The molecular basis for the initiation of fruit development and parthenocarpy

by

Adam Vivian-Smith, Assc. Dip. App. Sc., B. Sc (Hons)

A thesis submitted for the degree of

Doctor of Philosophy

at

The University of Adelaide

Department of Plant Science

in collaboration with

CSIRO Plant Industry, Horticulture Unit

Urrbrae, Adelaide

1st November, 2000

TABLE OF CONTENTS

Abstract

Parthenocarpy, or seedless fruit development, has an agronomic importance in many horticultural crops. In most fruit, fertilization or seed set usually determines whether fruit growth is sustained. Naturally occurring parthenocarpy results from a genetic lesion that permits fruit to develop in the absence of fertilization and seed development. Parthenocarpy can also be induced artificially with cytokinin, gibberellin or auxin plant growth regulators applied to anthesis pistils. This thesis describes genetic research using *Arabidopsis* as a model plant to identify integral mechanisms that control parthenocarpy and the initiation of fruit development.

The growth and structure of the *Arabidopsis* pistil was determined post-fertilization. Experiments were designed to understand how plant growth regulators induce *Arabidopsis* silique (fruit) development in emasculated anthesis stage pistils. Exogenous gibberellin (GA_3) induced growth and cellular differentiation most comparable to pollinated pistils. Dependencies on gibberellins during silique development were examined in mutants defective for gibberellin biosynthesis (*ga1*, *ga4-1*, *ga5-1*) or perception (*spy-4*, *gai-1*). Although exogenous GAs are effective at inducing parthenocarpy, mutant studies concluded that GAs are not the sole cue for fruit development in *Arabidopsis*. Mutants blocked in GA perception could develop siliques in response to pollination, auxin, cytokinin but not to exogenously applied gibberellins. Silique structure in pollinated *gai-1* and *ga5-1* provided strong evidence for a model supporting evidence of an auxin-like signal regulating structural development and that GAs limit anticlinal cellular division. A specialized function for *GAI* and related *GRAS* family members in controlling cellular division during fruit development was uncovered.

A mutant that forms parthenocarpic siliques without fertilization (*fwf*), was also characterized. The presence of surrounding floral whorls reduced the extent of parthenocarpic silique formation in *fwf*. Silique growth in the *fwf* background was examined when hormone perception, ovule and carpel identity functions were removed genetically. This established that *FWF* functions independent of *GAI*-mediated GA perception. Carpel identity conferred by *FUL* was critical for parthenocarpic silique elongation and ovule development beyond integument initiation, nucellar specification and subsequent morphogenesis, was essential for parthenocarpic silique development in *fwf*. Silique elongation occurs over a four-day period post-pollination or post-anthesis. This coincides with a similar time period in which *fwf* ovules remained receptive to fertilization. These observations are congruent with the hypothesis that *FWF* potentially represses a signal transduction process initiated within the ovule that mediates subsequent transition from carpel to silique development. Further analysis revealed that *aberrant testa shape* (*ats*) a mutant defective in integument formation enhanced parthenocarpic development in *fwf*, indicating that an ovule located repressor other than *fwf* can function to affect silique formation.

Other studies have shown that ethylene can modulate auxin-dependent growth in both aerial and root tissues by altering both polar and lateral auxin transport. The contribution of ethylene perception to signal transduction between ovule and carpel was also genetically assessed. Constitutive ethylene responses, conferred by *ctr1-1*, enhanced cellular expansion in *fwf* and also the autonomous silique development in *fis-2,* which develops autonomous endosperm. *ats ctr1-1* and *ino ctr1-1* double mutants were also found to be parthenocarpic. This indicates that ethylene perception and integumentary structure play an important role in autonomous silique development, conceivably by

changing the polar and lateral movement of an auxin-like signal within the integumentary tissues of the ovule.

fwf and *ats* were fine mapped on chromosome 5 of *Arabidopsis*. Candidate genes were identified corresponding to both mutations but only the identity of *FWF* was established. *Auxin Response Factor 8* (*ARF8*) was cloned and sequenced from the *fwf* mutant background. The gene encodes a protein with a amino-terminal DNA binding domain and a carboxy-terminal protein binding domain which homo- and hetero-dimerizes with other ARF or Aux / IAA class proteins. *ARF8* sequence from *fwf* mutants encoded a mutation in the translation start site. Complementation of *fwf* plants by the transformation of wild type copies of *ARF8* into *fwf* plants was hampered by reduced transformation efficiency. However wild type L.*er* and No.O plants transformed with mutant copies of *ARF8* were obtained in higher frequency, and these formed parthenocarpic siliques when primary transformants were emasculated. This indicated that an interfering protein is produced from the mutated *ARF8* gene that has altered regulatory activity. Sequence analysis indicated this and found that interference resulted from functional activity of the Q-rich and carboxy-terminal domains of the ARF8 protein. This inference is consistent with other published molecular data, which has demonstrated that the carboxy-terminal domain, together with the Q-rich region of selected ARF members, can activate auxin-responses. Thus the FWF / ARF8 protein may have a dual role, repressing carpel growth development through the DNA binding domain and then ensuring activation of silique development through the carboxy-terminal domain.

The combined molecular and genetic data has been used to construct models concerning the genetic control of silique development. The first model considers the role of plant hormones and how signals from floral whorls surrounding the carpel and from within the ovule control silique growth. A model is also presented for the control of adaxial

growth and development of the outer integument by the *INNER NO OUTER* gene. Finally the role of *FWF* and *SPY* in controlling floral tissue identity and boundary tissue specification is considered in a third model. Modification of the *FWF* / *ARF8* gene could be used as a tool to improve fruit set and retention in horticultural crops, in addition to creating seedless parthenocarpic fruit.

Declaration

I declare that this work contains no material, which has been accepted for the award of any other degree or diploma in any University or any other tertiary institution. To the best of my knowledge and belief this thesis is original and contains no material previously written or published by another person, except where due reference has been made in the text.

I give consent to this copy of my thesis, when deposited in the University library, being available for loan and for photocopying. A twelve-month embargo effective from the 1st day of November, 2000 was placed on this thesis.

Adam Vivian-Smith 

November, 2000

Acknowledgements

Firstly I would like to thank my supervisor Dr Anna Koltunow for her patience, encouragement and also for providing me with the opportunity to work in her lab on such a great project. This project and her support have provided me with many stimulating years of enjoyment.

I would like to thank Luo Ming for isolating the *fwf* mutant and for generous technical advice, Carol Horsman and Dr Anna Koltunow for their excellent illustration skills in Figure 3.1, and also to Carol Horsman for DNA preparation, help with transformation of *ARF8* clones and looking after plants. I thank Dr Anna Koltunow for performing cloning steps involved in the *ARF8* complementation, and I thank the Australian Genome Research Facility for sequencing *ARF8*.

I also would like to thank Prof Peter Langridge, Dr Susan Barker, and Dr Abed Chaudhury for helping to make this project possible and also for their advice during the project. I also thank the University of Adelaide for the Australian Postgraduate Award and the Horticultural Research and Development Corporation and the Commonwealth Scientific Industrial Research Organization (Australia) for funding and supplementary scholarship. I also thank the organizing members of the 10th International Arabidopsis conference for the travel scholarship to the 11th Arabidopsis conference in Madison, Wisconsin, 24th to 28th June 2000.

I thank Dr Kay Schneitz for providing *ant* and *ino* alleles, Dr Steve Swain for *spy-4*, Jason Walker and Prof John Larkins for molecular markers, and the *Arabidopsis* Biological Resource Center for seed. Dr Lyn Waterhouse at CEMMSA provided help with SEM microscopy facilities.

Special thanks go to past and present lab members, Susan, Nick, Matt Tucker, Matt Lynch, Sandra, Georgina, Jenny, Yoshi, Tohru, Debbie, Peter and Anne, for their technical know-how, payouts, chats and their discussions. I thank Dr Cameron McConchie and Dr Anna Williamson for inspiring me to pursue a career in science.

Warmest thanks go to Clare Gambley, Bec Short, Jade Herriman, Penny Richards, Luke Faulkner, Bree Bickmore, Kirrilley Becker, Toby Bramwell, Bart Rossel, Flavia Pellerone, Toby Knight, Anthony Otten, Danielle Smyth, Anna Stines, Jacqui Martin, Kylie Noonan, Dave Tattersall, Sarah and Phil Bricher, Steph Vaughan, Monaz Mehta, Abbie Collinson, Ava Blässe, the Reservoir Dogs and Whatthefoxhat? football teams and all other friends for enduring support, riotous behavior and memorable times.

Lastly, tremendous thanks go out to Ashley Bowen, Gabrielle, Brendan, Blake and my parents for never-ending support, wisdom and encouragement, right from the start of my study days. This thesis is dedicated to you.

Abbreviations

A	adenine
AFLP	Amplified fragment length polymorphism
ARF	auxin response factor
BA	benzyl adenine
bp, kbp, mbp	nucleotide base pairs, kilobase pairs, megabase pairs
CAPS	cleaved amplified polymorphic sequence
C	cytosine
cDNA	deoxyribonucleic acid complementary to mRNA
cm, mm, μm	centimetre, millimetre, micrometre
Col	*Arabidopsis* Columbia ecotype
dH_20	distilled water
DNA	deoxyribonucleic acid
DPA	days post-anthesis
EDTA	ethylenediaminetetraacetic acid
er	*erecta* mutation
G	guanine
GA, GA_X	gibberellin, gibberellic acid X,
g, mg, µg	gram(s), milligram(s), microgram(s)
IAA	indole acetic acid
L.*er*, L.*ER*	*Arabidopsis* Landsberg *erecta*, *Arabidopsis* Landsberg *ERECTA* ecotypes

L, ml, μl	litre(s), millilitre(s), microlitre(s)
M	molarity
min, hr	minute(s), hour(s)
mol	moles
mRNA	messenger ribonucleic acid
n	number of replicate measurements
NAA	napthyl acetic acid
°C	degrees celsius
PGR	plant growth regulator
PCR	polymerase chain reaction
RFLP	restriction fragment length polymorphism
RNA	ribonucleic acid
rpm	revolutions per minute
SDS	Sodium dodecyl sulphate
SSLP	simple sequence length polymorphism
T	thymidine
TAE	Tris-acetate-EDTA
Taq	*Thermus aquaticus* DNA polymerase
TE	Tris-EDTA buffer
Tris	Tris[hydroxymethyl]amino methane
U	Units of enzyme
%(v/v)	percent volume per volume
%(w/v)	percent weight volume

Chapter 1: Current issues in fruit initiation, development and parthenocarpy

1.1 Introduction

Fruit development is an integral part of angiosperm reproduction because the mature fruit protects, nurtures and then acts as the basic agent for facilitating seed dispersal. Fruits from different taxa are diverse in structure because during the course of evolution plant species have developed a variety of strategies for seed dispersal to maximize the distribution and success of the progeny. Some plant species use fruit structures to provide a mechanical device for seed dispersal, while other species are dependent on the consumption of the fleshy fruit tissues by megafauna to act as an agent in seed dissemination. In agriculture, numerous fruit varieties have been selectively bred to increase flesh content for human consumption. A typical human dietary intake consists of several different fleshy fruit per day and the seeds, which usually tend to form the inedible component, are disposed of and hence dispersed.

Fruit development begins following successful fertilization in the ovules of the flower and occurs concomitantly with that of the developing seed (Figure 1.1). There is evidence that suggests that developing seeds control the development of the fruit, at least to some extent (Denny, 1992; Meinke and Sussex, 1979). If fertilization is absent, flowers do not develop further and all or some of the floral organs abscise (Figure 1.1). However, fruit can develop without seeds in natural seedless variants or if treatments of plant growth hormones are applied to flowers (Figure 1.1). The development of seedless fruit without fertilization and the initiation of seed formation is called parthenocarpy and it is an agronomically important trait in horticultural crops. Control of fruit set, development and quality is also achieved by the application of plant growth regulators to horticultural fruit crops (Rappaport, 1979), yet little is known about the molecular basis of their action in fruit initiation and development. The present study is concerned with elucidating the molecular and genetic basis for parthenocarpy and the initiation of fruit development.

Figure 1.1 Fruit development requires the initiation and completion of flower development. Successful pollination of the stigma and subsequent fertilization events in the ovules allow seed and fruit development to proceed (top panel). Fruit development concludes when mature fruits ripen and shed seed. Fruits are diverse in structure, but a number of fruits are composed of exocarp, mesocarp and endocarp tissues that develop from the carpel. Without fertilization some or all of the floral organs abscise (bottom panel). Parthenocarpy is a process whereby fruit development occurs without fertilization and hence the initiation of seed development. Parthenocarpic fruit development has a genetic basis and it can be induced with exogenous application of plant growth regulators (bottom panel). This has led to the hypothesis that lesions relating to heritable parthenocarpic fruit development might relate to alterations in the synthesis or perception of endogenous hormones?

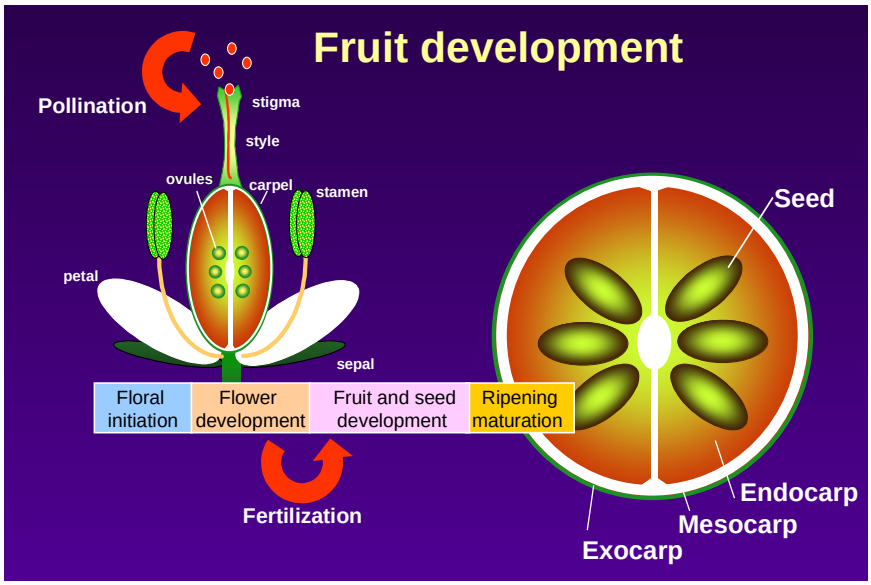
Fruit development
Pollination
stigma
style
ovules
carpel
stamen
petal
sepal
Floral initiation
Flower development
Fruit and seed development
Ripening maturation
Fertilization
Seed
Endocarp
Mesocarp
Exocarp

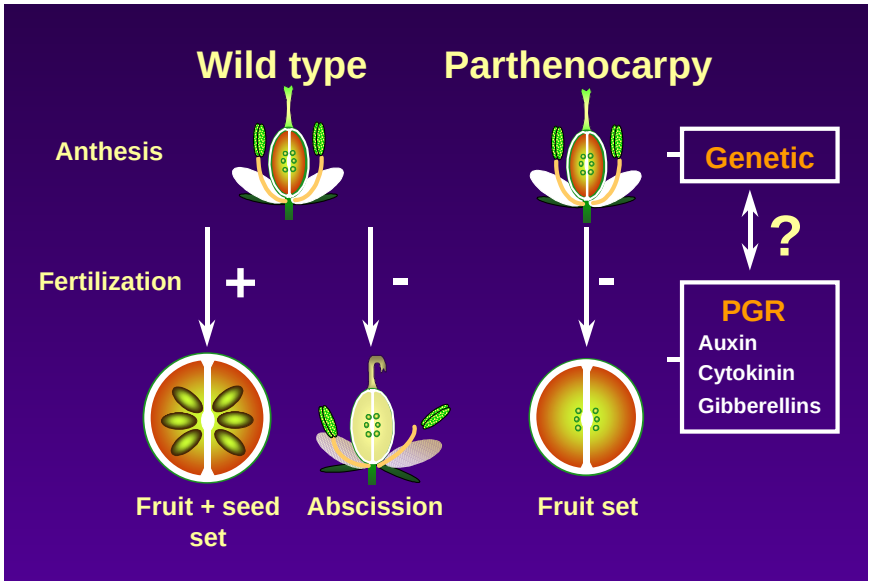
Wild type
Parthenocarpy
Anthesis
Fertilization
+
-
-
Genetic
?
PGR
Auxin
Cytokinin
Gibberellins
Fruit + seed set
Abscission
Fruit set

1.2 Diversity in floral development and fruit structure

Fruits are diverse in structure and function and the components of the flower that make up fruit tissues are also radically different amongst species. Fruits are not necessarily derived in their entirety from gynoecial tissues of the carpel and they can incorporate other tissues derived from other floral structures such as bracts, receptacles and complete inflorescence tissues (Coombe, 1975; Hulme, 1970). Fruits, like figs, strawberries and apples, which are derived from tissues other than the gynoecium proper are said to be pseudocarpic. Therefore the form of an angiosperm fruit depends upon three parameters including the number of components in a floral organ that eventually comprise them, the position of the contributing organs, and how these organs differentiate post-fertilization (Coombe, 1975).

Components of the pedicel, the peduncle, exocarp, mesocarp, endocarp and placental-intralocular tissue can all undergo various differentiation strategies (Coombe, 1975). For example some arilate fruit, like *Litchi chinensis*, part of the seed testa undergoes rapid expansion to form a succulent tissue inside the pericarp (Kumcha, 1999). In *Arabidopsis*, the fruit is simple and develops as an elongating pericarp or carpel that accommodates the developing seeds (Meinke and Sussex, 1979). The ripening process is the last step in fruit development and prepares the fruit ready for dissemination. This involves colour changes and tissue softening processes and sometimes dehiscence to release seed.

Growth in those component tissues that form the fruit is usually dependent upon post-fertilization signals to initiate development (Coombe, 1975). The number and types of cell divisions either periclinal and anticlinal in addition to the relationships between cell division and expansion, are important for determining the final shape and size of the fruit

(Lyndon, 1990). Gross cell expansion is often a feature of the late stages of fleshy fruit development, prior to ripening. This is a common feature of fruits where seeds are disseminated by megafauna. By contrast, plants that have developed fruit specialized for abiotic seed dispersal, are usually not fleshy. As the molecular processes regulating fruit development in *Arabidopsis thaliana*, a member of the Brassicaceae, is the focus of this research the events of flower and fruit development in this plant are introduced in the sections below.

1.3 Carpel, ovule and female gametophyte development

Floral development in *Arabidopsis* has been described and divided into various stages (Bowman, 1993). At floral maturity the *Arabidopsis* flower is composed of four whorls of organs. The outer whorl comprises four sepals that surround a set of four petals, followed by a whorl of six stamens (Figure 1.2A). The central whorl of the flower is the pistil, comprising a stigma, a short style and two fused carpels (Figure 1.2B and 1.2C). The gynophore tissue separates the carpels and the floral receptacle. The carpels enclose approximately 50-60 ovules that are borne on placental tissue that forms from the carpel margins (Figure 1.2C and 1.2D). The funiculus is a stalk that connects the placental tissue to the base of the ovule (Figure 1.2D and 1.2E). In *Arabidopsis*, the fruit forming component is a six cell layered carpel (Figure 1.2A; Sessions and Zambryski, 1995).

Male and female haploid gamete development occurs in the multicellular sporophytic diploid tissues of the anthers and ovules respectively (Figure 1.2A and 1.2D). Female gametophyte development is initiated during floral development when ovules are undergoing morphogenesis (Schneitz et al., 1995). Ovules develop from one or two sub-epidermal layers of placental tissue in the developing pistil (Schneitz et al., 1995). In the developing nucellar region of the ovule primordia, a single cell called a megaspore mother

Figure 1.2 *Arabidopsis* flower structure. (A) A mature flower showing the sepals, petals, dehiscent stamens and the pistil (center). (B) SEM picture of a pistil showing stigmatic papillae (p), carpel valve (demarcated) and floral receptacle (r). (C) A carpel valve has been removed from the pistil to reveal the rows of ovules (arrow; style, t). (D) SEM picture of an ovule showing micropyle (m), funiculus (f) and septum (sm). (E) A diagram showing a section through a mature ovule. a, antipodal cells; cc central cell; cr, chalazal region; e, egg cell; f, funiculus; fv, funiculus vascular tissue; ii, inner integument; m, micropyle; oi, outer integument; pn, polar nuclei; s, synergid cell; sm, septum-carpel margin.

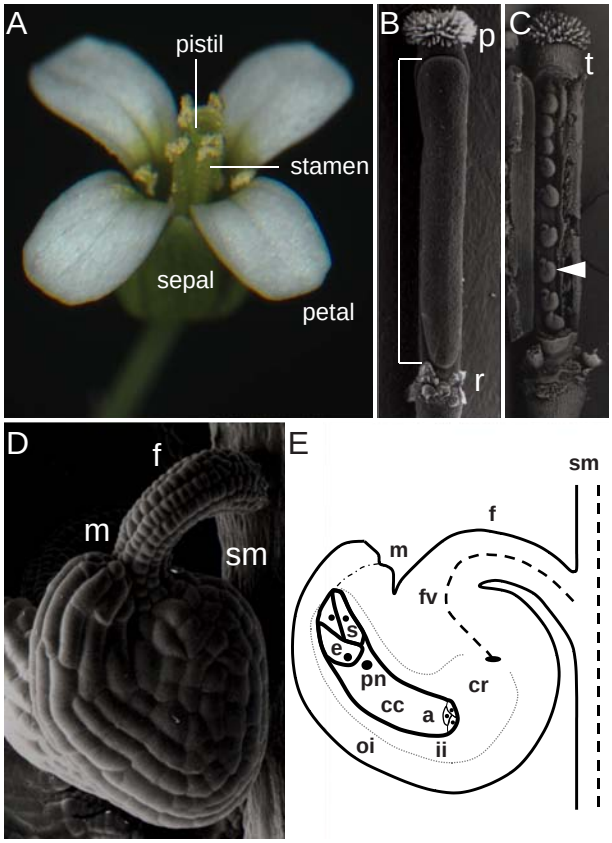
A
pistil
stamen
sepal
petal
B
p
r
C
t
D
f
m
sm
E
sm
f
m
fv
s
e
pn
cc
a
cr
oi
ii

cell is specified to undergo meiotic division. *Arabidopsis* forms a Polygonum-type of embryo sac. A tetrad of four megaspores is generated and one is selected as a functional megaspore while the other three haploid spores undergo cell death and degenerate. The selected megaspore undergoes mitosis, nuclear migration and cellularization events (Reiser and Fischer, 1993; Figure 1.2E). The mature haploid embryo sac that is composed of two synergid cells, an egg cell, three antipodal cells and a binuclear central cell (Figure 1.2E). In *Arabidopsis* the development of the ovule integument and funiculus is complete once the gametophyte has attained this stage (Schneitz et al., 1995). At anther dehiscence *Arabidopsis* pollen is tricellular and is composed of a vegetative cell and two sperm cells (Bowman, 1993).

1.4 Pollination and fertilization

Following the transfer of pollen from anthers to stigma, successful pollination in numerous species induces changes within the floral organs. Pollination can either accelerate or induce the senescence of the outermost floral organs, alter pigmentation, increase nutrient mobilization within floral organs and increase ethylene biosynthesis (reviewed O'Neill, 1997). Auxin is known to be a primary signal from pollen (O'Neill, 1997). Ethylene biosynthesis typically initiates within the stigma following pollen contact and facilitates the senescence of floral organs that are no longer required during fruit development. Ethylene regulates these interorgan processes and also serves to prepare the pistil for the coordinated growth of ovules and carpel following post-fertilization events (O'Neill, 1997). Ethylene biosynthesis most notably affects pigmentation and senescence in petal and perianth whorls, to perhaps signal to pollinators that a flower has previously been visited (O'Neill, 1997; O'Neill and Nadeau, 1997; O'Neill et al., 1993). Unlike many species, which produce a characteristic and noticeable climacteric ethylene response, the

post-pollination ethylene response in members of the Brassicaceae, are not climacteric (Khan, 1994) and ethylene responses following pollination in *Arabidopsis* have remained largely unstudied.

In *Arabidopsis*, fertilization involves the delivery of two sperm cells, transmitted via the pollen tube growth, to the mature female gametophyte (Figure 1.3A). The pollen tube is guided towards the female gametophyte and enters the micropyle of the ovule (Figure 1.3B). Upon fusion of the tube tip with a synergid cell, the pollen tube discharges its contents. Double fertilization involves one sperm cell uniting with the egg cell and the second sperm cell fuses with the central cell and its nucleus migrates to the polar nuclei (Figure 1.3C). This results in the initiation of a diploid zygote and triploid endosperm development (Figure 1.3C). The remaining synergid deteriorates and the integuments expand and divide to accommodate the developing embryo and endosperm. In *Arabidopsis* and other angiosperms, the integuments latter differentiate to form the testa, to protect the seed, and facilitate the transfer of nutrients into seeds via the funiculus (Bowman, 1993; Wittich, 1998). If fertilization is absent, the carpel and all other floral organs may senesce and the flower abscise completely without further differentiation.

1.5 Floral organ signal transduction and parthenocarpy

Signal transduction events must occur between ovule and carpel wall to ensure coordinated post-fertilization seed and fruit development. Gustafson, (1936) first discovered that the application of exogenous auxin to flowers induced parthenocarpy and the effects of various growth regulators on the initiation of fruit development have been studied since. Many different exogenously applied growth hormones, with the exception of ethylene and abscisic acid, have been shown to induce fruit development (Schwabe and Mills, 1981), and as such they have all been implicated in the control of fruit set and

Figure 1.3 Fertilization in *Arabidopsis*. (A) A pollen tube containing two sperm cells is guided to the ovule micropyle by signals emanating from a fertile female gametophyte. (B) The tube tip enters the micropyle of the ovule and unites with a synergid cell that degenerates upon fusion. Two sperm cells migrate to combine with the egg cell and polar nuclei of the central cell respectively. (C) Synergid cells degenerate and the diploid zygote, triploid endosperm and testa begin development. cc, central cell; e, egg cell; en, endosperm; g, generative cell; m, micropyle; p, pollen tube; s, synergid; sp, sperm cells; z, zygote.

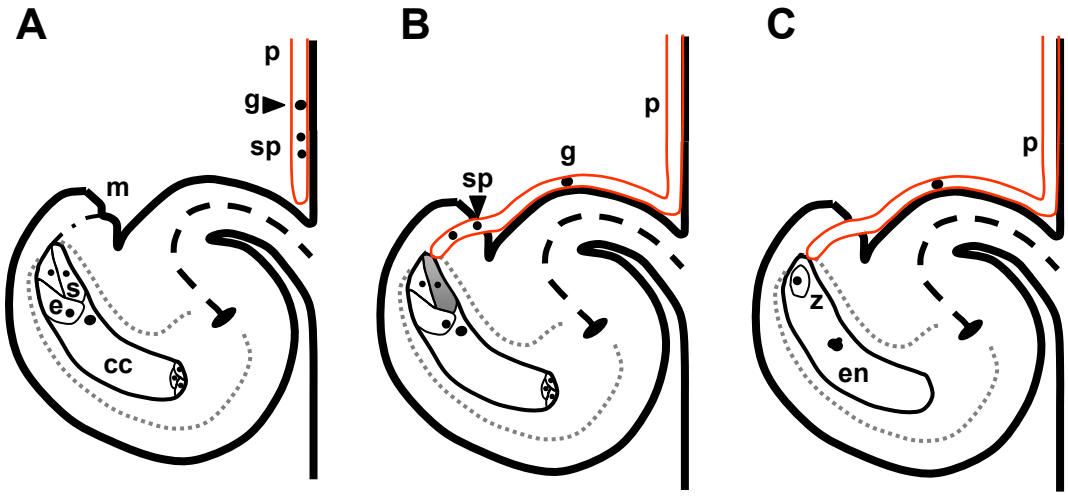
A
p
g
sp
m
s
e
cc
B
p
g
sp
C
p
z
en

initiation. The success of inducing parthenocarpy using exogenous growth regulators is dependent on a range of variables including the hormone type, wetting agent, amount of surface area, the amount of spray, type of solvents and even environmental conditions. Combinations of hormonal treatments are also commonly applied to try and ensure normal fruit development (Schwabe and Mills, 1981).

Gibberellins (primarily GA_1, GA_3 and GA_4), auxins (natural IAA; synthetic 2,4-D and 4-chloro-IAA) and to a lesser extent cytokinins (synthetic CPPU and BA) are all known to induce parthenocarpic fruit development in a wide variety of species (Schwabe and Mills, 1981). The growth regulator is usually applied to the flower but application of GA_3 to leaves proximal to emasculated pea flowers can also induce parthenocarpy (Peretó et al., 1988). This suggests GA_3 or another intermediate product is transported from the leaf to the flower and induces fruit set. Infrequently, maleic hydrazide, streptomycin and polyamines have also been used to induce seedlessness (Pommer et al., 1996; Schwabe and Mills, 1981). Brassinolide was also shown to be effective for inducing parthenocarpic fruit in eggplant (Khripach et al., 1999). Generally one particular growth regulator appears to be optimal at initiating fruit development independent of fertilization in one species, but not in another (Schwabe and Mills, 1981).

Gustafson, (1939) and later also Nitsch, (1970) suggested that natural parthenocarpy resulted from the production of a threshold level of endogenous growth substances in the ovary that maintained fruit growth independent of fertilization. Seeds are also known to produce copious amounts of growth hormones soon after their induction (Jensen and Bandurski, 1994; Swain et al., 1995b; Van Overbeek et al., 1941). Many studies have therefore focussed on identifying and determining the levels of endogenous hormones within fruit, to elucidate the mechanisms governing fruit initiation (Ben-Cheikh et al., 1997; de Bouille et al., 1989; Eeuwens and Schwabe, 1975; El-Otmani et al., 1995;

Fos et al., 2000; García-Martínez et al., 1997; García-Martínez et al., 1991a; García-Martínez et al., 1991b; García-Martínez et al., 1987; Kim et al., 1992; Kim et al., 1995; Koshioka et al., 1994; Mehouachi et al., 2000; Ozga et al., 1992; Rodrigo et al., 1997; Santes et al., 1993; Swain et al., 1995a; Takeno and Ise, 1992; Talon et al., 1990a; Talon et al., 1992; van Huizen et al., 1995).

Comparisons of auxin and gibberellin levels in parthenocarpic (*pat*; *pat-2*) and non-parthenocarpic tomato, have revealed differences in both auxin and gibberellin levels between parthenocarpic and non-parthenocarpic lines (Fos et al., 2000; Mapelli et al., 1993; Mapelli et al., 1978). The temporal patterns of hormone levels during seeded and parthenocarpic growth in these studies are complex, and to date, unequivocal evidence that changes in the levels of endogenous hormones play a role in fruit initiation processes in tomato and other species is lacking (Kim et al., 1992; Kojima et al., 1999; Koshioka et al., 1994; Takeno and Ise, 1992; Talon et al., 1990a; Talon et al., 1992; Varge and Bruinsma, 1976). Currently it is not known whether hormones are required to initiate fruit development, or are downstream components that form part of various developmental cascades occurring post-fertilization. It is also possible that exogenous growth regulators overwhelm various processes in the plant to induce fruit development.

Determinants of fruit set also include carbohydrate sink strength. Developing ovules and seeds are carbohydrate sinks (Wittich, 1998) and fruits that lack photosynthetic tissues also have a high carbohydrate demand (Wardlaw, 1990). Sucrose synthase is a key enzyme in determining sink strength in plant organs and sucrose synthase over expression can determine organ size (Zrenner et al., 1995). Down regulating the level of sucrose synthase in tomato fruit was shown to decrease fruit set (D'Aoust et al., 1999). Thus control of fruit set by endogenous carbohydrate demand could be a factor determining

whether fruit tissues develop or abscise. The relationship between sink strength, hormone levels and the primary fruit inductive signal remain to be determined.

Parthenocarpic fruit development has also been demonstrated to occur following stimulation using sterile pollen application to wild type plants (Gustafson, 1942; Rao et al., 1992; Yasuda, 1930; Yasuda, 1935). The process by which this occurs also is unknown.

1.6 Parthenocarpy and fertilization independent fruit set as tools to understand factors controlling fruit initiation

Parthenocarpy uncouples fruit development from fertilization-dependent processes and could be used to study the interorgan communication events that lead to fruit development. Two types of naturally occurring parthenocarpy have been identified on the basis of whether the genotype produces a viable seed in the presence of fertile pollen (George et al., 1984). Plants facultative for parthenocarpy produce viable seed if fertilized, and accordingly, the absence of fertile pollen or mechanisms preventing fertilization are required to observe parthenocarpy (George et al., 1984). Genotypes obligate for parthenocarpy are unable to produce viable seed in either the presence or absence of fertile pollen (George et al., 1984). Thus plants with the obligate condition are thought to be also defective during female gametophyte development. Agriculturally, obligate parthenocarpic genotypes are absolutely dependent on vegetative propagation.

The genetic basis for facultative parthenocarpic fruit development has been studied in tomato (Nuez et al., 1986; Pecaut and Philouze, 1978; Philouze, 1983a; Vardy et al., 1989a; Vardy et al., 1989b) and cucurbits (Pike and Peterson, 1969; Prohens et al., 1998). In the tomato line RP 75/59, parthenocarpy is inherited as three recessive genes with additive effects (Vardy et al., 1989a). Two of the recessive genes in the tomato line RP 75/59 have been mapped to chromosome 1 and 6. Crosses in other parthenocarpic lines,

between Montfavet 191 and Severianin, have revealed two separate recessive parthenocarpic loci called *pat* and *pat-2* respectively (George et al., 1984). Efforts to map the *pat-2* locus in tomato through linkage analysis have shown that *pat-2* locus is modified by a minor locus called *mp* and that *pat-2* is located on chromosome 3 between the visible markers *sf* and *bls* (Vardy et al., 1989b). One other cultivar, Sub Arctic Plenty, exhibits parthenocarpic fruit set that appears to be controlled by another recessive locus (Nuez et al., 1986). Thus there is evidence for at least three different loci controlling facultative parthenocarpic fruit development in tomato.

One other type of naturally occurring process also displays fruit development in the absence of fertilization. Apomixis results in the initiation of both seed and fruit development and as such apomixis is mechanistically distinct from parthenocarpy. Cells close to the megaspore mother cell in ovules of some apomictic plants such as *Hieracium* initiate an aberrant developmental program that eventually displaces the meiotically derived gametophyte with an unreduced cell that begins autonomous embryo and endosperm development (Koltunow, 1993). This gives rise to seeds identical in genotype to the maternal parent and autonomous fruit set.

What are the signals or mechanisms that enable natural parthenocarpic silique development? Do the signals form part of the normal senescence pathway? Or are they part of the post-fertilization response pathway? Are hormonal factors related to carpel development or to ovule development? Can the lesions causing parthenocarpic fruit development be genetically isolated? Is parthenocarpy a gain of function or a loss of function mutation?

At the time of initiation of the present study, *Arabidopsis thaliana* was selected as the genetic system to investigate the molecular processes governing the initiation and coordination of seed and fruit development. Fruit development in *Arabidopsis thaliana* had

received little attention in developmental and genetic terms. Significant progress has been made towards understanding the basis of asymmetric cell division, cell patterning, cell signaling and flower development through the use of molecular, developmental and genetic approaches in *Arabidopsis* (Dolan and Okada, 1999; Meyerowitz, 1997; Meyerowitz et al., 1991; Meyerowitz et al., 1998; Scheres, 2000; Scheres and Benfy, 1999). Therefore *Arabidopsis* was used to identify some of the molecular factors controlling the fruit initiation process.

1.7 Aims and expectations of this thesis

Parthenocarpy is a genetically inherited trait. Natural parthenocarpy may represent a mutation that uncouples or bypasses a signal transduction hierarchy that is normally dependent upon fertilization for fruit and seed initiation. From the information described in the literature, this might occur in at least four ways different ways. Firstly, hormonal perturbation or changes in plant growth hormone levels in particular ovary tissues may stimulate parthenocarpy (Gustafson, 1939). Secondly, the gene(s) involved in parthenocarpy could direct alterations in carbon partitioning and sink strength that influence the growth and expansion of the fruit (D'Aoust et al., 1999). Thirdly, lesions that give rise to parthenocarpy may relate to specific pollination dependent processes that influence fruit development (Yasuda, 1930) or finally, mutations that cause developmental lesions in specific tissues might permit the development of fruit to proceed without fertilization.

One way to identify the molecular factors controlling parthenocarpy is to try and induce the process via mutation. *Arabidopsis* has provided an excellent model for the identification of floral and reproductive mutants. *Arabidopsis* plants produce numerous fruits and this should allow the simple identification and characterization of mutants

affecting early fruit development and provide a convenient model in which to examine the hormonal and developmental control of parthenocarpy. During a visual mutagenesis screen designed for identifying components of apomixis (Chaudhury and Peacock, 1994), a parthenocarpic *Arabidopsis* mutation was detected and it formed the starting point for this study on parthenocarpy and the initiation of fruit development.

The aims of this thesis were to:

1) examine the development and genetic control of *Arabidopsis* fruit growth response to exogenous phytohormones application.

2) characterize a EMS induced parthenocarpic mutant in *Arabidopsis* and identify the mutated gene.

3) genetically examine what additional factors influence parthenocarpy in *Arabidopsis* by specifically examining the effects of alterations in hormone biosynthesis, perception and ovule development on parthenocarpy.

Chapter 2: Genetic analysis of growth regulator induced parthenocarpy in *Arabidopsis*

2.1 Introduction

Fruit and seed development are initiated following fertilization and are a coordinated process (Gillaspy et al., 1993). The absence of fertilization results in either senescence of the entire flower, or a cessation of carpel development following the abscission of other floral organs (Granell et al., 1992; O'Neill and Nadeau, 1997; Vercher and Carbonell, 1991; Vercher et al., 1989; Vercher et al., 1984). The limiting factors for growth of unpollinated carpels appear to be reduced endogenous growth hormone levels prior to the onset of senescence (Gillaspy et al., 1993; Pharis and King, 1985). Developing seeds are usually considered essential determinants of fruit growth (Archbold and Dennis, 1985; Nitsch, 1950) because they synthesize high levels of plant growth hormones (Ben-Cheikh et al., 1997; Eeuwens and Schwabe, 1975; García-Martínez et al., 1991a; García-Martínez et al., 1991b; Rodrigo et al., 1997; Sponsel, 1983; Talon et al., 1990a).

In some species, parthenocarpic fruit develops in the absence of fertilization and is seedless, indicating it is possible to uncouple fruit formation from seed development. Parthenocarpy has a genetic basis (Lin et al., 1984; Nuez et al., 1986; Pike and Peterson, 1969; Vardy et al., 1989a; Vardy et al., 1989b) and is selected for in seedless fruit breeding programs (Sykes and Lewis, 1996). Parthenocarpy can also be induced in a diverse range of agricultural species with the exogenous application of gibberellins, auxin, and cytokinin (Schwabe and Mills, 1981). It has been assumed that exogenous plant growth regulators (PGRs), substitute for hormones synthesized by developing seeds. Furthermore, elevated levels of endogenous auxins and gibberellins have been observed in the fruit of plants exhibiting naturally occurring parthenocarpy (George et al., 1984; Talon et al., 1990d; Talon et al., 1992), suggesting that elevated hormone levels in fruit tissue other than seed may be sufficient to induce fruit development. This was directly demonstrated by Rotino et al., (1997), when they obtained seedless transgenic tomato and eggplant by specifically

elevating auxin levels in ovules, by means of chimeric auxin biosynthesis genes. Although parthenocarpic fruit development can be induced following exogenous PGR application, and elevated endogenous hormone levels have been observed during parthenocarpic fruit set in some species, the molecular events controlling the initiation of fruit development and their linkage to plant hormone signal transduction processes remain unknown.

Arabidopsis can be used to identify the genes controlling carpel morphogenesis (Gu et al., 1998) and hormone signal transduction (Hobbie, 1998; Hobbie et al., 1994; Jacobsen and Oleszewski, 1993; Phillips, 1998). The functional fruit and seed dispersal unit of *Arabidopsis* are siliques, and their development in *Arabidopsis* is dependent on fertilization and seed set (Chaudhury et al., 1993; Meinke and Sussex, 1979; Ohad et al., 1996). Barendse et al., (1986) previously demonstrated that GA is an essential component for silique development in *Arabidopsis*, because both seed and fruit development in the *ga1* biosynthetic mutant were dependent on the application of exogenous GA_3 following pollination. Although reciprocal crosses between *ga1* mutants and wild-type plants showed that silique development was primarily determined by maternal endogenous GAs, Barendse et al., (1986) also showed that determinants, other than GAs, were also involved in silique development in the GA deficient genotypes.

The available biosynthetic and hormone perception mutants in *Arabidopsis* makes an ideal species with which to investigate how fruit growth is initiated at the molecular level and to understand the role of plant hormones during fruit development. Parthenocarpic silique development can occur in *Arabidopsis* following application of GA_3 (Chaudhury et al., 1994; Jacobsen and Oleszewski, 1993). Jacobsen and Oleszewski, (1993) reported that mutants at the *SPINDLY* locus have altered GA perception and that parthenocarpic silique elongation occurs independent of fertilization in these plants. Apart

from this genetic research, seedless fruit formation has not been studied to any great extent in *Arabidopsis*.

To further understand the molecular basis for parthenocarpy I have analyzed the ability of various plant growth regulators to elicit silique development following their application to the pistils of emasculated flowers. I then genetically analyzed how the process was mediated by comparing silique growth and morphology of PGR induced parthenocarpic siliques with those of *Arabidopsis* mutants blocked in GA biosynthesis and perception. In this chapter I demonstrate the relationships between growth regulator induced parthenocarpy, hormone signal transduction and silique development.

2.2 Materials and methods

2.2.1 Plant growth

Plants were grown at 20°C in a walk-in growth chamber (Phoenix Biosystems, Adelaide Australia) with 16 h day-length and a light intensity of 150 μmol m^{-2} s^{-1}. Eight plants were grown in 13 cm by 7 cm by 4 cm deep containers in a 1:1:1 peat, sand, and perlite mix containing 1 g L^{-1} Fe_2SO_4, 3 g L^{-1} of fertilizer (Osmocote plus, Scotts-Sierra chemicals, Mayville, OH), 2 g L^{-1} dolomite, 0.5 g L^{-1} gypsum, and 0.5 g L^{-1} lime. Plants were watered daily.

Seeds of *ga1-3*, which require GA for germination, were surface sterilized and plated onto Murashige and Skoog medium (Murashige and Skoog, 1962) containing 1% (w/v) sucrose, 1% (w/v) agarose, pH 5.7, to which sterile GA_3 had been added after autoclaving to a final concentration of 0.1 *m*M. Petri dishes were kept at 20°C in a 16 h day-length at 35 μmol m^{-2} s^{-1}. Seedlings were transferred to soil after 7 days.

2.2.2 Silique emasculation, controlled pollination and application of growth regulators

For each experiment, buds of *Arabidopsis thaliana* (L.) Heynh, Landsberg (L.*er* and L.*ER*) and Columbia (Col-1 and Col-1 *er*2) ecotypes, were emasculated at stage 11-12 (Bowman, 1993), approximately 1-2 days pre-anthesis. To avoid damage to the inflorescence meristem from emasculation, extra fine scissors (Castro-Viejo scissors, ProSciTech., Thuringowa, Australia), were used instead of fine forceps to remove sepals, petals and anthers, leaving an exposed pistil. Controlled pollinations were performed on anthesis stage pistils (Stage 13; Bowman, 1993), by dusting a freshly dehisced anther over the extended stigmatic papillae until pollen was seen adhering to the stigmatic surface. Alternatively pistils were left unpollinated as controls or treated with PGR.

Growth regulators were applied to emasculated pistils at stage 13 (Bowman, 1993), unless specified. Each pistil was uniformly coated, from the tip of the stigmatic papillae to the pedicel, with a 1 μl droplet containing either 0.01, 0.1, 1, or 10 *n*mol of either GA_3, BA, IAA or NAA, with 0.04% triton X-100 as a surfactant. Each solution was buffered to pH 7. Pistils treated with a control solution of 0.04% triton X-100, were identical in length to unpollinated pistils 7 days post-anthesis (DPA).

Final silique length following pollination or PGR treatment was measured 7 DPA. The growth rates of individual *Arabidopsis* siliques were measured over a 10-12 day period by taking repeated digital images of treated pistils at 12 h intervals (RD-175 camera, Minolta, Osaka, Japan). Growth data for each treatment were established by the examination of a minimum of five individual pistils, and each pistil was measured from a separate plant. Growth curves were fitted to data with an exponential growth function (Sigmaplot version 4.0, Jandel Scientific, San Rafael, CA).

2.2.3 Pistil receptivity to pollen and to GA_3

Emasculated flowers (*n* = 10 pistils) were pollinated or treated with a single application of 10 *n*mol GA_3 $pistil^{-1}$ (*n* = 7 pistils) at daily intervals post-anthesis to determine the period of receptivity to pollen or GA_3. Each GA_3 treated pistil from a separate plants was assessed. Final silique length was determined 12 DPA. Pistil receptivity was the period in which siliques elongated or set seed in response to pollination with respect to the day post-anthesis.

2.2.4 Morphological analysis of carpel and silique development

Pistils at anthesis and developing siliques following various treatments were fixed in 4% glutaraldehyde, 10 *m*M sodium-cacodylate (pH 6.9). Tissue was rinsed once in 10 *m*M sodium-cacodylate pH 6.9, then dehydrated through a graded ethanol series to 100% and embedded in Spurrs' resin (Spurr, 1969). Sections (0.6 μm) were cut from the embedded tissue using a microtome (Ultracut E, Reichert-Jung, Wien, Austria) and stained with 0.1% (w/v) toluidine blue. Stained sections were photographed using the digital camera attached to an Axioplan microscope (Carl Zeiss, Jena, Germany). Morphometric analysis was performed on captured images of each section by downloading to Photoshop (version 4.0, Adobe Systems Inc., San Jose, CA) and by measuring cells using imaging software (Image Tool version 1.27, The University of Texas Health Science, Texas, San Antonio; http://ddsdx.uthscsa.edu/).

To determine how the pattern of cell division and expansion occurred during silique development, the average number of cells in the exocarp, mesocarp and endocarp tissues was counted from cross-sections of pistils at anthesis and siliques at 7 DPA (*n* = 3-10). Mean cell length normal to the plane of silique elongation was also ascertained from lateral carpel longitudinal sections (*n* = 8-64 cells per section each from 3-10 sections). From

these data I determined the magnitude of extension of individual cell types and calculated the total number of cells in the longitudinal sectional area of a pistil or silique. The latter measurement was calculated directly by dividing the mean silique length by the cell length normal to the plane of silique growth.

2.2.5 Analysis of various *Arabidopsis* mutants for silique elongation following emasculation

A selection of existing *Arabidopsis* mutants were investigated for their ability to form a fruit following emasculation including: *amp1-1*; *ctr1-1*; *etr1-3*; *ein2-1*; *ein3-1*; *ein4*; *ein5-1*; *ein6*, *ein7*; *spy-1*; *spy-3*; *spy-4*; *gar2-1*; *gai-1*; *ga1-3; ga4-1; ga5-1*; *abi4*; *axr1-3*; *axr2*; *axr4-2*; *aux1-7*. Pistils were emasculated and assessed 12 DPA. All mutants were obtained from the *Arabidopsis* Biological Resource Center (Ohio State University, Columbus, Ohio) except *spy-4*, which was a gift from Dr Steve Swain, and *amp1-1*, from Dr Abed Chaudhury.

2.3 Results

2.3.1 Silique growth and elongation in *Arabidopsis*

Arabidopsis pistils from ecotypes L.*er*, L.*ER*, Col-1 and Col-1 *er*2, pollinated at stage 13 (anthesis; Bowman, 1993) increased in fresh weight until 6-7 DPA (not shown) and siliques were 4- to 5-fold longer than their initial anthesis length (Table 2.1). Other floral organs, excluding the developing silique, senesced soon after pollination and abscised during silique development. In pollinated pistils of L.*er* and Col-1 the siliques elongated exponentially until 3 and 5 DPA respectively (Figure 2.1 top and middle). The fruit matured and carpel valves became yellow from around 12 DPA, until the siliques shattered and shed matured seed several days later. I observed that Col-1 and L.*ER*

Table 2.1 Elongation of *Arabidopsis* siliques in response to pollination and PGR treatments.

	Ecotype/ Mutant (Mean silique length mm ± s.d.)							
Stage and Treatment	L.*er*	L.*ER*	Col-1 *er*2	Col-1	Ws-O	*spy*-4	*gai-1*[†]	*ga5-1*
Anthesis pistils	2.8 ± 0.2	3.2 ± 0.2	2.9 ± 0.3	3.2 ± 0.4	3.2 ± 0.2	2.8 ± 0.3	2.9 ± 0.3	3.2 ± 0.3
emasculated - pollination	4.1 ± 0.4[b]	4.8 ± 0.4[a]	3.7 ± 0.2[c]	4.1 ± 0.3[b]	4.5 ± 0.1[ab]	4.9 ± 0.4[a]	4.5 ± 0.4[a]	5.0 ± 0.2[a]
emasculated + pollination	11.5 ± 1.0[c]	16.7 ± 1.5[a]	11.3 ± 0.6[c]	16.0 ± 1.7[a]	17.3 ± 1.1[a]	14.6 ± 0.8[b]	9.5 ± 1.2[d]	10.5 ± 1.0[cd]
	(6.7)	(8.3)	(10.6)	(15.3)	(10.6)	(5.7)	(4.1)	(4.2)
IAA 10 *n*mol pistil^{-1}	7.5 ± 0.9	7.9 ± 2.4	6.9 ± 0.7	5.2 ± 0.4				
	(3.7)	(2.9)	(5.0)	(2.3)				
NAA 10 *n*mol pistil^{-1}	6.8 ± 0.8	8.9 ± 3.5	4.0 ± 1.7[NS]	5.9 ± 1.4		8.7 ± 1.4	7.6 ± 1.2	
	(3.1)	(3.6)	(1.4)*	(3.2)		(2.8)	(2.9)	
BA 0.1 *n*mol pistil^{-1}	5.9 ± 0.8	7.9 ± 0.5	5.3 ± 0.6	4.5 ± 1.3[NS]				
	(2.4)	(2.9)	(3.0)	(1.5)*				
BA 1 *n*mol pistil^{-1}	5.7 ± 0.4	6.2 ± 1.1	2.9 ± 0.3[NS]	5.1 ± 0.7		5.4 ± 1.1[NS]	6.1 ± 0.2	
	(2.2)	(1.9)*	(0) *	(2.2)		(1.3) *	(2.0)	
GA_3 0.1 *n*mol pistil^{-1}	8.2 ± 0.8	11.0 ± 3.2	5.9 ± 0.9	7.4 ± 0.4				
	(4.2)	(4.8)	(3.8)	(4.9)				
GA_3 1 *n*mol pistil^{-1}	9.5 ± 1.5	12.2 ± 1.6	7.6 ± 0.2	9.2 ± 1.1				
	(5.2)	(5.6)	(6.0)	(7.2)				
GA_3 10 *n*mol pistil^{-1}	10.0 ± 1.1	14.5 ± 1.9	9.2 ± 0.5	10.6 ± 1.4	9.8 ± 0.8	8.4 ± 1.1	5.3 ± 0.7	10.0 ± 1.1
	(5.6)	(7.0)	(7.9)	(8.9)	(4.9)	(2.7)	(1.5)*	(3.9)

[NS] Indicates the mean silique lengths are not significantly different from unpollinated pistils harvested at 7 day post-anthesis. [†] represents the mean silique length of cross-pollinated *gai-1* siliques (*gai-1* self pollinated siliques attained 7.99 ± 1.7 mm). Numbers in parentheses represent the fold increase silique length as described in the results. * Siliques less than two fold the length difference between anthesis and unpollinated 7 day pistils.

Figure 2.1 Silique elongation of emasculated anthesis pistils after pollination (p), without pollination (up), or treated with GA_3 (10 *n*mol pistil^{-1}), NAA (10 *n*mol pistil^{-1}) or BA (1 *n*mol pistil^{-1}), in Landsberg *erecta* (L.*er*; top panel), and Columbia ecotypes (Col-1; middle panel). Silique elongation in the *gai-1* background (bottom panel), after emasculation of anthesis stage pistils, and left unpollinated (up), or after cross pollination (p) or NAA treatment (10 *n*mol pistil^{-1}). For estimates of error (± s.d) refer to Table 2.1.

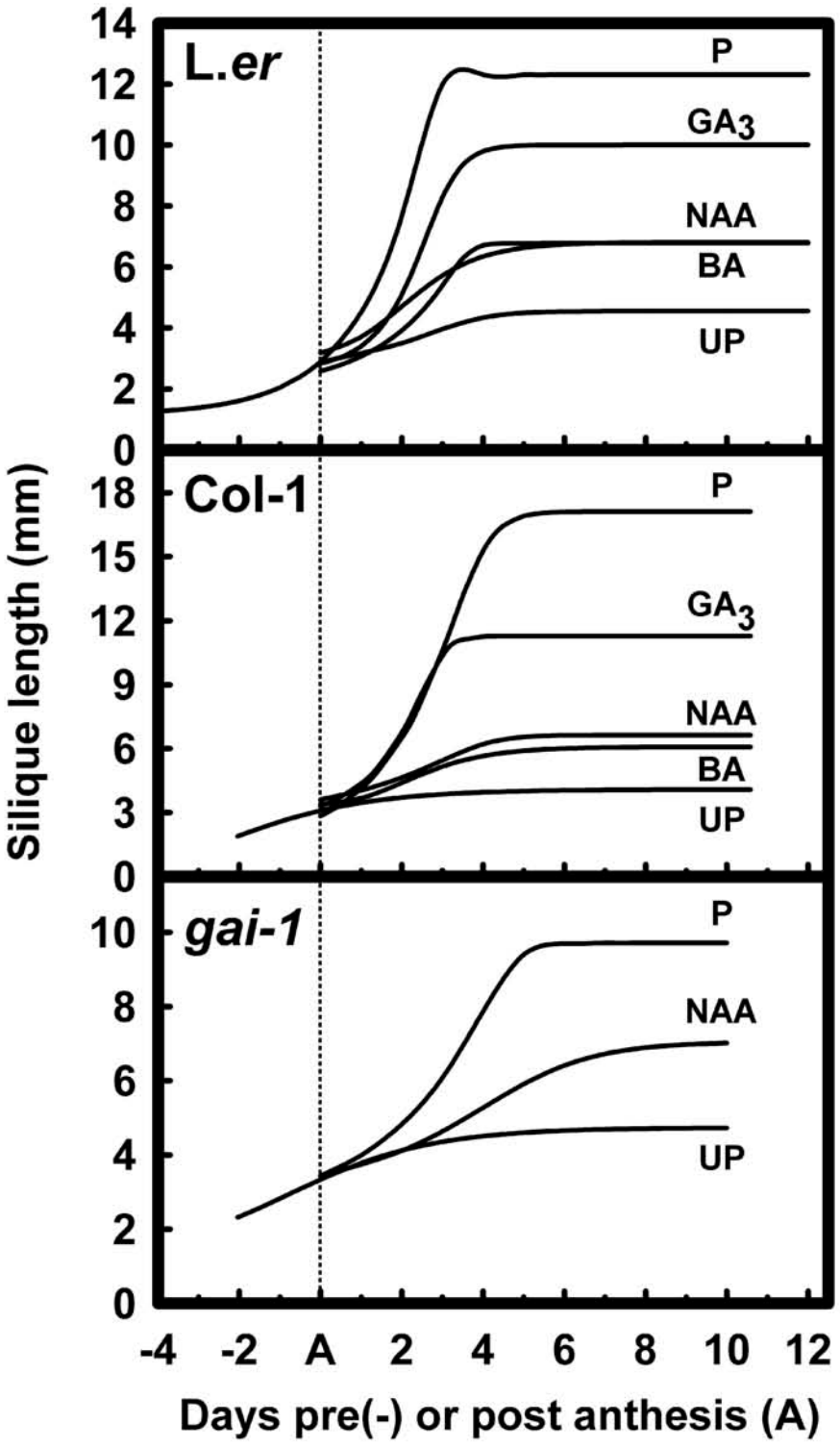
L.er
P
GA3
NAA
BA
UP
Col-1
P
GA3
NAA
BA
UP
gai-1
P
NAA
UP
Silique length (mm)
Days pre(-) or post anthesis (A)
-4
-2
A
2
4
6
8
10
12

ecotypes were comparable with respect to final pollinated silique length, but significantly longer than those of Col-1 *er2* and L.*er* (Table 2.1), indicating that regardless of the ecotype background the *erecta* mutation significantly reduced the ability of pollinated pistils to elongate. The final post-pollination silique length obtained in these backgrounds was comparable to that observed by Torii et al., (1996).

Unpollinated pistils also shed their floral organs, yet they continued to elongate slightly from their normal anthesis length at a considerably reduced rate of growth compared to pollinated siliques (Figure 2.1 top and middle). Unpollinated pistil elongation continued for 3 and 4 DPA in Col-1 and L.*er* ecotypes respectively (Figure 2.1, top and middle), and after 7 DPA, the unfertilized pistils senesced yet failed to dehisce. These pistils had increased in length approximately another one-third to one-half of their original anthesis length (Table 2.1). Therefore, an assessment of unpollinated pistil length at 7 DPA, was used as the baseline to evaluate and compare post-anthesis silique development induced by pollination or PGR application in the different ecotypes. It was noted that the final length attained by unpollinated pistils was ecotype dependent, and also determined by the presence or absence of the *erecta* mutation (Table 2.1).

2.3.2 *Arabidopsis* silique growth responses to PGRs

I compared the parthenocarpic responses of pistils following PGR application in different ecotype backgrounds that either contained or lacked the *erecta* mutation. I used a modified measurement of elongation to discriminate between parthenocarpy and the ability of an unpollinated pistil to slightly elongate. I subtracted the mean anthesis length from the final length attained at 7 DPA and then divided this difference by the mean difference between the anthesis length and unpollinated pistil length. Those pistils that exceeded a two-fold increase in this measure were considered to be parthenocarpic siliques (Table 2.1,

numbers in parentheses). Dehiscence of carpel valves was also used as an indicator of silique maturation.

Auxins (NAA or IAA), cytokinin (BA) and gibberellin (GA_3) applied at anthesis to emasculated pistils stimulated fertilization-independent silique growth in L.*er*, L.*ER*, Col-1 *er2* and Col-1 ecotypes (Table 2.1). The type and amount of PGR applied differentially influenced the magnitude of elongation and the external morphological appearance of the silique as examined at 7 DPA (Figure 2.2). In all cases, however, the extent of PGR induced silique elongation was always significantly lower than that observed in fertilized pistils ($P < 0.05$). Nevertheless, the elongated siliques that formed following auxin and GA_3 treatment matured at 10 DPA and shattered open several days later, indicating carpel valve dehiscence zones were functional. Compared with auxin and GA_3 induced siliques, pollinated siliques matured from 12 DPA. Cytokinin treatment often delayed silique maturation and carpel valve dehiscence compared to pollinated siliques.

Auxin treatments of 10 *n*mol pistil^{-1} NAA or IAA produced parthenocarpic siliques in all the ecotypes tested, except Col-1 *er2*, in which there was no apparent elongation observed following NAA application at 10 *n*mol pistil^{-1} (Figure 2.2 and Table 2.1). In general, the application of auxin at levels below 10 *n*mol pistil^{-1} did not result in significant elongation (Figure 2.2), while auxin levels above 50 *n*mol pistil^{-1} caused pistils to degenerate (not shown). Application of BA at 0.1 *n*mol pistil^{-1} was only effective in inducing parthenocarpic silique elongation in L.*er*, L.*ER* and Col-1 *er2* ecotypes. However, a higher level of BA (1 *n*mol pistil^{-1}) was able to induce parthenocarpy in the Col-1 ecotype. In all ecotypes, BA application below 0.1 *n*mol pistil^{-1} failed to yield a parthenocarpic response, while treatments above 10 *n*mol pistil^{-1} frequently damaged the pistils (Figure 2.2). These results indicated the Col-1 ecotype was least sensitive to auxin and generally less sensitive to BA than Landsberg ecotype (Table 2.1 and Figure 2.2).

Figure 2.2 Siliques 7 days post-anthesis after treatment with IAA, NAA, GA_3 or BA in the L.*er* background (top panel) or Columbia (bottom panel), with respective application levels in *n*mol $pistil^{-1}$ indicated in each panel.

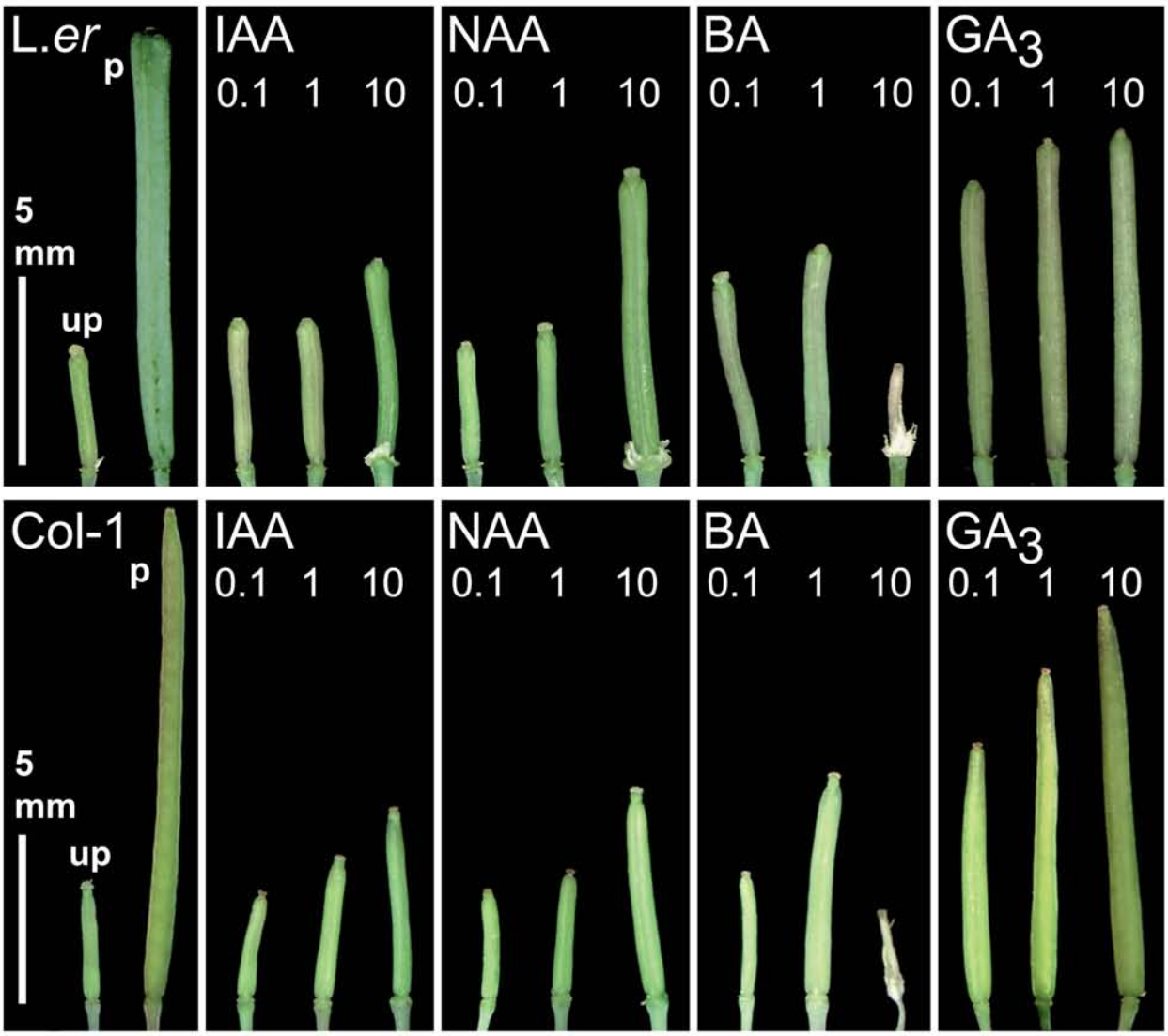
L.er
p
5
mm
up
IAA
0.1 1 10
NAA
0.1 1 10
BA
0.1 1 10
GA3
0.1 1 10
Col-1
p
5
mm
up
IAA
0.1 1 10
NAA
0.1 1 10
BA
0.1 1 10
GA3
0.1 1 10

Treatment of *Arabidopsis* pistils with GA_3 at 10 *n*mol pistil^{-1} was most effective at inducing silique elongation and resulted in the longest siliques at 10 DPA compared with those induced after auxin or cytokinin treatment (Table 2.1 and Figure 2.2). GA_3 was also effective at inducing silique elongation in the presence of the *erecta* mutation, and elongation was evident in both Col-1 and L.*er* ecotypes from levels as low as 10 *p*mol pistil^{-1} (not shown). Elongation of L.*er* and Col-1 pistils following 10 *n*mol pistil^{-1} GA_3 treatment resulted in a growth rate comparable to that observed in pollinated pistils (Figure 2.1 top and middle). Ecotype-specific differences in elongation and outward appearance following GA_3 application were also apparent (Table 2.1 and Figure 2.2). GA_3-treated Col-1 pistils were the most similar to pollinated siliques, even considering pistil elongation was dosage dependent (Table 2.1). In both ecotypes, silique growth following NAA and BA treatment progressed at a slower rate than the GA_3 treatment or fertilized pistils (Figure 2.1 top and middle).

2.3.3 Pistil receptivity to pollen and GA_3 in Col-1 and L.*er* ecotypes

I tested the receptivity period of emasculated pistils to pollination- and GA_3-induced growth by applying pollen or GA_3 on sequential days post-anthesis and then assessing final silique length. Figure 2.3 shows that pistil receptivity to pollen extends from anthesis (stage 13; Bowman 1993) to 3-4 DPA in L.*er* and 3 DPA for Col-1 (Figure 2.3 top and middle). Silique length and seed set declined beyond 4 DPA and once the pistils reached 5 DPA seeds were not set following pollination (Figure 2.3). Pistils were responsive to 10 *n*mol pistil^{-1} GA_3 treatment up to 6 DPA (Figure 2.3), indicating that they were receptive to GA_3 for a significantly longer period of time than they were to pollination.

Figure 2.3 The receptivity period for pollination and GA_3 induced silique elongation was determined by a single treatments of either GA_3 (triangles; 10 *n*mol $pistil^{-1}$) or pollination (circles) to emasculated pistils of *Arabidopsis* at varying days post-anthesis in L.*er* (top panel) and Col-1 ecotypes (middle panel). Seed set (lower panel) was also determined with respect to day pollinated post-anthesis.

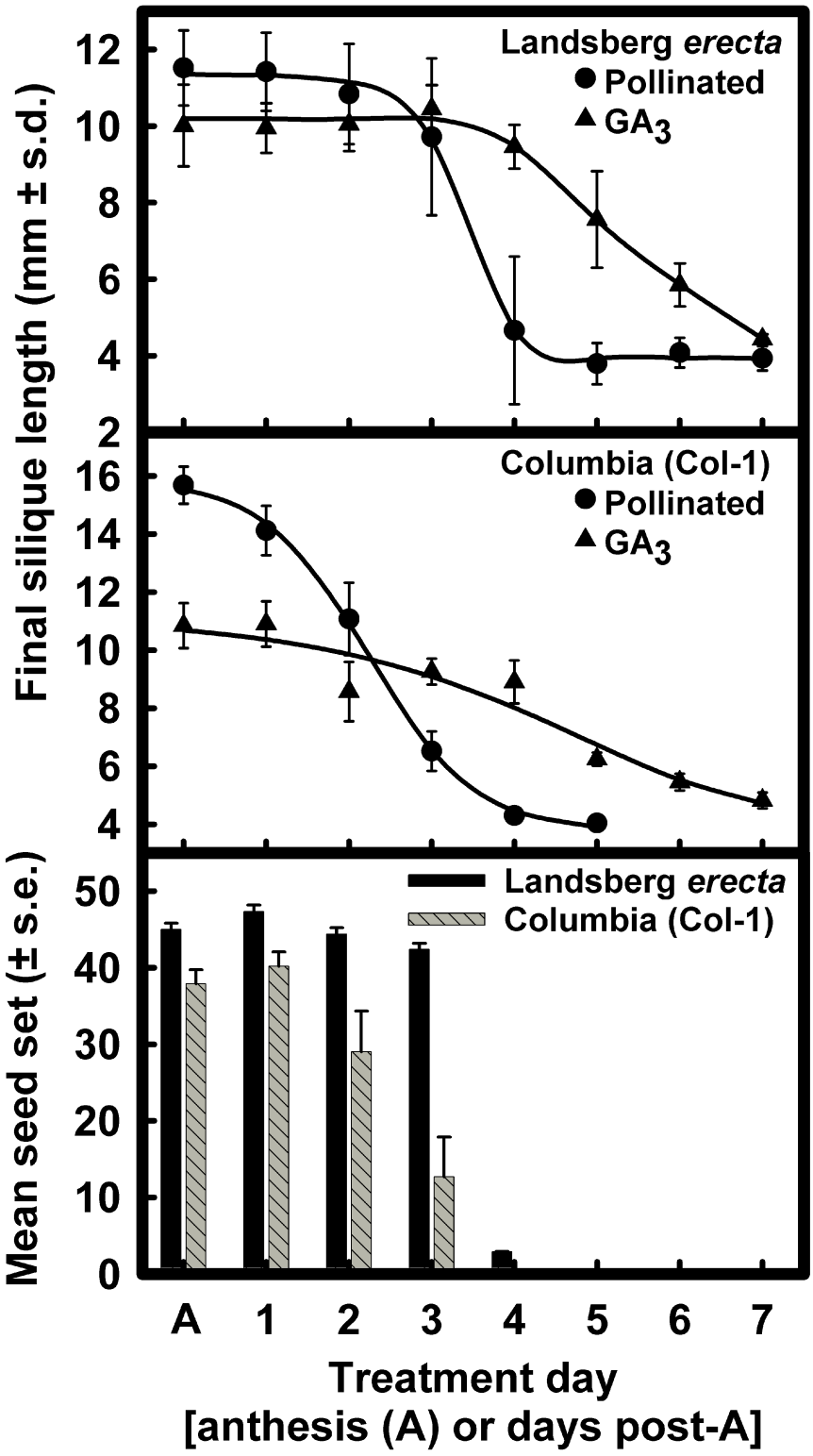
Landsberg erecta
Pollinated
GA3
Columbia (Col-1)
Pollinated
GA3
Final silique length (mm ± s.d.)
Landsberg erecta
Columbia (Col-1)
Mean seed set (± s.e.)
A
1
2
3
4
5
6
7
Treatment day
[anthesis (A) or days post-A]

2.3.4 Analysis of hormone biosynthesis and perception mutants for silique elongation following emasculation

Given that different plant growth regulators stimulate fertilization-independent silique development, various *Arabidopsis* mutants altered in their biosynthesis and perception of hormones were surveyed for silique elongation independent of fertilization. Emasculation of these mutants revealed that they were unable to significantly elongate their siliques over the slight elongation normally observed in unpollinated pistils. These non-parthenocarpic mutants included *amp1-1*, a mutant exhibiting elevated endogenous cytokinin levels; *abi4*, an abscisic acid insensitive mutant; *ctr1-1*, *etr1-3*, *ein2-1*, *ein3-1*, *ein4*, *ein5-1*, *ein6*, *ein7*, ethylene perception mutants; *gar2-1* and *gai-1*, GA perception mutants; *ga1-3*, *ga4-1* and *ga5-1*, GA biosynthesis mutants; and *axr1-3*, *axr2*, *axr4-2* and *aux1-7*, auxin perception mutants. Auxin application (NAA, *n*mol pistil^{-1}) to emasculated auxin-resistant mutants *axr1-3*, *axr2*, and *aux1-7* induced silique elongation (data not shown), indicating that these lesions were independent of auxin-induced parthenocarpy. Additional experiments were carried out with the GA perception mutants *spy-1*, *spy-3*, *spy-4* and *gai-1*; and also the GA biosynthesis mutants *ga1-3*, *ga4-1* and *ga5-1*. These are described in the sections below.

2.3.5 *spy-4* silique development following emasculation and response to PGR application

Jacobsen and Oleszewski, (1993) reported that several alleles of the *SPINDLY* locus exhibit parthenocarpic silique development. I assessed the involvement of *SPINDLY* during growth-regulator-induced parthenocarpy by comparing the elongation response of emasculated *spy-4* pistils with and without PGR application (Figure 2.4 and Table 2.1). Initially the length attained by emasculated *spy-4* pistils was compared with emasculated

Figure 2.4 Siliques from Ws.O ecotype background pollinated (p), unpollinated (up) and treatment with GA_3 (10 *n*mol pistil^{-1}), compared with *spy-4* unpollinated (up), pollinated (p) and after treatment with GA_3, NAA, or BA (10, 10 and 1 *n*mol pistil^{-1} respectively; top panel). *gai-1* and *ga5-1* unpollinated pistils and pollinated siliques (in the L.*er* background; bottom panel) as compared to GA_3, NAA and BA treatment (10, 10 and 1 *n*mol pistil^{-1} respectively), described in materials and methods.

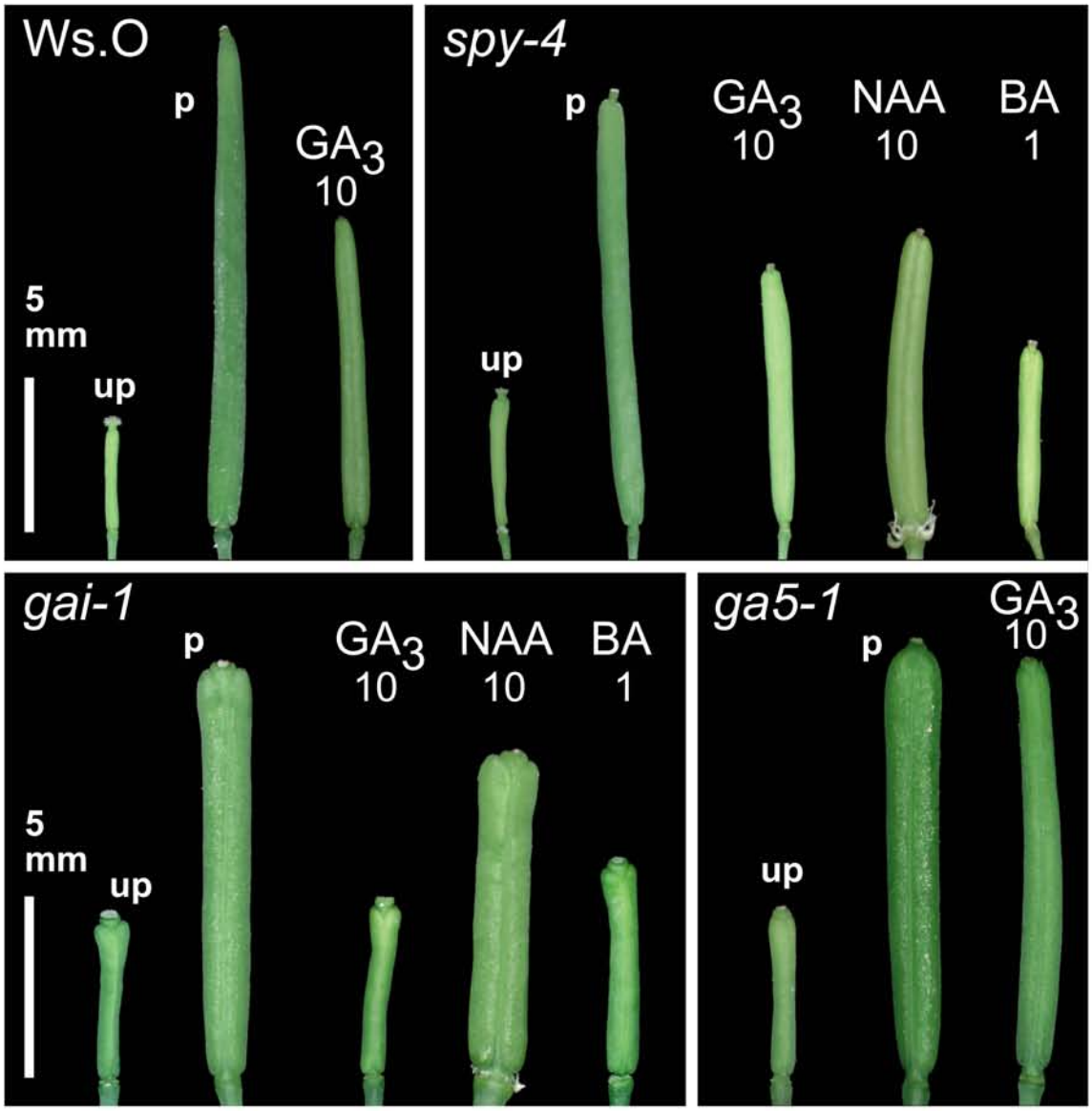
Ws.O
p
GA3
10
5
mm
up
spy-4
p
GA3
10
NAA
10
BA
1
up
gai-1
p
GA3
10
NAA
10
BA
1
5
mm
up
ga5-1
GA3
10
p
up

pistils of Wassilewskija-O (Ws-O), the parental background of the *spy-4* mutation, and I found that emasculated *spy-4* pistils did not significantly elongate further than emasculated Ws-O (Table 2.1 and Figure 2.4). Even though numerous *spy-4* plants were assessed (*n* = 87), parthenocarpic silique elongation was not observed (Figure 2.4 top panel and Table 2.1). Similar results were obtained when *spy-1* and *spy-3* plants were emasculated and examined (*n* = 24 and 18 plants, respectively).

To determine whether there was a difference in the response of emasculated *spy-4* pistils to the perception of various PGRs, I applied GA_3 and NAA at 10 *n*mol pistil^{-1}, and BA at 1 *n*mol pistil^{-1}. GA_3 and NAA application resulted in elongation of siliques (Table 2.1 and Figure 2.4), indicating *spy-4* pistils were able perceive these PGRs in pistil tissues at anthesis. Although *spy-4* pistils responded to these PGRs, emasculated pistils treated with BA did not significantly exceed the length of unpollinated Ws.O pistils at 7 DPA (Table 2.1). Nonetheless, when BA was applied to emasculated *spy-4* they expanded (Figure 2.4). Comparison of the silique length attained from GA_3 treated Ws.O pistils with GA_3 treatment of *spy-4* pistils revealed a slight, in-significant reduction in the capacity to elongate in response to exogenously applied GA_3. Taken together, these results show that under our growth conditions, *spy* alleles do not exhibit parthenocarpy following emasculation and that the *spy-4* allele is responsive to GA_3-induced parthenocarpic silique elongation.

2.3.6 PGR induced silique elongation in the *gai-1* background

Considering that GA application to L.*er* and Col-1 pistils produced the longest siliques with similar outward morphology to pollinated siliques, GA perception during fruit set was further examined by assessing responses of emasculated pistils to PGRs in the gibberellin insensitive mutant background, *gai-1*. The *gai-1* mutant displays repressed

growth and reduced GA responsiveness, caused by a semi-dominant mutation that confers dysfunctional activity to the *GAI* protein (Peng et al., 1997), but does not confer GA deficiency (Talon et al., 1990c).

Initially I found that self-pollinated *gai-1* pistils frequently produced shorter siliques with a higher degree of variability in silique length than that observed in L.*er*, the ecotype background of the *gai-1* mutant allele (Table 2.1). Seed set was also low and variable in self-pollinated *gai-1*. By contrast, *gai-1* siliques following cross-pollination with L.*er* pollen were not significantly different in length and were less variable than *gai-1* siliques following self-pollination (Table 2.1). I interpreted that *gai-1* had defective pollen that decreased seed set and silique elongation. In subsequent experiments, silique growth in *gai-1* pistils was therefore determined following cross-pollination with L.*er* pollen.

Following pollination, siliques of *gai-1* mutants elongated until 5-6 DPA, which was 2-3 day longer than that observed for L.*er* (Figure 2.1 bottom). Comparisons between the top and bottom panel of figure 2.1 show that the difference in elongation period was because pollinated *gai-1* siliques had a reduced growth rate and a significantly reduced mean silique length (Table 2.1). Given that the mean lengths of anthesis stage pistils of *gai-1* and L.*er* were similar (Table 2.1), differences in silique length arose during post-anthesis development. Following pollination, *gai-1* siliques were dehiscent, indicating the development of functional dehiscence zones.

Emasculated *gai-1* pistils would not elongate following application of 10 *n*mol pistil^{-1} GA_3. Unpollinated and GA_3 treated *gai-1* pistils were morphologically alike (Figure 2.4 and Table 2.1) and indehiscent, indicating that GA_3 induced parthenocarpy was blocked in the mutant *gai-1* background. However, silique elongation was still observed following exogenous application of NAA and, to a lesser degree, BA (Figure 2.4 and Table 2.1). NAA treatment also substantially increased silique expansion over that observed following

pollination of *gai-1* pistils (Figure 2.4 bottom left). Comparison of silique elongation in auxin induced *gai-1* pistils to pollinated *gai-1* pistils also revealed that the initiation, the rate and cessation of silique development differed (Figure 2.1, bottom). Therefore, while it appears that normal functional activity of *GAI* is necessary for transducing GA signals, the analysis of the *gai-1* mutant allele indicated this pathway does not appear to be critical for alternative PGR induced parthenocarpic responses.

2.3.7 Structural comparisons of unpollinated, pollinated and induced siliques

Up to this point, parthenocarpic induction had been measured as the ability of a silique to elongate and dehisce. I also compared the structure of anthesis pistils, unpollinated pistils and elongated siliques following pollination or PGR treatment in several mutant backgrounds by histological sectioning.

Arabidopsis gynoecium structure and post-pollination development has been described previously (Gasser and Robinson-Beers, 1993; Gu et al., 1998; Sessions and Zambryski, 1995), but without specific reference to exocarp, mesocarp, supportive sclerenchyma and endocarp development. Figures 2.5 and 2.6 show there are six to seven cell layers associated with the carpel wall, of which four form distinct cell types. The single outer epidermal layer of the carpel differentiates into the exocarp layer of mature siliques. Three to four chlorenchyma or parenchymal cell-type layers develop as the mesocarp layer. A supportive sclerenchymal layer adjoins the innermost mesocarp layer, and an adjacent endodermal layer forms the endocarp that faces into the locule. Cell counts from semi-thin carpel cross sections were used to specifically determine how carpel valves expand in width (Table 2.2). I also determined the cell length, normal to the plane of elongation from longitudinal sections, as shown in Table 2.3. Using the mean cell length

Figure 2.5 Carpel wall cross sections illustrating the degree of carpel expansion and development from an anthesis stage pistil compared with 7 days post-anthesis unpollinated, pollinated, and PGR treated siliques from the *gai-1* and L.*er* backgrounds; (A) L.*er* anthesis stage pistil, (B) L.*er* unpollinated pistil, (C) L.*er* pollinated silique, (D) emasculated pistil induced with 10 *n*mol pistil^{-1} GA_3, (E) L.*er* emasculated pistil induced with 10 *n*mol pistil^{-1} NAA, (F) *gai-1* pollinated silique. Unmarked arrowheads indicate dehiscence zones; f, funiculus; m, mesocarp; n, endocarp; o, ovule; p, septum; r, replum; s, seed; t, supportive sclerenchyma; x, exocarp. 250 μm scale bar.

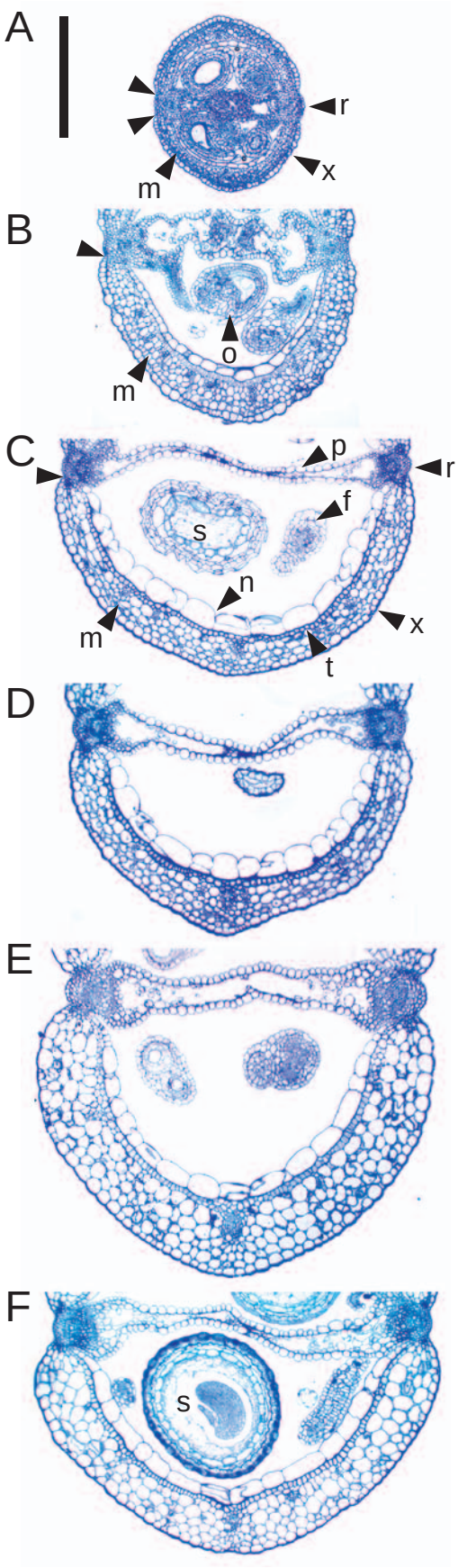
A
r
x
m
B
o
m
C
p
r
f
s
n
m
x
t
D
E
F
s

Figure 2.6. Longitudinal carpel wall sections of L.*er* at (A) anthesis, and 7 days post-anthesis for (B) an unpollinated silique, (C) pollinated silique, and parthenocarpic siliques induced by (D) 10 *n*mol pistil^{-1} GA_3, (E) 1 *n*mol pistil^{-1} BA, (F) 10 *n*mol pistil^{-1} NAA. Silique wall sections of the respective L.*er* treatments in the *gai-1* background (G to L). Carpel wall sections of *spy-4*, (M) anthesis pistil; and 7 days post-anthesis for (N) an unpollinated pistil; (O) pollinated silique; (P) emasculated *spy-4* pistil induced to grow with 10 *n*mol pistil^{-1} GA_3. Rescue of carpel wall structure in the *ga5-1* biosynthetic mutant, (Q) 7 day pollinated *ga5-1* silique, (R) *ga5-1* parthenocarpic silique induced with 10 *n*mol pistil^{-1} GA_3. e, endocarp; f, funiculus; o, ovule; m, mesocarp; t, supportive sclerenchyma; x, exocarp. 100 μm scale bar.

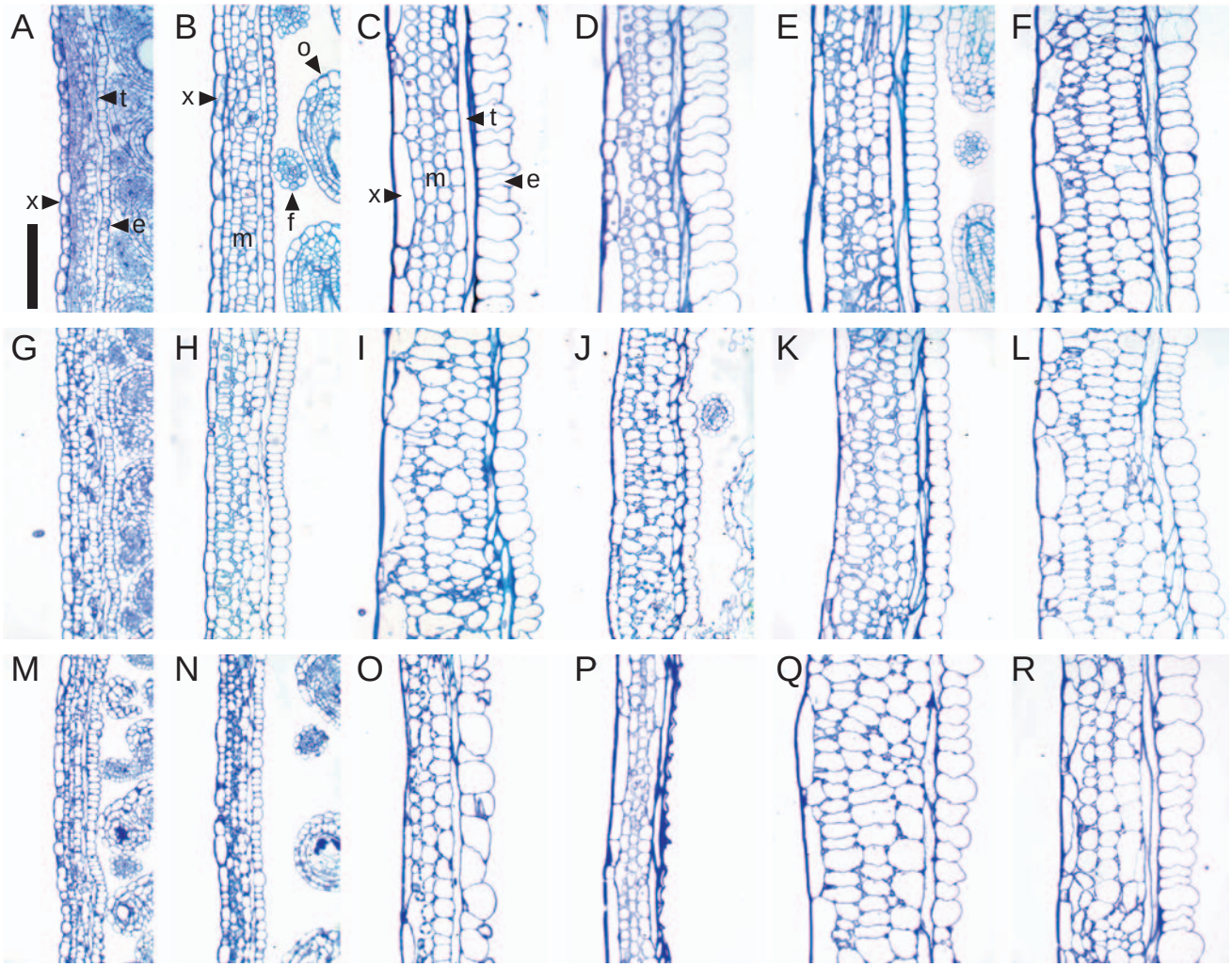
A
t
x
e
B
o
x
f
m
C
t
x
m
e
D
E
F
G
H
I
J
K
L
M
N
O
P
Q
R

Table 2.2 Comparison of cell number in cross-sections of different *Arabidopsis* carpels at anthesis and 7 day post-anthesis.

		Carpel cell number per tissue type (± s.d.)		
Treatment	**Day post-anthesis**	Exocarp	Mesocarp	Endocarp
anthesis	0	81 ± 18.5	177 ± 5.0	25.3 ± 5.0
L.*er* unpollinated	7	82 ± 10.6	171 ± 33	28.0 ± 8.7
L.*er* + pollination	7	79 ± 10.6	167 ± 7.0	32.7 ± 12.2
L.*er* + 10 *n*mol^{-1} pistil GA_3	7	69 ± 2.3	154 ± 6.9	23.3 ± 4.2
L.*er* + 10 *n*mol^{-1} pistil NAA	7	67 ± 8.1	180 ±17.8	24.0 ± 6.9
gai-1 + pollination	7	67 ± 11.7	149 ± 7.6	20.7 ± 1.2
ga5-1 + pollination	7	67 ± 10.0	131 ± 18.1	20.0 ± 4.3

for a given cell type, the total cell number was calculated for the length of a silique for a single longitudinal lateral section (Table 2.4).

Our observations of cross sections showed that the increase in the carpel width of unpollinated pistils and mature, pollination-induced siliques was entirely due to cellular expansion in all of the component tissues (Table 2.2 and Figure 2.5). This was because cell numbers in each tissue post-anthesis were not significantly greater than the mean number present in cross sections of anthesis pistils (Table 2.2). This indicates that the number of cells in a given cross section of a mature silique is determined prior to anthesis and remains static during silique formation. Therefore pollination and fertilization directly influence the degree of cell expansion in this plane, as pollinated pistils expanded far more than 7 day unpollinated pistils (Figure 2.5).

The length of unpollinated pistils increased slightly post-anthesis because cell length normal to the plane of elongation increased in the exocarp and endocarp layers (Table 2.3). However, the cell number per longitudinal section remained similar to anthesis pistils (Table 2.4). Endocarp and exocarp were composed of relatively uniform cells (Figures 2.5B and 2.6B). Mesocarp cells remained similar in length to anthesis pistils, but their numbers were greater than those observed in anthesis stage pistils (Table 2.3 and 2.4). This indicated that some cellular division occurred in the mesocarp cell layer. In contrast to mature siliques (Figures 2.5C and 2.6C), the secondary wall thickening of sclerenchyma cells and development of mature senescent zones were characteristically absent in unpollinated pistils (Figures 2.5B and 2.6B).

Pollination induced a significant increase in cell division and length normal to the plane of elongation, in specific tissue layers (Table 2.3). Unlike the unpollinated pistils, the exocarp of pollinated siliques was composed of cells varying in length (Figure 2.6C). The number of exocarp cells was increased slightly, as compared to that observed at anthesis

Table 2.3 Comparison of the mean cell length (μm ± s.d.), normal to the silique elongation axis, in *Arabidopsis* carpel tissue layers from anthesis and 7 day post-anthesis pollinated or PGR treated pistils.

	Stage of silique development and treatment type (Mean silique length for each treatment)							
Tissue	Anthesis (2.8 ± 0.2)	L*er* UP[a] (4.1 ± 0.4)	L*er* +P[b] (11.5 ± 1.0)	L*er* +GA_3[c] (10.0 ± 1.1)	L*er* +NAA[d] (6.8 ± 0.8)	*gai-1* +P[b] (9.5 ± 1.2)	*ga5-1*+P[b] (10.5 ± 1.0)	*ga5-1* +GA_3[c] (10.0 ± 1.1)
Exocarp	15 ± 8	28 ± 15	49 ± 32	82 ± 48	59 ± 24	46 ± 41	67 ± 42	60 ± 33
Mesocarp 1[e]	10 ± 4	11 ± 4	13 ± 5	13 ± 3	16 ± 6	20 ± 6	19 ± 5	20 ± 6
Mesocarp 2[e]	11 ± 3	11 ± 3	12 ± 3	17 ± 4	13 ± 5	20 ± 6	23 ± 6	18 ± 7
Mesocarp 3[e]	11 ± 4	14 ± 5	21 ± 8	17 ± 7	17 ± 6	29 ± 10	26 ± 8	30 ± 10
Endocarp	7 ± 2	13 ± 3	22 ± 6	20 ± 7	20 ± 7	28 ± 7	28 ± 8	24 ± 8

[a] UP, unpollinated; [b] P pollinated; [c] 10 *n*mol pistil^{-1} GA_3; [d] 10 *n*mol pistil^{-1} NAA; [e] Mesocarp 1 relates to mesocarp cells adjacent to the exocarp, mesocarp 2 cells bounded by other mesocarp cells and mesocarp 3, cells adjacent to the sclerenchyma layer.

Table 2.4 Comparison of the mean cell numbers (± s.e.), in longitudinal sections of *Arabidopsis* carpel tissues from anthesis and 7 day post-anthesis pollinated or PGR treated pistils.

	Stage of silique development and treatment type (Silique length for each treatment)							
Tissue	Anthesis (2.8 ± 0.2)	L*er* UP[a] (4.1 ± 0.4)	L*er* +P[b] (11.5 ± 1.0)	L*er* +GA_3[c] (10.0 ± 1.1)	L*er* +NAA[d] (6.8 ± 0.8)	*gai-1* +P[b] (9.5 ± 1.2)	*ga5-1*+P[b] (10.5 ± 1.0)	*ga5-1* +GA_3[c] (10.0 ± 1.1)
Exocarp	227 ± 20	196 ± 23	277 ± 26	176 ± 38	133 ± 13	241 ± 33	223 ± 26	232 ± 29
Mesocarp 1[e]	315 ± 17	396 ± 15	951 ± 41	788 ± 28	494 ± 25	440 ± 28	609 ± 18	567 ± 35
Mesocarp 2[e]	287 ± 12	389 ± 11	983 ± 34	642 ± 24	601 ± 28	437 ± 23	489 ± 14	623 ± 21
Mesocarp 3[e]	289 ± 19	326 ± 17	617 ± 30	664 ± 34	493 ± 22	306 ± 13	446 ± 16	440 ± 20
Endocarp	420 ± 19	351 ± 14	556 ± 28	560 ± 25	420 ± 35	303 ± 16	415 ± 18	450 ± 20

[a] UP, unpollinated; [b] P pollinated; [c] 10 *n*mol $pistil^{-1}GA_3$; [d] 10 *n*mol $pistil^{-1}$ NAA; [e] Mesocarp 1 relates to mesocarp cells adjacent to the exocarp, mesocarp 2 cells bounded by other mesocarp cells and mesocarp 3, cells adjacent to the sclerenchyma layer.

(Table 2.4). I inferred exocarp cells predominantly expand post-pollination. Mesocarp cells were separated into three layers to analyze cell length and number normal to the plane of elongation (Table 2.4). Cells adjacent to the exocarp were designated mesocarp 1, cells bounded by other mesocarp cells, mesocarp 2, and cells adjacent to the sclerenchyma layer, mesocarp 3. Mesocarp 1 and mesocarp 2 cells from mature siliques post-pollination were wider (Figures 2.5C and 2.6C) and longer than those observed in both unpollinated and anthesis stage pistils (Table 2.3). Mesocarp 3 cells in mature siliques were twice their original anthesis length (Table 2.3). Cell number for all mesocarp layers in this longitudinal section increased approximately 3-fold over the number present at anthesis (Table 2.4).

The number of endocarp cells, normal to the plane of elongation, increased almost two-fold after pollination (Table 2.4). These cells increased in length (Table 2.3) and in width by expanding into the carpel locule space (Figures 2.5C and 2.6C). During silique development following pollination, vascular differentiation also occurred in the replum, and also in the medial and lateral bundles of the carpel valve. Fully developed carpel valves were demarcated by mature dehiscence zones, subadjacent to the replum (Figure 2.5C, unmarked arrowheads).

I found that GA_3 treatment of unfertilized pistils induced differentiation analogous to mature pollinated siliques (Figures 2.5D and 2.6D). This was illustrated by similar cell numbers (Tables 2.2 and 2.4) and the degree of cellular elongation in each layer (Table 2.3), except in the mesocarp, where cell number was slightly reduced compared with pollinated siliques following GA_3 treatment (Table 2.4). Structural comparison of auxin induced siliques and pollinated pistils indicated gross cellular expansion primarily in the exocarp and mesocarp cell layers (Figures 2.5E and 2.6F). This resulted in increased silique wall width and only a small increase in cell length perpendicular to the plane of

elongation (Table 2.3). Generally, cell numbers normal to the plane of elongation, in the mesocarp and endocarp of auxin treated siliques were more similar to unpollinated siliques than the GA_3 treated or pollinated pistils (Figure 2.5E and 2.6F; Table 2.3 and 2.4). NAA induced siliques also displayed less secondary wall deposition in sclerenchyma cells and the endocarp cells had reduced expansion into the carpel locule. Siliques forming following auxin and cytokinin treatment frequently contained four mesocarp cell layers (Figure 2.5E, 2.6E and 2.6F).

2.3.8 Silique structure in GA perception mutants

Carpel valve structure was examined in *gai-1* and *spy-4* mutants following pollination and PGR application. Gross cellular expansion was observed in the exocarp and mesocarp cell layers of pollinated *gai-1* siliques (Figures 2.5F and 2.6I). This was similar to that observed following auxin treatment to unfertilized L.*er* pistils (Figure 2.6F). Closer inspection indicated that the mesocarp and endocarp cells of pollinated *gai-1* (Figure 2.6I) were longer than those of pollinated L.*er* or NAA treated pistils (Table 2.3). Furthermore, their cell number, normal to the plane of elongation, was essentially the same as L.*er* unpollinated siliques (Table 2.3). Therefore *gai-1* silique elongation following pollination occurred principally by cellular expansion with minimal cell division. This was not a result of cross-pollination with L.*er* pollen, because self-pollinated *gai-1* silique structure was comparable (data not shown).

Treatment of *gai-1* pistils with GA_3, failed to stimulate elongation and the pistils resembled unfertilized pistils (Figure 2.4). Following sectioning, I also observed that a small amount of mesocarp expansion and increased secondary thickening in sclerenchyma occurred in GA treated *gai-1* pistils (Figure 2.6J), indicating minimal differentiation. Treatment of emasculated *gai-1* pistils with BA and NAA (Figures 2.6K and 2.6L,

respectively) produced carpel valves with structures similar to that observed following application of these hormones to emasculated L.*er* pistils.

I also examined *spy-4* silique structure after pollination or treatment with GA_3 (Figures 2.6M-P). Both unpollinated pistils and pollinated *spy-4* siliques displayed a slender carpel valve phenotype and small mesocarp cells (Figures 2.6N and 2.6O), compared with the respective treatment in L.*er* and *gai-1* siliques. Like unpollinated L.*er* pistils, unpollinated *spy-4* pistils remained undifferentiated (Figure 2.6N). Furthermore, parthenocarpic *spy-4* siliques induced by GA_3 treatment, had extreme reduction in mesocarp cell size and the endocarp cells failed to form normally (Figure 2.6P). These results may be a function of the Ws-O background in *spy-4* plants and requires further investigation to exclude ecotype-specific responses.

2.3.9 Analysis of silique structure in GA biosynthetic mutants after pollination or PGR treatment

The dependency of silique elongation on endogenous levels of GA was examined by comparing unpollinated and post-pollination silique structures in the GA biosynthesis mutants *ga4-1* and *ga5-1*. Both mutants examined were in the L.*er* background. *ga4-1* is blocked in the 3β-hydroxylation step of GA_{20} to GA_1 and also GA_9 to GA_4 (Chiang et al., 1995; Figure 2.7). The *ga5-1* mutant is impaired at the 20-oxidation step but is still responsive to exogenous GA_3, as is *ga4-1* in shoots and rosettes (Talon et al., 1990b; Figure 2.7). Both *ga4-1* and *ga5-1* mutants have reduced levels of endogenous active GA_4 and GA_1 (Talon et al., 1990b). The 20-oxidase encoded by *GA5* has also been shown to be regulated by both *GAI* and *SPY* (Peng et al., 1997; Xu et al., 1995; Figure 2.7).

The structure of unpollinated and pollinated *ga4-1* siliques (data not shown) resembled unpollinated pistils and pollinated siliques of L.*er* (Figures 2.6B and 2.6C,

Figure 2.7 Model for how biosynthesis and perception of GAs determine silique structure in *Arabidopsis*. Signals from fertilization allow cell division, cell expansion and differentiation during development. This may include activation of certain steps within the GA signal transduction cascade for normal differentiation. Levels of active GAs (GA_1, GA_3 or GA_4) would specifically limit cell division and the biosynthetic mutants (italics) would block or alter this process. One exception occurs at *GA4*, where other known 3ß-hydrolyases may allow synthesis of active GAs. Also on the basis of mutant analysis, *GAI* may participate in GA perception by transducing signals that regulate cell division. a) At high GA levels cells develop like normal pollinated siliques; b) at low levels of active GA the auxin-like effect dominates with limited cellular division; and c) at very low levels of GA, siliques are blocked in differentiation. The steps in GA biosynthesis between *ent*-copalyl diphosphate and GA_{19} or GA_{24} are abbreviated for simplicity. Other steps are detailed in Hedden and Kamiya (1997) or Sponsel et al., (1997). e, endocarp; m, mesocarp; x, exocarp.

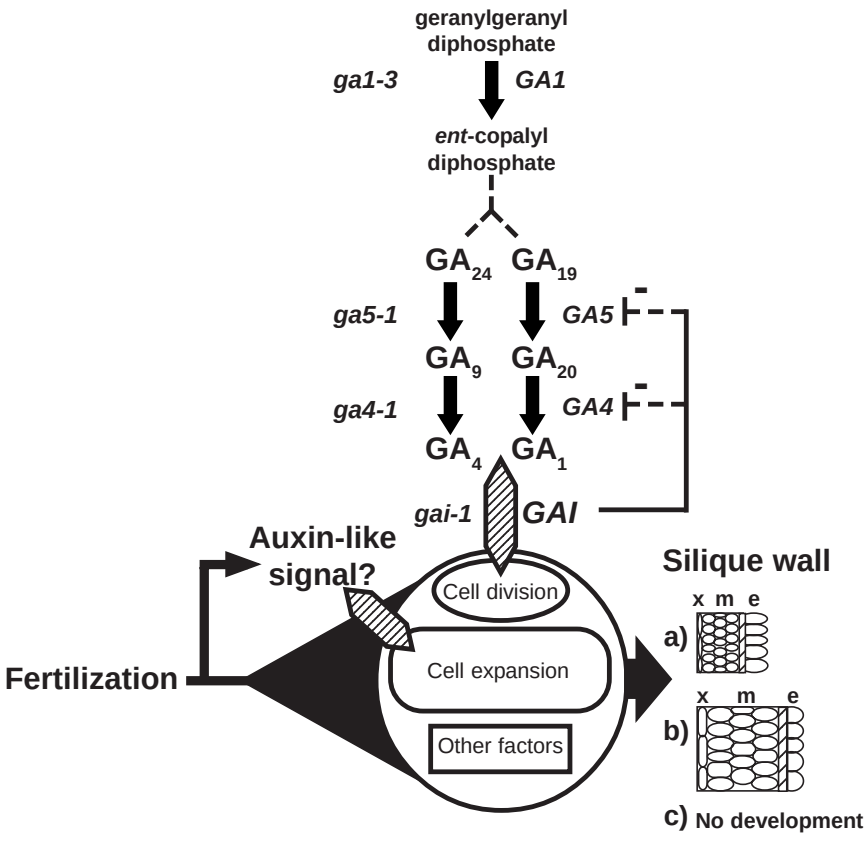
geranylgeranyl diphosphate
ga1-3
GA1
ent-copalyl diphosphate
GA24
GA19
ga5-1
GA5
GA9
GA20
ga4-1
GA4
GA4
GA1
gai-1
GAI
Auxin-like signal?
Fertilization
Cell division
Cell expansion
Other factors
Silique wall
x m e
a)
x m e
b)
c) No development

respectively). By contrast, pollinated *ga5-1* siliques (Figure 2.4, bottom right and Figure 2.6Q) exhibited a carpel valve phenotype similar to pollinated *gai-1* siliques and also to parthenocarpic siliques obtained from NAA treatment of L.*er* pistils. Cell length in mesocarp and endocarp was similar in both *ga5-1* and *gai-1* siliques post-pollination (Table 2.3). However, unlike *gai-1*, parthenocarpic silique elongation was induced in *ga5-1* following GA_3 application (Figure 2.4, bottom right), and carpel valve structure following this treatment was similar to that observed in L.*er* siliques following pollination (Figure 2.6R and Table 2.3). This indicates that appropriate levels of endogenously active GAs are required for normal carpel development post-pollination in L.*er* and that the GA response in *gai-1* was blocked.

I have shown that parthenocarpic silique development was induced in both *spy-4* and *gai-1* following application of auxin. However, *ga1-3* mutants that lack normal functional *ent*-copalyl diphosphate synthase (Figure 2.7), an enzyme that catalyzes the first committed step in the GA biosynthesis pathway (Sun and Kamiya, 1994), did not produce parthenocarpic siliques after auxin application (1 and 10 *n*mol NAA $pistil^{-1}$; data not shown). This indicates that the alternate parthenocarpy pathway induced by NAA is only active if the early steps in endogenous GA biosynthesis are correctly maintained.

2.4 Discussion

Pollination and subsequent double fertilization events in the carpel induce a coordinated sequence of cell division, cell expansion and cell differentiation events that result in mature fruit and seed structures. The nature and sequence of the signals that stimulate or limit these processes are unknown. In the absence of fertilization, *Arabidopsis* pistils treated with gibberellin, auxin and cytokinin produced parthenocarpic siliques that varied in length and morphology depending on the ecotype and the growth regulator

applied. The ability to induce silique growth with different classes of PGR indicates that *Arabidopsis* pistils are receptive to a variety of hormonal signals that can subsequently promote parthenocarpic growth and thus uncouple silique growth from the normally linked process of seed development.

Structural differences between fertilization-induced fruit and various PGR-induced parthenocarpic fruit have also been observed in tomatoes (Bünger-Kibler and Bangerth, 1982), blueberry (Cano-Medrano and Darnell, 1997), rape (Srinivasan and Morgan, 1996), *Citrus* (Guardiola et al., 1993), watermelon (Sedgley et al., 1977) and pea (Vercher and Carbonell, 1991; Vercher et al., 1987). In *Arabidopsis*, the application of a single PGR could not reproduce the exact silique length, shape and growth rate observed following pollination. However, application of GA_3 at 10 *n*mol pistil^{-1} gave the greatest silique elongation and most similar structural development compared with pollination-induced siliques.

The shorter silique length following GA application in *Arabidopsis* may reflect the lack of seeds that may physically add to the gross structural arrangement of the silique, as was observed in *Brassica napus* (Srinivasan and Morgan, 1996). It is conceivable that the *Arabidopsis* seeds also contribute morphogenic molecules that influence maternal carpel tissue development as has been suggested for other species (Denny, 1992). Comparable post-pollination silique length in *Arabidopsis* might be obtained following repeated PGR application or combinations PGRs, as observed in *Brassica napus* (Srinivasan and Morgan, 1996) and pea (van Huizen et al., 1997).

GA_3 primarily influenced mesocarp cell division in a manner similar to that observed following pollination in *Arabidopsis*. By contrast, gross mesocarp and exocarp cell enlargement occurred following auxin treatment in *Arabidopsis*. In tomato, GA_3 treatment has been observed to induce mesocarp cell expansion with restricted cellular

division while auxin treatment stimulated cell division (Bünger-Kibler and Bangerth, 1982). PGR-induced parthenocarpy in *Arabidopsis* was also different to that observed in the related crucifer *Brassica napus*, where GA_3 induced cellular expansion in mesocarp tissues (Srinivasan and Morgan, 1996).

Taken together, these observations demonstrate that while pollination-independent fruit development can occur following PGR application in some species, a particular PGR can induce cell division in the fruit tissue of one species but produce cell enlargement during fruit development in another. The potential to successfully induce parthenocarpic fruit development with PGRs may reflect the status of the carpel with respect to the developmental potential for cell division, expansion and cell differentiation processes at the time of growth regulator application. Therefore, endogenous hormone synthesis and the perception of an endogenous hormone or exogenously applied PGR in a particular tissue are likely to be key factors in hormone-induced parthenocarpy.

2.4.1 GA biosynthesis and parthenocarpic silique development in *Arabidopsis*

Barendse et al., (1986) determined that GAs and other additional maternally derived factors were essential for post-pollination silique development in *Arabidopsis*. Here I have shown that exogenous GA application stimulates parthenocarpic silique development, producing siliques with a structure most similar to siliques derived post-pollination. How does the biosynthesis of GAs determine parthenocarpic fruit growth and what are the critical steps in the GA biosynthesis pathway that affect parthenocarpic silique development?

To address these questions, I examined parthenocarpic silique development in various GA biosynthesis mutants showing reduced endogenous GAs in shoots (Talon et al., 1990b). Figure 2.7 shows the mutants examined in relation to their role in the known GA

biosynthetic pathway in *Arabidopsis*. *ga1-3* mutants lack functional *ent*-copalyl diphosphate synthase (Sun and Kamiya, 1994; Figure 2.7), and produce very low levels of active GAs (Hedden and Kamiya, 1997). Barendse et al., (1986) showed that these mutants have an absolute requirement for exogenous GA to produce siliques following fertilization and I found *ga1-3* mutants do not produce parthenocarpic siliques following NAA treatment, indicating that a threshold of endogenous biosynthesis of GAs is an essential component for both parthenocarpic and pollination-induced silique development (Figure 2.7). This is supported by the observation that *spy* mutants partially rescue the *ga1-3* phenotype (Jacobsen and Oleszewski, 1993; Silverstone et al., 1997b) by possibly elevating the basal response level that would normally be suppressed in wild type plants (Jacobsen and Oleszewski, 1993), thus avoiding sub-threshold levels of GA biosynthesis that would prevent a variety of essential processes.

The *ga4-1* mutant is blocked in the 3-β-hydroxylation of GA_{20} to GA_1 or GA_9 to GA_4, a final step in yielding active GAs (Chiang et al., 1995; Talon et al., 1990b; Figure 2.7). Levels of GA_1 and GA_4 observed in this mutant are three-fold lower than L.*er* (Talon et al., 1990b). Following pollination, the silique walls of the *ga4-1* mutant were similar in structure to that of pollinated L.*er*. This could mean that the lower level of active GAs in the *ga4-1* mutant can sustain structural development of the pollinated silique (Figure 2.7), which would agree with our observations that parthenocarpy can be induced in *Arabidopsis* with low levels of GA_3. Products from the recently identified *GA4H* gene (Yamaguchi et al., 1998) which has similarity to the *GA4* gene can catalyze the 3ß-hydroxylation of GA_{20} to GA_1 and may contribute to the active GA levels in *ga4-1*. Alternatively, g*a4-1* mutants may not block the synthesis of all biologically active GAs (Sponsel et al., 1997). Thus *GA4-1* may not be a critical determinant of silique development in *Arabidopsis* because of its functional redundancy.

GA5-1 is one of three 20-oxidase cDNAs thought to encode a stem specific isoform that can catalyze several steps in GA biosynthesis including the conversion of GA_{24} to GA_9 and their 13-hydroxylated counterparts, GA_{19} to GA_{20} (Phillips et al., 1995; Sponsel et al., 1997; Figure 2.7). Xu et al., (1995) and Talon et al., (1990b) have confirmed that the mutant has low levels of active GA_1 and GA_4 compared to L.*er*. Sponsel et al., (1997) observed that the *ga5-1* mutant had slightly smaller siliques following fertilization (8.3 ± 0.3mm) and suggested the low levels of GA 20-oxidase activity were responsible for the short silique phenotype. In the present study, there was no significant difference in length between pollinated *ga5-1* and pollinated L.*er* siliques or after GA_3-induced parthenocarpy in the *ga5-1* mutant (Table 2.1), but there were visible differences in carpel valve structure. Pollination of *ga5-1* pistils resulted in reduced mesocarp cell division and increased mesocarp cell expansion, resembling aspects of NAA-induced parthenocarpy. By contrast, parthenocarpic silique structure following emasculation and GA_3 treatment in *ga5-1* was identical to the normal structure of pollinated L.*er*. The act of pollination coupled with lower active GA levels in *ga5-1*, resulted in altered mesocarp structure, indicating that endogenous GAs limit cell division and structural differentiation of specific silique tissues (Figure 2.7).

It is possible that fertilization induces an auxin-like signal in the pistil (O'Neill and Nadeau, 1997) and this signal is in turn regulated in the mesocarp by an appropriate level of GA, resulting in the observed silique development in wild type plants (Figure 2.7). Regulation of GA 20-oxidase activity and mRNA levels during pea pod growth by both auxin and GA_3 has been previously reported (García-Martínez et al., 1997; van Huizen et al., 1997; van Huizen et al., 1995). Recent double mutant analysis of *ga5-2 ga6-2* by Sponsel et al., (1997) supports that sub-threshold levels of biologically active GAs severely limit silique development. Therefore, development may proceed if there are sub-optimal

levels of active GA in *Arabidopsis* mesocarp, as in the *ga5-1* mutant, but the auxin-like effect would dominate resulting in greater cellular expansion and an alteration in mesocarp structure (Figure 2.7).

The GA biosynthesis mutants show that a basal level of endogenous GA activity is essential for parthenocarpic silique development, that subtle alterations in GA biosynthesis can lead to changes in differentiation of specific silique tissues, and that while GAs are critical for silique development they do not appear to be the sole endogenous developmental cue.

2.4.2 GA perception and parthenocarpic silique development

Endogenous synthesis of GA is important in maintaining silique development post-pollination. I have also demonstrated exogenous GA_3 application can stimulate parthenocarpic silique development, indicating exogenous GA_3 is perceived in addition to endogenously synthesized GA. *GAI* is important for perception of GA (Koornneef et al., 1985; Figure 2.7). Active GA_1 levels in the *gai-1* mutant are 27 times greater than the normally observed levels in L.*er* (Talon et al., 1990c). Therefore, in contrast to the GA biosynthesis mutants, active GAs are overabundant in *gai-1*. This is perhaps because transcript levels of *GA4* and *GA5* genes are upregulated and allow higher levels of GA biosynthesis (Cowling et al., 1998; Peng et al., 1997). Experimental evidence indicates that *GAI* appears to regulate transcription of the 20-oxidase, encoded by *GA5,* in a manner that represses transcript levels when endogenously active GAs are sufficiently present (Cowling et al., 1998; Peng et al., 1997). Thus *GAI* functions as a GA derepressable modulator of plant growth (Peng et al., 1997). *GAI* encodes a protein that appears to be a nuclear encoded transcriptional coactivator that is similar to the *Arabidopsis SCARECROW* and *RGA* genes (Silverstone et al., 1998). I utilized the *gai-1* mutant allele that encodes an

altered product lacking 17 amino acids, a domain critical for GA response and repression (Peng et al., 1997).

Contrary to previous findings (Koornneef et al., 1985), I have found that the *gai-1* mutation does extend to the floral unit because parthenocarpic silique growth was blocked when *gai-1* mutants were treated with GA_3. However, silique development was not blocked following pollination, and parthenocarpy was also triggered in this mutant following auxin and cytokinin treatment. Silique growth in pollinated *gai-1* plants proceeded primarily by cell expansion and resembled auxin-induced parthenocarpic siliques. A post-pollination auxin-like signal, that acts independently of GA perception may explain the cellular expansion phenotype (Figure 2.7) because the *gai-1* mutant may be blocked in one or more down stream processes required for mediating correct structural development post-pollination.

spy mutants display a phenotype similar to plants repeatedly exposed to GA (Jacobsen and Oleszewski, 1993) and the *spy-4* allele is completely epistatic to *gai-1* (Jacobsen et al., 1996). There is some debate whether *SPY* activates or deactivates *GAI* and *RGA* in *Arabidopsis* (Silverstone et al., 1998), which could affect *GA4* and *GA5* transcription levels. *spy* mutants were reported as parthenocarpic (Jacobsen and Oleszewski, 1993), but I found *spy-4* did not exhibit parthenocarpic silique elongation and differentiation when left unpollinated. Emasculated *spy-4* pistils did, however, respond to GA_3 treatment, in that they had even smaller mesocarp cells than pollination-induced siliques. Control points other than *SPY* may allow exogenously induced GA_3 parthenocarpy in *Arabidopsis* to proceed.

2.4.3 *Arabidopsis* can be used to elucidate the molecular basis of parthenocarpy

In this study I have described roles for GA biosynthesis and perception during *Arabidopsis* silique development. I observed that application of a range of PGRs can induce parthenocarpic silique development with various structural differentiation. Analysis of GA mutants indicate that active GAs and their perception can limit or stimulate cell division and differentiation in *Arabidopsis* carpels (Figure 2.7). However, *gai-1* mutants appear to have dependencies on alternative endogenous signals that allow pollination- and auxin-induced silique development to occur. Perhaps in one of several steps activated post-fertilization, *GAI* functions to balance signals from GA and other sources (Figure 2.7). The possibility of fertilization-stimulated auxin-like cues for silique development and cellular expansion could be investigated using appropriate perception mutants or hormone-induced genetic elements.

Experimental evidence indicates that ethylene and auxin do play a significant part during pollinated ovary development and senescence of unpollinated pistils (Komori et al., 1997; O'Neill and Nadeau, 1997; O'Neill et al., 1993), but empirical evidence is required for understanding interaction of ethylene perception. Appropriate mutagenesis screens in *Arabidopsis* should identify mutants that are parthenocarpic and can elongate siliques in the absence of fertilization. A basis for such a screen would be similar to those conducted to identify mutants exhibiting components of apomixis (Chaudhury et al., 1997; Ohad et al., 1996) except that plants producing seedless siliques would be examined. This approach could clarify the roles of endogenous hormones during the initiation of fruit development and may also aid in the elucidation of the molecular basis of parthenocarpy.

Chapter 3: Characterization of seedless silique development in the parthenocarpic *Arabidopsis* mutant *fruit without fertilization* (*fwf*)

3.1 Introduction

In flowering plants seed and fruit formation are usually coordinated developmental processes that occur after fertilization (Figure 3.1). This occurs in the ovule, a female gamete forming structure located within the carpel of the flower (Figure 3.1). Following fertilization the ovule develops into a seed and the carpel of the flower differentiates into a fruit that protects and nourishes the developing seed often aiding in its dispersal. The events of fruit and seed development are uncoupled during parthenocarpic fruit development where a fruit forms in the absence of fertilization and seed formation. Parthenocarpy is genetically controlled in tomato (Vardy et al., 1989a; Vardy et al., 1989b), banana (Ortiz and Vuylsteke, 1995) and cucumber (Rudich et al., 1977) and can also be induced in a large number of horticultural species following the application of growth regulators to unfertilized pistils (Schwabe and Mills, 1981). Information concerning the molecular events that trigger and sustain parthenocarpic development would contribute towards our understanding of the processes that initiate fruit formation.

Arabidopsis thaliana is being used as a model to study the molecular process that enable carpel and subsequent silique (fruit) development (Alvarez and Smyth, 1999; Bowman et al., 1999; Ferrándiz et al., 1999; Gasser and Robinson-Beers, 1993; Nemhauser et al., 1998; Sessions et al., 1997; chapter 2). The structural components of the *Arabidopsis* carpel are indicated in figure 3.1A. Silique development in *Arabidopsis* is fertilization dependent (Chaudhury et al., 1997; Meinke and Sussex, 1979; Ohad et al., 1996). If fertilization does not occur, the carpel (Figure 3.1A) expands slightly in length prior to progressing into a terminal senescence phase without further tissue differentiation (Figure 3.1B).

Following fertilization the ovule forms a seed and the cell layers of the carpel differentiate into the exocarp, mesocarp, structural sclerenchyma and endocarp of the

Figure 3.1 Silique development in *Arabidopsis*. Morphological features of the *Arabidopsis* pistil at anthesis (A), an unpollinated senescing pistil (B) and a maturing seeded silique (C) prior to dehiscence are shown whole and in section. (A) At anthesis *Arabidopsis* flowers contain a central pistil surrounded by six dehiscent stamens, four fully recurved petals and four sepals. The pistil is comprised of two fused carpels adjoined by medial replum tissues, with a false septum dividing the ovary into two locules (Bowman et al., 1999; Gasser and Robinson-Beers, 1993; Sessions and Zambryski, 1995). Ovules are attached via their funiculus to placental tissue located on the false septum. (B) In the absence of fertilization, pistils cease growth and then undergo senescence without further differentiation. (C) Silique development is not initiated until fertilization occurs or growth regulator treatment is applied. (C) Carpel valves initiate silique development and differentiate exocarp, mesocarp, endocarp, supportive sclerenchyma and lateral vascular bundle development. Cells in the carpel that will comprise the single cell exocarp layer in the silique are coloured green. Those that give rise to the mesocarp, supportive sclerenchyma and endocarp are coloured yellow, red and blue respectively.

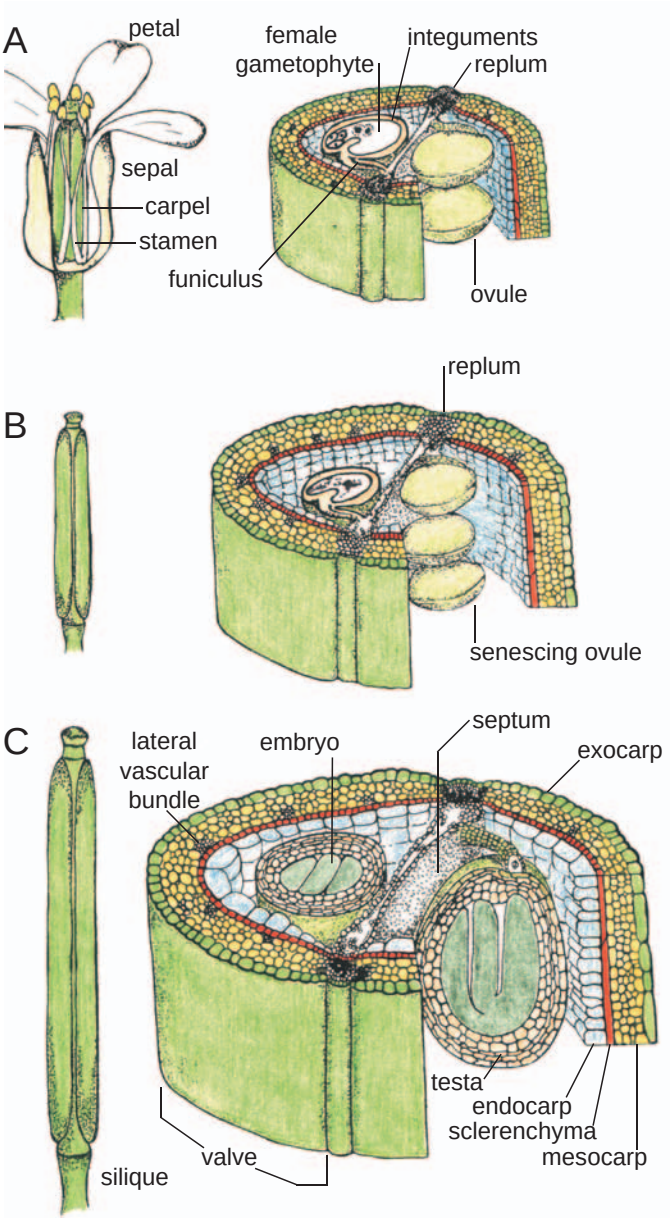
A
petal
sepal
carpel
stamen
female gametophyte
integuments
replum
funiculus
ovule
B
replum
senescing ovule
C
lateral vascular bundle
embryo
septum
exocarp
testa
endocarp
sclerenchyma
mesocarp
valve
silique

silique (Figure 3.1C). Exocarp formation mainly results from cell expansion. The mesocarp forms primarily by anticlinal divisions and cellular expansion. The single cell layer of supportive sclerenchyma elongates and develops secondary wall thickening during silique development, and endocarp formation involves anticlinal divisions and cellular expansion (chapter 2.3.7). Silique growth occurs over a four day period post-pollination and later at seed maturity the silique dehisces along the replum carpel-valve boundary to release the seeds (Liljegren et al., 1998; Meinke and Sussex, 1979). Therefore, fruit development in *Arabidopsis* involves a commitment to cell division, cell expansion, differentiation and then dehiscence. However, critical determinants in the commitment to silique growth therefore appear to regulate mesocarp cell division and expansion.

Parthenocarpic silique development can also be induced in *Arabidopsis* by the application of various plant growth regulators including gibberellins, auxins and cytokinins to anthesis stage carpels (Spence et al., 1996; chapter 2.3.2). Growth regulator application influences the development of silique tissue layers in different ways and gibberellin (GA_3) application results in siliques that are morphologically most similar to that observed post-pollination (chapter 2.3.7). Genetic analysis of plant growth regulator-induced silique development indicates that GA perception controls the processes of mesocarp cell division and that mesocarp expansion can be controlled by auxin (chapter 2.3.7). *GAI*, a member of the *SCARECROW*-like or *GRAS* gene family (Pysh et al., 1999) appears to be essential for coordinating anticlinal mesocarp cell division in response to active GAs during silique development (chapter 2.3.8).

This chapter describes *fwf* (*fruit without fertilization*), a parthenocarpic *Arabidopsis* mutant. I characterize the genetic interaction of *fwf* with *Arabidopsis* mutants disrupted in hormone perception, carpel identity and ovule integument formation to define the processes facilitating parthenocarpic silique development. I provide genetic evidence that

suggests *FWF* activity is required for the repression of silique development in the absence of fertilization and that signal transduction from ovules and the outer floral whorl organs may modify parthenocarpic fruit development in *fwf* mutants.

3.2 Materials and Methods

3.2.1 Isolation of the *fwf* mutant, scoring parthenocarpy and histological sectioning

The *fruit without fertilization* (*fwf*) mutant was isolated during a genetic screen for *fertilization independent seed* (*fis*) development (Chaudhury et al., 1997). Landsberg *erecta* (L.*er*) seeds heterozygous for the male sterile *pistillata* (*pi*) mutation were mutagenized with ethyl methane sulfonate (EMS) and M2 plants were specifically screened for mutants that formed siliques. In contrast to the characterized *fis* mutants (Chaudhury et al., 1997), the *fwf* mutant failed to initiate seed development. The *fwf* lesion was separated from *pi* by crossing with L.*er* pollen and was then backcrossed to L.*er* seven times. A near isogenic line (NIL) was created in Columbia by backcrossing *fwf* three times to L.*er* followed by five backcrosses to Col-1. Parthenocarpic plants were identified by the emasculation of a minimum of five pistils on the main apical meristem after the formation of the first 15 flowers. Plants producing siliques that consistently elongated greater than 5.5 to 6 mm in length post-emasculation were scored as parthenocarpic.

Plant growth conditions, methods for emasculation (which involves removing all floral organs except the pistil), assessment of pistil receptivity, silique growth measurements, application of plant growth regulators and histology are essentially as described in chapter 2.2. Histological sections and mature siliques 7 day post-anthesis were photographed using a SPOT2 camera (Diagnostic instruments Inc., Sterling Heights, Michigan) fitted to either an Axioplan or Stemi-2000C microscope (Carl Zeiss, Jena,

Germany). *fwf* siliques above flower position 30 were observed, photographed and collected for sectioning during subsequent genetic analysis unless stated.

3.2.2 Map position of *fwf* and *aberrant testa shape* (*ats*)

Col-1 plants were crossed as pollen donors to *fwf* homozygote plants for preliminary analysis. In the segregating F_2 population 26 *fwf* plants were identified and cleaved amplified polymorphic sequences (CAPS; Konieczny and Ausubel, 1993) and simple sequence length polymorphism (SSLP; Bell and Ecker, 1994) markers were used to assign *fwf* to a linkage group. Analysis with visible markers provided additional mapping data. *aberrant testa shape*, (*ats*; Léon-Kloosterziel et al., 1994) was crossed with *fwf* and 5 homozygous *ats fwf* plants were identified from 341 F_2 plants. A single *ats fwf* plant was then crossed to Col-4 to obtain coupling phase recombination data for assessment using the Haldane function (Koornneef and Stam, 1992). SSLPs were used to verify the position of *fwf* relative to *ats*.

3.2.3 Genetic analysis of *fwf* with multiple mutant lines

In all double and triple mutant analyses the L.*er* ecotype was used. The *ats*, *ga1-3*, *gai-1* mutants were obtained from the Arabidopsis Biological Resource Center. The EMS mutant, *frt1-3* (a gift from Prof. Robert Fischer, University of California, Berkeley, CA) displayed a phenotype similar to the previously described *agl8* mutant, *ful-1* (Gu et al., 1998) which is defective in carpel and fruit morphogenesis. *frt1-3* was shown to be allelic to *ful-1*, and thus *frt1-3* has been designated as an allele of *ful-1*, named *ful-7*.

Multiple mutant lines were obtained either by crossing homozygous lines together and identifying homozygous *fwf* F_2 individuals that segregated in the F_3 for the alternative

mutation (*ga1-3*, *ful-7*) or multiple mutants were identified as F_3 homozygous plants for the desired genotype. When necessary these plants were progeny checked or testcrossed.

Plants containing the conditional male sterile *pop1* mutation (allelic to *cer6*) were male sterile at relative humidities less than 50%, but set fertile seed when transferred to 95% relative humidity (Hülskamp et al., 1995). To create *ga1-3 fwf* double mutants, *ga1-3* mutant seed was germinated on MS media, pH 5.7 (Murashige and Skoog, 1962; Sigma Co.), containing 2% sucrose, 1% agarose supplemented with 0.1 mM GA_3. Seedlings were transferred to soil and treated with GA_3 to produce fertile flowers for crosses with *fwf* pollen. Homozygous *fwf* F_2 lines segregating for *ga1-3* at F_3 were analyzed by initially germinating seed on GA_3 supplemented MS media but without further GA_3 treatment to allow homozygous *ga1-3* individuals to become GA deficient.

3.3 Results

3.3.1 *fwf* is facultatively parthenocarpic

A parthenocarpic mutant, fruit without fertilization (*fwf*) was identified in a mutagenesis screen carried out in the L.*er* background containing the male-sterile *pistillata* (*pi*) background because it displayed significantly elongated siliques in the absence of pollination. When the *pi* mutation was outcrossed, all of the segregating plants set fertile seed and emasculation was required to identify those with the *fwf* lesion indicating that parthenocarpy in *fwf* is facultative. Seed development was not observed in emasculated *fwf* plants (Fig 3.2A). This feature distinguishes *fwf* from the previously characterized *fis* (Chaudhury et al., 1997), *fie* (Ohad et al., 1996) and *mea* (Grossniklaus et al., 1998) mutants shown to develop siliques and non-viable autonomous seed-like structures in the absence of fertilization.

Figure 3.2 Features of the *fwf* phenotype. (A) Comparisons of a pistil dissected from a anthesis stage L.*er* flower (a), L.*er* silique 7 days post-pollination (p), an emasculated unpollinated L.*er* pistil 7 day post-anthesis (up), compared with a parthenocarpic *fwf* silique in the L.*er* background and in the near isogenic line (Col-1) following emasculation. A carpel has been removed from the anthesis stage pistil, the maturing L.*er* silique following pollination, and also from the *fwf* silique following emasculation, to display the presence and absence of seeds. (B) Partially cleared siliques showing decreased seed set in proximal region of the *fwf* silique following cross-pollination with L.*er* pollen. (C) and (D) show comparative sections from unpollinated L.*er* and *fwf* ovules at stage 3-VI to 4-I according to Schneitz et al. (1995). (E-H) Comparison of *fwf* floral morphology with that of ethylene mutants. Anthesis stage L.*er* (E) and *fwf* (F) flowers. *fwf* develop large petals with pronounced vasculature and pistils precociously elongate but the petals do not fully recurve. *ctr1-1* flowers (G) develop excess petal recurvature in late flower positions and *ein6* (H) has greatly enlarged stigmatic tissue with constitutively recurved petals post-pollination. Lateral sections of carpel valves examined 7 days post-anthesis from unpollinated (I) and pollinated L.*er* (J) showing the degree of development of exocarp (x), mesocarp (m), supportive sclerenchyma (s) and endocarp (e). Unpollinated *fwf* plants (K) develop enlarged exocarp and mesocarp cells, with less endocarp cell expansion. Pollinated *fwf* siliques (L) show similar development to pollinated L.*er* but with greater expansion of exocarp and mesocarp cells. This difference is also apparent in transverse sections of pollinated L.*er* (M) and *fwf* (N). Unpollinated *fwf* pistils (O) at early flower positions develop large lateral vascular bundles and associated exocarp cells are enlarged (arrowhead). Above flower position 30 (P), mesocarp cells generally greatly enlarged. Ovule (o). Scale bars: A 3mm; C,D, 30 μm; I to P 50 μm.

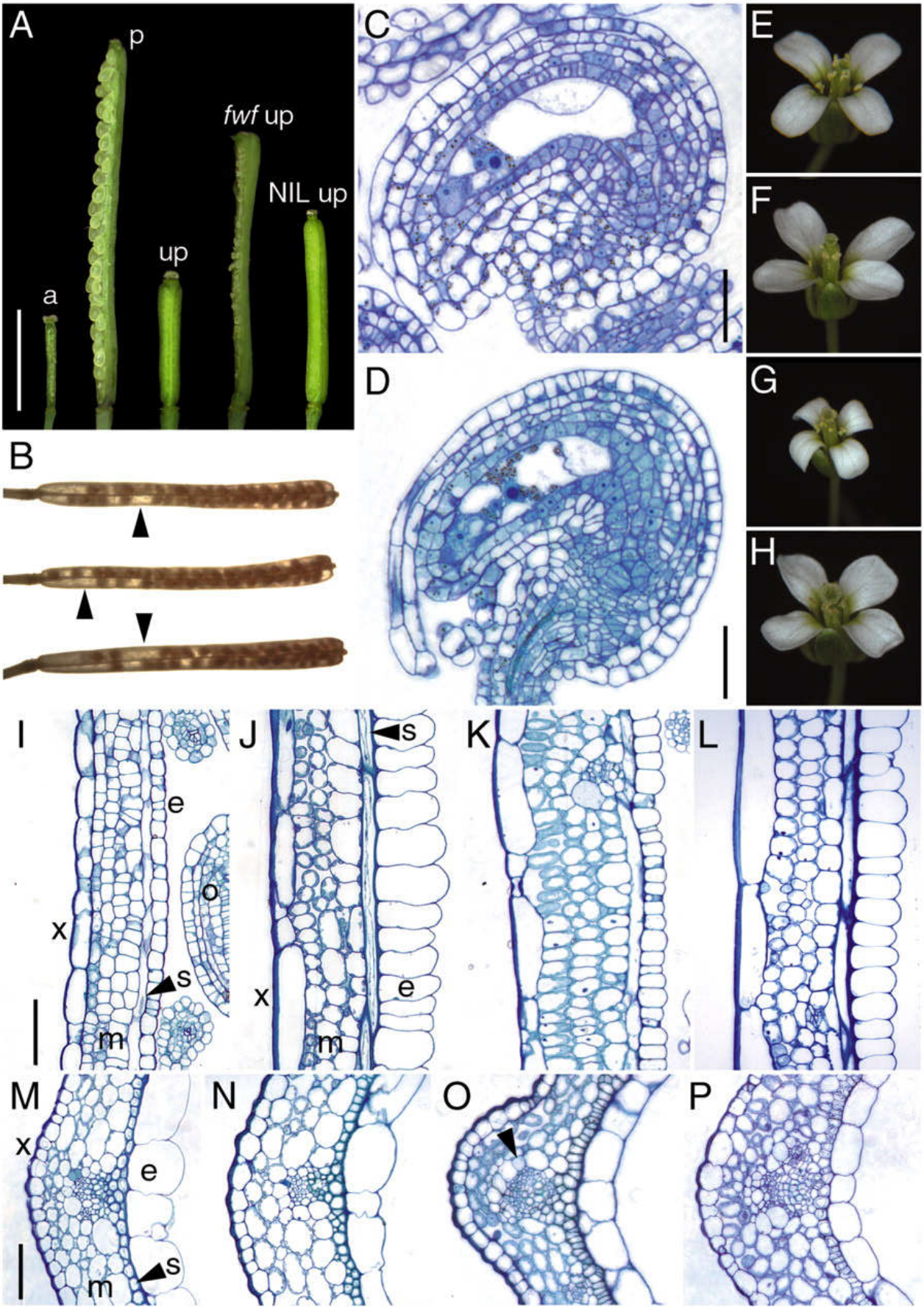
A
p
fwf up
NIL up
up
a
B
C
D
E
F
G
H
I
e
o
x
s
m
J
s
x
e
m
K
L
M
x
e
s
m
N
O
P

Emasculated *fwf* plants also produced dehiscent siliques indicating that silique development proceeds to completion in the absence of developing seeds. Parthenocarpic *fwf* siliques were shorter than siliques formed post-pollination in *fwf* and L.*er* (Figure 3.2A; Table 3.1) suggesting that either the developing seeds or processes associated with seed formation may contribute to the terminal size of the silique. The *fwf* lesion also displayed a degree of ecotype specificity. Shorter parthenocarpic siliques were formed in the NIL Col-1 background compared to those observed in L.*er* (Figure 3.2A; Table 3.1).

Reciprocal crosses between *fwf* and wild type (Col-1) showed that *fwf* segregated as a recessive mutation (46 *fwf* in 184 F_2 plants). Seed abortion indicated by brown shriveled seeds was rare in reciprocal crosses. However, seed initiation was reduced in the proximal positions of *fwf* siliques following pollination with L.*er*, as indicated by empty positions within the silique (Figure 3.2B). Pollination of emasculated *fwf* and L.*er* pistils on sequential days post-anthesis showed comparable duration in female receptivity (Figure 3.3A) confirming that *fwf* pollen was capable of germination and growth over the same four day period as observed for L.*er*. Ovule numbers in *fwf* and L.*er* pistils were comparable (53.4 ± 6.5 and 54.0 ± 5.2; respectively). Sections of anthesis stage ovules from proximal pistil positions showed that embryo sac structure in unfertilized *fwf* pistils and L.*er* were structurally similar (Figure 3.2C), however, 19% of *fwf* ovules (n = 37) displayed extended outer integuments compared to wild type L.*er* (Figure 3.2D and 3.2C respectively). Collectively these data suggest that the decreased seed initiation in proximal portions of the *fwf* silique is associated with an unknown maternal defect.

3.3.2 *fwf* exhibits altered petal morphology and precocious silique formation

Plant stature in *fwf* plants was indistinguishable from wild type. Subtle alterations in floral morphology were however observed. *fwf* flowers randomly exhibited missing

Table 3.1. Pistil and silique lengths at 7 days post-anthesis in wild type and mutant genotypes.

	Silique length (mm ± s.d.)		
genotype / treatment	**male sterile**	**emasculated**	**pollinated**
L.*er*	-	4.5 ± 0.5	12.8 ± 1.1
pop1	4.3 ± 0.4	-	-
fwf	-	7.5 ± 1.0	11.0 ± 1.4 [a]
pop1 fwf	5.5 ± 0.7	-	-
pop1 fwf / +	4.7 ± 0.7	-	-
Col-1	-	4.1 ± 0.3	14.1 ± 1.2
fwf NIL (Col-1)	-	5.7 ± 0.4	-
gai-1	-	4.8 ± 0.4	9.5 ± 1.1
gai-1 fwf	-	6.1 ± 0.6	8.2 ± 0.5
ful-7	-	2.9 ± 0.2	3.9 ± 0.1
ful-7 fwf	-	2.4 ± 0.2	-
ats	-	4.2 ± 0.5	12.1 ± 0.6
pop1 ats	5.3 ± 0.5	-	-
pop1 ats fwf	9.1 ± 0.6	-	-
ats fwf	-	9.3 ± 0.7	-
gai-1 ats fwf	-	7.9 ± 0.7	-

Plants containing *pop1* were assayed under male sterile conditions; [a] pollinated with L.*er*

Figure 3.3 (A) Receptivity period for pollinated L.*er* and *fwf* pistils, determined by pollinating emasculated pistils with L.*er* pollen at various days post-anthesis and determining seed set. (B) The relationship of floral position on the primary inflorescence meristem and final parthenocarpic silique length in male sterile *pop1* (circles) and *pop1 fwf* (squares), emasculated *fwf* (diamonds) and male sterile *pop1 ats fwf* triple mutant (triangles). (C) Silique growth of pollinated L.*er* (p), emasculated *fwf* and male sterile *pop1 ats fwf* compared to emasculated and unfertilized L.*er* (up).

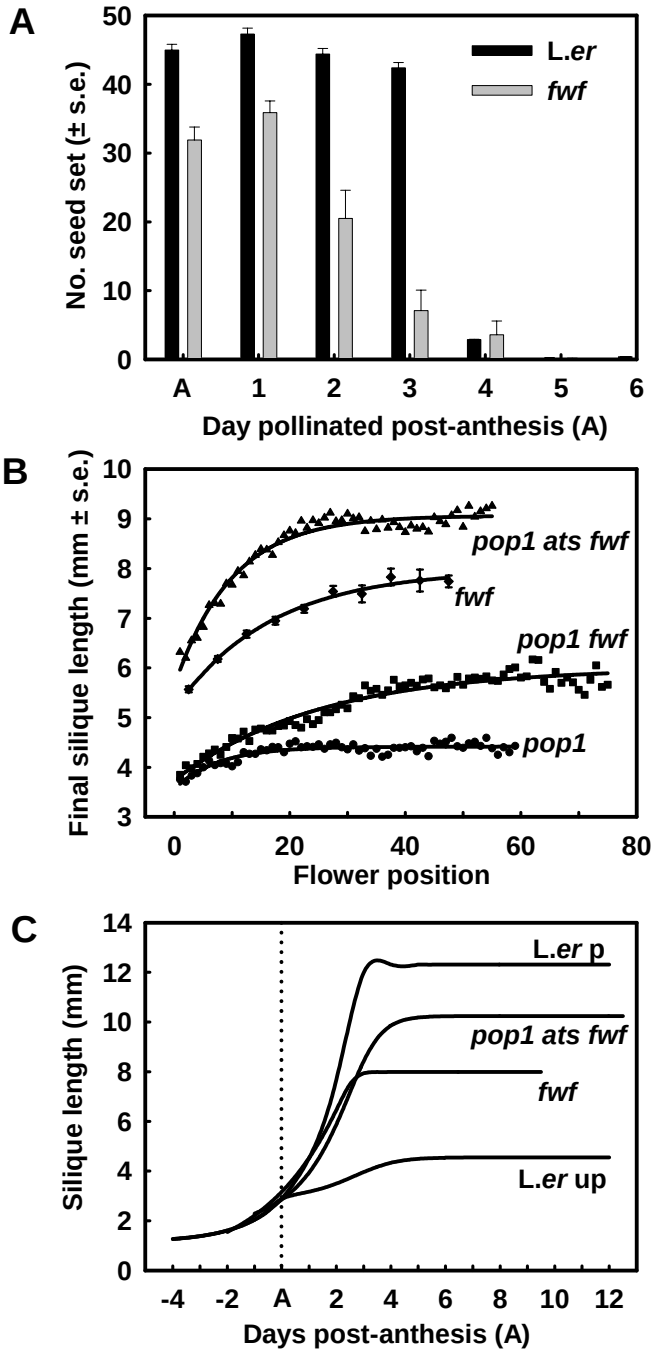
A
No. seed set (± s.e.)
L.er
fwf
Day pollinated post-anthesis (A)
B
Final silique length (mm ± s.e.)
pop1 ats fwf
fwf
pop1 fwf
pop1
Flower position
C
Silique length (mm)
L.er p
pop1 ats fwf
fwf
L.er up
Days post-anthesis (A)

stamens, increased vasculature on enlarged petals, occasional crinkly petal edges, incomplete petal recurvature and decreased stigmatic papillae length compared with L.*er* (Figure 3.2E and 3.2F). Silique growth was often precocious in unemasculated flowers of aging *fwf* plants resulting in decreased seed set because stigmatic papillae often extended above the anthers prior to their dehiscence at anthesis. Some of these floral features resembled those observed in early flower positions of the ethylene perception mutant *ctr1-1* and *ein2-5*:CEND (Alonso et al., 1999). However, *ctr1-1* flowers display excessive petal recurvature and dehiscent stamens level with stigmatic tissues at later floral positions (Figure 3.2G), unlike *fwf*. Floral morphology in *fwf* was also distinct from that in the ethylene insensitive *ein6* mutant which displays constitutively recurved petals post-anthesis and enlarged stigmatic papillae (Figure 3.2H). Therefore the *fwf* mutation appears to primarily influence flower and silique development.

3.3.3 *fwf* is located on chromosome 5

The *fwf* lesion was located on chromosome 5 linked to the SSLP and CAPS markers nga106, nga139, AthSO191 and DFR as shown in figure 3.4. Analysis of 52 chromatids revealed that the recombination frequencies between *fwf* and nga106, and *fwf* and nga139 were 19.2 ± 5.2 (24.2 cM) and 11.5 ± 4.4 (13.1 cM) respectively. Recombination frequencies between *fwf* and AthSO191, and *fwf* and DFR were 13.5 ± 4.7 (15.7 cM) and 25 ± 6 (34.7 cM) respectively. This positioned *fwf* between markers nga139 and AthSO191 on the recombinant inbred map using the Haldane function (Figure 3.4; Rhee et al., 1998) and confirmed that *fwf* is distinct from the *fis*, *mea* and *fie* loci.

The visible markers *aberrant testa shape* (*ats*) and *bel1-1* were also used to confirm the map position for *fwf*. The map position of *ats* on the genetic map was reported at 64 cM on chromosome 5. When *ats fwf* double mutants were crossed in coupling phase as pollen

Figure 3.4 Map positions for *fwf*, *bel1-1* and *ats* mutants on chromosome 5.

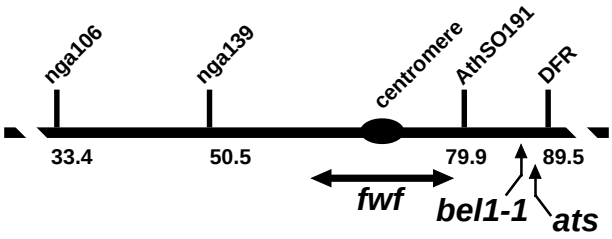
nga106
nga139
centromere
AthSO191
DFR
33.4
50.5
79.9
89.5
fwf
bel1-1
ats

donors to Col-4 female parents the recombination frequency was 7.39 ±1.98 (n = 181) indicating that the map distance between *ats* and *fwf* was 8 ± 2.32 cM using the Haldane function. Additional data indicated that *ats* maps to a distinct locus between *bel1-1* and DFR (Figure 3.4; chapter 6.2.2).

3.3.4 Flower position and emasculation influence parthenocarpy in *fwf*

Parthenocarpic fruit development in *fwf* was influenced by the flower position on the inflorescence meristem and also when all of the floral organs surrounding the pistil were removed to assess parthenocarpy. Figure 3.3B shows that emasculation of *fwf* flowers above floral position 30 resulted in the maximal terminal silique elongation of 7-8 mm. By contrast, the first few pollinated L.*er* and *fwf* flowers immediately attained maximal silique lengths of 11-12 mm (not shown).

I examined whether the process of emasculation influenced parthenocarpic silique development in *fwf*. As a comparable alternative to floral organ emasculation, a conditional male sterile mutation, *pop1* was used to control pollen viability. Under low humidity conditions *pop1* pollen is unable to germinate and plants are male sterile. Emasculated L.*er* and male sterile *pop1* pistils did not grow further than 4.5 mm (Figure 3.3B and 3.3C). Emasculation of *pop1 fwf* flowers produced parthenocarpic siliques of lengths similar to those observed in emasculated *fwf* plants (Figures 3.3B; Table 3.1). Surprisingly, non-emasculated *pop fwf* plants produced siliques that were significantly reduced in length compared to those observed in emasculated *fwf* plants (Figure 3.3B; Table 3.1). Emasculation does not stimulate parthenocarpy in wild-type pistils but the resultant wounding may enhance parthenocarpic development in *fwf*. Alternatively, the presence of the surrounding floral whorls may act to inhibit parthenocarpic silique development in *fwf*.

The latter is plausible considering *fwf* was originally isolated from a screen in *pistillata* plants that do not form stamens and petals.

3.3.5 *ats* enhances parthenocarpic development in *fwf* negating the requirement for emasculation of the surrounding floral whorls

During the mapping of *fwf*, double mutants were made with *ats* a mutant that has a lesion in ovule integument formation. Wild type *Arabidopsis* ovules consist of a two-cell layer outer integument and three-cell layer inner integument (Schneitz et al., 1995). In *ats*, a three-cell layer unitegmic structure replaces both integuments and this results in modified ovule and testa shape (Léon-Kloosterziel et al., 1994). Emasculated *ats fwf* plants formed parthenocarpic siliques that exceeded the mean emasculated *fwf* silique length at all floral positions (Table 3.1). The mean parthenocarpic silique length after flower position 30 was only slightly shorter than that of siliques from self-pollinated *ats* plants (Table 3.1). The *ats* mutation did not restore seed development in the proximal portion of the silique or affect the total amount seed set compared with pollinated *fwf* plants.

To further examine the effects of emasculation and the influence of surrounding floral whorls on parthenocarpic development in *fwf*, a *pop1 ats fwf* triple mutant was created. When the triple mutant was assessed under male sterile low humidity conditions (Figure 3.3B) it achieved a mean parthenocarpic silique length of 9.1 ± 0.7 mm at flower position 30 (n = 20 plants ± s.d.). This was equal to the silique length obtained in the emasculated *ats fwf* double mutant (Table 3.1). Therefore *ats* enhances parthenocarpic silique development in *fwf* negating the requirement for emasculation to achieve siliques comparable in length to that obtained post-pollination. This suggests that a wounding response resulting from the removal of floral tissues during emasculation is not required to

observe parthenocarpy in *fwf*, and that fruit growth may be modulated by both signals from surrounding floral whorls and from events within the ovule.

3.3.6 Parthenocarpic *fwf* siliques undergo mesocarp cell division and expansion

Silique development is precocious in *fwf* (Figure 3.2F and 3.3C), however the rate of silique elongation in emasculated *fwf* and *pop1 ats fwf* is comparable to that observed in pollinated L.*er* until siliques cease elongation 3 and 4 days post-anthesis respectively (Figure 3.3C). The parthenocarpic elongation and silique growth in *pop1 ats fwf* triple mutants was identical to that observed in emasculated L.*er* pistils treated with GA_3 (10 *n*mol $pistil^{-1}$; chapter 2.3.2). The latter have been shown to undergo mesocarp cell division and expansion in a similar manner observed in pollination-induced siliques (chapter 2.3.7).

Mutations that allow fertilization-independent silique development might individually or collectively affect cell expansion, cell division and cell differentiation in developing tissue layers (Figure 3.1). Therefore, silique formation in *fwf* mutants was examined by determining the mean cell length (Table 3.2) and calculating relative cell numbers from longitudinal sections in the different tissue layers during development (Table 3.3). Comparisons were made between anthesis pistils, unpollinated pistils and mature parthenocarpic siliques at 7 days post-anthesis (Figure 3.2I to 3.2L).

Mesocarp cell division occurred normal to the plane of silique elongation in emasculated *fwf* pistils and *pop1 ats fwf* siliques (Table 3.3). The number of mesocarp and endocarp cells in anthesis *fwf* pistils was elevated compared to anthesis stage wild type L.*er* (Table 3.3). This was because these cell layers were already undergoing precocious anticlinal cell division. Endocarp cells divided anticlinally, but their expansion into the locule was not as great as in pollination-induced siliques (Figure 3.2J and 3.2K; Table 3.3). Exocarp and supportive sclerenchyma cells expanded longitudinally during parthenocarpic

Table 3.2 Comparison of the mean cell length (μm ± s.d.), normal to the silique elongation axis, in *Arabidopsis* carpel tissue layers from anthesis and 7 days post-anthesis in mutants containing combinations of *fwf*, *ats* and *gai-1*.

	Stage of silique development, treatment and genotype (Mean silique length for each genotype / treatment)							
Tissue	L.*er* A [†] (2.8 ± 0.2)	L.*er* UP [†] (4.1 ± 0.4)	L.*er* +P [†] (11.5 ± 1.0)	*fwf* A (3.2 ± 0.1)	*fwf* UP (7.5 ± 1.0)	*pop1 ats fwf* UP (9.1 ± 0.6)	*gai-1 fwf* UP (6.1 ± 0.6)	*gai-1 ats fwf* UP (7.9 ± 0.7)
Exocarp	15 ± 8	28 ± 15	49 ± 32	17 ± 8	37 ± 21	51 ± 30	36 ± 20	35 ± 30
Mesocarp 1 [a]	10 ± 4	11 ± 4	13 ± 5	8 ± 3	14 ± 4	9 ± 2	16 ± 4	13 ± 4
Mesocarp 2 [a]	11 ± 3	11 ± 3	12 ± 3	9 ± 2	14 ± 3	10 ± 2	17 ± 5	14 ± 5
Mesocarp 3 [a]	11 ± 4	14 ± 5	21 ± 8	10 ± 3	17 ± 6	15 ± 6	21 ± 5	15 ± 6
Endocarp	7 ± 2	13 ± 3	22 ± 6	7 ± 2	15 ± 4	16 ± 5	17 ± 5	16 ± 6

[†] data described in chapter 2.3.7; A, anthesis; UP, emasculated and unpollinated; +P, pollinated; [a] Mesocarp 1 relates to mesocarp cells adjacent to the exocarp, mesocarp 2 cells bounded by other mesocarp cells and mesocarp 3, cells adjacent to the sclerenchyma layer.

Table 3.3 Comparison of the mean cell number (± s.e), in a longitudinal section of *Arabidopsis* carpel tissue from anthesis and at 7 days post-anthesis in mutants containing combinations of *fwf*, *ats* and *gai-1*.

	Stage of silique development, treatment and genotype (Silique length for each genotype / treatment)							
Tissue	L.*er* A [†] (2.8 ± 0.2)	L.*er* UP [†] (4.1 ± 0.4)	L.*er* +P [†] (11.5 ± 1.0)	*fwf* A (3.2 ± 0.1)	*fwf* UP (7.5 ± 1.0)	*pop1 ats fwf* UP (9.1 ± 0.6)	*gai-1 fwf* UP (6.1 ± 0.6)	*gai-1 ats fwf* UP (7.9 ± 0.7)
Exocarp	227 ± 20	196 ± 23	277 ± 26	222 ± 13	255 ± 30	264 ± 45	213 ± 19	397 ± 52
Mesocarp 1 [a]	315 ± 17	396 ± 15	951 ± 41	411 ± 12	590 ± 20	1024 ± 22	410 ± 12	687 ± 34
Mesocarp 2 [a]	287 ± 12	389 ± 11	983 ± 34	398 ± 11	579 ± 17	978 ± 27	393 ± 15	658 ± 28
Mesocarp 3 [a]	289 ± 19	326 ± 17	617 ± 30	343 ± 15	480 ± 24	719 ± 37	312 ± 14	649 ± 37
Endocarp	420 ± 19	351 ± 14	556 ± 28	496 ± 13	550 ± 19	652 ± 32	391 ± 18	568 ± 28

[†] data described in chapter 2.3.7; A, anthesis; UP, emasculated and unpollinated; +P, pollinated; [a] Mesocarp 1 relates to mesocarp cells adjacent to the exocarp, mesocarp 2 cells bounded by other mesocarp cells and mesocarp 3, cells adjacent to the sclerenchyma layer.

development, with the latter developing secondary wall thickenings in pollinated L.*er* (Figure 3.2J). Therefore the development of parthenocarpic siliques in *fwf* was relatively similar to siliques formed post-fertilization in wild type plants but parthenocarpic siliques initiated earlier in development and they were also 41 % shorter than pollination-induced siliques. This related to decreased cell division in the mesocarp relative to wild type siliques forming post-pollination.

Cell numbers in transverse valve sections remained constant in all tissues from anthesis to maturity in parthenocarpic and post-fertilization siliques in both *fwf* and L.*er* (not shown) indicating that the degree of cellular expansion determines silique width. Pollination-induced *fwf* siliques were, however, altered in mesocarp expansion compared to pollination-induced L.*er* siliques. Pollination-induced *fwf* siliques exhibited greater mesocarp cell expansion compared to L.*er* (Figure 3.2M and 3.2N), indicating pollination stimulates mesocarp cell expansion in a manner additive to that induced by the *fwf* lesion.

3.3.7 Lateral vascular bundle development and adjacent mesocarp cell expansion is affected in *fwf*

Parthenocarpic siliques forming prior to floral position 30 in *fwf*, *fwf* (NIL), and *ats fwf*, contained a group of mesocarp cells adjacent to the lateral vascular bundle that expanded, forming a crescent of enlarged cells (Figure 3.2O). In parthenocarpic *fwf* siliques above flower position 30, the degree of mesocarp cell expansion became even more pronounced and expansion was not as restricted to mesocarp cells adjacent to the lateral vascular bundle (Figure 3.2P). This observation correlates with the stronger parthenocarpic *fwf* phenotype observed at later floral positions.

Differences were also found within lateral vascular bundles in parthenocarpic siliques. Lateral vascular bundles were larger and contained more vascular elements than

pollination-induced siliques (Figure 3.2O and 3.2P). *FWF* may therefore suppress vascular differentiation and mesocarp expansion in unfertilized pistils and this suppression might be modulated relative to changes in floral meristem age or a basipetal-acropetal gradient along the inflorescence meristem.

3.3.8 Parthenocarpy in *fwf* requires *FUL activity*

The *AGL8* MADS-box gene is essential for carpel valve identity and growth. Mutations in *AGL8* abolish silique elongation and carpel valve dehiscence (Gu et al., 1998). Mesocarp cell expansion and division, and also vascular differentiation within the carpel becomes impaired prior to anthesis. This lesion persists post-pollination but the final endocarp cell number is twice the normal amount (Gu et al., 1998). Mutant *ful* pistils set seed normally but because silique elongation is abolished, developing seeds become crowded and later rupture the carpel during maturation. A *ful-7 fwf* double mutant was created to determine the effects on parthenocarpic silique development.

Neither parthenocarpic nor significant pollination-induced silique elongation was observed in *ful-7 fwf* plants (Figure 3.5B). Therefore *FUL* activity is also required for parthenocarpic silique development in the *fwf* background. However, replum growth and expansion continued in the absence of silique elongation in both pollinated *ful-7* and *ful-7 fwf* double mutant pistils resulting in a zigzag arrangement of the replum tissue (Figure 3.5B, inset). Emasculated *ful-7 fwf* and *ful-7* plants did not initiate silique development or further replum growth and lacked the distinctive replum zigzag patterning observed post-pollination (Figure 3.5B, inset). Therefore, pollination and fertilization can trigger further replum growth in a manner that is independent of *FUL* and *FWF* activity. However, functional *FUL* activity is required for continued replum growth during parthenocarpic development in the *fwf* background. Thus the *ful-7* mutant is completely epistatic to

Figure 3.5 (A) Unpollinated L.*er* pistil or following pollination in L.*er* or after emasculation in *fwf* at 7 days post-anthesis. (B) *ful-7* and *ful-7 fwf* double mutants following pollination (p) or emasculation (up) in *ful-7 fwf*. Pollinated *ful-7* double mutants have continued replum development and replum cells expand (B, inset arrow). This development is absent in emasculated and unpollinated *ful-7 fwf* pistils (B, inset). Silique development in the *gai-1* background (C), and when *fwf* is combined with *gai-1* and together with *ats* (D). Sections of unpollinated *gai-1* (E), parthenocarpic *gai-1 fwf* (F), and pollinated *gai-1 fwf* (G) after 7 days post-anthesis. *ats* restores anticlinal mesocarp cell division in the parthenocarpic *gai-1 ats fwf* triple mutant (H) but mesocarp cells adjacent to vascular bundle remain enlarged (arrowhead). *ats* also increases the mesocarp cell division in parthenocarpic *fwf* (I). e, endocarp; m, mesocarp; s, supportive sclerenchyma; x, exocarp. Scale bars: A to D, 3 mm; E to I, 50 μm.

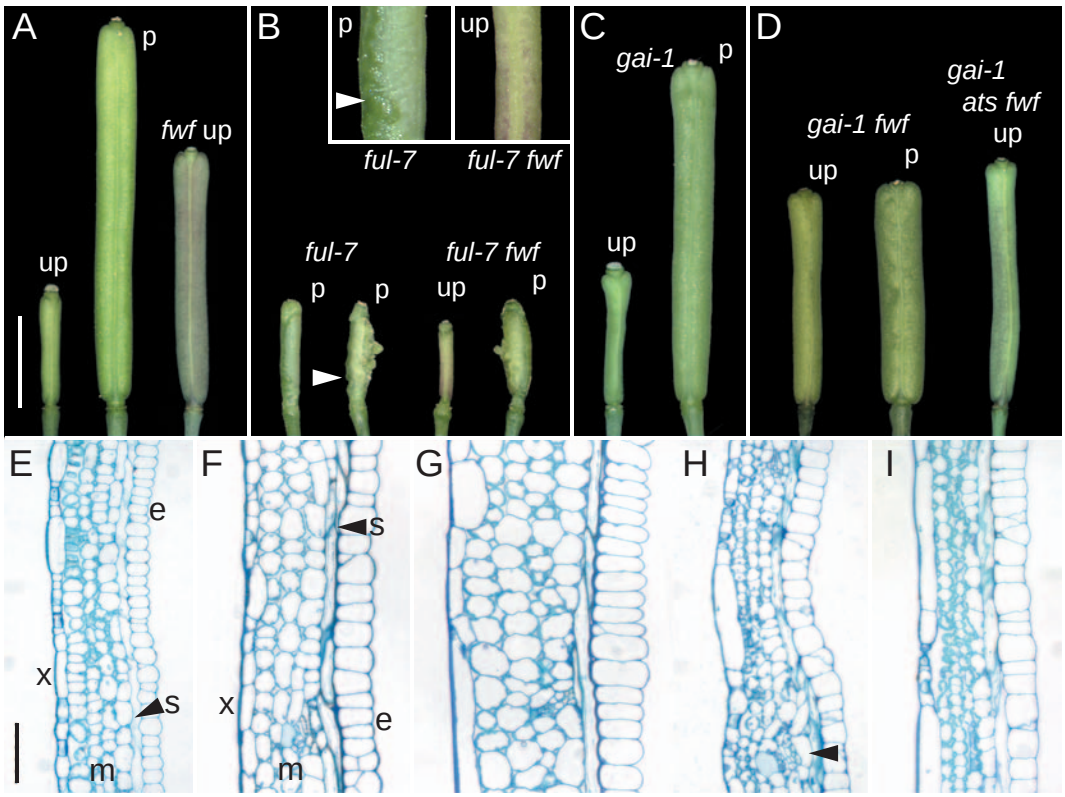
A
p
fwf up
up
B
p
up
ful-7
ful-7 fwf
ful-7
ful-7 fwf
p
p
up
p
C
gai-1
p
up
D
gai-1 fwf
gai-1
ats fwf
up
up
p
E
e
x
s
m
F
s
x
e
m
G
H
I

parthenocarpic silique development conferred by the *fwf* lesion, and it appears that the tissues comprising the valve solely mediate silique elongation in unpollinated *fwf* pistils.

3.3.9 Interaction with GA biosynthesis and perception

The application of GA_3 to anthesis stage *Arabidopsis* pistils results in the formation of parthenocarpic siliques that are 13 - 22% smaller than, but morphologically similar to pollination-induced siliques (chapter 2.3.2). Treatment with 10 *n*mol pistil^{-1} GA_3 together with either 1 *n*mol pistil^{-1} BA or NAA induced parthenocarpic siliques comparable in length to pollinated wild type plants (11.2 ± 1.4 and 12.1 ± 0.3 mm, respectively). When emasculated *fwf* pistils were treated at early flower positions (10 to 20), with either exogenous GA_3 or NAA at 10 *n*mol pistil^{-1}, parthenocarpy was enhanced, indicating *fwf* pistils respond to the exogenously applied growth regulators. GA_3 application to *fwf* pistils resulted in parthenocarpic siliques comparable to pollination induced siliques (11.9 ± 0.8). NAA enhanced lengthwise parthenocarpic silique growth (8.4 ± 0.7 mm) and also induced significant silique expansion. As parthenocarpic silique lengths approaching that observed following pollination could be achieved following the application of primarily GA_3 in combination with other growth regulators to *fwf* pistils, then it was formally possible that *fwf* represents a lesion in hormone biosynthesis or perception.

To test whether *fwf* was associated with GA perception or GA biosynthesis, *fwf* was combined with the *gai-1* and *ga1-3* mutations respectively. The *gai-1* mutation is a semi-dominant GA perception mutant that constitutively blocks GA responses because the truncated *gai-1* protein lacks a portion of the N-terminal domain (Peng et al., 1997). Homozygous *gai-1* plants are blocked in GA_3 induced parthenocarpic silique development (chapter 2.3.6). *gai-1* pistils do form siliques in response to pollination but these siliques have restricted anticlinal mesocarp cell division and predominantly grow by cellular

expansion. Mildly GA deficient plants containing the *ga5-1* biosynthesis mutation differentiate pollination-induced siliques in a manner similar to that observed in *gai-1* plants, indicating that GAs limit anticlinal mesocarp cell division (chapter 2.3.9). Severely GA deficient plants such as the *ga1-3* mutant fail to form siliques following pollination (Barendse et al., 1986).

Plants homozygous for *ga1-3 fwf* were identical to *ga1-3* single mutants and did not form siliques post-emasculation or pollination (not shown). This indicates *fwf* does not rescue silique development in *ga1-3* pistils and is distinct from the *spindly* (*spy*) and *repressor of ga1-3* (*rga*) mutants that partially restore a wild type phenotype to plants containing the *ga1-3* mutation (Jacobsen et al., 1996; Silverstone et al., 1997b).

When *gai-1 fwf* double mutants were created, emasculated pistils formed siliques that elongated and expanded further than that observed in unpollinated *gai-1* pistils (Figure 3.5C and 3.5D; Table 3.1). Comparisons between sections of unpollinated *gai-1* pistils (Figure 3.5E) and parthenocarpic *gai-1 fwf* siliques (Figure 3.5F) showed that mesocarp cell expansion and differentiation were the primary cause of parthenocarpic silique development in the *gai-1 fwf* double mutant. Anticlinal mesocarp cell division was not observed because anthesis *fwf* pistils and parthenocarpic *gai-1 fwf* siliques contained similar cell numbers (Table 3.3). Pollinated *gai-1 fwf* pistils also developed siliques by mesocarp expansion (Figure 3.5G), but pollination induced cell expansion greater than that observed in parthenocarpic *gai-1 fwf* siliques following emasculation (Figure 3.5F). These results confirm that the *fwf* lesion functions independently of *GAI* mediated GA perception. The development of shorter parthenocarpic siliques principally by mesocarp expansion with decreased anticlinal mesocarp cell division in the *gai-1* background (Figure 3.5D; Table 3.1) indicates that activation of GA perception through *GAI* in the mesocarp together

with other unidentified factors, is required to enable parthenocarpic silique development to a size comparable to emasculated *fwf* (Figure 3.5A).

The *gai-1 ats fwf* triple mutant developed parthenocarpic siliques superior in length to unpollinated *gai-1 fwf* (Figure 3.5D) but of a similar mean length to emasculated *fwf* single mutants (Figure 3.5A and Table 3.1). Sections showed that unpollinated *gai-1 ats fwf* siliques (Figure 3.5H) had much smaller mesocarp cells than emasculated *gai-1 fwf* (Figure 3.5G; Table 3.2) or pollinated *gai-1* (chapter 2.3.8). Mesocarp cell numbers in *gai-1 ats fwf* were greater than those observed in unpollinated *gai1-1 fwf* (Table 3.3). This indicates that *ats* restores or circumvents the blockage in anticlinal cell division conferred by *gai-1*. Longitudinal silique sections taken from parthenocarpic *pop1 ats fwf* triple mutants (Figure 3.5I), also showed that the *ats* lesion results in smaller mesocarp cells (Table 3.2) and final cell numbers in all tissue layers were comparable to L.*er* following pollination (Table 3.3). Therefore, the effects of *ats* on anticlinal mesocarp cell division in the *pop1 ats fwf* triple mutant are additive to that observed in siliques of *fwf* alone.

3.4 Discussion

FWF regulates the carpel to fruit transition and is affected by signals from the ovule and surrounding floral whorls. The carpel of *Arabidopsis* flower and the ovules inside them are one of the last floral organs to initiate and differentiate. Carpel primordia identity is specified by the floral homeotic gene *AGAMOUS* and genes such as *ETTIN*, *CRABS CLAW*, *SPATULA, FRUITFULL* and others like *PICKLE* subsequently act to specify carpel tissue polarity, identity, tissue boundaries, and growth and differentiation during gynoecium development (Alvarez and Smyth, 1999; Bowman et al., 1999; Eshed et al., 1999; Sessions et al., 1997). Carpel growth diminishes towards anthesis ensuring that the stigma tip becomes aligned with the dehiscing anthers to enable efficient self-pollination

(Figure 3.1). The molecular processes that cause carpels to diminish growth, determine carpel size relative to stamen length, and permit initiation of silique development are relatively unknown.

Silique growth and differentiation then resumes post-fertilization as the surrounding floral whorls abscise and the carpel differentiates into a seeded silique (Figure 3.1). Double fertilization occurs in the ovule and how information from this event is transduced to coordinate development of the carpel into a fruit remains to be determined. However, mutations in either one of three genes *MEDEA* (Grossniklaus et al., 1998), *FIS* (Luo et al., 1999) or *FIE* (Ohad et al., 1999) result in silique development and the initiation of seed and endosperm formation in the absence of fertilization. Proteins encoded by these genes are thought to form a repressive complex that inhibits seed and silique development in the absence of fertilization (Chaudhury et al., 1997).

3.4.1 *FWF* activity is affected by floral whorls and integument structure

Here it has been shown that *fwf* is a novel mutant that appears to be floral specific, affecting developmental events in petals and the ovule integuments which also allows a silique to develop independently of fertilization and seed development. It can be postulated that *FWF* may be involved in processes that repress the development of silique tissues prior to pollination and fertilization (Figure 3.6). The role of *FWF* in processes of silique development mediated by *MEDEA*, *FIS* and *FIE* requires further investigation.

The observation that removal of sepals, petals and stamens was required to maintain significant elongation of the silique in the *fwf* background suggests that *FWF* activity in carpels and siliques may be modified by events in the surrounding floral whorls.

Figure 3.6 A model for the regulation of silique development by GA mediated signal transduction, *FWF* and fertilization dependent processes. *FWF* primarily acts within a signal transduction pathway during pre-fertilization stages in pistil tissues to repress mesocarp expansion and vascular differentiation required for further silique development. Fertilization dependent events would mitigate *FWF* repression allowing the initiation of a hypothetical silique differentiation signal (red arrows). This pathway integrates with an auxin-like signal, which mediates mesocarp expansion that occurs independent of *GAI* mediated GA perception. Anticlinal mesocarp cell division during silique development is dependent on GA perception because the absence of anticlinal divisions in the *gai-1 fwf* double mutant was observed. *FWF* would precede the activation of GA signal transduction, which allows anticlinal mesocarp division. Processes occurring in integument and floral whorl tissues may modify activity of *FWF* or alter the signal transduction between ovule and carpel post-fertilization. Early steps in GA biosynthesis (*GA1*) that occur in vascular tissues appear to be essential for silique development.

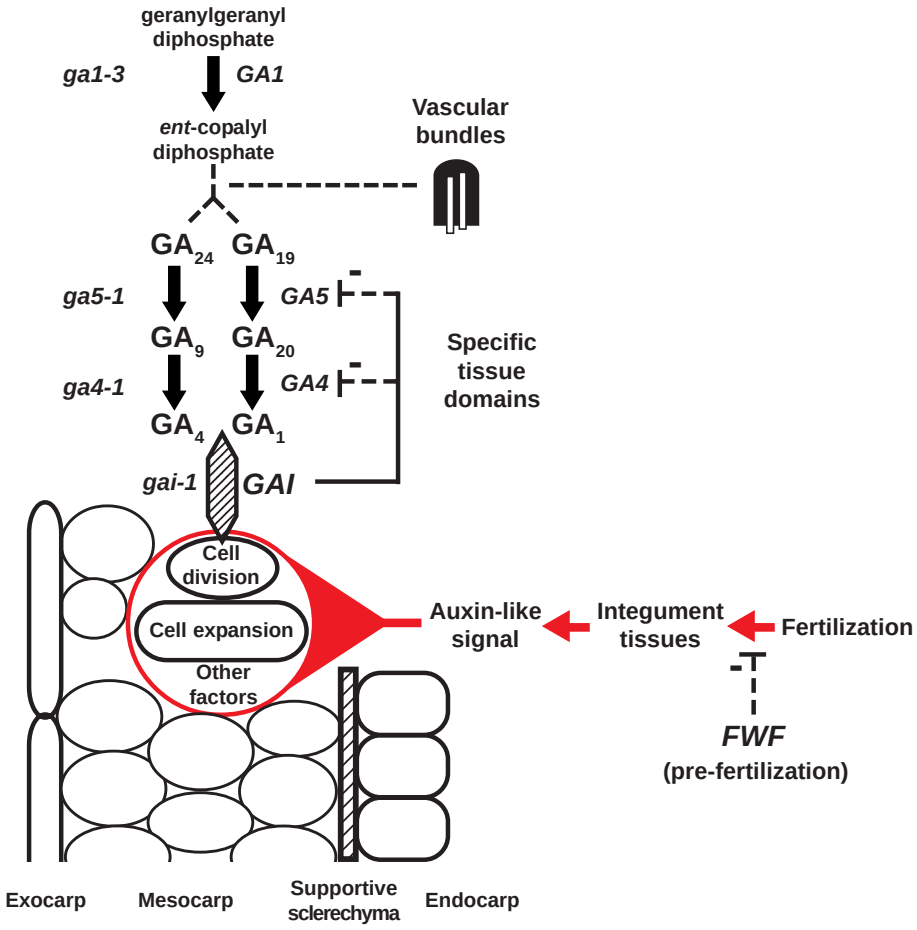
geranylgeranyl diphosphate
ga1-3
GA1
ent-copalyl diphosphate
Vascular bundles
GA24
GA19
ga5-1
GA5
GA9
GA20
ga4-1
GA4
GA4
GA1
Specific tissue domains
gai-1
GAI
Cell division
Cell expansion
Other factors
Auxin-like signal
Integument tissues
Fertilization
FWF
(pre-fertilization)
Exocarp
Mesocarp
Supportive sclerechyma
Endocarp

The petal phenotype of *fwf* resembles in some respects that observed in ethylene mutants. The plant hormone ethylene is known to play a role in coordinating the processes of floral senescence and post-pollination carpel development in a number of species (O'Neill and Nadeau, 1997). Ethylene can also modulate polar and lateral movement of auxin in aerial and root tissues (Chen et al., 1998; Morelli and Ruberti, 2000). However, the linkage of *FWF* to the ethylene or auxin perception pathway and its subsequent potential role in floral senescence and silique development remain to be determined.

The combination of *fwf* with the unitegmic ovule mutation *ats*, where the total number of integuments cell layers is reduced from five to three (Léon-Kloosterziel et al., 1994), relieved the requirement for emasculation of surrounding floral whorls and enhanced parthenocarpic silique development. This suggested that in wild type ovules, additional repressive signaling originating from the integument might be occurring to restrict silique growth in the absence of fertilization. This infers that events in the ovule might modify silique development in a manner dependent on long range signaling. However, the identity of *ATS* and its expression in the flower are unknown. The observed *ats* lesion in the ovule does not eliminate the possibility that *ATS* may also be expressed in the developing carpel and silique, acting to alter or direct the activity of genes in the carpel and silique tissues. Furthermore the composite integument structure in *ats* mutants may have resulted in a novel enhancing activity not functionally relevant in wild type ovules with distinct integument tissues. The inhibition of parthenocarpic silique development by outer floral whorls also implies a long range signaling influence from these floral organs on silique growth and further suggests that *FWF* may play a central but multifunctional role in the developmental transition between carpel maturation and the initiation of fruit development.

3.4.2 *FUL* and *FWF* are regulators of silique growth

Activity of the developmental gene *FRUITFULL* is also required for the transition between carpel and silique development. *FUL* determines the competency of the carpel tissues to develop into siliques. Mutations in *FUL* appear to prohibit mesocarp cell division and expansion normal to the plane of elongation post-fertilization even though the six cell layers of the carpel appear to differentiate (Gu et al., 1998; Bowman, 1999). Transverse sections however, show that *ful-1* fails to correctly control endocarp cell division pre-fertilization and *ful-1* carpels form twice the number of endocarp cell observed in wild type (Gu et al., 1998). Vascular bundle development in *ful-1* mutants is also dramatically reduced in carpels and in cauline leaves (Gu et al., 1998). By contrast the *fwf* mutation allows mesocarp cells to divide and expand during silique development and the *fwf* mutation enhances vascular development in lateral vascular bundles in parthenocarpic siliques. Siliques do not form in *ful-7 fwf* double mutants indicating that the cellular activity induced by the *fwf* lesion cannot compensate for the deficiency generated in the *ful-7* mutant. Thus, functional *FUL* activity is required for both parthenocarpic and pollination-induced silique growth and differentiation.

The activities of *FUL* and *FWF* pre-fertilization appear antagonistic in that *FUL* is a positive regulator of silique growth and tissue identity, and that *FWF* appears to have a repressive function. The effects of lesions in both of these genes on mesocarp tissue and vascular bundle development underscores the importance of these tissues in establishing and maintaining silique growth to achieve maximum growth potential. *FUL* and *FWF* may directly interact to modulate silique development and this can be tested once *FWF* is cloned.

3.4.3 *FWF* modulates mesocarp expansion but requires *GAI* for determining anticlinal cell division

Cell division and expansion in mesocarp are critical components for attaining final silique length. Growth contributing to silique width occurs by cellular expansion in all tissues (chapter 2.3.7; Figure 3.1). *FWF* might play a role in the regulation of mesocarp expansion and in the control of lateral vascular bundle development according to the model described in Figure 3.6. Autonomous mesocarp expansion and anticlinal mesocarp cell division occur in *fwf* suggesting that it may affect signal transduction that alters auxin and or GA perception. To elucidate the role of *FWF* in parthenocarpic silique development double mutants were constructed with the GA insensitive mutant, *gai-1* and the GA biosynthetic mutant, *ga1-3* (Figure 3.6).

GA1, which catalyzes the first step in GA biosynthesis, is expressed in the vascular tissues of the carpel (Sun and Kamiya, 1994), and *ga1-3* mutants require exogenous treatment with active GAs for silique development (Barendse et al., 1986). *spy* mutants, *rga* mutants and the complete loss of *GAI* function alleles (*gait-6* allele) partially restore GA deficient growth in vegetative tissues in *ga1-3* plants (Silverstone et al., 1998). Parthenocarpic silique development was not restored in *ga1-3 fwf* double mutants, demonstrating that parthenocarpic silique growth initiated by the *fwf* mutation is dependent on early GA biosynthesis steps regulated by *GA1* function (Figure 3.6).

GAI is a member of the *GRAS* or *SCARECROW*-like family (*SCL*; Pysh et al., 1999) and is required for the perception of active GAs (Figure 3.6). The mutant *gai-1* allele acts as a constitutive repressor of GA induced responses and siliques develop only in response to exogenous auxin application or pollination but not to exogenously applied GA_3 (chapter 2.3.6). The *gai-1 fwf* double mutants were found to be parthenocarpic when

emasculated, although, parthenocarpic siliques that developed, were reduced in silique length compared to the *fwf* single mutant.

Structural analysis of parthenocarpic and pollination-induced *gai-1 fwf* siliques revealed that anticlinal cell divisions observed in mesocarp tissues were absent and that silique development proceeded by cell expansion. These results indicate that mesocarp expansion, which is primarily repressed and mitigated by *FWF*, occurs independently of, or might precede *GAI* mediated GA perception (Figure 3.6). GA biosynthesis could also be activated in steps downstream of mesocarp expansion (Figure 3.6). Evidence that *FWF* limits the expansion of mesocarp cells, was also obtained when mesocarp cells of pollination-induced L.*er* and *fwf* mutant siliques were compared, revealing that mesocarp cells in pollination-induced *fwf* silique were larger in cross-sectional area. This suggests *FWF* would normally act in response to signals derived from pollination to limit gross mesocarp expansion. Gross mesocarp cell expansion is observed following auxin treatment to emasculated pistils (chapter 2.3.7). Therefore, the *gai-1 fwf* parthenocarpic phenotype could be explained if *FWF* was involved in repressing an auxin-like signal transduction cascade primarily controlling mesocarp cell expansion and also be involved in controlling GA related aspects of silique development mediated by *GAI* (Figure 3.6).

Recently several papers have demonstrated that GA 20-oxidase, a biosynthetic enzyme that catalyzes multiple steps in GA biosynthesis, has specific expression domains within the developing tomato fruit (Rebers et al., 1999), in watermelon integument tissues (Kang et al., 1999) and within tissues of the *Arabidopsis* inflorescences and siliques (Phillips et al., 1995; Sponsel et al., 1997). In *Arabidopsis GAI* and *RGA* negatively regulate the abundance of GA 20-oxidase (Peng et al., 1997; Silverstone et al., 1998; Figure 3.6) and this forms a self-regulating loop between GA signal transduction and GA

biosynthesis. Exogenous auxin, however, has been shown to increase GA 20-oxidase levels in developing pea pericarps (García-Martínez et al., 1997; van Huizen et al., 1995). Therefore expression domains of GA biosynthetic enzymes in inflorescences may play a role in the control of tissue proliferation within fruit, in response to auxin or auxin-like signal transduction cascades (Figure 3.6).

3.4.4 *GAI* mediated mesocarp anticlinal cellular division is uncoupled by lesions in *ATS*

Mesocarp anticlinal cell division occurs in parthenocarpic *fwf* siliques post-anthesis and is controlled by *GAI* and other factors (Figure 3.6). The *ats* mutation was found to alter parthenocarpic silique development and restore anticlinal mesocarp cell division in the gibberellin insensitive *gai-1 ats fwf* triple mutant. The *ats* lesion was also found to negate the requirement for emasculation of the *fwf* mutant when *fwf* was combined in the *pop1 ats fwf* triple mutant and siliques from this triple mutant approached lengths observed following pollination in wild type plants.

In *ats* mutants integument development is defective and single unitegmic structure replaces the outer and inner integuments that are normally observed in wild type plants (Baker et al., 1997; Léon-Kloosterziel et al., 1994). Genetic analysis has shown that the single integument in *ats* has attributes of both inner and outer integuments (Baker et al., 1997). Two explanations might explain the role of *ATS* in parthenocarpic silique development. One interpretation is that *ATS* forms a component of the GA signal transduction cascade within the ovule and floral whorls, and directly regulates GA biosynthesis or perception. An alternative explanation is that *ATS* occupies a central role in

Figure 3.7 (A) *SCL* or *GRAS* polypeptide consensus structure. The typical *SCL* gene has several domains and these include a variable N-terminal domain with homopolymeric repeat regions (NVD), a leucine heptad region (LHRI), a conserved VHIID motif, a second leucine heptad region (LHRII), a P-F-Y-R-E and a SAW motif. (B) A neighbor-joining tree constructed for amino acid sequences from the *Arabidopsis SCL* or *GRAS* family members including the *LATERAL SUPPRESSOR* amino acid sequence from tomato (Schumacher et al., 1999). Members of the *SCL* or *GRAS* family cloned on the basis of a mutant phenotype are indicated in red. The *SCL* gene member most similar to *SCR* (Genbank accession number, AB017067), maps close to *ATS* (chapter 6.2.2). Unnumbered *SCL* members have genbank accession numbers in superscript. Northern analysis has shown that *SCL1*, *SCL3*, *SCL5*, *SCL7* and *SCL14* are expressed in silique tissues (Pysh et al., 1999). Recent analysis of flanking sequences from a *Ds* insertion element database (Parinov et al., 1999) has revealed several other *SCL* genes already have *Ds* insertions (open triangles). Analysis of insertional mutants may help elucidate the role *SCL* gene family plays in fruit development. Distances between neighboring polypeptides were determined using the Juke-Cantor algorithm (Rice, 1994) and displayed using the TreeView program (Page, 1996).

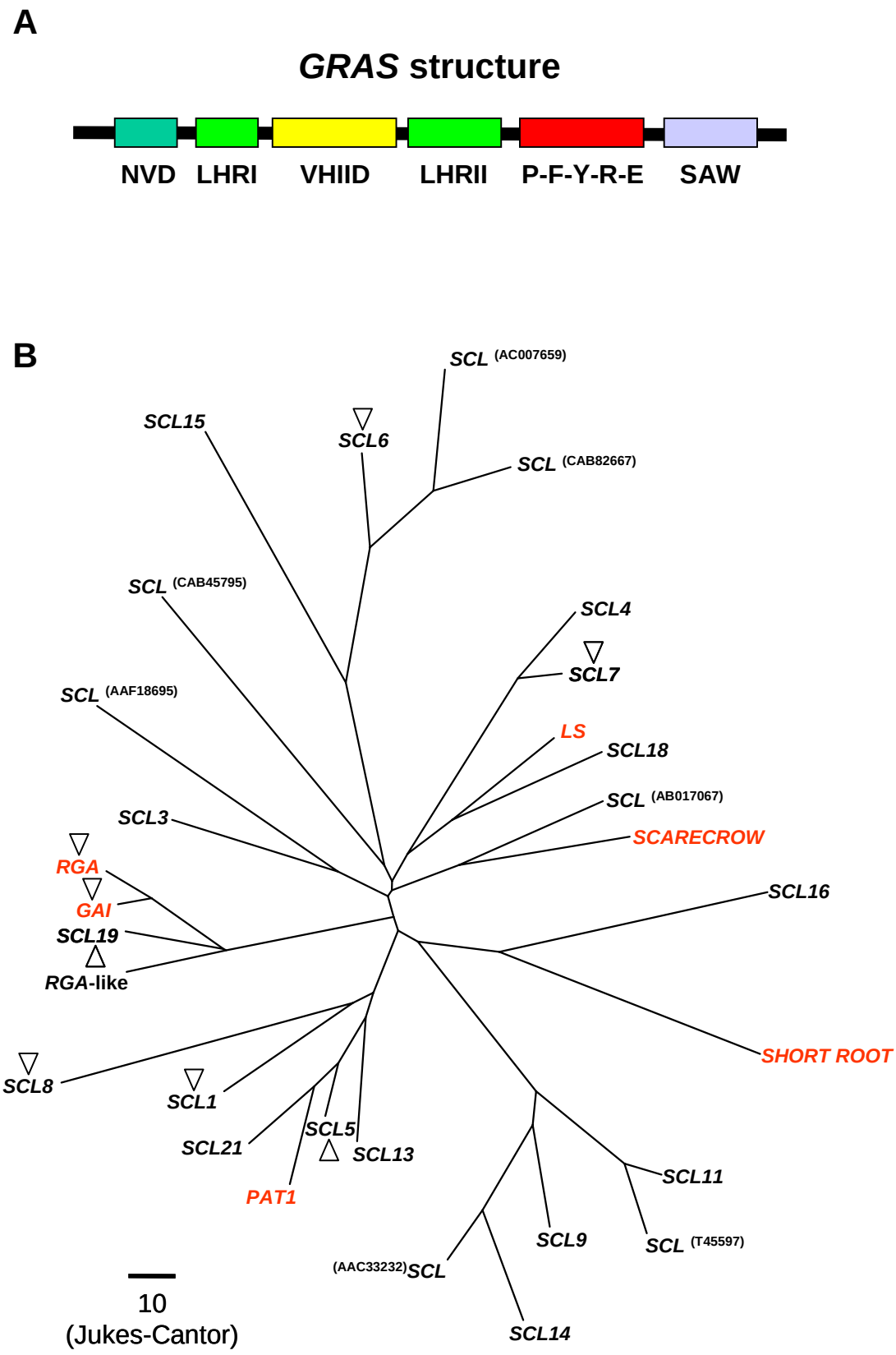
A
GRAS structure
NVD
LHRI
VHIID
LHRII
P-F-Y-R-E
SAW
B
SCL (AC007659)
SCL15
SCL6
SCL (CAB82667)
SCL (CAB45795)
SCL4
SCL7
SCL (AAF18695)
LS
SCL18
SCL (AB017067)
SCL3
SCARECROW
RGA
SCL16
GAI
SCL19
RGA-like
SHORT ROOT
SCL8
SCL1
SCL5
SCL21
SCL13
SCL11
PAT1
SCL9
SCL (T45597)
(AAC33232)SCL
SCL14
10
(Jukes-Cantor)

coordinating or communicating cell division and cell specification processes in ovules and carpels.

3.4.5 Is *ATS* a *SCL* gene or *GRAS* member ?

Asymmetric cell divisions play a critical role in the propagation and establishment of cellular patterns in plant development. Functional analysis of the *GRAS* or *SCL* gene family and their mutations (Di Laurenzio et al., 1996; Helariutta et al., 2000; Peng et al., 1997; Pysh et al., 1999; Silverstone et al., 1998; chapter 2.3) has shown that this gene family plays an important role in specifying asymmetric cell divisions and also in the control of transmissible growth signals. In *scr* mutants periclinal cell divisions are missing in the cortex-endodermal initial cells (Di Laurenzio et al., 1996). Cell lineages arising from these layers produce a composite cortex-endodermis tissue with missing cell layers compared to wild type roots. The mutant phenotype exhibited by *ats* has several similarities to the *scr* mutant in that *ats* mutants have missing integument cell layers and form a composite integument tissue. A *SCR*-like gene, most similar to *SCR* is present in the map location of *ats* (chapter 6.2.2; Figure 3.7) and as such seems a choice candidate for gene cloning.

3.4.6 Roles for *SCR*-like or *GRAS* members in silique growth and development

Searches of the *Arabidopsis* genomic sequence database and phylogenetic analysis show that the *SCL* gene family forms a large assemblage of proteins (Figure 3.7). The *SCL* gene family appears to have high conservation amongst plants, as one EST has been found in moss (*Physcomitrella patens*; Genbank accession number, AW497238) and has most similarity to the *SHORT ROOT* (*SHR*) gene of *Arabidopsis*. Several subfamilies of *SCL*

genes can be resolved in *Arabidopsis* and one cluster contains the *GAI* / *RGA* gibberellin signal transduction genes (Figure 3.7). Most information concerning the role of *SCL* genes in developmental processes has been obtained from studies of the genes of *GAI* (chapter 2.3.8), *SCR* and *SHR* (Di Laurenzio et al., 1996; Helariutta et al., 2000).

SCR is expressed in cells adjacent to vascular tissues and expression of *SCR* is ramified throughout the entire vegetative development (Wysocka-Diller et al., 2000). Intriguingly *SCR* expression is dependent on *SHR* that is expressed in the pericycle and vascular tissue of the root and controls asymmetric cell division in the endodermis (Helariutta et al., 2000). The mechanism by which *SHR* regulates *SCR* expression in adjacent cells is thought to be dependent on non-cell-autonomous factors (Helariutta et al., 2000). The mutants *shr* and *scr* mutants are also agravitropic, suggesting that *SCR* and *SHR* are involved in specifying cells in the endodermis and preparing these for gravity perception (Fukaki et al., 1998). In chapter 2.3.8 and in this study, the semi-dominant *gai-1* allele was shown to block anticlinal mesocarp cell division in the developing silique and the *ats* lesion restored anticlinal mesocarp cell division in a manner independent to that of the *gai-1* mutation in the *gai-1 ats fwf* triple mutant. This suggests *ATS* may modify *GAI* mediated processes in a manner similar to other members of the *GRAS* family.

GRAS gene function can also be extended to parthenocarpic fruit development in tomato. Mutations in another member of the *GRAS* family, the *LATERAL SUPRESSOR* gene (*LS*; Schumacher et al., 1999; Figure 3.7), suppresses secondary meristem initiation in tomato, and *ls* mutant flowers do not initiate petal formation (Szymkowiak and Sussex, 1993). An epistatic interaction has previously been found between the *ls* mutant and the *pat-2* allele that confers parthenocarpic fruit development in tomato (Philouze, 1983b). *ls* in this case, blocks the development of parthenocarpic fruit. Future approaches to studying

the roles other *SCL* genes play in fruit development may utilize insertional mutations already found in *Arabidopsis* (Figure 3.7).

The data presented in this chapter suggests that the manner by which *FWF* mitigates repression of silique development is likely to incorporate mechanisms for long-range signal transduction between ovule and carpel tissues. It has been shown that the activity of one *SCL* family member, *GAI*, is important for mesocarp cell development. The role of *ATS* in the process will be clarified once the identity of the gene is known.

The enhanced effect of the *ats* lesion on parthenocarpic silique development in the *fwf* background raises the question whether other specific ovule tissues have an effect on parthenocarpic silique growth. The involvement of cell division and specification by *SCL* gene members, and roles of vascular tissue during silique development, requires further developmental-genetic data to understand the transition between carpel and silique development, a step that is ultimately controlled by the female gametophyte.

Chapter 4: Fertilization independent fruit growth is governed by ovule organization and two distinct signal transduction pathways

4.1 Introduction

In flowering plants the reproductive cycle initiates with a change in plant growth phase from vegetative to floral and ends in the production of seeds and the surrounding fruit structures that facilitate seed dispersal. Once a flower is formed, growth of the floral organs diminishes. Double fertilization is the cue that triggers both the developmental transition of the female reproductive structure the carpel into a fruit, and the ovules inside the carpels into seeds in a coordinated manner to facilitate seed dispersal at maturity. If fertilization does not occur by the end of a specific developmental window of time referred to as female receptivity, the flower undergoes senescence and some or all of the floral organs will abscise. The molecular cues that trigger and coordinate the transitions between flower and fruit development and senescence are largely unknown.

Double fertilization occurs inside the ovule and involves defined fusion events between sperm cells of the male gametophyte with specific cell types of the female gametophyte (Russell, 1993). An important question is how information from this event within the female gametophyte, which directly results in seed formation, is transmitted or used to enable the coordinated development of the carpel into the fruit. In different plant species, the fruit growth response is determined by the number of fertilized ovules (García-Martínez et al., 1991a; Gonzalez et al., 1998; Meinke and Sussex, 1979; Srinivasan and Morgan, 1996; Varge and Bruinsma, 1976) suggesting that each fertilized ovule contributes individually, but in an additive manner to control the overall growth of the fruit.

Recently *Arabidopsis* mutants designated *mea*, *fis* and *fie* have been characterized, in which the initiation of seed and fruit development is uncoupled from fertilization (Grossniklaus et al., 1998; Luo et al., 1999; Ohad et al., 1999). When these mutants are in a

male sterile background, autonomous endosperm formation is initiated in the central cell and the fruit or silique forms, matures and dehisces. The functionally different *MEA*, *FIS* and *FIE* proteins are thought to form a complex that represses seed development in the absence of fertilization (Chaudhury et al., 1997; Ohad et al., 1999). In agreement with this prediction, expression of these genes co-localizes to nuclei of the mature female gametophyte but they are also co-expressed in nuclei formed during the early events of endosperm formation (Luo et al., 2000; Vielle-Calzada et al., 1999). While the molecular cues that enable silique development in these mutants are unknown, it has been suggested that silique formation might result from developmental cues elicited from endosperm formation in the unfertilized ovules (Ohad et al., 1999).

Seed and fruit development is also uncoupled from fertilization in flowering plants that undergo parthenocarpy, or seedless fruit formation. Parthenocarpy has a genetic basis in examined species (chapter 3) but it can also be induced in non-parthenocarpic plants by the exogenous application of various plant growth regulators to carpels (chapter 2). Nitsch, (1970) proposed that parthenocarpy may result from alterations in the spatial and temporal synthesis of plant hormones within carpel tissues. Rotino et al., (1997) and Ficcadenti et al., (1999) demonstrated that the expression of a bacterial auxin biosynthesis gene in the ovules of eggplant and tomato leads to the production of parthenocarpic fruit supporting the concept of Nitsch, (1970), but further indicating increased auxin synthesis within ovules can induce parthenocarpic fruit development. An understanding of how fruit initiation occurs in the absence of fertilization should provide information concerning the molecular factors that regulate the floral to fruit transition, influence fruit growth and differentiation, and affect entry into the senescence pathway.

Chapter 3, described the characterization of a parthenocarpic *Arabidopsis* mutant called *fruit without fertilization* (*fwf*). Genetic analysis showed that *fwf* is a recessive

mutation. As this is consistent with a loss of function, it was proposed that in wild type plants *FWF* functions to suppress fruit growth in the absence of fertilization and that cues from fertilization may mitigate this repression enabling the coordinated development of the seed and fruit (chapter 3.4).

Characterization of the *fwf* mutant provided several lines of evidence that signaling from ovules might play a role in parthenocarpic fruit formation (chapter 3) as has been implied from fertilization-dependent processes. For example, the period that *fwf* ovules are receptive to fertilization coincides with the period of parthenocarpic silique development suggesting that functional ovules may be required to transduce a signal that allows silique formation to occur (chapter 3.3.1). The control of cell division, expansion and differentiation in developing silique mesocarp tissue was shown to involve GA biosynthesis and perception together with an auxin-like signal (chapter 3.3.9). The control of mesocarp cell proliferation was altered in the *aberrant testa shape* (*ats*) mutant background that modifies integument development in the ovule (Léon-Kloosterziel et al., 1994). This suggested that structural determinants of the ovule might be producing molecules that modulate silique growth in the *fwf* mutant background. However, as *ats* has not been cloned the possibility that the mutation may subtly affect expression in carpel and silique tissues could not be discounted. The possibility that events in specific ovule tissues may influence the carpel to silique transition requires further investigation in other ovule mutants where the genetic lesions are known.

The plant hormone ethylene is known to affect floral growth, senescence and fruit development (O'Neill and Nadeau, 1997; O'Neill et al., 1993; Orzáez et al., 1999; Sato-Nara et al., 1999). Ethylene is also thought to coordinate post-pollination inter-organ responses (O'Neill and Nadeau, 1997). Data concerning the expression of ethylene biosynthesis and perception components suggests linkage of ethylene to carpel and ovule

growth and senescence. In *Arabidopsis* the molecular components of ethylene perception *ERS2* and *ETR2* are expressed at high levels in petals, ovules and in the funiculus, a tissue that connects the ovule to the ovary wall (Hua et al., 1998; Sakai et al., 1998). In tobacco, down regulation of ACC oxidase an enzyme responsible for the synthesis of ethylene from ACC results in the arrest of ovule development (De Martinis and Mariani, 1999) indicating that ethylene biosynthesis is required for subsequent cellular organogenesis. *Arabidopsis ctr1-1* mutants exhibit constitutive ethylene response (Kieber et al., 1993), precocious pistil elongation prior to anthesis (Alonso et al., 1999) and have reduced transmission through the female gametophyte (Roman et al., 1995). A reduction in transmission through the female gametophyte and precocious pistil elongation indicate *CTR1* maybe required for fertilization dependent processes or the induction of seed development (Drews et al., 1998), however unlike *fwf*, they do not form parthenocarpic siliques.

In this chapter, the hypothesis that signal transduction events between the ovule and the carpel are essential for the initiation of parthenocarpic fruit development in *Arabidopsis* is tested. The role of ethylene perception in coordinating the initiation and regulation of silique development is also examined by double mutant analysis. The data shows that the presence and integrity of specific ovule tissues is required to regulate the carpel to silique transition and that ethylene perception plays an important role in the control of fertilization independent silique formation.

4.2 Materials and methods

Plant growth conditions, methods for emasculation, application of plant growth regulators and histology are as described in chapter 2.2. Unless stated, *fwf* siliques above flower position 30 were observed, photographed and collected for sectioning during

subsequent genetic analysis. Ovules were cleared using Hoyers solution (Zhang and Somerville, 1997; 100 g chloral hydrate; 5 ml glycerol; 30 ml H_2O).

4.2.1 Genetic analysis of *fwf* and multiple mutant lines

In most genetic crosses the L.*er* ecotype was used unless stated. The following mutants were obtained from the Arabidopsis Biological Resource Center; *ats*, *bel1-1, ctr1-1* (Col), *etr1-3* (Col), and *ein6*. The *ant* and *ino* mutants were a gift from Kay Schneitz.

The majority of multiple mutant lines containing *fwf* or *ctr1-1* were obtained by crossing homozygous lines together and identifying homozygous *fwf* or *ctr1-1* F_2 individuals that segregated in the F_3 for the alternative mutation. At times, homozygous multiple mutants could be identified unequivocally amongst the F_2 segregants and when necessary these plants were progeny checked or testcrossed.

Several multiple mutants required media supplements or a specific selection procedure. Identification of the *bel1-1 fwf* double mutants was facilitated by a PCR based method (Western and Haughn, 1999) because mutations were closely linked. *Bsa* AI (New England Biolabs, Beverly, MA, USA) was used to cleave *bel1-1* PCR products and to identify homozygous *fwf* lines segregating for *bel1-1* mutation. Homozygous lines containing *ctr1-1* were selected on the basis of their seedling phenotype. The *fwf* NIL (Near Isogenic Line in the Col-1 background; chapter 3.3.1) was used to create the *ctr1-1 fwf* double mutant and maintain the Columbia background for comparison of silique growth with *ctr1-1* plants. This also avoided the *erecta* mutation, which enhanced the *ctr1-1* mutant phenotype (not shown). Plants containing the *pop1* mutation (allelic to *cer6*) were male sterile at relative humidities less than 50%, but set fertile seed when transferred to 95% relative humidity (Hülskamp et al., 1995).

Double and triple mutant combinations with *fis* required a backcrossing strategy due to reduced female transmission (Chaudhury et al., 1997). *fis-2*, a kanamycin resistant *Ds* tagged line (Luo et al., 1999) was used as the pollen donor to homozygous *pop1 fwf, ats fwf* or *ctr1-1* mutants. Progeny containing *fis-2* were selected on MS media containing 50 μg ml^{-1} (w/v) kanamycin and were backcrossed to the respective homozygous lines up to three times. Lines containing *ats*, could not be surface sterilized, and plants that grew on MS media containing 1% agar and 50 μg ml^{-1} kanamycin were transferred to soil after 7 days growth and analyzed for 50% seed lethality associated with *fis-2*. *fis-2* plants do not exhibit strong phenotypic expression when grown under low light (M. Luo and A. Chaudhury, unpublished observations). The degree to which *pop1 fwf*, *ats fwf*, and *ctr1-1* interacted with *fis-2* was determined by comparing silique development under two different growth regimes. Single, double and triple mutant combinations were grown and assessed at 20°C with a 16 h day length (150 μmol m^{-2} s^{-1} light) or at 25°C under continuous light (250 μmol m^{-2} s^{-1}).

4.3 Results

4.3.1 Selection of mutants for the examination of the relationship between ovule structure and silique development in *fwf*

Mature *Arabidopsis* ovules are composed of a centrally located mature female gametophyte surrounded by an endothelium, a three-cell layer inner integument and a two-cell layer outer integument (Figure 4.1A). *fwf* mutants develop comparatively normal ovules (Figure 4.1A), however the outer integument extends further than the inner integument in 19% of ovules (chapter 3.3.1). One interpretation of the observation that parthenocarpic silique development in *fwf* is enhanced in the *ats* mutant background is that alterations in the integrity of the integument tissues modulate silique growth (chapter 3.4.1

Figure 4.1 Parthenocarpic silique development at 7 days post-anthesis in *fwf* (A) or in double mutants combining *fwf* with various ovule mutants designated in the cartoon (B-F). (B) The *ant* mutant is blocked in integument morphogenesis. Parthenocarpic development of *ant* carpels occurs following GA_3 or NAA treatment (10 *n*mol pistil^{-1}), however emasculated *ant fwf* double mutants are non-parthenocarpic. (C) *bel1-1* mutants have aberrant integument identity and lack a functional female gametophytes. Emasculated *bel1-1* pistil 7 day post-anthesis in comparison to a non-parthenocarpic *bel1-1 fwf* pistil from a flower at position 20-30 that lacks homeotic conversions of the ovule outer integument into carpel-like structures. Carpel-like structures do proliferate at later flower positions (see figure 4.3). (D) *ino* mutants do not develop an outer integument but *ino fwf* double mutants are parthenocarpic. *ino* mutants heterozygous for *fwf* also display weak parthenocarpic silique development. (E) *ats* mutants have a unitegmic ovule structure comprised of a composite or fused inner and outer integument. *pop1 ats fwf* triple mutants have enhanced parthenocarpic silique development compared to non-emasculated *pop1 fwf* and emasculated *fwf* (A). (F) *fis-2* mutants have autonomous silique growth and initiate seed-like structures when endosperm development occurs. Silique growth in *pop1 fwf fis-2* / + triple mutants grown either (a) under low light or (b) high light growth conditions suggests that *fwf* and *fis-2* are independent or in the same pathway. up, unpollinated. Scale bar: 3 mm

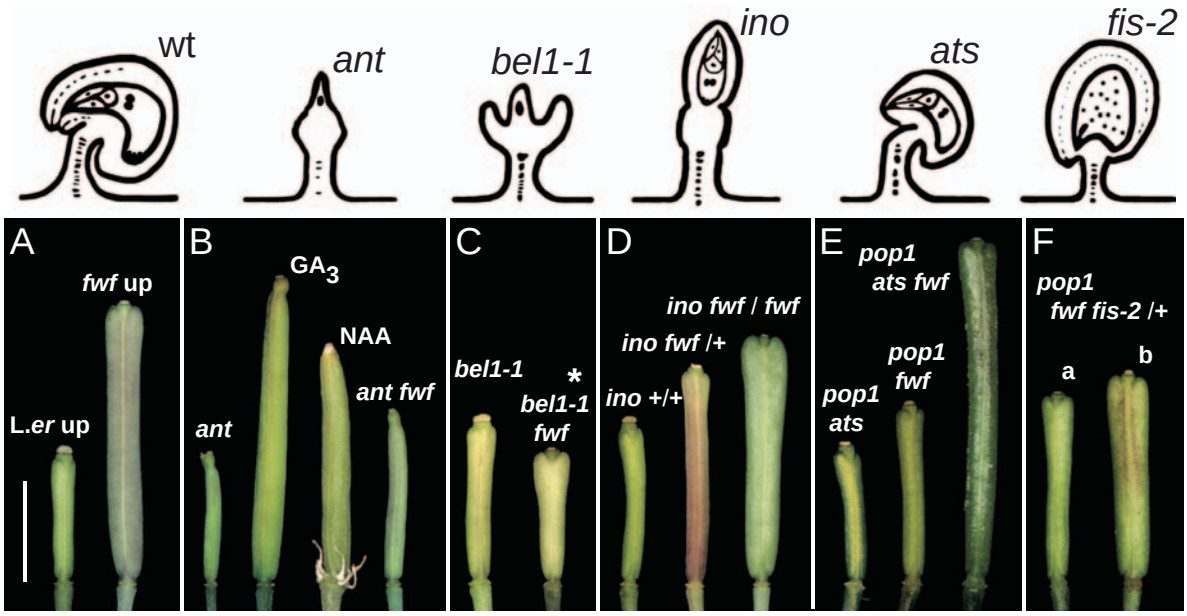
wt
ant
bel1-1
ino
ats
fis-2
A
fwf up
L.er up
B
GA3
NAA
ant fwf
ant
C
bel1-1
*
bel1-1
fwf
D
ino fwf / fwf
ino fwf /+
ino +/+
E
pop1
ats fwf
pop1
fwf
pop1
ats
F
pop1
fwf fis-2 /+
a
b

and 3.4.4). To determine whether ovules contain tissue specific regulatory elements involved in controlling the extent to which siliques develop crosses were performed between *fwf* and other *Arabidopsis* ovule mutants that arrest at various stages of ovule growth and differentiation (Baker et al., 1997; Schneitz et al., 1997).

Mutants were selected where the genetic lesion has been fully characterized and the spatial and temporal pattern of gene expression within the ovule and carpel is known. Figure 4.1 shows the types of ovule mutants selected and the developmental stages at which they arrest. *ant* mutants have severely disrupted integument development and megaspore mother cells sometimes arise, but fail to form a functional female gametophyte (Figure 4.1B; Elliott et al., 1996). *BEL* is required early during ovule identity to promote integument initiation (Western and Haughn, 1999), and *bel1-1* mutants lack an inner integument (Figure 4.1C). The outer integuments arise but stochastically develop into carpel-like structures (Modrusan et al., 1994). *ino* mutants lack outer integument development, but develop an orthotropous ovule with inner integument and functional embryo sac (Figure 4.1D; Villanueva et al., 1999). *fis-2* is a female gametophytic mutation and mutants develop autonomous seed-like structures containing diploid endosperm (Figure 4.1F; Luo et al., 1999). The effects on silique development from each resulting mutant combination with *fwf* are described below (Figure 4.1).

4.3.2 *ant fwf* and *bel1-1 fwf* double mutants indicate a functional ovule is required for parthenocarpic silique formation

The *ant fwf* double mutant did not develop parthenocarpic siliques (Figure 4.1B; Table 4.1). This was not related to an associated *ant* defect that influenced silique formation. Figure 4.1B shows that treatment of emasculated *ant* pistils with GA_3 and NAA (10 *n*mol pistil^{-1}) resulted in the formation of siliques indicating that these hormones are

Table 4.1 Silique lengths in mutant genotypes

	Silique length (mm ± s.d.)		
genotype / treatment	**male sterile (non-emasculated)**	**emasculated**	**pollinated**
L.*er*	-	4.5 ± 0.5	12.8 ± 1.1
pop1	4.3 ± 0.4	-	-
fwf	-	7.5 ± 1.0	11.0 ± 1.4 [a]
pop1 fwf	5.5 ± 0.7	-	-
fwf / +	4.8 ± 0.3	-	-
ant	4.3 ± 0.5	5.3 ± 0.6	-
ant + NAA [b]	-	7.1 ± 0.6	-
ant + GA3 [b]	-	8.3 ± 1.3	-
ant + BA [c]	-	5.2 ± 0.4	-
ant fwf	4.9 ± 0.7	5.0 ± 0.4	-
ant ctr1-1	4.7 ± 0.6	5.0 ± 0.4	-
bel1-1	5.3 ± 0.6	-	-
bel1-1 ctr1-1	5.7 ± 0.8	-	-
bel1-1 fwf	8.2 ± 0.2 [d]	-	-
ino	-	4.3 ± 0.7	-
ino fwf / +	-	5.8 ± 0.5	-
ino fwf / *fwf*	-	7.9 ± 0.5	-
ino ctr1-1	-	6.8 ± 0.8	-
ats	-	4.2 ± 0.5	12.1 ± 0.6
pop1 ats	5.3 ± 0.5	-	-
ats fwf	-	9.3 ± 0.7	-
pop1 ats fwf	9.1 ± 0.6	-	-
pop1 ats fwf [e]	9.9 ± 0.8	-	-
ats ctr1-1	-	8.2 ± 1.2	14.2 ± 0.9
pop1 ats ctr1-1	6.7 ± 0.5	-	-
fwf NIL (Col-1)	-	5.7 ± 0.4	-
ctr1-1	-	3.9 ± 0.4	12.1 ± 0.3
pop1 ctr1-1	4.4 ± 0.3	-	-
ctr1-1 fwf NIL	-	5.9 ± 0.5	-
ctr1-1 fwf ER (F_2)	-	6.8 ± 0.8	-
ein2	-	4.4 ± 0.5	-
ein2 + BA [c]	-	6.6 ± 0.9	-
ein6	-	3.6 ± 0.5	12.6 ± 0.9
ein6 + GA_3 [b]	-	8.4 ± 2.0	-
ein6 ant	-	4.8 ± 0.3	-
ats fwf fis-2 / + [e]	-	8.9 ± 0.6	-

pop1 containing were assayed under male sterile conditions; [a] pollinated with L.*er*; [b] emasculated pistil treated with 10 *n*mol pistil^{-1}; [c] emasculated pistil treated with 1 *n*mol pistil^{-1}; [d] with carpel-like structures; [e] high light growth condition

perceived by *ant* carpels and enable silique formation in the absence of a functional ovule. Flowers immediately above the GA_3 treated pistil also developed parthenocarpically indicating that GA_3 or a GA stimulated product is transported to induce parthenocarpic development in other receptive *ant* flowers. The inability to form parthenocarpic siliques in the *ant fwf* double mutant indicates that in *fwf*, silique formation is categorically dependent upon ovule development beyond the point arrested by the *ant* lesion.

Similarly, parthenocarpic silique development was not observed when *bel1-1 fwf* double mutant flowers were emasculated at early flower positions (Figure 4.1C). *bel-1* single mutants have a stochastic capacity to develop carpel-like structures from positions where the outer integuments of the ovule would form (Modrusan et al., 1994). The development of such carpel-like structures contributed slightly to pistil growth in emasculated *bel-1* mutants (Table 4.1; Figure 4.1C). When *bel1-1 fwf* pistils lacking carpel like structures were examined for growth post-emasculation between flower positions 20 and 30, the mean final pistil length was 4.4 ± 0.4 (n = 15). This is not significantly different to wild type L.*er* emasculated pistils, but is significantly less than the 7.2 to 7.5 mm parthenocarpic silique lengths obtained following emasculation of the *fwf* mutant flowers (chapter 3.3.1;Figure 4.1A and 4.1C; Table 4.1). Therefore *bel1-1* is epistatic to *fwf* in the context where carpel-like structures are not initiated inside *bel1-1 fwf* pistils.

In *bel1-1 fwf* mutants after flower positions 20 to 30, however, a distinct alteration in the frequency of carpel-like structures was observed compared to that in *bel1-1* mutants and this correlated with increased silique elongation (Figure 4.2A and 4.2B). The longest siliques were observed when all ovules in *bel1-1 fwf* mutants were converted to carpel-like structures. Funicular development was impaired as long aberrant green funiculi were produced (Figure 4.2B). The septum appeared to tear as the silique expanded and siliques were broad shouldered possibly because replum development was incomplete.

Figure 4.2 Frequency of homeotic conversions of ovules into carpel-like structures in *bel1-1* single mutant and *bel1-1 fwf* double mutants. (A) Homeotic conversion of *bel1-1* shaped ovules into carpel-like structures in *bel1-1* (circles) and the *bel1-1 fwf* double mutant (triangles) and the relationship of this to final silique length. (B) *bel1-1* single and *bel1-1 fwf* double mutants showing silique morphology and the distribution and proliferation of carpel-like structures within the silique. Funiculi of *bel1-1 fwf* double mutants develop aberrantly and are long, green and thin (arrow). Scale bar: 3 mm.

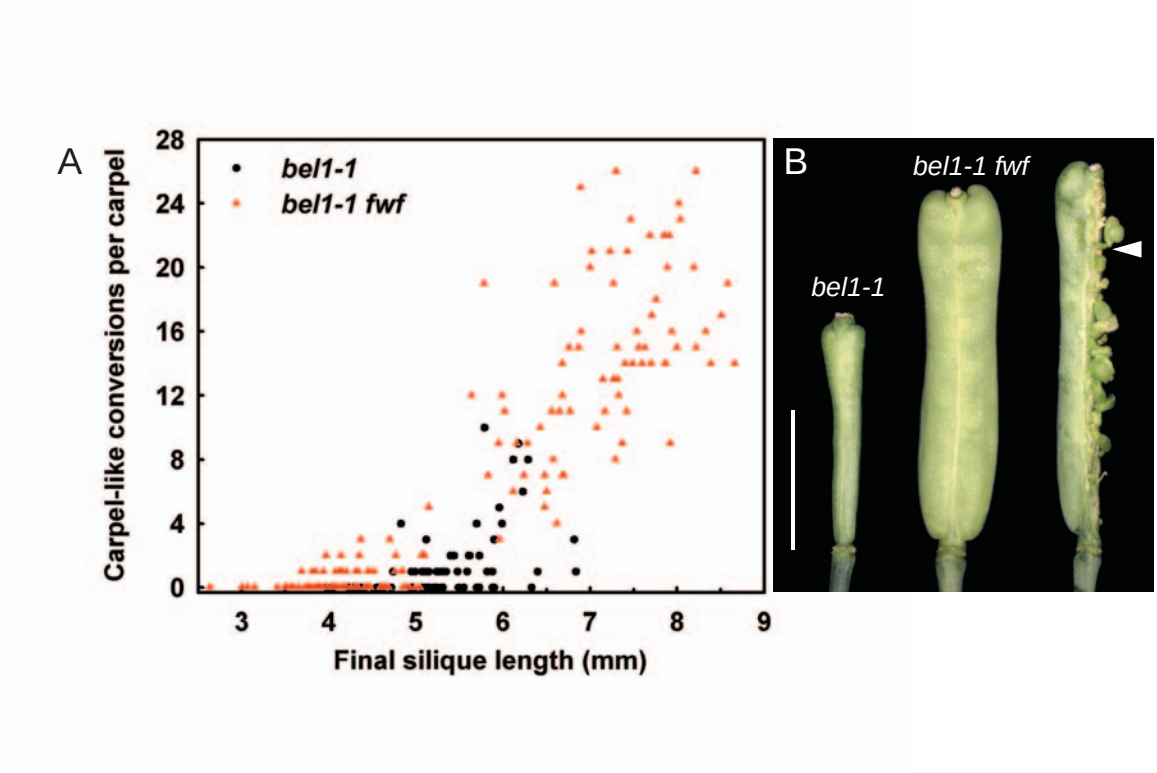
A
Carpel-like conversions per carpel
28
24
20
16
12
8
4
0
bel1-1
bel1-1 fwf
3
4
5
6
7
8
9
Final silique length (mm)
B
bel1-1
bel1-1 fwf

Like *ant*, parthenocarpic development could also be induced in *bel1-1* single mutants with the application of GA_3 or NAA (10 *n*mol pistil^{-1}; Table 4.1), but neither treatment was able to phenocopy the carpel-like development seen in the *bel1-1 fwf* double mutant (not shown). This indicates that the *fwf* lesion reinforces the homeotic conversion and autonomous proliferation of carpel-like structures in later floral positions, and further indicates that autonomous silique development only occurs in *bel1-1 fwf* double mutants when development of the carpel-like structures are initiated. Analysis of *bel1-1 fwf* and *ant fwf* mutants indicates that the stimulus for silique development in the *fwf* background originates from tissues fated within a functional ovule, or in the case of *bel1-1 fwf* a developing carpel-like structure.

4.3.3 Dissection of ovule tissues critical for parthenocarpic silique development using *ino fwf*, *ats fwf* and *fwf fis-2* mutants

ino fwf double mutants developed parthenocarpic siliques (Figure 4.1D). The genetic removal of the outer integument by the *ino* lesion did not alter the final parthenocarpic silique length or the degree of parthenocarpic development compared to emasculated homozygous *fwf* plants (Figure 4.1D; Table 4.1). The outer integument is therefore not a critical component in the control of parthenocarpic silique development in the *fwf* background.

A secondary effect of the *ino* mutation was also uncovered in an analysis of the F_2 segregants resulting from the selfing of F_1 individuals from the *fwf* and *ino* intercross. F_2 plants emasculated above flower position 30, showed an additional parthenocarpic phenotype with a mean silique length that was intermediate between homozygous emasculated *fwf* and emasculated L.*er* (Table 4.1). This intermediate class correlated with the *ino* mutation in a heterozygous *fwf* background (Table 4.1; Figure 4.1D). Observed

segregation ratios in this cross were 73 : 45 : 12 : 15 : 5, where the phenotypic classes were, wild type : *fwf* : *ino* : *ino fwf* / + : *ino fwf*. The number of *fwf* individuals were greater than expected, when the *ino* and *ino fwf* / + classes were combined, and the observed segregation ratio compared to the expected ratio of 9 : 3 : 3 : 1 for two independently segregating loci ($\chi^2 = 13.8$, $P < 0.005$). Therefore, *fwf* does not segregate in a normal mendelian recessive manner in an *ino* mutant background. *fwf* might alternatively be semi-dominant, or be involved in a threshold type response in particular mutant backgrounds.

The observed phenotypic ratios of parthenocarpic *ino fwf* / +, *ino* and *fwf* plants could otherwise indicate a gametophytic interaction between *INO* and *FWF* in the ovule. A possibility existed that the elevated *fwf* class and the observed *ino fwf* / + class could occur because FWF activity might be required to repress fertilization-dependent silique development from within the female gametophyte and INO is required in maternal sporophytic tissues to modulate FWF related activity. If this were the situation, the expected ratio for parthenocarpic silique development classes resulting from a segregating F_2 intercross would be 5 : 7 : 1 : 2 : 1, where the phenotypic classes are wild type : *fwf* : *ino* : *ino fwf* / + : *ino fwf*. However, when the observed segregation was tested against the expected ratio for a gametophytic interaction between INO and FWF the observed pattern remained significantly different ($\chi^2 = 24.5$, $P < 0.001$). This suggests that FWF may not function explicitly in a gametophytic manner modulated sporophytically by INO.

Figure 4.1E shows the degree of silique elongation in *pop1 ats fwf* triple mutants compared with male sterile *pop1 ats* and *pop1 fwf* double mutants. It has been shown genetically that the *ats* mutant has a composite integument nature (Baker et al., 1997) and parthenocarpy is enhanced when *fwf* is combined with this background (chapter 3.3.5). *ino fwf* homozygous mutants did not show enhanced parthenocarpic silique development

(Table 4.1). This indicates that the outer integument plays a minor role in regulating signal transduction regulating fruit initiation when *FWF* is mutated. In *ats* mutants, the function of inner integument cell layers or the endothelium may be altered, accounting for the enhanced parthenocarpic silique development.

fis-2 mutants have a female gametophytic mutation that allows the initiation of fertilization-independent seed and silique development, *fwf* was combined with *fis-2* to examine if a genetic interaction existed between these two mutants. Double mutants were assayed under low light and high light conditions (Figure 4.1F; Table 4.2). As previously reported, male sterile homozygous and heterozygous *fis-2* lines develop autonomous seed-like structures and produce diploid endosperm in 100% and 50% of ovules respectively, but only when grown under high light conditions described in the materials and methods (Table 4.2). Male sterile *pop1 fwf* mutants heterozygous for *fis-2* did not display enhanced silique development nor was the number of seed-like structures altered under low light or high light growth conditions when compared with the level expected for *fis-2* heterozygous plants (Table 4.2). Enhanced silique development was not observed in emasculated *ats fwf fis-2* / + mutants (Table 4.2). An additive effect on either autonomous silique development or endosperm proliferation would be expected if *fis-2* and *fwf* acted in a separate pathway. Therefore the *fwf* and *fis-2* genetic lesions may act independently or *fwf* could function as a repressor of silique development that acts directly downstream of endosperm development conferred by the maternal effect *fis-2* mutation.

Taken together these data indicate that the outer integument of the ovule is not critical for parthenocarpic silique development but that the female gametophyte, endothelium and inner integument may individually or collectively synthesize molecules that direct parthenocarpic silique development.

Table 4.2. Autonomous seed-like structures and silique length when *fwf* and *ctr1-1* are combined with *fis-2*.

genotype	seed-like structures (± s.d.)	silique length (mm ± s.e.)
pop1 fwf [a]	0	5.4 ± 0.4
[†]*fis-2 fis*-2 [a]	0.3 ± 0.8	3.8 ± 0.4
[†]*fis-2 fis-2* [b]	39.6 ± 4.0	6.2 ± 1.0
ant fis-2 / + [b]	-	4.7 ± 0.5
pop1 fwf fis-2 / + [a]	0.8 ± 1.1	5.6 ± 0.5
pop1 fwf fis-2 / + [b]	23.7 ± 7.6	6.3 ± 0.4
[†]*ctr1-1 fis-2* / + [a]	13.6 ± 7.9	8.0 ± 1.2
[†]*ctr1-1 fis-2* / + [b]	11.9 ± 9.1	6.8 ± 0.6

[a] low light regime and [b] high light regime; [†] emasculated; *pop1* containing individuals were assayed under male sterile conditions

4.3.4 Vascular development in ovules during silique development

Examination of parthenocarpic silique development in *fwf* plants containing various ovule defects showed that the structured integrity of the ovule is an important factor in enabling parthenocarpic silique development. An important question is how is the information from the ovule being transmitted to the carpel to enable these processes of silique development. In chapter 3.4.1 it was hypothesized that *FWF* may repress mesocarp expansion and vascular differentiation within the silique through a pathway that may involve an auxin-like signal. A preliminary study was carried out to examine vascular development between the ovule and carpel in wild type and selected mutants. This study was primarily aimed to further understand the relationship between the higher frequency of carpel-like structures and the increased silique length in *bel1-1 fwf* plants, and also the absence of parthenocarpic silique development in *ant fwf* double mutants.

Vascular differentiation at different stages in cleared wild type L.*er* ovules and pistils is shown in Figure 4.3. The staging of ovule development used was that described by Schneitz et al., (1995) and their studies have determined that the development of vasculature in the ovule funiculus is initiated at stage 2-III when integument primordia become visible at stage 10 of floral development (Bowman, 1993). Contrary to the observations of Schneitz et al., (1995), pro-vascular development in L.*er* was not visible in cleared ovules until stage 3-II to 3-III (Figure 4.3A and 4.3B). At stages 3-IV to 3-V the differentiation of vascular tissue begins and vascular strands are observed towards the chalazal end of the funiculus and the funiculus base (Figure 4.3C). At this stage ovules have an inner integument that completely surrounds the nucellus and female gametophyte development is in transition from a four-nucleate state to an eight nucleate embryo sac. In stage 12 wild type flowers, the ovule is mature (stage 3-VI; Schneitz et al., 1995) and pre-fertilization vascular development is complete. A single vascular element is evident that

Figure 4.3 Vascular differentiation during ovule development in L.*er*. (A) Vascular differentiation is not apparent in wild type ovules at stage 2-IV to 2-V. (B) Pro-vascular differentiation begins in stages 3-II to 3-III. (C) At ovule stage 3-IV vascular and pro-vascular strands become visible in the chalazal region and at the base of funiculus respectively. (D) At anthesis vascular differentiation is complete at stage 3-VI and a single vascular element is observed. This begins in the chalazal region of the ovule and terminates at the base of the funiculus with a tear-drop tracheid element (arrow). (E) In unfertilized *pop1* pistils 3 days post-anthesis further vascular differentiation was not observed. (F) Post-fertilization, vascular differentiation was observed in the funiculus-replum boundary region when embryos reached late globular (F) and heart stage (G, arrows). Post-fertilization vascular differentiation results in a contiguous vascular element that extends from the base of the funiculus towards the replum vasculature. c, chalazal region; fv, funiculus vasculature; ii, inner integument; n, nucellus; oi, outer integument; pv, pro-vascular tissue; rv, replum vasculature; m, micropyle. Scale bar, 40 μm

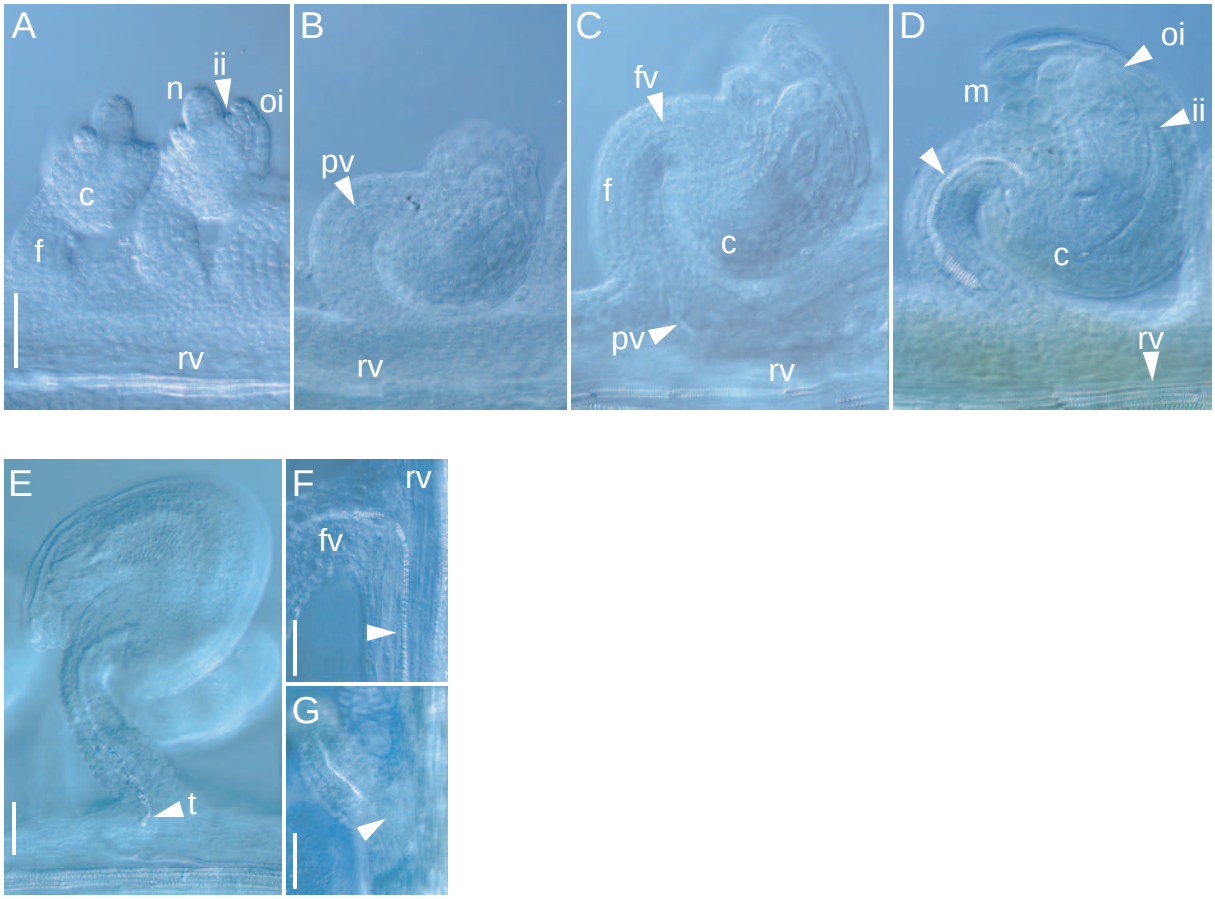
A
ii
n
oi
c
f
rv
B
pv
rv
C
fv
f
c
pv
rv
D
oi
m
ii
c
rv
E
t
F
rv
fv
G

initiates in the chalazal region and terminates adjacent to the replum vasculature with a tear-drop tracheid element (Figure 4.3D). Examination of unfertilized pistils 3 days post-anthesis (n = 6) showed that no further vascular differentiation occurred and as such funiculus vasculature and replum vasculature remained separated (Figure 4.3E). Further vascular development occurs post-fertilization in developing seeds once the embryo reaches the globular stage of development. A new vascular element differentiates and there is a contiguous vascular connection between the funiculus and replum (Figure 4.3F and 4.3G arrow).

Vascular differentiation in *ant* ovule primordia has been studied by Schneitz et al., (1997) who examined several *ant* alleles and showed that vascular development did not occur in *ant* ovule primordia and funicular tissue. Vascular differentiation was also absent in *ant fwf* double mutant ovules and funiculi (Figure 4.4A). A single tear-drop tracheid element was occasionally observed in the position normally occupied by a differentiating megaspore mother cell (Figure 4.4B). This has also been previously observed in *ant* single mutants (not shown; Elliot et al., 1996).

The early pattern of vascular development in *bel1-1* and *bel1-1 fwf* at early flower positions resembled that observed during ovule development in L.*er* (Figure 4.4C) and a single vascular element formed, that initiated in the chalazal region of the ovule and terminated at the base of the funiculus with a tear-drop tracheid element (Figure 4.4C arrow, and Figure 4.4D). A considerable gap was observed between the terminating tear-drop tracheid element and the sub-adjacent replum vascular elements (Figure 4.4C). However in *bel1-1* and also *bel1-1 fwf* ovules that had initiated development of carpel-like structures, vascular differentiation continued so that a contiguous junction formed between the funicular and the replum vascular elements (Figure 4.4E).

Figure 4.4 Vascular development in ovules. (A) *ant fwf* mutants do not develop vascular elements within the funiculus. (B) Infrequently a tear-drop shaped tracheid elements forms in place of the megaspore mother cell. (C) *bel1-1* mutant ovules develop vasculature in the same manner as wild type ovules, however, vascular differentiation terminates at the base of the funiculus and contiguous vasculature connection to the replum vascular elements is not made (D, t, arrowhead). (E) Only when carpel-like structures develop in *bel1-1* ovules is a contiguous connection made with replum vascular elements (j). j, adjoining vasculature; rv, replum vascular tissues; t, terminating vasculature. Scale bar, 50 μm.

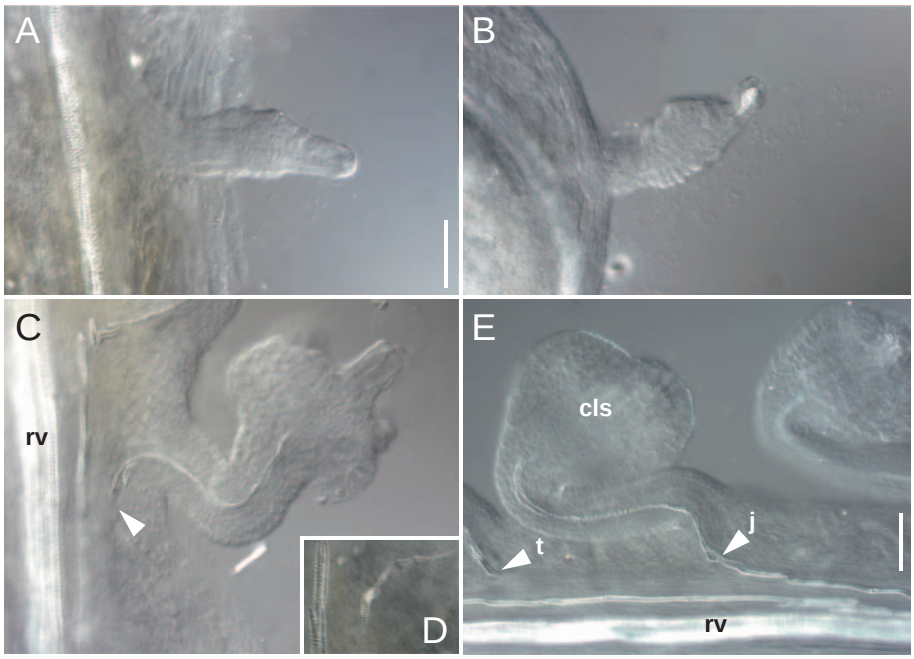
A
B
C
rv
D
E
cls
t
j
rv

The examination of vascular development in *fwf* mutants was not complete at the time of writing this thesis. However the correlation between increased silique length and the formation of a continuous vascular connection in *bel1-1 fwf* mutants when carpel-like structures form suggests that vascular development might be another critical factor for sustained silique development. The observed deficiencies in vascular development within *ant fwf* ovule primordia and the lack of parthenocarpic silique development in *ant fwf* double mutants supports this argument. Vascular development needs to be observed in *fwf* to determine if a continuous vascular connection forms during parthenocarpic silique growth in this mutant. Firm conclusions cannot be made from this study regarding the correlation of funicular-replum vascular development and silique formation in parthenocarpic *fwf* mutants, until this has been studied.

4.3.5 Constitutive ethylene responses allow parthenocarpic silique development when ovules are altered in integument structure

The plant hormone ethylene is thought to have a role as a secondary signal for coordinating post-pollination inter-organ responses and floral senescence (Fernandez et al., 2000; O'Neill and Nadeau, 1997). *ctr1-1* and *ein6* mutants display floral defects during development that reflect a constitutive ethylene response and an ethylene insensitive phenotype respectively, and similar but not identical floral defects are also observed in *fwf* (chapter 3.3.2). Parthenocarpic silique development in *fwf* is inhibited by the presence of the outer floral whorls (chapter 3.3.4) but the introduction of the *ats* lesion in the *fwf* background negated this inhibition (chapter 3.3.5). In order to examine the genetic interaction between constitutive ethylene responses, integument structure, floral whorls and post-fertilization events, a set of double and triple mutants were created between *ctr1-1* and the ovule mutants described in section 4.1 (Figure 4.5A to 4.5C).

Figure 4.5 Parthenocarpic silique development in the *ctr1-1* background when mutations in ovule development described in Figure 4.2 are combined in double mutants. (A) Emasculated *ctr1-1* pistils elongate only in response to pollination. (B) Parthenocarpic silique elongation occurs in the *ctr1-1* background when the outer integument is removed (*ino ctr1-1*) or modified by the *ats* mutation (*ats ctr1-1*), but does not occur in *ant ctr1-1* or *bel1-1 ctr1-1* double mutants. (C) Enhancement of autonomous silique development occurs in emasculated *ctr1-1 fis-2* / + double mutants grown under low light conditions. (D) Longitudinal section of an unpollinated *ctr1-1* carpel valve 7 days post-anthesis and (E) a pollination-induced *ctr1-1* silique valve. (F) Longitudinal section of an emasculated *ats ctr1-1* silique at 7 days post-anthesis. (G) Longitudinal section of a pollination-induced *ein6* silique valve at 7 days post-anthesis. (H) A longitudinal section of a parthenocarpic *fwf* NIL silique at 7 days post-anthesis compared with (I), a parthenocarpic *ctr1-1 fwf* NIL silique. f, funiculus; e, endocarp; up, unpollinated; m, mesocarp; o, ovule; p, pollinated; s, supportive sclerenchyma; x, exocarp. Scale bars: A to C, 3 mm; D to I, 50 μm scale for all.

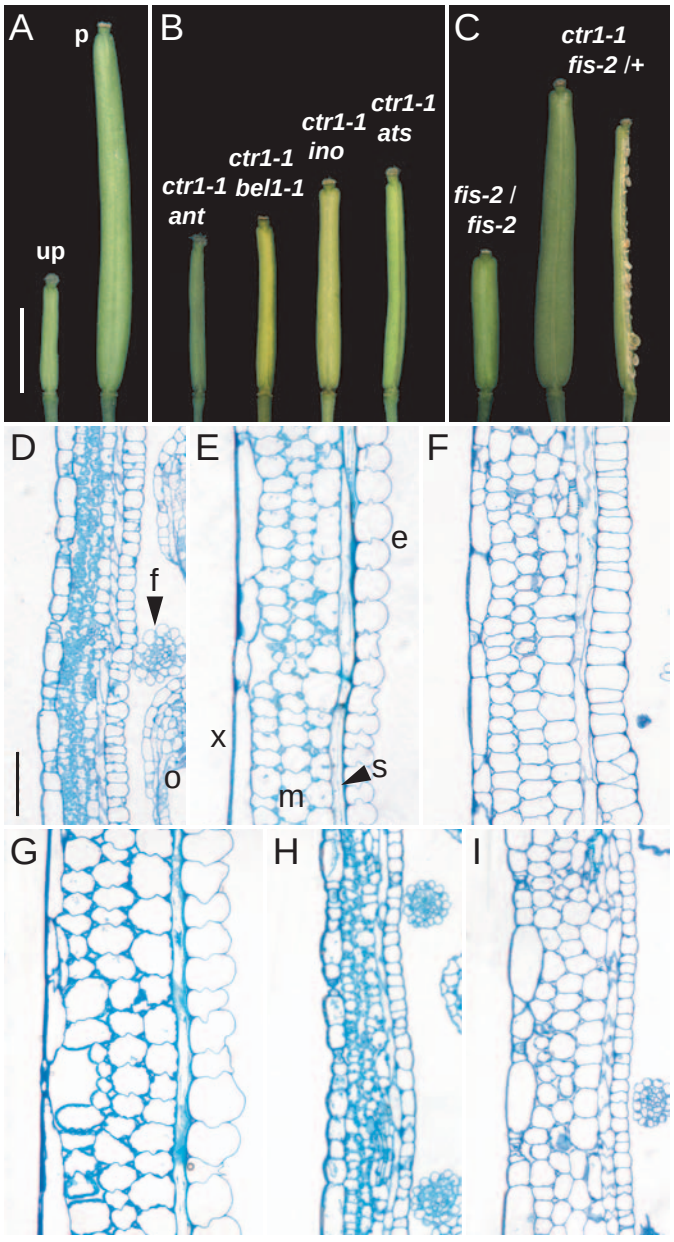
A
p
up
B
ctr1-1
ant
ctr1-1
bel1-1
ctr1-1
ino
ctr1-1
ats
C
ctr1-1
fis-2 /+
fis-2 /
fis-2
D
f
o
E
e
x
s
m
F
G
H
I

In *ctr1-1* plants the gynoecium frequently protrudes through the petals before the bud opens, but the mutant is not parthenocarpic because the final pistil length observed in unpollinated *ctr1-1* is similar to the wild type background (chapter 2.3.5; Table 4.1; Figure 4.5A). *ant ctr1-1* double mutants displayed very narrow pointed rosette and cauline leaves, suggesting both of these genes are required for normal leaf blade expansion. However *ant ctr1-1* mutants are not parthenocarpic as pistils remained small and were similar in length to emasculated *ant* flowers (Figure 4.5B; Table 4.1). *ctr1-1* mutants containing the *bel1-1* mutation, had pistils slightly longer than the mean for *bel1-1* alone at maturity (Table 4.1). The number of carpel-like structures in *bel1-1 ctr1-1* double mutants was also comparable to *bel1-1* alone, indicating that *ctr1-1* has no effect on this process, unlike the *fwf* lesion which greatly increases the frequency of carpel-like structures in the *bel1-1* background.

ino ctr1-1 double mutants developed parthenocarpic siliques after emasculation that were significantly greater in length than pistils observed from emasculated *ino* flowers (Figure 4.5B; Table 4.1). This indicates that the genetic removal of the outer integument in combination with the constitutively activated ethylene responses conferred by *ctr1-1* are sufficient to initiate silique development. The observation that neither mutation individually permits parthenocarpic silique development implies that the ethylene responses might have an active role initiating silique development while the outer integument would negate the parthenocarpic silique development stimulated by the loss of *ctr1-1* function. Since the outer integument does not significantly influence silique development in the *fwf* background, the outer integument might produce signals negating parthenocarpic silique development in *ctr1-1*. Alternatively the outer integument could have a passive role permitting the diffusion of morphogenic molecules into these cell layers, reducing the overall parthenocarpic response conferred by the constitutive activation of target responses downstream of *CTR1*.

Emasculated *ats ctr1-1* double mutants also displayed a parthenocarpic response and siliques that formed were longer than those observed in emasculated *ino ctr1-1* double mutants (Figure 4.5B; Table 4.1). However *ats ctr1-1* siliques were slender and lacked the degree of silique wall expansion observed in *fwf* mutants. Analysis of longitudinal sections revealed that anticlinal mesocarp cell division occurred in parthenocarpic *ats ctr1-1* siliques (Figure 4.5F), because comparisons between cell numbers from longitudinal sections of anthesis stage *ats ctr1-1* pistils and mature parthenocarpic *ats ctr1-1* siliques showed a two-fold increase in mesocarp cell number. Endocarp and supportive sclerenchyma development in emasculated *ats ctr1-1* siliques was however not as extensively thickened as that observed in *ctr1-1* siliques following post-pollination (Figure 4.5F).

pop1 ats ctr1-1 triple mutants were constructed to test if parthenocarpy could occur without emasculation. *pop1 ats ctr1-1* triple mutants elongated independent of emasculation, but the siliques were smaller than those observed in emasculated *ats ctr1-1* double mutants (Table 4.1). Therefore silique elongation in the *ats ctr1-1* background is subject to inhibition from the outer floral whorls, but unlike the situation in *fwf*, the inhibition from outer floral whorls is not relieved by *ats*.

Collectively the data shows that parthenocarpic silique development in a constitutive ethylene response condition, resembles that seen in *fwf* because it is dependent upon signals from within the functional gametophyte and inner integument, and modulated by the presence of outer floral whorls. Parthenocarpic silique development in a *ctr1-1* background is nevertheless unlike *fwf* because it is entirely moderated by integumentary structure and the loss of specific cell layers.

4.3.6 *ctr1-1* enhances autonomous silique development in *fis-2* mutants

When *ctr1-1* and *fis-2* were combined in a double mutant, it was found that *ctr1-1* enhanced autonomous silique and seed-like development in heterozygous *fis-2* plants under the low light growth conditions described in the materials and methods (Table 4.2). There is normally low penetrance of the homozygous *fis-2* single mutant phenotype under low light conditions (Table 4.2). *ctr1-1* marginally improved autonomous silique development under high light conditions. Emasculated *ctr1-1 fis-2* / + plants developed less seed-like structures than expected for an emasculated heterozygous *fis-2* individual under both conditions (Table 4.2). Genes that require ethylene for induction are constitutively expressed in *ctr1-1* (Kieber et al., 1993). Therefore the enhanced growth of the *fis-2* / + siliques in the *ctr1-1* background under low light conditions suggests that *fis-2* / + siliques do not reach maximal elongation in these conditions because steps in ethylene signal transduction or a related signal pathway are limiting.

4.3.7 Control of silique mesocarp cell expansion is defective in the *ethylene insensitive 6* perception mutant

EIN2 and EIN6 act after *CTR1* in the signal transduction cascade (Johnson and Ecker, 1998). Examination of the valve structure in mature pollination-induced *ein6* siliques revealed that the siliques were wider than those observed in the L.*er* parental background and the *ein6* siliques formed mesocarp cells that were extremely expanded compared with those observed in *ctr1-1* siliques (Figure 4.5G and 4.5E respectively). Sections of pollination-induced *ein6* siliques (Figure 4.5G) resembled those in the GA perception mutant *gai-1* (chapter 2.3.8). However, development of parthenocarpic *ein6* siliques can occur following treatment of pistils with 10 *n*mol pistil^{-1} GA_3 (Table 4.1) indicating that GA can induce silique development independent of *EIN6* function and that the *gai-1* and *ein6* silique phenotypes are unrelated.

EIN2 is also central component of ethylene perception and a genetic model proposed that it mediates ethylene signal transduction downstream of *CTR1* (Johnson and Ecker, 1998; Urao et al., 2000). Expression of the C-terminal domain of *EIN2* is sufficient to mimic the floral phenotype of the *ctr1-1* mutant (Alonso et al., 1999). Unlike *EIN6*, sections of pollination induced siliques from *ein2* mutants did not reveal defects in mesocarp expansion (not shown). Root tissues of *ein2* mutants are also cytokinin resistant (Cary et al., 1995). However the application of 1 *n*mol pistil^{-1} BA permitted parthenocarpic silique development in *ein2* mutants demonstrating that this mutant is able to perceive cytokinin in pistils and initiate silique development independent of *EIN2* function (Table 4.1). The silique phenotypes observed in *ino ctr1-1*, *ats ctr1-1* and *ein6* mutants show that ethylene perception has a role controlling cellular differentiation in *Arabidopsis* siliques.

4.3.8 *ctr1-1* enhances mesocarp expansion in the *fwf* NIL

The relationship of *FWF* with ethylene signal transduction and perception was examined because of the similarities in the regulation of parthenocarpy in *fwf* and *ctr1-1* backgrounds and the role of ethylene perception in controlling cell differentiation in *Arabidopsis* siliques. *ETR1* acts as an ethylene receptor, upstream of *CTR1* in the ethylene signal transduction pathway (Johnson and Ecker, 1998). Double mutant analysis between *etr1-3* and *fwf* showed that parthenocarpic silique elongation induced in *fwf* was independent of the dominant ethylene insensitive mutation, *etr1-3* (not shown). Although it remains possible that functional redundancy at the level of ethylene perception could conceal possible interactions. Examination of silique structure in pollination-induced *etr1-3* siliques showed they were identical to wild type (not shown).

The effect of constitutive ethylene responses conferred by the *ctr1-1* mutant in the *fwf* background was tested using the near isogenic *fwf* line in the Col-1 ecotype (NIL;

chapter 3.3.1) because the *erecta* mutation enhanced the *ctr1-1* phenotype. However F_2 intercross progeny between *ctr1-1* and *fwf* in the L.*er* ecotype that did not contain the *erecta* mutation were also examined. Final silique lengths obtained following emasculation in *ctr1-1 fwf ER* lines derived from F_2 intercross progeny showed that *ctr1-1* did not enhance the final silique length compared to *fwf* single mutants (Table 4.1). Parthenocarpic silique development in *fwf* was found to be less penetrant in Col-1 than the L.*er* ecotype where *fwf* was originally isolated (chapter 3.3.1). Examination of silique structure revealed that mesocarp expansion was greatly diminished in this line (Figure 4.5H). When *ctr1-1* was combined in a *ctr1-1 fwf* NIL double mutant, *ctr1-1* did not enhance parthenocarpic silique elongation (Table 4.1). Longitudinal sections of emasculated *ctr1-1 fwf* NIL double mutant silique walls did however, reveal that *ctr1-1* enhanced mesocarp expansion (Figure 4.5I).

The *ctr1-1* mutation is therefore functionally distinct from the *fwf* lesion. Parthenocarpic silique development only occurs in the *ctr1-1* background when the outer integument is removed genetically by combing *ctr1-1* with *ino* or if the integument structure is modified by the *ats* lesion. The observation that *FWF* is functionally separated from *CTR1* pathway is further strengthened because *ctr1-1* enhances autonomous silique development in the *fis-2* mutant under low light growth conditions, while the *fwf* lesion does not. Furthermore, *ctr1-1* does not enhance the development of carpel-like structures in the *bel1-1* mutant background. Therefore ethylene responses appear to act in a positive manner to enhance silique development. This is separate to the de-repression of silique development conferred by the *fwf* mutation because *ctr1-1* does not enhance the silique length independent of *fwf* (Table 4.1) but *ctr1-1* does enhance mesocarp expansion in the *fwf* Col-1 background.

Discussion

4.4.1 Signals from ovules regulate silique growth in *Arabidopsis*

The initial response to pollination in many flowers is an early burst in ethylene production in the stigma, style, ovary and petals that helps to co-ordinate ovary growth and floral organ senescence. Auxin is also involved in this process (Larsen et al., 1993; O'Neill and Nadeau, 1997; O'Neill et al., 1993). Double fertilization, which subsequently occurs within the ovule, is required to initiate both seed and fruit development. The double fertilization event directly results in the initiation of embryo and endosperm of the seed, however, it is not clear how signals from this event induce development of the surrounding ovary tissues into the fruit or how co-ordinate development of both seed and fruit is maintained.

In this chapter it has been shown using a genetic approach that silique development in the absence of fertilization is dependent upon signals from tissues within the ovule in two functionally distinct mutant backgrounds. Lesions in *FWF* enable parthenocarpic silique development and it has been postulated that FWF acts as a repressor of silique development in the absence of fertilization. Genetic analysis by combining mutants defective in ovule development with *fwf* showed that parthenocarpy was dependent on a functional female gametophyte, endothelium and inner integument. This implies that these tissues act as source tissues and contribute morphogenic molecules that induce silique development. Perhaps the FWF product that is expressed in one or more of these tissues blocks this activity.

The observation that lesions in *ATS*, which produces a composite single integument structure, enhances parthenocarpic silique growth in the *fwf* background suggests that signals from the integument mediated by *ATS*, modulate *FWF* activity, and act to restrict

silique development. However, firm conclusions regarding *ATS* function cannot be made until the identity of this gene and its pattern of expression are known.

The importance of ethylene response for coordinating silique development in *Arabidopsis* was demonstrated following the analysis of parthenocarpy in the constitutive ethylene response mutant *ctr1-1* and silique growth in fertilization-independent *ctr1-1 fis-2* double mutant. The induction of parthenocarpic silique growth in *ctr1-1* was dependent on the presence of a functional gametophyte and endothelium and also lesions in the integument tissues because parthenocarpic growth was observed only in *ats ctr1-1* and *ino ctr1-1* double mutants. It is conceivable that the constitutive ethylene responses mimic the pollination-induced burst of ethylene that accompanies fertilization dependent processes (O'Neill and Nadeau, 1997). In wild type plants ethylene perception maybe required to modulate signals within the integuments that normally suppress silique development in the absence of fertilization. Enhanced silique growth observed in the absence of fertilization in *ctr1-1 fis-2* plants could be explained because *ctr1-1* would provide the appropriate down-stream post-pollination cues to negate inhibitory signals from integuments and the autonomous endosperm development induced by *fis-2* would negate fertilization-dependent processes in the gametophyte.

The data obtained from the analysis of parthenocarpic silique development in this chapter, combined with data obtained from the analysis of fertilization-independent seed mutants, suggests that morphogenic signals from ovule tissues are required for the initiation and modulation of silique development. Morphogenic molecules like auxin and GA are perceived in the carpel because mutations early in ovule development do not affect growth-regulator-induced parthenocarpic silique development. Therefore specific ovule components are key regulators of both fertilization-dependent and fertilization-independent fruit development.

4.4.2 Vascular development between the ovule and the carpel is required for silique development

Transmission of signals between the ovule and the carpel to initiate fruit development may occur via the symplast, apoplast or vasculature. In mature wild type ovules, vascular development between the base of the funiculus and the adjacent vascular tissue of the replum was found to be fertilization-dependent. Parthenocarpic silique development in the *fwf* mutant was blocked in the presence of the *ant* mutation that forms ovule primordia but does not develop pro-vascular vascular tissue. Continuity between funicular and replum vascular tissue also correlated with the formation of carpel-like structures and silique elongation in the *bel1-1 fwf* mutants. Collectively these data suggest that the development of pro-vascular tissues between the funiculus and the replum of the carpel may be an important factor associated with the carpel to silique transition. The funicular-replum vascular differentiation process or the vascular tissue itself may aid in the transmission of morphogenic factors between the ovule and carpel tissues.

fwf mutants display enhanced lateral vascular bundle differentiation and mesocarp expansion in the adjacent tissues (chapter 3.3.7). *FWF* product may therefore modulate formation or transmission of morphogenic molecules from ovules to control mesocarp and vascular differentiation during silique development.

4.4.3 Functional FWF activity is required to promote ovule identity and control cell proliferation

The MADS-box transcription factor *AGAMOUS* (*AG*) specifies both carpel and ovule identity in *Arabidopsis* (Bowman et al., 1999; Western and Haughn, 1999; Figure 4.6A). *AG* is initially expressed in stamen and carpel primordia (Yanofsky et al., 1990) and

Figure 4.6 Expression domains of *AGAMOUS* during *Arabidopsis* flower development (modified from Ferrándiz et al. 1999). (A) For floral development stages 6, 8, 10 and 12 both longitudinal (bottom) and transverse (top) sections are shown. *AG* is detected in stage 3 flowers in the central meristematic region (blue) that later forms the two inner whorls of floral organs. *AG* transcripts become abundant and then are uniformly expressed throughout stamen and carpel primordia between stages 4 to 7. High-level transcript abundance becomes limited to ovule primordia before stage 9 and persists at elevated levels within all ovule tissues until stage 12. Lower levels are detected in carpel wall and stamen tissues during these stages. (B) Between stages 12 and 14, the *AG* expression domain becomes confined to the endothelium of the inner integument layer (red) and does not appear to be expressed in other integument cell layers or within the embryo sac (Bowman et al., 1991; Modrusan et al., 1994; Reiser et al., 1995). fm, floral meristem; st, stamen; c, carpel; cw, carpel wall; o, ovule; m micropyle; p, false septum-carpel margin; f, funiculus; fv, funiculus vascular tissue; cr, chalazal region; ii, inner integument; oi, outer integument; s, synergid cell; e, egg cell; pn, polar nuclei; cc, central cell; a, antipodal cells; rv, replum vascular tissues.

A

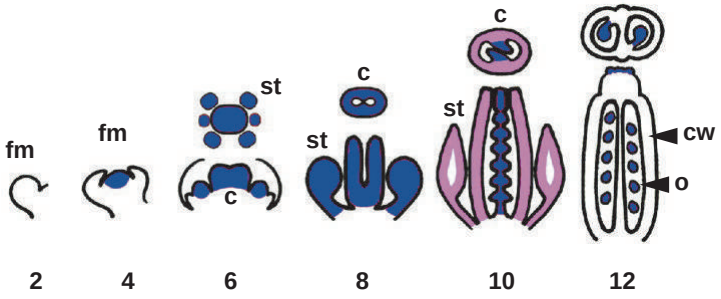

B

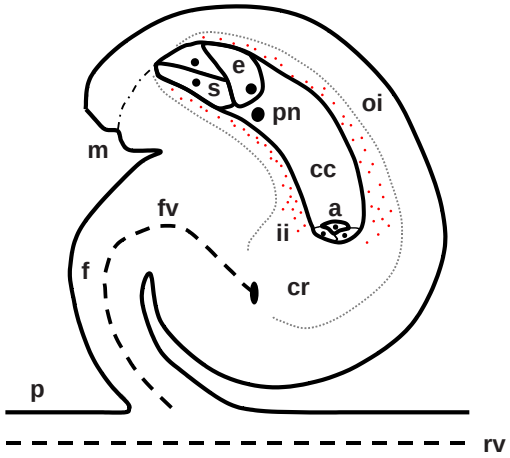

then expression becomes restricted to the stigma, ovule primordia and then to the endothelium of the ovule (Bowman et al., 1991; Reiser et al., 1995; Figure 4.6B). The homeodomain gene *BEL* acts in parallel with *AG* to control both ovule identity and inner integument development (Western and Haughn, 1999). Loss of *BEL* function results in abnormal ovules that lack an inner integument and have an irregular-shaped outer integument that can stochastically develop carpelloid properties complete with stigmatic tissue and ovules (Modrusan et al., 1994). Ectopic over-expression of *AG* in *Arabidopsis* also leads to carpelloid structures developing in positions normally occupied by ovules as well as ovule development occurring in first whorl floral organs (Mizukami and Ma, 1992). As excess *AG* activity positively induces ectopic ovule formation in first whorl organs and promotes a carpelloid identity to wild type ovule primordia, then *BEL* activity is required to modulate *AG* in ovules (Ray et al., 1994). *bel1-1* mutants do not exhibit altered *AG* mRNA accumulation during the early stages of ovule development indicating that *BEL* may act post-transcriptionally to control *AG* activity (Reiser et al., 1995).

Ovule development does not occur in first whorl organs in the *fwf* mutant but when *fwf* is combined with *bel1-1*, carpelloid organ initiation and outgrowth is promoted at a much greater frequency than in the *bel1-1* single mutant. One interpretation of the increased carpelloidy is that *FWF* functions downstream of *AG* and *BEL* to control sporophytic cell proliferation in the ovule. The observation that 19% of *fwf* ovules develop a longer outer integument is consistent with this hypothesis. The possibility that there may be an interaction between *FWF* and *AG* in the endothelium also requires further investigation. It is tempting to speculate that the same morphogenic molecules, which are responsible for silique growth in the *bel1-1 fwf* double mutant are active in permitting carpel-like structures to initiate in *bel1-1* ovule primordia and also permit the vascular differentiation in the funiculus-replum boundary.

4.4.4 *FWF* may mediate effects relating to the morphogen auxin

There are several lines of evidence that suggest alteration in auxin activity may be involved in the *fwf* mutant and that auxin may be directly or indirectly involved in the transmission of signals from the ovule to facilitate silique development. The plant hormone auxin plays many roles during plant development including the induction of vascular tissue formation and cell expansion (Berleth and Mattsson, 2000; Jacobs, 1952; Sachs, 1991). *fwf* mutants display enhanced vascular bundle development and cell expansion in mesocarp tissues. The double mutant analysis between *fwf* and ovule defective mutants showed that completion of vascular tissue between the ovule and the replum were important for silique growth.

Parthenocarpic fruit development can be induced by auxin in eggplant, tomato and tobacco when auxin levels are upregulated specifically in ovules using chimeric gene constructions in transgenic plants (Ficcadenti et al., 1999; Rotino et al., 1997). This suggests that localized induction of auxin biosynthesis in the ovule is sufficient to initiate and sustain silique development. Parthenocarpy is also induced in *Arabidopsis* by auxin and GA application and the former has a significant effect on mesocarp cell expansion (chapter 2.3.2 and 2.3.7). Combination of *fwf* with the GA insensitive mutant *gai-1* results in parthenocarpic silique development strongly resembling auxin-induced parthenocarpy (chapter 3.3.9). This further supported a role for auxin in silique development and the involvement of *FWF* in auxin-related events during silique development.

The remainder of this discussion concerns the formulation of a model for events regulating the transition between carpel and silique development. The model is based upon on the current knowledge of the genes controlling early gynoecium development in *Arabidopsis*, observations obtained in this chapter concerning *fwf*, ovule defective mutants

and ethylene signal transduction, and considers the role of auxin in mediating a range of events essential to this transition.

4.4.5 Auxin gradients and patterning in leaf, root and carpel development

A conceptual framework for auxin action in cellular organization and vascular differentiation within the leaf has been proposed on the basis of polar auxin transport inhibitor studies (Mattsson et al., 1999; Sieburth, 1999). The model for leaf vein initiation during leaf development is that auxin is first synthesized in leaf margins and auxin then partly self-regulates its own transport away to the center of the leaf. Auxin flow is canalized into discreet channels that then differentiate into a network of veins (Mattsson et al., 1999). Reducing polar auxin transport in developing leaf organs increases the number of vascular stands and alters the vascular differentiation pattern, confining vascular tissue development towards the leaf margin (Mattsson et al., 1999; Sieburth, 1999). Data from these studies indicates that auxin plays a role in the self-organization of vascular development through apical-basal polarization of cells while also supporting the existence of auxin biosynthesis sites in the margins of developing leaf organ primordia (Berleth and Mattsson, 2000; Mattsson et al., 1999; Sieburth, 1999).

In root tissues an auxin concentration is maximal in the vascular apex (Sabatini et al., 1999). Gravitropic responses in root tissues occur through the formation and maintenance of auxin gradients within cell files (Morelli and Ruberti, 2000). Auxin efflux carriers play an immediate role in the polar auxin transport system (see Morelli and Ruberti, 2000 for review). Responses to specific environmental stimuli augment the asymmetric growth and elongation which in part occurs through the modulation of auxin gradients. Ethylene perception is an important modulator of gravitropic responses in hypocotyl and root tissues, where ethylene perception modulates specific aspects of polar

and lateral transport of auxin through auxin efflux carrier expression and activity (Gälweiler et al., 1998; Morelli and Ruberti, 2000; Roman et al., 1995). Alternative modulators of polar and lateral auxin transport include the *ATHB2* homeodomain protein that mediates a shade avoidance response and responses to Red and Far Red light ratios (Steindler et al., 1997; Steindler et al., 1999).

Carpels appear to have evolved from leaf-like structures. Primitive and ancestral carpels resemble folded leaf-like structures with unfused carpel margins and placental tissue from which the ovules developed. It is thought that genetic networks were recruited to direct the growth of leaf-like structures into sporophyllous organs to produce the advanced closed angiosperm carpel (Bowman et al., 1999; Gasser and Robinson-Beers, 1993). In support of this theory, Alvarez and Smyth, (1999) found that combinations of loss of function mutations in *AG*, *PISTILLATA*, *APETALA2*, *CRABS CLAW* and *SPATULA* are required for the homeotic conversion of carpels into leaf-like organs. Furthermore, in *spt-2 ap2-2 pi-1 ag-1* quadruple mutants, ovule primordia arise from the reduced carpelloid organ margins (Alvarez and Smyth, 1999). As such, the *Arabidopsis* carpel in Figure 4.7 is drawn as a stylized flattened structure with ovules at the margins.

ETTIN (*ETT*) is an auxin response factor gene and *ETT* function is essential for tissue patterning during carpel development in *Arabidopsis.* Comparison of carpel development in wild type and *ett* mutants treated with polar auxin transport inhibitors has provided evidence that auxin acts as a morphogen directing regional patterning in the developing *Arabidopsis* carpel (Nemhauser et al., 2000). A model has been proposed suggesting that an apical-basal gradient of auxin during early carpel development provides a mechanism that links *ETT* and its putative role in the transcriptional regulation of auxin responsive genes to the establishment of tissue pattern in early carpel development (Nemhauser et al., 2000). This model can be extended to the mature stage of carpel

Figure 4.7 Model describing the participation of integumentary tissues in parthenocarpic silique development conferred by the *fwf* or *ctr1-1* mutation. The diagram is simplified to show a single flattened carpel with ovules on the margins. (A) *FWF* represses the transport or initiation of a morphogenic signal initiated either separately or collectively within the inner integument, the endothelium or female gametophyte of the *Arabidopsis* ovule. (B) Fertilization dependent signals mitigate *FWF* repression and each fertilized ovule contributes to the net morphogen efflux (black dotted arrows) at the carpel margin. This permits mesocarp differentiation and carpel vascular development. A fertilized ovule would also reinforce funiculus-replum vascular development (thick black line). *ant fwf* double mutants do not develop vascular tissue in the funiculus (gray dotted line) and thus can not initiate parthenocarpic silique development. *bel1-1 fwf* double mutants initiate parthenocarpy only when carpel-like structures are initiated from ovule primordia. *ats* and *ino* mutants have three integument cell layers and can initiate parthenocarpy in the *fwf* and *ctr1-1* backgrounds. *ats* integumentary cell layers have an altered composition accounting for the enhanced parthenocarpy observed in the *ats fwf* mutant. Transmission of morphogenic molecules in the three inner integument cell layers of *ino* mutants is unaffected. Polar and lateral routes for auxin transport within the ovule integument cell layers in (C) wild type, in (D) the *ctr1-1* mutant and in (E) the *ctr1-1 ino* double mutant. Constitutive ethylene responses could enhance polar and lateral movement of auxin (arrows) from the inner integument (blue) and female gametophyte (red), to the chalazal region and the outer integument (gray). Loss of the outer integument, in the *ctr1-1 ino* mutant (E), confines auxin distribution reaching a threshold able to activate silique differentiation.

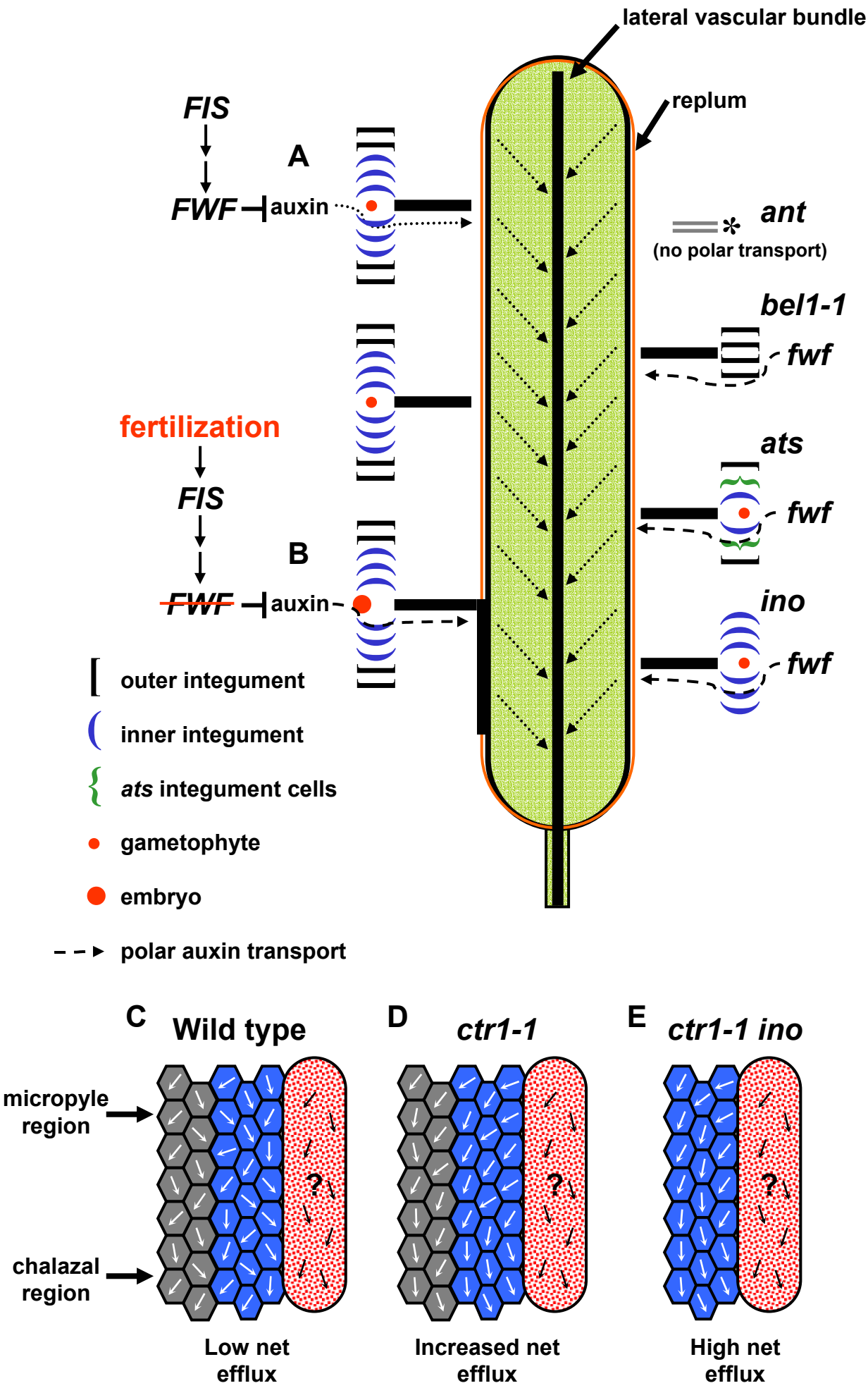
lateral vascular bundle
replum
FIS
A
FWF
auxin
ant
(no polar transport)
bel1-1
fwf
fertilization
FIS
ats
fwf
B
FWF
auxin
ino
fwf
outer integument
inner integument
ats integument cells
gametophyte
embryo
polar auxin transport
C
Wild type
D
ctr1-1
E
ctr1-1 ino
micropyle region
chalazal region
?
Low net efflux
Increased net efflux
High net efflux

development to incorporate the observations in *fwf* and *ctr1-1* mutants concerning morphogenic signals from ovule tissues that regulate the stage of silique initiation.

4.4.6 Auxin gradients and polar auxin transport may mediate the carpel to silique transition

I propose a model whereby polar and lateral transport of a morphogenic molecule possibly auxin creates a threshold level of morphogen to activate the silique development program. In this model FWF influences the repression of auxin signal transduction in ovule source cells and ethylene perception modulates polar auxin transport between the ovule and the carpel tissue. The model is summarized in Figure 4.7, which shows an opened carpel with ovules at the carpel margins.

Normally a basal level of auxin would be synthesized in the ovule and the molecule would diffuse towards the funiculus and then to the carpel margin as occurs in the leaf model (Figure 4.7A). Morphogenic molecules synthesized in the gametophyte and the surrounding inner integument tissues would diffuse to the outer integument, and also to the chalazal region, and then collectively towards the funiculus. The overall net efflux of auxin from an unfertilized ovule would not permit parthenocarpic silique development because *FWF* activity either collectively or individually within the inner integument, endothelium, female gametophyte and funiculus of the *Arabidopsis* ovule would repress polar auxin transport or the initiation of the signal transduction process (Figure 4.7A). Post-fertilization signals initiated by an event in the female gametophyte would relieve *FWF* mediated restriction of auxin transport or signal transduction allowing each ovule to contribute an increased flux of morphogen or positive signal to the margin of the carpel (Figure 4.7B). This would be facilitated by the completion of vascular development between the funiculus and the replum, permitting further mesocarp and vascular development critical for overall

silique growth. Mutants in which ovules do not develop vascular tissue in the funiculus are unable to establish the vascular connection, and cannot initiate silique development.

Alterations in ovule integument structure may result in increased flux or concentration of morphogen and receptors. The outer integument, however, does not appear to play a major role in parthenocarpic silique development, because *ino fwf* mutants do not have enhanced parthenocarpic silique development. Mutations in *FWF* would lead to a loss in repressive function allowing a net efflux of auxin, from the source cells within the inner integument and or female gametophyte, that would be sufficient to induce parthenocarpic silique development (Figure 4.7).

Biosynthesis and perception of GA is also essential for silique development (Barendse et al., 1986). *GA1* catalyzes the first step in GA biosynthesis and its expression is restricted to the vascular tissues of the funiculus, replum and lateral vascular bundles (Sun and Kamiya, 1997). Polar auxin transport could regulate vascular development and in turn modulate the abundance of GA precursor molecules entering the GA biosynthesis pathway thus regulating silique growth and differentiation.

4.4.7 Ethylene perception in the ovule

The role of ethylene perception in ovule-carpel signal transduction is postulated to function in terms of ethylene perception modulating polar and lateral movement of auxin transport as has been shown to occur in the root and hypocotyl tissues. However in the ovule and carpel, transport would follow the path outlined in the model in Figure 4.7. Normally ethylene responses would be compartmentalized within the integumentary tissues and the known expression of ethylene receptors in the ovule (Hua and Meyerowitz, 1998; Sakai et al., 1998) would act to suppress cellular differentiation and silique development. This is consistent with the double mutant analysis with various ovule

defective mutants in the *ctr1-1* background where the primary regulation of parthenocarpy was observed in the integuments. A burst of ethylene from pollination-induced events would raise ethylene concentrations above a threshold level and would trigger ethylene biosynthesis. The ethylene receptors, *ETR2* and *ERS2* which are expressed in the ovule (Hua and Meyerowitz, 1998; Sakai et al., 1998) could help coordinate the movement of morphogenic molecules through phosphorylation and inactivation of the CTR1 kinase as part of the known ethylene perception and response pathway (Alonso et al., 1999; Johnson and Ecker, 1998).

It follows that the *ctr1-1* mutation would enhance the movement of auxin between gametophyte and sporophytic tissues and may facilitate the lateral movement of auxin into the outer integument. As such the net efflux would be slightly increased above the overall basal export to the chalazal region seen in wild type ovules (Figure 4.7C). This would permit some carpel expansion, as observed in the *ctr1-1* pistil, but this efflux alone would be insufficient to result in parthenocarpic silique development (Figure 4.7D). Combining the *ctr1-1* mutant with *ino* would reduce the lateral diffusion of auxin because the total number of cell layers acting as integumentary tissues has been reduced from five to three. This would enhance net auxin export collectively from the gametophyte, endothelium and inner integument tissues to the chalazal region where it would be transported to the carpel margin through the funiculus, allowing the carpel to expand and initiate silique differentiation (Figure 4.7E). Alterations in both outer an inner integument structure and a reduction in the number of cell layers, as occurs in the *ats* mutation, result in enhanced silique development in the *ctr1-1* background. In this case the composite integument structure might change the number and arrangement of receptors affecting the process of auxin transfer and or other morphogenic molecules.

The developmental-genetic data described in this chapter indicates that *FWF* is involved in a repressive function controlling fertilization-dependent silique development via the movement of morphogenic molecules from source cells within the inner integument, endothelium, and or gametophyte to the target tissues in the carpel margin. Cloning of *FWF* and *in situ* localization of *FWF* in various mutant backgrounds may provide information on the role played by *FWF* and how *FWF* integrates auxin signal transduction in these tissues. Future experiments to verify the identity of the source cells may utilize mutants that form normal integuments but are defective in female gametogenesis.

Chapter 5: *FWF* controls the carpel-gynophore boundary specification, marginal boundary differentiation, and C-class organ identity together with *SPY*

5.1 Introduction

Flower development can be subdivided into several periods that include the initiation of floral primordia from the shoot apical meristem (SAM), the patterning and growth of floral meristems, and floral organ morphogenesis. Ovule primordia are initiated during the process of gynoecium morphogenesis from adaxial margins of the carpel. In *Arabidopsis*, floral development ceases at anthesis when the mature pistil is receptive to pollination and stamens dehisce pollen. Immediately after double fertilization in the ovule, post-fertilization flower development commences and includes seed and fruit set, and floral organ abscission.

Lateral organ primordia and organ development occurs from the flanks of the SAM by processes known to be dependent upon positional cues and determinants (Bowman and Eshed, 2000). A repertoire of genes that actively maintain a stem cell population and the interactions between different zones in the SAM (Bowman and Eshed, 2000) provide the framework for these positional cues and determinants. One determinant of organ initiation and positioning in the floral and vegetative meristem appears to be the hormone auxin (Reinhardt et al., 2000). Topical application of auxin to the flanking regions of the *pin-formed1-1* mutant meristem permits the formation of floral organs (Reinhardt et al., 2000). Positions of incipient organ primordia induced in these mutants by auxin were always restricted to a radial zone below the shoot apex, that invariably corresponded with the site of auxin application (Reinhardt et al., 2000).

The plant hormone gibberellin, in addition to the morphogen auxin, is also known to influence the regular pattern of organ initiation and position, or phyllotaxis (Schwabe, 1971). Gibberellins, however, characteristically alter cell division and expansion properties between developing organs (Cho and Kende, 1997; Lester et al., 1997; Sauter et al., 1995; van der Knaap et al., 1997).

Auxin mediated processes also act later, after organ initiation, during floral organ patterning and growth to ensure correct tissue organogenesis during gynoecium development and carpel morphogenesis. Genetic analysis of carpel development in *Arabidopsis* has revealed that several independent pathways act to impart carpel identity and tissue polarity in the developing floral primordia and during organ patterning (Bowman et al., 1999; Eshed et al., 1999). The role auxin plays in the apical-basal positioning of the carpel margin is highlighted by the phenotypic analysis of the *pinoid* (*pid*), *pin1* and *ettin* (*ett*) mutants. Each of these mutants has altered carpel-gynophore boundaries in developing gynoecia (Ferrándiz et al., 1999; Okada et al., 1991; Sessions and Zambryski, 1995).

The molecular identity of the *PIN1* gene reveals it is a member of the membrane bound polar auxin efflux carriers (Gälweiler et al., 1998), while *PID* is a protein kinase that regulates auxin responses (Christensen et al., 2000). *ETT* encodes a protein that is a member of auxin response factor (ARF) family of transcriptional regulators that bind to auxin response elements in DNA (AuxREs; Sessions et al., 1997; Ulmasov et al., 1999b). Applications of a polar auxin transport inhibitor (NPA) to developing gynoecia alters the carpel margin position and phenocopies the *ett* mutation (Nemhauser et al., 2000). Increased levels of applied NPA apically shifts the basal margin during wild type carpel development but also lowers the apical style-carpel margin (Nemhauser et al., 2000). The similarity between the NPA induced phenotype and that observed in *ETT* mutants led Nemhauser et al., (2000) to propose a model in which auxin gradients within the developing gynoecia establish boundaries for tissue differentiation and that *ETT* has an integral role in translating these auxin gradients into regional boundaries.

Double mutant analyses show that *ETT* is not required for the development of the carpel valve as such, but that it is required in carpel margins to determine where valve cell

types will actually form. The *SPATULA* (*SPT*) gene is involved in a variety of aspects controlling carpel development and promotes carpel identity in an *AGAMOUS* (*AG*) independent pathway (Alvarez and Smyth, 1999; Bowman et al., 1999). *spt* mutants display a loss in postgenital carpel fusion and misspecification of transmitting tract and vascular tissues, but in general retain carpel valve identity because carpel development can largely be specified through other redundant pathways (Alvarez and Smyth, 1999). The finding that *spt* is completely epistatic to *ett*, because *spt ett* double mutants do not have altered apical-basal carpel margins, suggested that in particular tissues *SPT* is regulated directly by *ETT* activity (Alvarez and Smyth, 1999; Bowman et al., 1999; Heisler et al., 1999). *In situ* data reveal that *ETT* is expressed in petal, stamen and carpel whorls in an *AG*-independent manner (Sessions et al., 1997). Therefore *ETT* and *SPT* may work together in an *AGAMOUS* independent pathway to control the carpel margin position and identity, and the differentiation of the transmitting tract, septum and placental tissue.

Gibberellins are important for the control of both stamen and carpel growth. The *GA1* gene encodes a primary step in the biosynthesis of active GAs (Sun and Kamiya, 1994) and is expressed in vascular tissues of the carpel and in anther tissues (Silverstone et al., 1997a). Mutations in *GA1* disrupt the biosynthesis of active GAs and *ga1-3* mutants are entirely dependent on exogenous active GAs for silique development (Barendse et al., 1986). Plants containing mutations at the *SPINDLY* (*SPY*) locus can restore vegetative growth and development in *ga1-3* plants (Jacobsen et al., 1996). *spy* single mutants display a phenotype that resembles plants repeatedly treated with active GAs, because they have increased internode length and a reduced requirement for GA during seed germination (Jacobsen et al., 1996).

The *spy-4* mutant was initially combined with the *fwf* mutant to understand the interaction of *FWF* with genes involved in GA perception specifically in silique tissues.

Parthenocarpy was unaffected in early flower positions because emasculated pistils in *spy-4 fwf* double mutants elongated parthenocarpically. However analysis of the *spy-4 fwf* phenotype also revealed an interaction between the *fwf* and the *spy-4* mutant in almost all floral whorls. Stamen, carpel and ovule identities were severely affected. Sepals and petals retained their identity, but sepal margins underwent homeotic conversion. The interaction was further examined in this chapter and the similarities between the *spy-4 fwf* double mutant phenotype and the *ett* mutant in late floral positions implicate *FWF* in mediating auxin signal transduction.

5.2 Materials and methods

Plant growth conditions, methods for emasculation, application of plant growth regulators and histology are as described in chapter 2.2. *fwf* siliques above flower position 30 were observed and photographed during subsequent genetic analysis unless stated.

Double mutants were created by intercrossing mutant lines and obtaining homozygous *fwf* F_2 progeny. Homozygous *fwf* F_3 progeny segregating for the alternative mutation were then analyzed for their mutant phenotype. The *spy-4* mutation contains a T-DNA insertion with kanamycin resistance in a Ws.O parental ecotype. Homozygous *fwf* lines that yielded F_3 plants segregating *spy-4* were grown and selected on MS media (described in chapter 3.2.3) supplemented with 50 μg ml^{-1} (w/v) kanamycin. Double mutant studies with *ett* used the *ett-2* allele in the Ws-2 background and were selected on the basis of phenotype.

5.3 Results

5.3.1 *fwf* in combination with *spy-4* increase carpelloid identity in stamens and create petalloid margins in sepals

The *spy-4 fwf* double mutant displayed a series of heterochronic alterations in organ identity in sepal margins, stamens, carpels and ovules when compared with wild type plants (Figure 5.1 and Figure 5.2). Parthenocarpy however, was unaffected in early flower positions because emasculated pistils in *spy-4 fwf* double mutants formed seedless siliques (Figure 5.2A and 5.2B; Table 5.1). Heterochronic changes were also previously observed in *fwf* mutants (chapter 3.3.1) and also in mutant *bel1-1 fwf* mutants (chapter 4.3.2), where the predisposition for parthenocarpic silique development, or carpel-like development in the *bel1-1 fwf* ovule primordia respectively, increased with the meristem age or flower position.

Floral development in *spy-4* mutants is comparable to wild type (Figure 5.1A). At anthesis, *spy-4* flowers are however, slightly larger than wild type. Early flowers up to position 15 on the main apical meristem of *spy-4 fwf* double mutants displayed stamens with carpelloid properties and short filaments (Figure 5.1B). At later flower positions, anthers became increasingly chlorophyllous and carpelloid, exhibiting significant elongation and expansion of carpelloid anthers (Figure 5.1C and 5.1D). In flowers forming above position 20, the anther locule position became shifted to toward the outer margins of the anther (Figure 5.1C, 5.1D and 5.1E). Carpelloid stamens and filaments without anthers were also observed in late flower positions (Figure 5.1D). Stamen filaments without carpelloid anthers were thinner than filaments with carpelloid tissue (Figure 5.1D). These results suggest that that *FWF* and *SPY* might control the proliferation of stamenoid tissues, effectively reducing cell division and expansion within the anther.

Petals retained normal identity but were reduced in length in late forming flowers (Figure 5.1D). Sepals also retained normal organ identity, except petalloid margins differentiated on the perimeter of the sepal tissue (Figure 5.1C and 5.1F). In rare instances sepal margins further differentiated vestigial ovule primordia (not shown). The sepal

Figure 5.1 Comparison of *spy-4* and *spy-4 fwf* double mutant flowers. (A) Anthesis stage *spy-4* flower with sepal removed. Flowers from early to late flower positions from anthesis stage *spy-4 fwf* double mutant flowers are shown left to right (B to D). These flowers were taken from meristems prior to heterochronic gynophore-carpel boundary alteration. *spy-4 fwf* double mutant flowers have expansion and pronounced carpelloid conversion of anthers. (D) At late flower positions anthers were missing from some filaments. (E) A carpelloid anther showing locules in chlorophyllous marginal tissue. (F) Petalloid margins observed on a *spy-4 fwf* double mutant sepal. cs, carpelloid stamen; fs, filamentous stamen; pm, petalloid margin. Scale bars: A to D, 1 mm; E, F, 0.5 mm

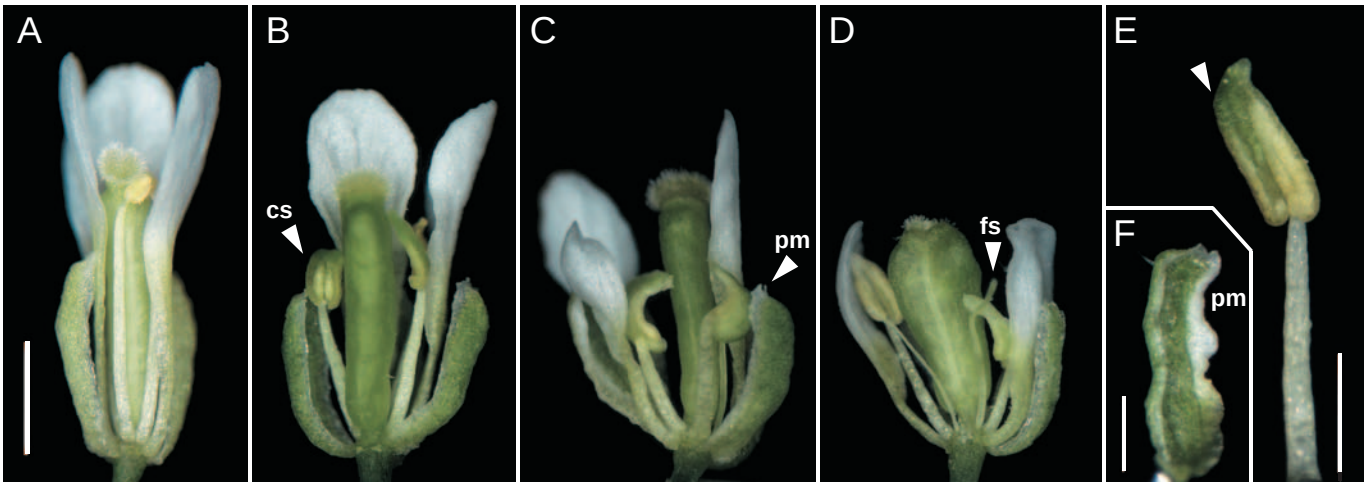
A
B
cs
C
pm
D
fs
E
F
pm

Figure 5.2 (A) Post-pollination growth response in *spy-4* siliques (p) and in unpollinated (up) parthenocarpic *spy-4 fwf* double mutants (B). *spy-4 fwf* double mutants show heterochronic defects that increase with flower position (B, left to right) and include gynophore-carpel boundary being shifted apically, and carpels becoming more unfused. (C) *spy-4 fwf* mutants with homeotic conversions of ovule primordia to carpel-like structures. At later positions these structures reiterated from the proximal region of the carpel and become linear pointed and flat (D). (F) Outermost carpels were removed (at the thin line) from the silique in B (asterisk), to show the reiterated gynophore and carpel-like structures with vestigial ovules on their margins. The reiterated gynophore (arrowhead) formed from the basal region at the rear. Frequently these carpel-gynophore structures erupt from fourth whorl carpels and become indeterminate (G). Wild type (H) and *spy-4 fwf* (I) seedlings grown on MS media at 14 and 16 days respectively, showing that *spy-4 fwf* double mutants have extra sets of cotyledons. Siliques from pollinated and unpollinated *ett-2* and *ett-2 fwf* double mutants (J). Scale bars: A, B, G, J, 3 mm; C, 200 μm; D, E, 2 mm; F, 1.5 mm; H, I, 1 mm.

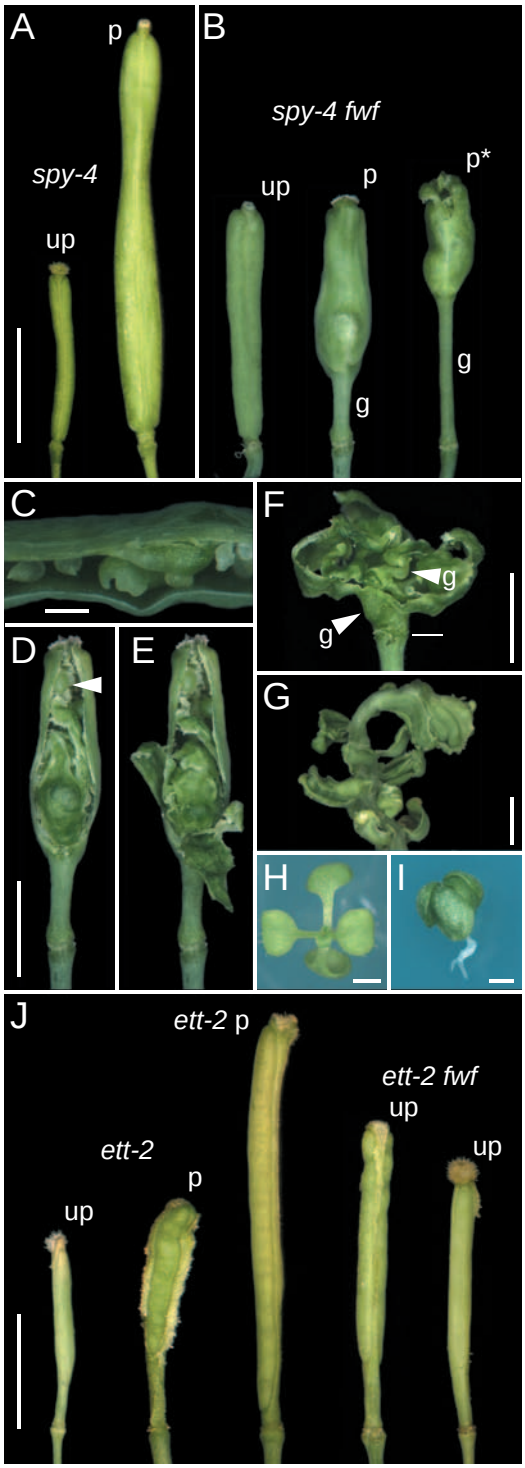
A
p
spy-4
up
B
spy-4 fwf
up
p
p*
g
g
C
F
g
g
D
E
G
H
I
J
ett-2 p
ett-2 fwf
up
up
ett-2
p
up

Table 5.1 Parthenocarpic silique lengths of mutant genotypes

	Silique length (mm ± s.d.)	
genotype / treatment	**emasculated**	**pollinated**
L.*er*	4.5 ± 0.5	12.8 ± 1.1
fwf	7.5 ± 1.0	11.0 ± 1.4 [a]
spy-4	4.7 ± 0.4	14.2 ± 1.3
spy-4 fwf	5.6 ± 0.5 [b]	-
ett-2	4.7 ± 0.6	-
ett-2 fwf	7.6 ± 0.9	-
axr2	3.8 ± 0.4	10.6 ± 0.7
axr2 fwf	6.6 ± 0.8	8.5 ± 0.4

[a] pollinated with L.*er*; [b] assessed at early floral positions

whorls were the least affected compared to stamen and carpel whorls, indicating that the *spy-4 fwf* double mutation primarily affects C-class organ identity that is principally controlled by the *AGAMOUS* gene.

5.3.2 Carpel boundaries in *fwf* mutants are altered in the presence of *spy-4*

A dramatic spectrum of heterochronic developmental defects occurred in carpel and ovule tissues of *spy-4 fwf* double mutants that were not apparent in either single mutant (Figure 5.2A and 5.2B). The defects seen in carpels and ovules increased and changed acropetally with flower position on the primary inflorescence meristem (Figure 5.2B).

At an early stage when carpel morphogenesis was largely unaffected, homozygous *spy-4 fwf* plants displayed both normal ovules, and ovules that form long carpelloid structures (Figure 5.2C). Stigmatic papillae were usually absent from carpelloid-ovule tips (Figure 5.2C). Later, the apical-basal boundary of the carpel valve and gynophore became apically shifted and fourth whorl carpels became syncarpous with a fusion of multiple carpels (Figure 5.2B). Dissected siliques showed that septal tissues were replaced with even more severely reduced carpelloid structures (Figure 5.2D). These structures developed preferentially from the central basal carpel region and reiterated in an indeterminate manner (Figure 5.2D). The reiterative structures become flattened and had vestigial ovules on the margins and the structures usually crumpled within the closed carpel (Figure 5.2E). Seeds were set in the apical portion of the silique where ovules were functional (Figure 5.2D).

As the defects become extreme, the main gynophore length increased, the stigmatic tissue was lost and carpels became unfused (Figure 5.2B, asterisk). Dissected siliques showed that the gynophore was reiterated within itself a couple of times from the innermost basal area of the carpel (Figure 5.2F). Reiterated carpelloid-gynophore

structures did not arise directly from the proximal carpel center but from the side, from homeotic conversion of ovule primordia (Figure 5.2F, arrowhead). Occasionally, the fourth whorl carpel erupted with a thickened gynophore-carpel structure that displayed carpelloid tissues with adaxial margins recurving back (Figure 5.2G).

spy-4 fwf double mutants also had an embryonic phenotype. Compared to wild type seedlings (Figure 5.2H), *spy-4 fwf* seedlings displayed cotyledon bifurcation or extra sets of cotyledons upon germination (Figure 5.2I). Subsequent leaf development was normal. Together these results suggest that in addition to the presumptive role of *SPY* in GA perception, *FWF* and *SPY* potentially function in separate pathways together to repress growth and the reiteration of structural fate in carpels and ovules and also in cotyledons.

5.3.3 *fwf* and *ett-2* have independent functions in silique development and gynophore-carpel boundary specification

To test how the shift in gynophore-carpel boundary position was related to *SPY* or *FWF* activity I examined the interaction between the *fwf* and *ett* mutations. Both *ett* and *pid* are two auxin related mutants that have shifted apical-basal gynophore carpel boundaries in *Arabidopsis* pistils (Ferrándiz et al., 1999; Christensen et al., 2000). *ett* mutants also have altered stigmatic-replum boundaries (Sessions et al., 1997; Figure 5.2J), but stigmatic-replum boundaries are preserved in *pid* mutants (Ferrándiz et al., 1999). In early flower positions in *spy-4 fwf* double mutants, stigmatic-replum boundaries are preserved, but subsequently become reduced and marginallized to unfused carpel tips in late forming flowers.

The weak *ett-2* allele was used to construct *ett-2 fwf* double mutants. *ett-2* single mutants display a moderate apical shift in the gynophore-carpel and stigma-replum boundary positions (Figure 5.2J). Some variation in *ett-2* penetrance was observed within

each plant (compare the two pollinated siliques Figure 5.2J). In *ett-2 fwf* double mutants, neither flowers nor siliques displayed changed apical stigmatic-replum or basal carpel-gynophore boundaries compared to *ett-2* alone (Figure 5.2J). No new phenotype was observed in *ett-2 fwf* stamens, indicating that *FWF*'s role in stamen development is independent of *ETT*. Parthenocarpic silique development conferred by the *fwf* mutation was also maintained in emasculated pistils (Figure 5.2J; Table 5.1). This indicates that *ETT* and *FWF* function independently, but that *FWF* has a unique role in specifying apical-basal carpel boundary position. The alteration in carpel-gynophore boundary specification in *fwf* is as a result specific, only in the context of reduced *SPY* activity.

ett-2 fwf double mutants did nevertheless have an embryo phenotype. Of 500 *ett-2 fwf* seeds plated on MS media (described chapter 3.2.3), 77.2% of the seedlings germinated. 25.1% of the germinating seedlings showed a mutant phenotype. These included cotyledons without roots and or hypocotyl, missing cotyledons, roots and hypocotyl tissues without cotyledons, fan-shaped leaves or single cotyledons without the plant body. Thus *ETT* and *FWF* together may control aspects of embryogenesis.

5.3.4 *fwf* and *axr2* have independent functions

AXR2, encodes a member of the Aux / IAA protein family (Nagpal et al., 2000). Auxin responses in the semidominant *axr2* mutant are altered such that plants are agravitropic and have distorted shoot, root and hypocotyl growth (Nagpal et al., 2000). Parthenocarpic silique development in *fwf* was shown to be independent of *axr2* (Table 5.1) and siliques had normal gynophore-carpel boundaries. Additionally *axr2 fwf* double mutants did not have an embryonic phenotype. *FWF* function and the gynophore-carpel boundary specification therefore appear to be independent of *AXR2* mediated auxin signal transduction.

5.4 Discussion

5.4.1 *SPY* and *FWF* control floral organ identity

Mutations in both *SPY* and *FWF* cause multiple heterochronic effects in the patterning and growth of floral organs. C-class floral organ identity functions were primarily affected in *spy-4 fwf* double mutants and the phenotypes observed, were similar to the *ett* mutant (Sessions and Zambryski, 1995) and to the *spt* mutant (Alvarez and Smyth, 1999). Extra sets of cotyledons were also observed when the *spy-4* and *fwf* mutant were combined.

Heterochronic developmental defects have also been observed in other mutants including the *altered meristem program1* (*amp* allelic to *pt*, *cop2* and *hpt*; Chaudhury et al., 1993; Mordhorst et al., 1998), *extra cotyledon1* (*xtc1*) and *xtc2* (Conway and Poethig, 1997). In these mutants, changes in the relative timing of developmental decisions are thought to occur within the shoot meristem during embryogenesis (Conway and Poethig, 1997). This subsequently influences the identity of cotyledon and leaf tissues in mutant *xtc* plants, and both phyllotaxy and organogenesis in the case of *amp1*. Changes in the timing of developmental decisions during floral organogenesis and cotyledon specification could also account for the observed phenotypes in *spy-4 fwf* mutants. Signals transduced independently through *SPY* and *FWF* may act as a type of scaffold upon which developmental fate decisions are made in stamens, the carpel and ovules. As the defects observed were primarily confined to these floral whorls, the *spy-4* and *fwf* mutations could disrupt an *AG*-dependent carpel morphogenic pathway (Figure 5.3A) and also an *AG*-independent pathway affecting *SPT*-dependent carpel margin specification (Figure 5.3B). The similarity between the *ett* and *spy-4 fwf* phenotype additionally implicates *FWF* in mediating auxin signal transduction and *SPT* dependent processes.

5.4.2 *LEAFY* (*LFY*), *AGAMOUS* and *SPINDLY* in floral organogenesis

Heterochronic transformation of flower to shoot development can also be induced in *ag* and heterozygous *leafy* (*lfy*) mutant pistils (Okamuro et al., 1996). When these mutants were shifted from a long day to a short day environment, flowers underwent reversion and produced ectopic shoot primordium from the proximal region of the pistil (Okamuro et al., 1996). Corresponding treatment of wild type flowers did not result in floral reversion, demonstrating that the reversion process was specific to haploinsufficient *lfy* plants and homozygous *ag* plants. Mutations in *SPY* repressed floral reversion in *ag* and heterozygous *lfy* mutants leading Okamuro et al., (1996) to infer that phytochrome and hormonal control through the SPY protein controls the maintenance of floral meristem identity when *AG* or *LFY* functions are compromised under short day conditions. It has been recently shown that the *LFY* promoter is activated in response to active GAs and high sucrose, and that the *spy-5* mutant expresses upregulated *LFY-GUS* reporter activity (Blázquez et al., 1998; Blázquez and Weigel, 2000). *LFY* directly regulates transcriptional activity of *AG* by binding motifs in the *AG* promoter (Busch et al., 1999). Therefore *SPY* is an important regulator of floral meristem identity because it can repress the activation of downstream *LFY* and subsequent *AG* transcription (Figure 5.3B).

SPY encodes a tetratricopeptide repeat protein (TPR) with a c-terminal catalytic domain that has sequence similarity to *O*-GlcNAc transferases (TPR; Jacobsen et al., 1996). While the function of the TPR domain remains unknown (Thornton et al., 1999), *O*-GlcNAc transferase activity for the *SPY* protein has been demonstrated in a baculovirus expression system (Thornton et al., 1999). Cellular expression patterns for *SPY* have not been determined, but RT- PCR analysis has shown that *SPY* and the homologue *HvSPY* in Barley are expressed at low levels throughout the plant (Jacobsen et al., 1996; Robertson et

Figure 5.3 Control of floral organogenesis by *SPY* and *FWF*. (A) Description of floral phenotypes observed in the *spy-4 fwf* double mutant and their relationship with floral organ identity class A, B and C functions. (B) Model describing the control of organ identity by *SPY* and *FWF* in sepal, stamen and ovule whorls (shown by triangles in A). (C) A model describing the control of boundary and marginal specification by *ETT*, *SPT*, *FWF* and *SPY* in the carpel whorl. (D) A mutually exclusive model describing the role of *SPY* in gynophore elongation, and roles of *ETT* and *SPT* in the carpel-gynophore boundary specification.

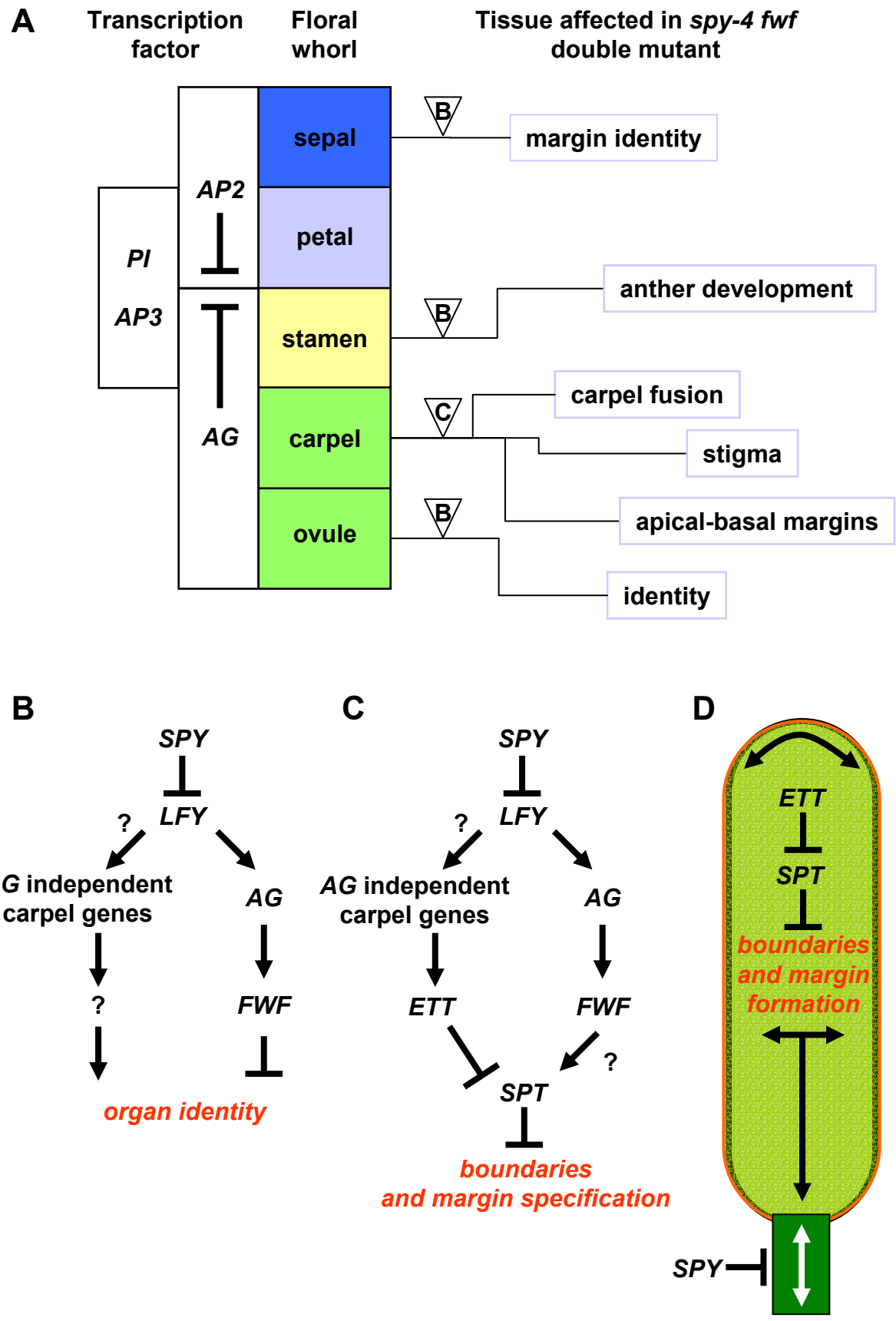
A
Transcription factor
Floral whorl
Tissue affected in spy-4 fwf double mutant
sepal
petal
stamen
carpel
ovule
AP2
PI
AP3
AG
B
B
C
B
margin identity
anther development
carpel fusion
stigma
apical-basal margins
identity
B
SPY
?
LFY
AG independent carpel genes
AG
?
FWF
organ identity
C
SPY
?
LFY
AG independent carpel genes
AG
ETT
FWF
?
SPT
boundaries and margin specification
D
ETT
SPT
boundaries and margin formation
SPY

al., 1998). Mutations in *SPY* are known to alter GA signal transduction (Jacobsen et al., 1996) and the transcription of the GA biosynthetic enzyme GA4 (Cowling et al., 1998). In the case of barley, the HvSPY protein can also alter ABA signal transduction (Robertson et al., 1998). The precise function for *SPY* in GA signal transduction however, remains unknown because the position and role of *SPY* in GA and ABA signal transduction pathways has not yet been determined. The information gained here from the *spy-4 fwf* double mutant provides further evidence that *SPY* and *FWF* have a role in floral organogenesis.

5.4.3 Models for role of *FWF* and *SPY* in sepal, stamen and ovule morphogenesis

FWF has been cloned (chapter 6) but its expression patterns in floral tissue remain to be determined. Genetic analysis in chapter 4 suggests, that *FWF* represses silique development by its activity either collectively or individually within the inner integument, endothelium and female gametophyte tissues of the ovule (chapter 4.4.1). Phenotypes observed in the *spy-4 fwf* double mutant show that *FWF* has a unique role earlier in flower development during floral patterning and organogenesis. The overall phenotypes of the *spy-4 fwf* double definitively show that *SPY* and *FWF* function in overlapping pathways to regulate many functions. In the sections below, models are provided to describe how *FWF* and *SPY* jointly regulate floral organogenesis and development in different floral organs (Figure 5.3A).

5.4.3.1 Sepal margin identity

The overall organ identity of sepals is largely unaffected in the *spy-4 fwf* double mutant, however petalloid margins and vestigial ovules were present on the sepal perimeters. This is indicates the margins of sepal tissues in the *spy-4 fwf* double are capable

of undergoing further differentiation following the specification of sepal organ identity. Excess *AG* activity or the loss in *AP2* organ identity activity in sepals permits the differentiation of ovules and stigmatic tissue in this floral whorl (Drews et al., 1991; Mizukami and Ma, 1992). The *AP2* gene restricts carpel differentiation in whorls one and two by negatively repressing *AG*-dependent differentiation (Figure 5.3A; Drews et al., 1991). Alterations in sepal margins in *spy-4 fwf* and the observation that *fwf* enhances carpelloid ovule development in *bel1-1* (chapter 4.3.2), suggest that *FWF* represses several specific functions downstream of *AG* activity, and that *SPY* and *FWF* function together to repress marginal differentiation and identity in the sepal (Figure 5.3C).

5.4.3.2 Stamen identity

Carpelloid anther development was seen in the *spy-4 fwf* double mutant. Similar defects are also seen in the parthenocarpic *pat* mutant of tomato (Mazzucato et al., 1998; Mazzucato et al., 1999). Gibberellin has been implicated in controlling sex expression and sex determination (reviewed Pharis and King, 1985). Many plant species also exhibit alterations in sexual dimorphism in response to ectopic GAs. In maize, anthers become feminized following ectopic application of active GAs during specific floral stages (reviewed Pharis and King, 1985). Anther and filament development appears to be regulated tightly by GA biosynthesis and perception (reviewed Fei and Sawhney, 1999; Pharis and King, 1985). In *Arabidopsis* the *GA1* biosynthetic enzyme is expressed to high levels in anthers (Sun and Kamiya, 1997) and GA stimulated genes are highly expressed in stamen filaments (Aubert et al., 1998; Herzog et al., 1995; Raventos et al., 2000). Mutational studies in *Arabidopsis* and tomato have uncovered mutants that are dependent on exogenous GA for functional stamen development (Fei and Sawhney, 1999; Sawhney and Greyson, 1973), or dependent on exogenous GA for petal identity in the case of *ap1*

and *ap2* mutants (Okamuro et al., 1997). *SPINDLY*'s role in GA signal transduction may therefore play an important role in stamen identity in *Arabidopsis* together with signal transduction repressed by *FWF*.

During plant evolution, stamen identity may have become dependent on the co-evolution of components within the GA signal transduction pathway together with homeodomain and MADS box proteins. Since most primitive types of flowers have large perianths, or modified leaves with adaxial sporogenous zones, while advance angiosperms have an extremely reduced stamen structure, the regulation of cell proliferation may have played a significant role in the morphogenesis and reduction of the advance angiosperm stamen. Modification of *SPY* and *FWF* activity, along with other homeodomain proteins, might have participated in this evolutionary process.

5.4.3.3 Carpel and gynophore morphogenesis

In late flower positions *spy-4 fwf* carpel development was severely disrupted by the reiteration of gynophore and carpelloid tissues. Reiterated tissue had reduced polarity and identity similar to that observed in *spt-2 ap2-2 pi-1 ag-1* mutants (Alvarez and Smyth, 1999). Such tissue proliferation results from a loss in fourth whorl determinacy and ovule identity. Loss in fourth whorl determinacy is also seen in *ag-1* and *crc-1 ag-1* / + mutants (Alvarez and Smyth, 1999). *SPY* and *FWF* might specifically prevent reiteration within the carpel whorl to stop second order carpelloid tissue, ovule and gynophore development to ensure that only one carpel forms.

ETTIN functions during carpel morphogenesis to regulate the formation of the stigmatic-replum and carpel-gynophore boundaries (Bowman and Smyth, 1999; Sessions and Zambryski, 1995). *ETT* expression is restricted to the abaxial regions of the carpel primordium and persists until the gynoecial cylinder differentiates new tissue (Bowman

and Smyth, 1999; Sessions et al., 1997). At later stages of carpel development, prior to anthesis, *ETT* expression becomes restricted to vascular tissues (Sessions et al., 1997). *ETT* encodes an ARF (Sessions et al., 1997) and the application of the polar auxin transport inhibitor, NPA, can phenocopy the *ett* phenotype, therefore, auxin gradients are considered an integral component for providing positional information to determine the carpel-gynophore boundary (Nemhauser et al., 2000).

PID also encodes a protein kinase essential for auxin responses and defects in *PID* affect the apical-basal carpel-gynophore boundary (Christensen et al., 2000). The function of *AtSK12* and *AtSK11* members of the SHAGGY-related protein kinase genes can also affect the apical-basal carpel gynophore boundary (Dornelas et al., 2000). Antisense analysis of *AtSK12* and *AtSK11* induced a phenotype similar to *ett-1* (Dornelas et al., 2000). In contrast to the *pid* mutation and the antisense analysis of *AtSK* genes, loss of function in the *TOUSLED* (*TSL*) protein kinase greatly affects gynoecium morphogenesis and strongly affects the *ett-1* phenotype, reducing the carpel morphogenesis in *ett-1* to a solitary gynophore structure with apically positioned ovules (Roe et al., 1997). *TSL* is expressed in an apical-basal gradient in developing pistils, with the highest expression confined to the stigmatic region and the lowest expression towards the carpel-gynophore boundary (Roe et al. 1997).

Altered carpel-gynophore boundaries are also observed when the rice *OsDD4* gene is overexpressed in *Arabidopsis thaliana* plants (van der Knaap et al., 2000; van der Knaap, 1998). These plants also produce leaf-like structures in carpel whorls and filamentous structures in place of ovules (van der Knaap et al., 2000; van der Knaap, 1998), a phenotype with greatest similarity to the *spy-4 fwf* double mutant described in this chapter. *OsDD4* is a GA regulated gene that encodes a *Brahma*-related (*BRG-1*) protein

(van der Knaap et al., 2000; van der Knaap, 1998). In other organisms, *BRG-1* group proteins are required for retinoblastoma-mediated cell cycle arrest (Strobeck et al., 2000).

Collectively the data suggest that protein kinase networks might be important in the formation of the two hypothetical carpel boundaries. The mechanism of boundary formation may act via phosphorylation during the auxin signal transduction cascades and through other processes. *FWF* may have an independent role to *ETT*, because the *ett-2 fwf* phenotype was not altered in either hypothetical carpel boundary (Figure 5.3C). A reduction in *SPY* activity early in carpel morphogenesis could decrease *ETT* activity or expression (Figure 5.3C). However as we do not see altered boundary specification in *spy-4* mutants, it is plausible that there are other compensatory factors and *FWF* may be one of these (Figure 5.3C). This model could account for the *ett*-like phenotype observed in the *spy-4 fwf* double mutant, and because *SPT* is a likely target of *ETT* (Alvarez and Smyth, 1999), the loss of transmitting tract tissue, disrupted carpel fusion and altered stigma-carpel boundaries could be due to reduced *SPT* activity (Figure 5.3C).

This model suggests that *ETT* may not strictly translate auxin gradients into carpel boundaries, but interprets positional information from a variety of gradients in addition to auxin. A factor that may determine *ETT* activity is the protein *FIL* because expression domains of *ETT* and *FIL* overlap in the carpel (Siegfried et al., 1999) and *FIL* physically interacts with *ETT* in a yeast two-hybrid system (Watanabe et al., 1999). *ETT* also lacks the hetero- and homo-dimerization domains III and IV which are required for interaction with *Aux* / *IAA* family members and other ARF members (Guilfoyle et al., 1998b) and therefore *ETT* activity could bind to AuxREs to protect these sites from being transcriptionally activated.

Since *SPY* is presumed to be part of the GA perception pathway, an alternative model is one where reduced *SPY* activity promotes internode elongation of the gynophore

(Figure 5.3D). Auxin gradients acting in concert with GA signal transduction would specify the position of the carpel-gynophore boundary. In this model *SPY* and *ETT* would compete in a mutually exclusive manner to control the carpel-gynophore boundary and adjust the length of the gynophore (Figure 5.3D). The role of *FWF* is hard to explain in this model and further theories are unconstrained.

5.4.3.4 Ovule identity

Ovule development and identity was also affected in the *spy-4 fwf* double mutant (Figure 5.3A). In chapter 4.3.2, the *fwf* mutation was shown to enhance carpelloid structures developing in *bel1-1* ovule primordia. Ectopic expression of *AG* can produce carpelloid ovule development (Mizukami and Ma, 1992). The loss of repressive elements downstream of *AG* could also hypothetically reproduce this phenotype. *FWF* may function downstream of *AG*, but in parallel with other floral identity genes regulated by *SPY*, to control ovule morphogenesis (Figure 5.3C). Loss of function in both pathways would then lead to the production of carpelloid ovules (Figure 5.3C).

5.4.4 Future work

Models described in this chapter provide testable hypotheses to examine the role of *FWF*, *ETT* and *SPY* in *AG*-dependent and *SPT*-dependent carpel morphogenic pathways. To test models described in figure 5.3C and 5.3D the construction of *spy4 ett-2* double mutants is required to determine how *SPY*, *ETT* and GA perception participates in the specification of the carpel-gynophore boundary. This double mutant may illuminate how reduced *SPY* activity alters the gynophore-carpel boundary in the presence of the *fwf* mutation. The creation of *spt fwf* double mutant would also reveal whether *FWF* and *SPT*

genes act in separate pathways. The cellular expression pattern of *SPY* during floral development is also required to understand how *SPY* controls carpel development.

Experiments are also required to determine the role of stamen and anther emasculation on the control of parthenocarpic silique development, to address the how the outer floral whorls suppress parthenocarpic development (chapter 3.3.1).

Chapter 6: Mapped based cloning of *FWF* and mapping *ATS*

6.1 Introduction to map based cloning approaches

Mutagenesis in *Arabidopsis* allows researchers to identify gene function by the examination of the mutated phenotype and provides a way of cloning genes (Koncz et al., 1992). Isolation of a mutated gene is largely dependent on the nature of the genetic mutation and whether the researcher is employing a forward or reverse genetic screen. Reverse genetic screens are based upon the study and characterization of a mutant phenotype and then subsequently isolating the genetic lesion using a map based cloning procedure or by locating an insertional gene-tag that has been used as a mutagen (Koncz et al., 1992). Construction of physical and integrated maps of chromosomes facilitates locating these mutations within the genome. A forward genetic screen focuses on a gene of interest and involves the identification of insertional mutations within this gene or gene family and therefore does not require genomic mapping (Tissier et al., 1999; Wisman et al., 1998; Yephremov and Saedler, 2000). Mutant phenotypes generated in this way provide data on gene function.

Insertional mutagenesis where T-DNA or a transposon disrupts a gene function by integration can be used in both reverse and forward genetic screens and provides a convenient method in which to mutagenise and to locate the mutated gene. Fine mapping of the insertional mutant is usually not required, as flanking DNA adjacent to the insertion can be recovered and the gene identity and position deduced relative to a physical or genetic map. The disadvantages of insertional mutagenesis is that much smaller mutant populations are generated in comparative periods of time to which populations of chemical or radiation induced mutants can be generated.

Chemical mutagenesis with ethane methane sulfonate (EMS) or radiation with fast neutron or gamma radiation is usually used in reverse genetic screens. A caveat to chemical or radiation mutagenesis is that mutant plants must be backcrossed to reduce the

likelihood of any deleterious mutations becoming linked to the allele of interest. Secondly it takes longer to map and clone EMS induced, fast neutron or gamma irradiated mutations, but this is now being expedited with the sequencing and mapping of the entire *Arabidopsis* genome.

fwf is an EMS induced mutation with only one single allele identified to date. EMS mutants frequently have base changes or frame-shift lesions and locating these particular point changes requires linkage mapping against known markers within the *Arabidopsis* genome. Several alternative methods offered feasible approaches for cloning *fwf*. One approach was to use fast neutron radiation to generate new deletion alleles and use a genomic subtraction method to isolate DNA fragments corresponding to the deletion (Koncz et al., 1992). Another approach was to map the *fwf* mutation and then use this information to select an *Arabidopsis* line with a suitably positioned *Ds* element to act as a background for regional transposon mutagenesis to create a new tagged *fwf* mutant allele (Seki et al., 1999). A third option was possible if the mutant mapped to a sequenced region of the genome. Fine mapping *fwf* to a suitable resolution would permit selection of candidate genes based on sequence data for cloning and molecular complementation. *fwf* was fine mapped to a small interval on a completely sequenced region of the genome which permitted the third option. Flanking markers surrounding *fwf* were first identified and then additional recombinants within this interval were generated and analyzed.

6.2 Methods and results

fwf was separated from the associated *pi* background and found to be a recessive mutation as described in chapter 3. Homozygous *fwf* lines were identified in each backcross generation by emasculation, careful observation of the *fwf* phenotype and also by testcrosses. Several individual lines were maintained during this procedure to backcross

five. These were found to be identical and one of these was selected and backcrossed another two times. Recombinant analysis required a comprehensive description of the *fwf* phenotype in both Columbia and Landsberg backgrounds. This was provided in chapter 3.

6.2.1 Linkage analysis with existing SSLP, CAPS and visible markers

SSLP and visible markers spanning all five *Arabidopsis* chromosomes established linkage of the *fwf* lesion to chromosome five (chapter 3.3.3). Additional SSLP and CAPS marker analysis on the 26 *fwf* individuals described in chapter 3.3.3 placed *fwf* between GA3 and AthSO191 (Figure 6.1; appendix 1.1). To delineate the region containing *FWF* further, additional recombinant progeny and markers were scored in this region. A cross was performed between Col-3 (female parent) and *fwf* (pollen donor). A total of 38 *fwf* individuals were identified from a population of 272 emasculated F_2 plants. Three informative recombinants within this population suggested that *fwf* was located centromeric to the AthSO191 marker (Figure 6.1). However, low recombination, incomplete *fwf* penetrance and the absence of a polymorphism at the AthPhyC marker in the Col-3 background precluded further analysis of F_2 individuals segregating in the Col-3 background. The three informative recombinants were retained for further marker analysis, as were an additional 20 *fwf* plants from a cross between Col-1 (female parent) and *fwf* (pollen donor; $n = 87$ F_2 emasculated plants).

6.2.2 The *ats* mutation maps telomeric to *BEL*

In order to map *ats* and *fwf* simultaneously, a cross was also performed using *ats fwf* in coupling phase as a pollen donor to Col-4 plants (chapter 3.2.2). By using *ats* in coupling phase, the linkage order of *fwf* with surrounding molecular markers could be established whilst also providing three point recombination estimates. The use of *ats fwf* in

Figure 6.1 Genetic and physical mapping of the *fwf* and *ats* mutations. (A) Genetic map of chromosome 5 shows the map position of *fwf* and *ats* (cM). (B) The physical map position of *fwf* and the number of recombinants between the AthPhyC and AthSO191 markers below. (C) Number of recombinants in the interval spanning the Col-4 dominant marker MLF18 #2 and the CAPS marker MJG14 #2. (D) A BAC / P1 map obtained from the KAOS database spanning the region containing *FWF*. (E) Open reading frames indicating potential genes in the delineated region containing *FWF*.

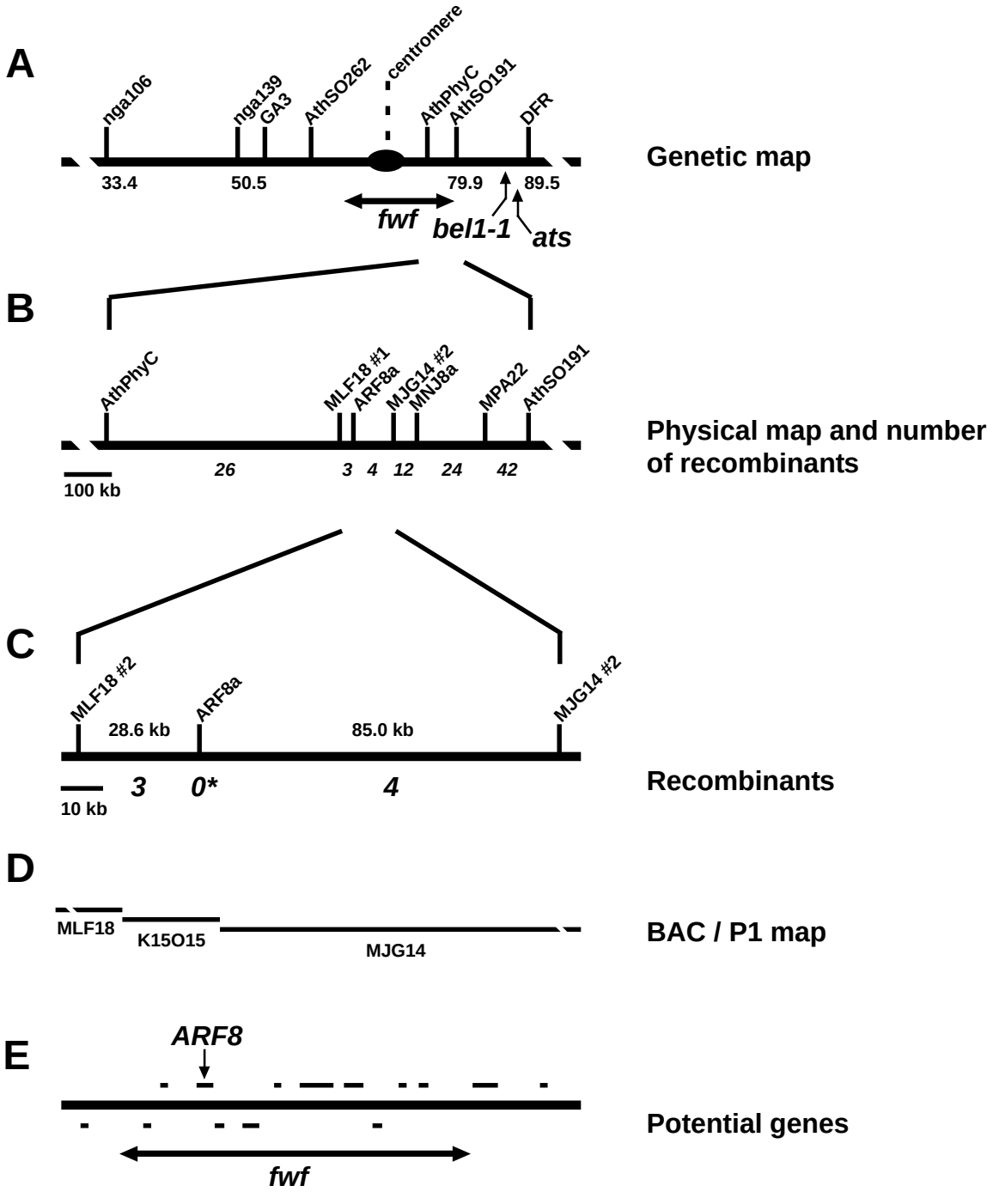
A
nga106
nga139
GA3
AthSO262
centromere
AthPhyC
AthSO191
DFR
33.4
50.5
79.9
89.5
fwf
bel1-1
ats
Genetic map
B
AthPhyC
MLF18 #1
ARF8a
MJG14 #2
MNJ8a
MPA22
AthSO191
26
3
4
12
24
42
100 kb
Physical map and number of recombinants
C
MLF18 #2
ARF8a
MJG14 #2
28.6 kb
85.0 kb
3
0*
4
10 kb
Recombinants
D
MLF18
K15O15
MJG14
BAC / P1 map
E
ARF8
fwf
Potential genes

coupling phase enabled the visual identification of rare single mutant individuals eliminating the requirement for molecular markers. In the first instance, 59 *fwf* plants were analyzed from 181 F_2 plants.

The position of *ats* on the genetic map of chromosome 5 was reported as 64 cM, close to the *bel1-1* mutation (chapter 4; KAOS and TAIR databases). F_1 plants from a cross between *ats* and *bel1-1* produced wild type seeds indicating that the two mutations had complemented each other and that *ats* and *bell* were independent loci.

ats was subsequently mapped to a region telomeric to the *bell* locus and located between the CAPS marker MJC20 #2 and MDH9 #1 marker (Figure 6.2) using informative recombination events and new CAPS and SSLP markers developed between AthPhyC and DFR (appendix 1.1). This indicated that the map position published for *ats* in the TAIR database at October 2000 is incorrect. Figure 6.2 shows that four *ats* recombinants span the 170 kb interval between MJC20 #2 and MDH9 #1 (Figure 6.2). This region spans the portions of the P1 vectors MJC20 and MDH9 and covers the entire TAC vector K5J14 (KAOS database; Figure 6.2).

Inspection of *Arabidopsis* sequence data in the 170 kb interval between MJC20 #2 and MDH9 #1 using the KAOS database revealed 34 potential coding regions. A total of 16 of these candidates could be excluded based on sequence similarity to genes known to have metabolic, chloroplast or other cellular functions. Functions for 7 have not yet been described. Eleven remaining coding regions encoded three protein kinases, a Skp1 homologue, a coding region with similarity to an auxin-induced protein, a Myb-transcription factor, a GTP binding-like protein, a flower bud expressed gene and a protein containing chromosome condensation motifs. Another two genes appear to encode transcription factors. One of these transcription factors encodes a putative protein with

Figure 6.2 Physical map position of the *ats* mutation on chromosome 5. Four recombinants position *ats* to a region between the markers MJC20 #2 and MDH9 #1. The position of a potential gene encoding *ATS* is indicated by a *SCL*-gene or *GRAS* gene family member.

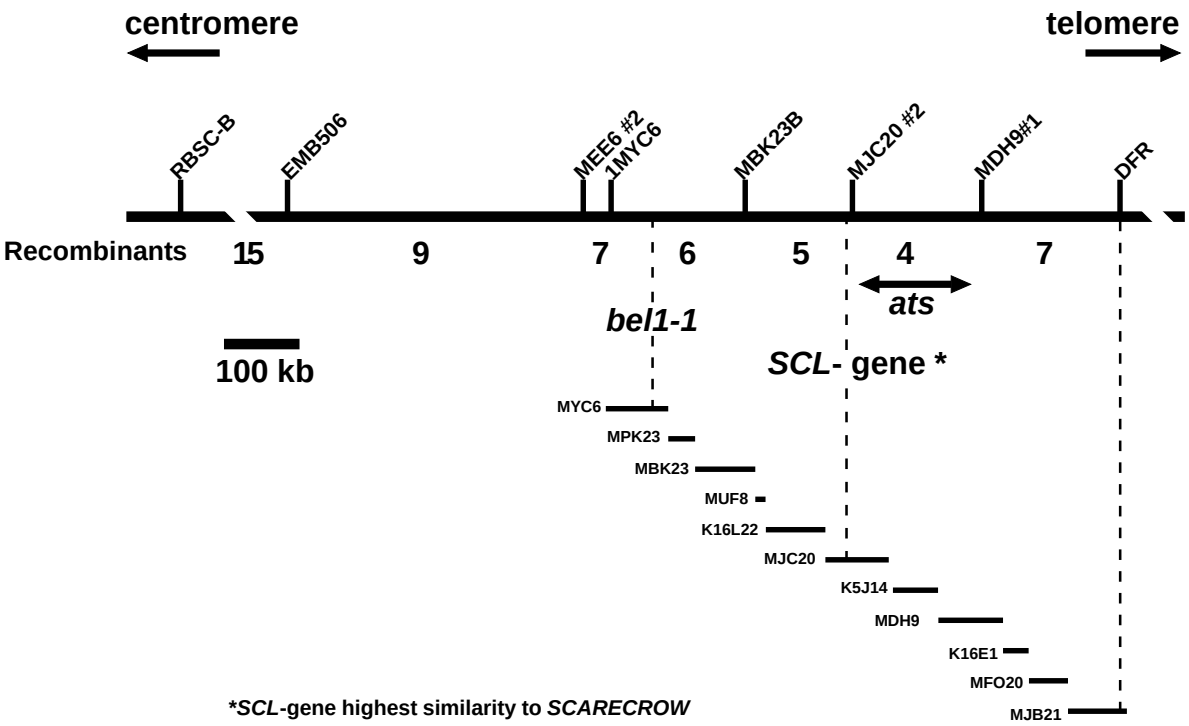
centromere
telomere
RBSC-B
EMB506
MEE6 #2
1MYC6
MBK23B
MJC20 #2
MDH9#1
DFR
Recombinants
15
9
7
6
5
4
7
ats
bel1-1
100 kb
SCL- gene *
MYC6
MPK23
MBK23
MUF8
K16L22
MJC20
K5J14
MDH9
K16E1
MFO20
MJB21
*SCL-gene highest similarity to SCARECROW

similarity in the final three exons to the *TRITHORAX* protein of *Drosophila melanogaster* and has similarity to another protein on chromosome 5.

Another gene that could also be considered as a candidate for *ATS* encodes a *SCR*-like or *GRAS* family member but it is located 30 kb centromeric to the MJC20 #2 marker (Figure 6.2), which conflicts with current mapping data indicating that *ats* is located telomeric to MJC20 #2. However, the *ats* phenotype has several features in common with mutants in other *GRAS* family members including *GAI*, *LATERAL SUPPRESOR* and *SCARECROW* (chapter 3). Mutations in these genes result in defective cell divisions in specific tissues. *lateral suppressor* (Schumacher et al., 1999) and *scarecrow* (Di Laurenzio et al., 1996) mutants have missing cell types as does *ats*, with two cell layers missing from integument tissues and *ats* forms a composite outer and inner integument (Léon-Kloosterziel et al., 1994).

Neighbor joining comparisons (Page, 1996; Rice, 1994) amongst the *GRAS* family members identified in the *Arabidopsis* genome revealed that the *SCR*-like candidate encoded on the P1 vector MJC20 has the most similarity to *SCARECROW* (chapter 3; Figure 3.7). Based on phenotypic analysis it is tempting to speculate that *ATS* is a *SCR*-like gene, however, the current map position conflicts with this concept. Additional recombinants or complementation with genomic fragments spanning this region are now required to reveal the identity of *ATS* and to further establish the role *ATS* plays in parthenocarpy and fruit development.

6.2.3 *fwf* is located between AthPhyC and AthSO191

The new physical map position for the visible marker, *ats*, helped locate *fwf*. From the analysis of 181 F_2 individuals resulting from the cross between Col-4 and *ats fwf*, the distance between *ats* and *fwf* was determined to be 8 ± 2.32 cM (chapter 3.3.3 and chapter

6.2.2), using the Haldane function (Koornneef and Stam, 1992) and the estimation of the recombinant fraction (Stevens, 1939). This data placed *fwf* between AthPhyC and AthSO191.

A revised genetic map was also calculated from the molecular marker analysis on plants pooled from all informative progeny in the above crosses (not shown; Koornneef and Stam, 1992; Stevens, 1939). Map distances between *fwf* and each molecular marker were determined and compared with the genetic distances established for the recombinant inbred map established for *Arabidopsis* (TAIR database). This confirmed that *fwf* was located between AthPhyC and AthSO191 on the genetic map (Figure 6.1). Analysis of SSLP and CAPS markers in near isogenic lines (NIL) containing *fwf*, facilitated mapping and provided data which also confirmed that *fwf* was located between the AthPhyC and AthSO191 markers (Figure 6.3). All of the informative recombinants from the above mapping populations were retained for further analysis.

6.2.4 PCR based screening for AthPhyC – AthSO191 recombinants

Fine scale mapping required the generation and assessment of additional informative recombinants in the AthPhyC and AthSO191 interval. A PCR screening method was employed to screen plants at an early plant stage to facilitate the identification of recombinants between AthPhyC and AthSO191 recombinants.

A DNA extraction procedure for large scale PCR based screening was modified from that described by Langridge et al., (1991). Small Hybond™ N+ nylon membrane discs were cut with a paper punch and placed individually into a 96-well microtitre plate. Each disc was adhered to the well using a drop of acetone to soften the plastic and the acetone was allowed to evaporate. A total of 1602 F_2 seedlings from crosses between Col-4 and *ats fwf* in the coupling phase, and also Col-4 and *fwf*, were grown to a four leaf stage

Figure 6.3 Analysis of recombinants in the near isogenic line containing *fwf*. *fwf* is contained between the markers AthPhyC and AthSO191 positioned on L.*er* DNA (blue) and flanked by Col-1 DNA (red).

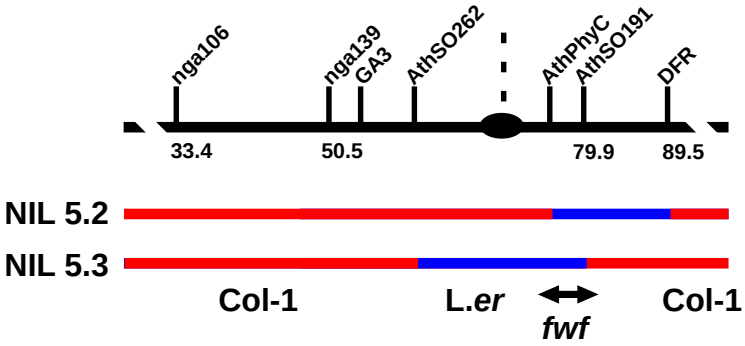
nga106
nga139
GA3
AthSO262
AthPhyC
AthSO191
DFR
33.4
50.5
79.9
89.5
NIL 5.2
NIL 5.3
Col-1
L.er
fwf
Col-1

on MS media (Murashige and Skoog, 1962; containing 2% suc, 1% agarose, pH 5.9). Seedlings were grown at a density of 24 plants per plate in 100 mm by 20 mm culture dishes. Seedlings were numbered and a single leaf was excised from each plant. Leaves were placed in individual wells to which 20 μl of 1M NaOH had been added and were crushed onto the membrane using a disposable pestle. 50 μl of high salt buffer (1.5 M NaCl, 0.5 M Tris.Cl pH 7.0, 1 *m*M EDTA) was added using a multi-channel pipette. The solution was removed after one minute and 100 μl of low salt buffer (1 *m*M EDTA, 10 *m*M Tris.Cl pH 7.5) was then added and subsequently removed after another minute. The membranes were washed with sterile dH_20 and then the DNA was eluted from each membrane in a 70 μl volume of dH_20 after heating at 95°C for 3 minutes on a waterbath. Eluted DNA was transferred to a new microtitre plate and further diluted to a final volume of 210 μl with dH_20. A 10 μl aliquot was directly used in each 20 μl PCR reaction or the extracted DNA was stored at –20°C for several days until required.

Plant DNA was screened using primers that corresponded to AthPhyC and AthSO191. Primer pairs for AthPhyC and AthSO191 were combined together in a multiplex PCR in 96 well PCR tube format. PCR products were separated on Metaphor® or SeaKem® LE 4% agarose gels. Recombinant plants were identified by comparing segregation patterns of AthPhyC-AthSO191 markers. Recombinants plants were transferred to soil, grown, scored for parthenocarpic silique elongation and F_3 seed was collected. Plant genotypes were then rechecked from individual leaves of transplanted seedlings using DNA extracted as described by Edwards et al., (1991). Once plant genotypes were verified, all of the informative recombinant progeny within the interval between AthPhyC and AthSO191 were pooled for further analysis.

6.2.5 Fine mapping by recombinant screening located *fwf* to a 110 kb region

A pool of 121 recombinants within the AthPhyC and AthSO191 interval was obtained. During fine mapping a number of plants were excluded from further analysis. It was revealed that six parthenocarpic plants homozygous for *ats*, were heterozygous for *fwf*. Two other parthenocarpic plants that were derived from crosses between Col-4 and Col-1 with *fwf* were also excluded because progeny testing and map data showed these parthenocarpic plants were also *fwf* heterozygotes. This data, together with the observation that *ino fwf* / + heterozygote plants were parthenocarpic (chapter 4.3.3), was the first indication that *fwf* might be a semi-dominant mutation and not necessarily be a null mutation. A threshold effect could account for parthenocarpic development of heterozygous *fwf* plants in different backgrounds.

Fine mapping necessitated the determination of the phase of *fwf* in the 121 pooled coupling and repulsion phase recombinants. Initially emasculation and scoring for *fwf* silique phenotype was performed on plants that were homozygous for L.*er* at one locus and heterozygous for Col-4 at the other. As additional CAPS and SSLP markers were mapped it was necessary to grow and assess *fwf* linkage in homozygous F_3 individuals from F_2 individuals that were in the opposite phase. Due to the intensive nature of emasculating and scoring individuals, only recombinants in critical map positions were examined in this phase. Homozygous F_3 recombinant plants were verified by SSLP and CAPS markers and by scoring for parthenocarpic silique elongation.

In total 68 plants, excluding the heterozygote *fwf* individuals, were emasculated and scored for segregation of both wild type and *fwf* alleles. Markers within the AthPhyC and AthSO191 interval were scored and recombinants were found centromeric and telomeric to the ARF8a marker respectively (Figure 6.1B). Markers surrounding the ARF8a marker had the least number of recombinants (Figure 6.1C). This revealed that *fwf* is located in a region spanning the TAC vector K15O15 and part of the P1 vector, MJG14 (KAOS

database; Figure 6.1C and 6.1D). Predicted gene sequences in this region were inspected (Kazusa database) and a candidate gene was identified for cloning and complementation analysis (Figure 6.1E).

Based on physiological data (chapter 2), developmental and genetic data (chapter 3 and chapter 4), the *Auxin Response Factor 8* (*ARF8*) gene appeared to have the highest likelihood of containing the *fwf* mutation. Members of the *ARF* family have been cloned previously and shown to bind AuxRE elements that contain a core DNA motif of TGTCTC and *ARF* members have capacity to activate or repress transcription in response to exogenous auxin (Ulmasov et al., 1999a; Ulmasov et al., 1999b). Figure 6.4A shows the structure of the *ARF8* genomic clone including the promoter region, exon positions and also the polypeptide produced by *ARF8* (Ulmasov et al., 1999b).

6.2.6 The ATG translation start in *ARF8* is mutated in *fwf*

A 6048 bp region of genomic DNA containing the *ARF8* coding sequence and 1834 bp of 5' sequence flanking the ATG was amplified by Dr Anna Koltunow from both *fwf* and L.*er* using eLONGase® and PCR primers (ARF8 –1830F and ARF8a +2817R; appendix 1.1) according to manufacturer instructions (Gibco BRL, Rockville, MD). Each product was subsequently cloned into the T-easy vector (pGEM® -5Zf+; Promega, Madison, WI) following the addition of adenosine residues using terminal transferase (Roche Molecular Biochemicals, Palo Alto, CA).

I performed single strand sequencing on the cloned fragments obtained from both *fwf* and L.*er* using the – 44 forward primer (appendix 1.1 and 1.2). Comparison of sequence data revealed that the ATG translation start site in *ARF8* cloned from *fwf* was mutated to ATA (Figure 6.4B). To test whether the mutation in the protein initiation codon was not a result of a PCR amplification error during the primary cloning step, a CAPS

Figure 6.4 (A) The cloned genomic DNA fragment (6048 bp) containing the *ARF8* gene. Exons are shown in blue. The *ARF8* promoter contains sequences with similarity to core motifs of the CArG box and auxin response elements (AuxRE). The *ARF8* protein has a DNA binding domain (DBD), a Q-rich region, and carboxy-terminal domains (CTD) III and IV (Ulmasov et al., 1999a). The predicted *ARF8* protein coding sequence in *fwf* lacks the DBD and contains a truncated Q-rich region but retains both CTD domains of the protein. (B) Sequence chromatograms comparing the wild type *ARF8* ATG translation start site (top) and the mutated ATA start site found in *fwf* (bottom). (C) *Hsp92 II* restriction endonuclease cleavage of PCR products amplified from DNA extracted from No.O, Col-4, L.*er*, heterozygote *fwf*, homozygous *fwf*, PCR products of cloned *ARF8* sequences from *fwf* (1.4) and L.*er* (2.6) and the recombinant *fwf* plant B4CAT48. The presence of the 82 bp fragment (arrow) indicates the presence of the ATG initiation codon in the *ARF8* sequence.

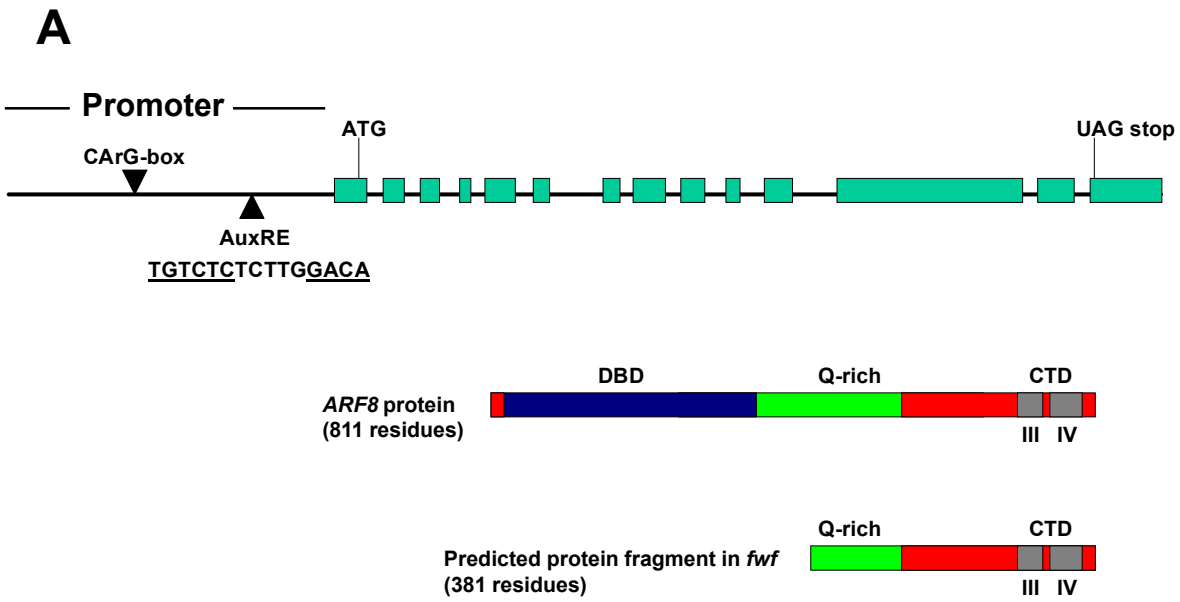
A
Promoter
ATG
UAG stop
CArG-box
AuxRE
TGTCTCTCTTGGACA
DBD
Q-rich
CTD
ARF8 protein
(811 residues)
III IV
Q-rich
CTD
Predicted protein fragment in fwf
(381 residues)
III IV

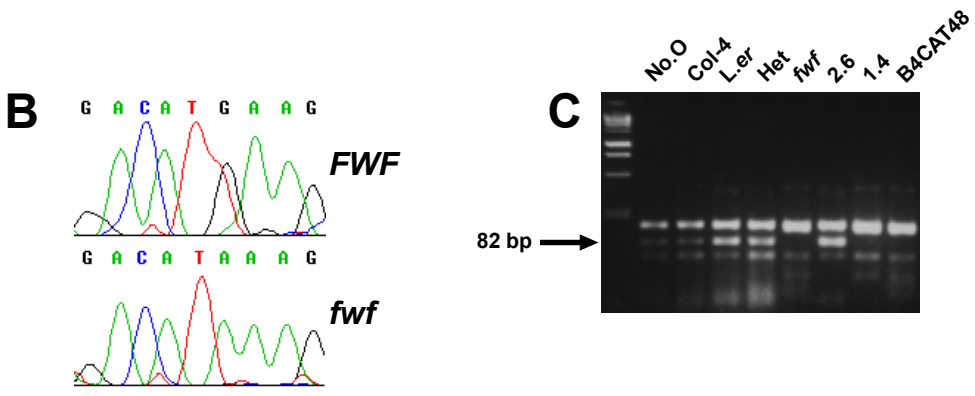
B
G A C A T G A A G
FWF
G A C A T A A A G
fwf
C
No.O
Col-4
L.er
Het
fwf
2.6
1.4
B4CAT48
82 bp

polymorphism was designed to assess that the ATA site was present in individual *fwf* plants and absent from wild type plants in mapping populations. Using the ARF8 – 44 forward primer and the reverse primer ARF8 15394R (appendix 1.1), PCR amplifications were performed on DNA isolated from wild type L.*er* plants, recombinant populations and also genomic *ARF8* DNA cloned from *fwf* and wild type L.*er* plants. *Hsp92 II* restriction endonuclease was used to cleave PCR products. PCR products amplified from wild type plants and also *ARF8* sequences cloned from wild type L.*er* were digested with *Hsp92 II* restriction endonuclease and produced an expected 82 bp fragment (Figure 6.4C), indicating that the ATG was present. *Hsp92 II* left PCR products amplified from *fwf* plants and also *ARF8* cloned from *fwf* plants uncut (Figure 6.4C). This indicated that the *ARF8* protein initiation codon is mutated to ATA in *fwf* plants and that the sequence is not an artifact resulting from the cloning of the *ARF8* sequence from *fwf* plants.

Both strands of the two *ARF8* genomic clones (6048 bp) isolated from *fwf* and wild type plants in the L.*er* background were sequenced by the Australian Genome Research Facility (AGRF). This also confirmed that the ATG start site was mutated to ATA in the clone isolated from *fwf* plants and also identified other base substitutions in the 6 kb region (Table 6.1). When *ARF8* genomic sequences from L.*er* and *fwf* were compared with the Col-4 genomic sequence obtained from the KAOS database four base substitutions were specific to *fwf*. Two base substitutions specific to the *fwf* sequence occurred in the 3' untranslated region (UTR; Table 6.1). These two substitutions would not affect *ARF8* protein activity, but it is not known if they alter message stability through modification of the 3'UTR stability motifs (Gil and Green, 1996). The fourth base substitution that was specific to *fwf* occurred at position 3418. This was a silent mutation with respect to *ARF8* amino acid composition (Table 6.1) and therefore unlikely to alter *ARF8* activity. Thus the

Table 6.1 Summary of base substitutions between Col-4, L.*er* and *fwf* (start site is position 1834)

	Base		
Position in L.*er* clone	**Col-4**	**L.*er***	***fwf***	
1730	G	T	T	
1802	T	C	T	5' UTR
1836	G	G	A*	start site mutation in *fwf*
1885	T	C	T	intron 1
2977	C	T	T	
3267	G	A	A	
3418	T	T	C*	silent substitution in exon XII
3687	A	C	C	
4058	T	G	G	
4164	G	T	T	
4326	A	T	T	
5581	T	C	C	
5626	A	T	T	
5804	T	T	C*	3' UTR
5986	A	A	G*	3' UTR

*indicates base substitutions specific to *fwf*

mutated protein initiation codon sequence was considered to be the primary lesion affecting *ARF8* function in *fwf* plants.

6.2.7 Transformation of mutated *ARF8* into wild type L.*er* induces parthenocarpic silique development

The wild type L.*er* and mutated copies *ARF8* cloned from *fwf* were subcloned into the pBIN19 vector (Bevan, 1984) and transformed into *Agrobacterium tumefacians* strain LBA4404 by Dr Anna Koltunow. I grew up *Agrobacterium* cultures and plants were transformed using the dipping method (Clough and Bent, 1998). Mutated *ARF8* and wild type *ARF8* were separately introduced into No.O, L.*er* and *fwf* plants. Kanamycin resistant plants (50 μg L^{-1}) were assessed for the presence of the T-DNA insert using PCR primers designed to detect the *NPTII* gene (appendix 1.1).

Complementation of the mutation was attempted by introducing wild type *ARF8* sequence into *fwf* plants and subsequent analysis of transformants by emasculation to examine if parthenocarpic fruit developed. It was expected that a wild type copy of *ARF8* would restore fertilization-dependent silique development in emasculated *fwf* transformants. It proved difficult to introduce and regenerate *fwf* plants containing the *ARF8* gene. Only three plants were obtained following the germination of 1.42 grams of seed on kanamycin and only one survived to flowering. When the surviving plant was emasculated it was parthenocarpic (Figure 6.5), as were 32 of its progeny plants, indicating that the mutation was not complemented in the only recovered plant. Southern analysis was not carried out to determine if the surviving plant actually contained an intact copy of the introduced *ARF8* gene. Following the floral dip transformation of the wild type *ARF8* copy to wild type No.O and L.*er* backgrounds, three No.O and three L.*er* plants were found to be kanamycin resistant following the germination 0.97 g and 0.29 g of seed respectively.

Figure 6.5 Some transformants containing the mutated *ARF8* cloned from *fwf* are parthenocarpic. (A) Emasculated 7 day wild type No.O pistil and a parthenocarpic No.O T_0 transformant containing *ARF8* cloned from *fwf* (1.4). (B) Fertilization-dependent silique development was not observed in the only kanamycin resistant plant obtained from transformation aimed at complementing the *fwf* mutation by introducing wild type *ARF8* sequence (2.6) into *fwf* mutants.

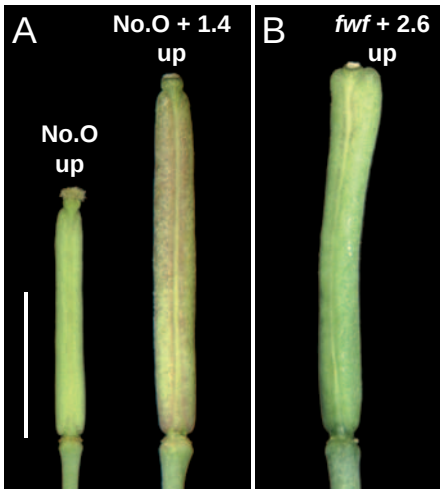
A
No.O + 1.4
up
No.O
up
B
fwf + 2.6
up

These plants were not parthenocarpic and appeared like wild type plants. Further work is required to establish if complementation can be achieved by either crossing the plants containing a wild type copy of *ARF8* with *fwf*, or through the complementation of wild type *ARF8* to *fwf* plants.

By contrast transgenic No.O and L.*er* plants containing the mutated *ARF8* gene were readily obtained. A total of 7 No.O and 9 plant L.*er* transgenic plants were obtained following the germination of 0.2 and 0.7 grams of seed respectively. Surprisingly, 3 of the 7 T_0 No.O plants and 4 of 9 L.*er* T_0 plants transformed with the mutated copy were found to be parthenocarpic when emasculated (Figure 6.5). One No.O plant containing mutated *ARF8* had fasciated meristems, another No.O plant developed leaves from root tissue and one also had irregular leaf margins. Plants 2511T10 (No.O) and 2003T3 (L.*er*) that were transformed with the mutated *ARF8* had mean emasculated silique lengths of 6.4 ± 0.4 (> flower position 25) and 6.1 ± 0.3 mm respectively (> flower position 30). This length approached that observed in homozygous *fwf* lines (7.5 ± 1.0 mm). Crosses were also performed between homozygous *fwf* lines and primary No.O transformants containing mutated *ARF8* that displayed a parthenocarpic silique phenotype. Kanamycin resistant progeny selected from this test cross were also found to be parthenocarpic (not shown).

Ten *fwf* plants transformed with the mutated *ARF8* were also obtained. Four of these plants remained small, became chlorotic and died. Four of the surviving plants displayed auxin like phenotypes that included fasciated stems, terminal meristems, trumpet shaped leaves or chlorotic flowers with alterations in carpel-gynophore boundaries. These phenotypes have also been observed in the *filamentous flower* mutant (Sawa et al., 1999a; Sawa et al., 1999b), *clavata* mutants (Clark et al., 1996), plants overexpressing of *yabby3* (Siegfried et al., 1999) and in plants containing antisense *AtSK11* and *AtSK12* (Dornelas et al., 2000). The *fwf* line containing mutated *ARF8* that displayed alterations in carpel-

gynophore boundaries was most similar to the *ettin* (Sessions et al., 1997), *pinoid* (Ferrándiz et al., 1999) and *the spy-4 fwf* double mutant phenotype (chapter 5.3.2).

These observations, together with those showing that the introduction of mutated *ARF8* into wild type plants induces parthenocarpy, indicate that *fwf* is unlikely to be a null mutation. Portions of the mutated *ARF8* gene must be transcribed and translated into functional protein capable of converting fertilization-dependent silique development into a fertilization-independent response in wild type plants and also creating the auxin-like defects in *fwf* plants when extra copies of mutated *ARF8* are introduced. Southern analysis is required to determine the copy number of the mutated *ARF8* in the transgenic plants and to determine whether the copy number relates to the phenotypes observed as this may indicate a dosage effects of the introduced gene. An alternative and unlikely explanation, where the introduced mutated *ARF8* copy silences *ARF8* expression producing the parthenocarpic phenotype, could be tested using RNAi (Chuang and Meyerowitz, 2000) or by *Arabidopsis ARF8* gene knockouts (Wisman et al., 1998; Parinov et al., 1999).

6.2.8 Protein initiation from another ATG in the mutant *ARF8* gene may allow translation of the Q-rich and carboxy-terminal domains

An alternative open reading frame was discovered in the mutant *ARF8* gene using the BCM BESTORF program (Smith et al., 1996). The program predicted that an in frame but truncated ARF8 polypeptide sequence could be produced beginning at amino acid position 430 and thus could contain a portion of the Q-rich region together with the entire carboxy-terminal domains III and IV of ARF8 (Figure 6.1A and Table 6.2).

The carboxy-terminal region of *ARF*s has been shown to be essential for the homo- and hetero-dimerization of *ARF* family members and is essential for the activation of auxin-dependent responses in carrot protoplasts (Ulmasov et al., 1999b). Molecular data

Table 6.2 Amino acid sequence for *ARF8* and the best-predicted protein sequence in the *fwf* mutant, indicating the alternative methionine translation initiation codon (arrow). The DNA binding domain is indicated in blue, the Q-rich region in green, and carboxy-terminal domains III and IV are underlined.

MKLSTSGLGQQGHEGEKCLNS**ELWHACAGPLVSLPSSGSRVVYFPQGHSEQVAATTN**
KEVDGHIPNYPSLPPQLICQLHNVTMHADVETDEVYAQMTLQPLTPEEQKETFVPIE
LGIPSKQPSNYFCKTLTASDTSTHGGFSVPRRAAEKVFPPLDYTLQPPAQELIARDL
HDVEWKFRHIFRGQPKRHLLTTGWSVFVSAKRLVAGDSVIFIRNEKNQLFLGIRHAT
RPQTIVPSSVLSSDSMHIGLLAAAAHASATNSCFTVFFHPRASQSEFVIQLSKYIKA
VFHTRISVGMRFRMLFETEESSVRRYMGTITGISDLDSVRWPNSHWRSVKVGWDEST
AGERQPRVSLWEIEPLTTFPMYPSLFPLRLKRPWHAGTSSLPDGRGDLGSGLTWLRG
↓
GGGEQQGLLPLNYPSVGLFPWMQQRLDLSQMGTDNNQQYQAMLAAGLQNIGGGDPLR
QQFVQLQEPHHQYLQQSASHNSDLMLQQQQQQQASRHLMHAQTQIMSENLPQQNMRQ
EVSNQPAGQQQQLQQPDQNAYLNAFKMQNGHLQQWQQQSEMPSPSFMKSDFTDSSNK
FATTASPASGDGNLLNFSITGQSVLPEQLTTEGWSPKASNTFSEPLSLPQAYPGKSL
ALEPGNPQNPSLFGVDPDSGLFLPSTVPRFASSSGDAEASPMSLTDSGFQNSLYSCM
III
QDTTHELLHGAGQINSSNQTKNFVKVYKSGSVGRSLDISRFSSYHELREELGKMFAI
IV
EGLLEDPLRSGWQLVFVDKENDILLLGDDPWESFVNNVWYIKILSPEDVHQMGDHGE
GSGGLFPQNPTHL

has shown that Q-rich *ARFs* can operate as potent activators of auxin responses in the absence of a functional DBD in carrot protoplasts (Ulmasov et al., 1999a). *ARF*s that lack a functional DBD do not bind AuxRE elements but appear to activate transcription through the dimerization with other intact endogenous *ARFs* that occupy AuxREs (Ulmasov et al., 1999a). The carboxy-terminal domain (CTD) of the predicted polypeptide from the mutant copy of *ARF8* gene may function to interfere with the activation and repression of auxin responses. Further work is required to test this prediction and to determine if copy number of the introduced mutant gene is important for the induction of a parthenocarpic response in wild type plants.

6.2.9 AuxRE, homeodomain and MADS-box binding motifs were identified in the *ARF8* promoter

The PLAnt Cis-acting Element program (PLACE; Higo et al., 1999), the Genomatix promoter-scan (Quandt et al., 1995) and TFSEARCH (Heinemeyer et al., 1998) programs were used to identify potential transcription factor binding motifs in the *ARF8* promoter. A MADS-box DNA binding motif with similarity to an *AGAMOUS* binding site or CArG box motif was found (Table 6.3 and Figure 6.1; Huang et al., 1993). In the forward orientation, the CArG box motif in *ARF8* resembles the *MCM1* motif found in yeast (Acton et al., 2000). In the reverse orientation the motif is most similar to the *AG* DNA binding motif (Huang et al., 1993). The identification of a potential MADS-box binding domain indicates that *ARF8* might be targeted and regulated by one or more MADS domain proteins. Potential candidates include the transcription factor *AGAMOUS* or *FRUITFULL*. The presence of a T nucleotide at position 1 in the forward orientation of the core CArG motif in *ARF8* may affect the recruitment, binding and orientation of MADS-box proteins to the core motif. However, a comparison of the reverse orientation

Table 6.3 CArG-box motif in *ARF8* promoter (position –1237)

	Nucleotide position																	
	-4	**-3**	**-2**	**-1**	**1**	**2**	**3**	**4**	**5**	**6**	**7**	**8**	**9**	**10**	**11**	**12**	**13**	**14**
ARF8	G	T	T	T	T	C	T	C	T	T	T	T	G	G	T	A	A	G
MCM1		T/a	T	-C	C	C	T/C	A	A	T/A	N	N	G	G	T	A	A	
AGAMOUS	N	T	T/a	A/T	C	C	A/T	A/t	A/t	T/A	N	N	G	G	-G	A/t	A	N
SRF	A	T	G	C	C	C	A/t	T	A	T	A	T/a	G	G	T/A	N	N	T

sequence against the consensus *AG* CArG box motif (Huang et al., 1993), shows that the 5' upstream *ARF8* motif does indeed represent a potential binding site. This is because the T nucleotide becomes inconsequential for binding interaction.

Several sequences resembling the core binding motif of the homeodomain protein *Athb1* (CAAT(A/T)ATTG; Sessa et al., 1993), were also observed in the *ARF8* promoter region. One *Athb1* motif sequence flanks the CArG-box motif in the *ARF8* promoter and is located 1264 bp upstream of the ATG translation initiation codon. Another *Athb1* motif is located at 841 bp upstream from the ATG translation initiation codon. *Athb1* is a member of homeobox proteins that share a common 60 amino acid sequence element that forms a DNA binding domain (Gehring et al., 1994; Sessa et al., 1997). *Athb1* is similar to the homeodomain protein *BEL* (Dong et al., 2000; Hertzberg and Olsson, 1998). *Athb2* is less similar to *BEL* (Bharathan et al., 1999; Dong et al., 2000) and also binds to the *Athb1* consensus sequence but with less efficiency (Sessa et al., 1997). If *BEL* recognizes similar motifs as *Athb1* then it may be involved in regulating *ARF8* transcription together with MADS box proteins that bind CArG box motifs. A precedent for interaction between MADS-box transcription factors and homeodomain proteins already exists in yeast, where the interactions of MATα2 and MCM1 proteins act cooperatively to bind a 31 bp specific operator (Gehring et al., 1994; Tan and Richmond, 1998).

A sequence with high similarity to an AuxRE element was also found in the *ARF8* promoter region (Ulmasov et al., 1999b; Figure 6.1). This suggests that *ARF8* activity might either be repressed or activated by other *ARF* proteins that bind and occupy the AuxREs or that *ARF8* may be capable of self regulating its own transcription.

6.3 Discussion

Nitsch, (1970) proposed that genetically controlled parthenocarpy was a consequence of temporal hormonal alterations in ovary tissues that triggered fruit development. In this chapter, a mutation in a gene involved in the auxin signal transduction cascade was found to confer parthenocarpy in *Arabidopsis*. The *ARF8* gene, a member of the Auxin Response Factor group of transcriptional regulators (Ulmasov et al., 1999a; Ulmasov et al., 1999b) was found to contain a mutated translation start site. Sequence analysis indicated that a *ARF8* truncated protein lacking a DNA binding domain might be produced. The introduction of the mutant *ARF8* gene into wild type plants induced the parthenocarpic phenotype indicating that the *fwf* lesion is not a null mutation and that a truncated protein may be interfering with the intact *ARF8* protein function to elicit parthenocarpy in transgenic plants. In contrast to the hypothesis of Nitsch, (1970), the lesion in *ARF8* suggests that aspects of primary events in the auxin signal transduction cascade rather than levels of the hormone alone may be involved in the mediation of parthenocarpic fruit development in *Arabidopsis*.

6.3.1 *ARF* genes and their roles in controlling auxin responses

Greater than 85% of the *Arabidopsis* genome has been sequenced and 13 members of the *ARF* family can be identified from available sequences (Figure 6.6). *ARF* members are conserved in higher plants and are found in tomato, potato, rice, maize and soybean (The Institute for Genomic Research database; TIGR). In *Arabidopsis* four *ARF* members, including that cloned from *fwf*, have now been assigned functions based on mutational studies (Figure 6.6). *NPH4* has been identified as a regulator of differential growth in aerial tissues and acts in concert with ethylene perception to control organ bending (Harper et al., 2000). *MONOPTEROS* (*MP*) is involved in provascular development during embryogenesis (Hardtke and Berleth, 1998). *MP* also occupies the root of the neighbor-

Figure 6.6 A neighbor-joining tree showing the phylogenetic relationships between ARF amino acid sequences from *Arabidopsis*. Members of the *ARF* family cloned on the basis of a mutant phenotype are indicated in red. Distances were determined using the Juke-Cantor algorithm (Rice, 1994) and displayed using the TreeView program (Page, 1996).

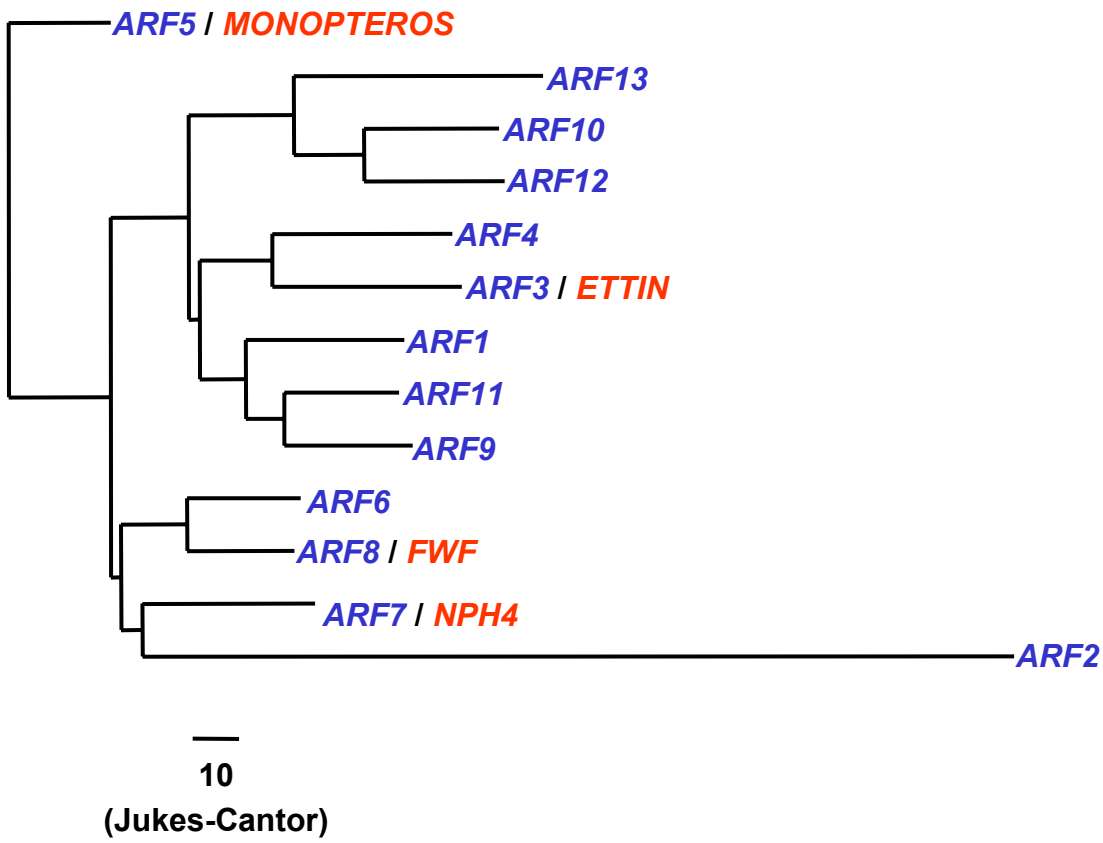
ARF5 / MONOPTEROS
ARF13
ARF10
ARF12
ARF4
ARF3 / ETTIN
ARF1
ARF11
ARF9
ARF6
ARF8 / FWF
ARF7 / NPH4
ARF2
10
(Jukes-Cantor)

joining tree (Figure 6.6), suggesting that the *MP* function may have arisen first during plant evolution in response to alterations in plant body-plan architecture or vascular development. *ETTIN* (*ETT*) controls the apical-basal and abaxial-adaxial tissue distributions within the carpel and also vascular development in the carpel (Sessions et al., 1997; chapter 4). *ARF8* is most similar to *ARF6* and *ARF7* (Figure 6.6). From studies documented in this thesis *ARF8* functions in the ovule to mitigate fertilization dependent signals that control subsequent silique development (chapter 4). Mutational analysis suggests that *ARF8* may have both repressor and activation functions, depending on the integrity of different protein domains, or also possibly by the binding of cofactors to these domains. *ARF8* also plays additional roles in the coordination of floral senescence, ovule development and floral organ identity subordinate to *AG* regulation (chapter 3, chapter 4 and chapter 5).

Members of the *ARF* transcription family bind AuxRE elements found in auxin-responsive promoters of genes that are activated early in response to increases auxin levels (Ulmasov et al., 1999a; Figure 6.7). Transcription of ARFs does not increase in response to exogenous auxin levels (Guilfoyle et al., 1998b). The proteins encoded by *ARF* genes have a characteristic structure (Figure 6.7). The DNA binding domain (DBD) in the N-terminal region interacts with an AuxRE that usually contains a core-binding motif TGTCTC in a direct or palindromic repeat (Ulmasov et al., 1999b; Figure 6.7). ARF proteins also contain a non-conserved middle region. This region is composed of either a Q-rich region (*ARF5*, *ARF6*, *ARF7* and *ARF8*), or a P / S / T-rich (*ARF1*), an S-rich region (*ARF3*), or an unbiased amino acid middle region (*ARF2*, *ARF4* and *ARF9*; Ulmasov et al., 1999a). The C-terminal domain (CTD) of an ARF protein is composed of a set of conserved domains III and IV, that appear to be critical in facilitating protein-protein interactions (Ulmasov et al., 1999a; Figure 6.7B an 6.7C).

Figure 6.7 Structure and function of ARF proteins in regulating expression of auxin responsive genes. The cartoon depicts how ARF proteins might repress and activate transcription of auxin response genes containing an auxin response element (AuxRE). (A) An ARF family member binds an AuxRE motif through the DNA binding domain (DBD) of the ARF protein. (B) The hetero- or homo-dimerization of ARF members through cooperative binding of the carboxy-terminal domains (CTD) III and IV facilitates the repression or activation of transcription of the downstream coding region in auxin responsive genes. (C) *Aux* / *IAA* family members also contain conserved CTD domains III and IV in addition to domains I and II. These can also form dimers with *ARF* members to repress transcription of the downstream coding region (Kim et al., 1997; Ulmasov et al., 1997b).

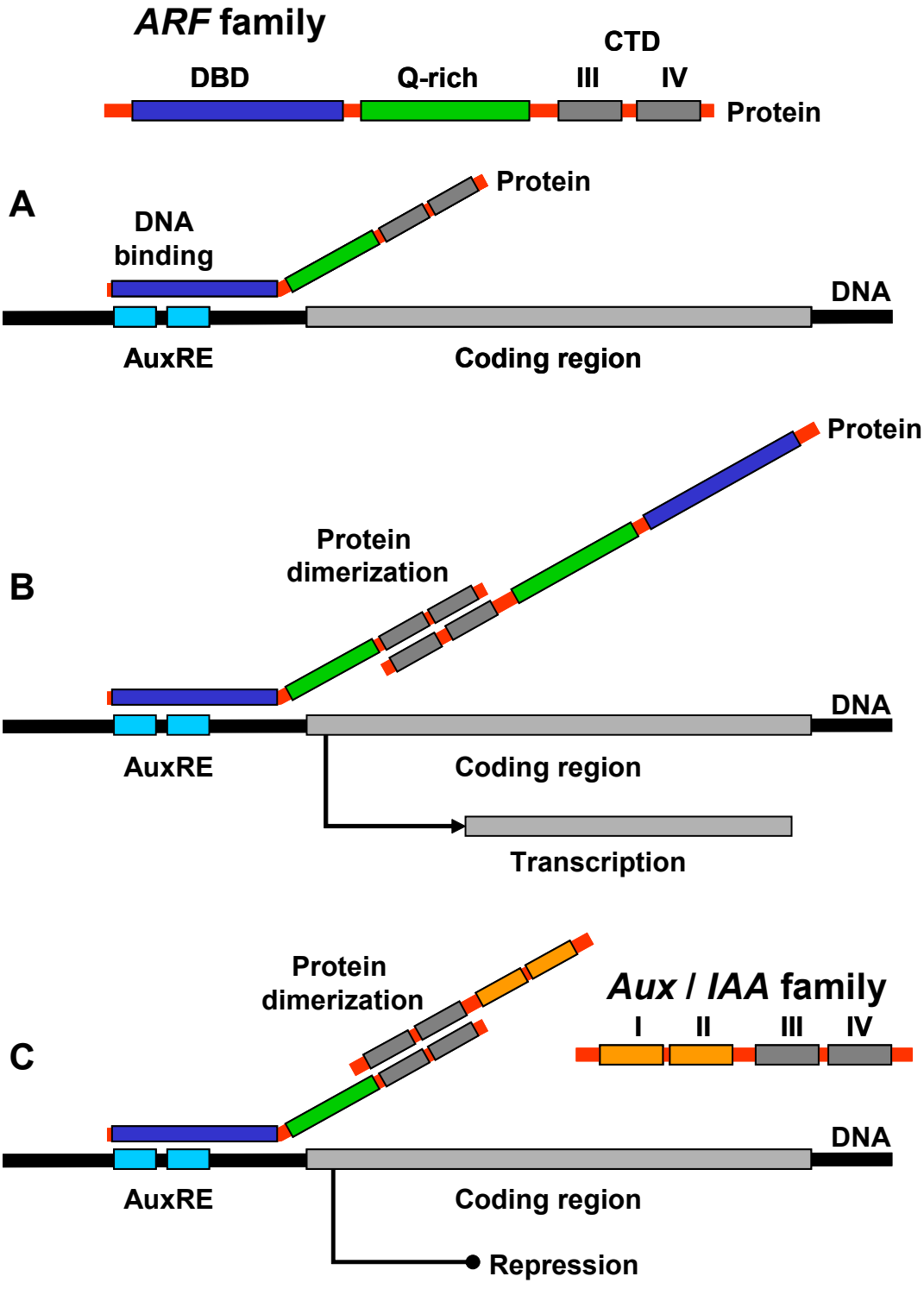
ARF family
CTD
DBD
Q-rich
III
IV
Protein
A
DNA binding
Protein
DNA
AuxRE
Coding region
B
Protein
Protein dimerization
DNA
AuxRE
Coding region
Transcription
C
Protein dimerization
Aux / IAA family
I
II
III
IV
DNA
AuxRE
Coding region
Repression

Experiments with yeast one- and two-hybrid systems (Ulmasov et al., 1997a; Ulmasov et al., 1997b) and assays using reporter genes in carrot protoplasts (Ulmasov et al., 1999a; Ulmasov et al., 1997b) have been used to define *ARF* function. AuxRE elements in the promoters of genes expressed in plant cells appear to be occupied by an *ARF* member (Figure 6.7A). The activation or repression of downstream coding regions in auxin responsive genes is dependent on the availability of unbound CTDs that can form homo- or hetero-dimers with *ARF*s (Ulmasov et al., 1999a; Figure 6.7B). Truncation of *ARF* genes and domain swapping experiments, where the middle region between *ARF1* and *ARF6* has been reversed, has established that the Q-rich middle region of *ARF*s functions as an activation domain (Ulmasov et al., 1999a). This contrasts with the roles of *ARF1*, *ARF2*, *ARF4* and *ARF9* that have middle regions that appear to act as repressors of auxin-induced gene expression (Ulmasov et al., 1999a). The expression of truncated Q-rich *ARF*s (*ARF*5 to *ARF8*) lacking the DBD result in the transcriptional activation of genes containing AuxREs without the ARF directly binding to the DNA (Ulmasov et al., 1999a). This indicates that a truncated Q-rich ARF would dimerize with a full-length ARF typically occupying the AuxRE and thus alleviate the transcriptional repression of the downstream coding region.

Hetero-dimerization can also occur between ARF members and the short-lived nuclear Aux / IAA protein family which also contain the conserved CTD domains III and IV (Ulmasov et al., 1997b; Figure 6.7C). In contrast to ARFs, these proteins are rapidly induced in the presence of auxin (Abel et al., 1994; Ballas et al., 1995; Oeller et al., 1993; Oeller and Theologis, 1995) and their rapid protein degradation is also essential for normal auxin signal transduction (Worley et al., 2000). Over-expression of the *Aux* / *IAA* class in transgenic plant cells results in the repression of auxin-induced transcription downstream from AuxRE elements (Ulmasov et al., 1997b). Thus the activation and repression of auxin

responses through AuxREs is likely to be complex and dependent on the competitive homo- and hetero-dimerization between ARFs and Aux / IAA members, together with the rate of Aux / IAA protein degradation (Leyser and Berleth, 1999).

All of the observed mutations in *MONOPTEROS* disrupt CTD function (Hardtke and Berleth, 1998). *MP* is initially expressed in provascular cells found in the basal domain of the embryo. In wild type plants this tissue gives rise to the hypocotyl and primary root. *mp* mutants lack these tissues and do not develop vascular tissues in this region (Przemeck et al., 1996). This suggests that the functional DBD domain enables binding to AuxRE motifs in upstream elements of genes coordinating provascular development. However, the lack of functional CTD activity in *mp* mutants would prevent transcriptional activation of these genes leading to the loss of provascular cell development and impaired development of hypocotyl and root organs that are dependent on auxin induced activation. *MP* is also expressed later in plant development and its expression is confined to funiculus, ovule and lateral vascular bundles of the carpel (Hardtke and Berleth, 1998), potentially indicating a role for this Q-rich *ARF* in the activation of auxin responses these tissues.

NPH4 (*ARF7*) is also a Q-rich *ARF* like *MP* (Harper et al., 2000). *NPH4* has a role in phototropic responses, apical hook maintenance, stem gravitropism and curvature (Harper et al., 2000; Stowe-Evans et al., 1998). Analysis of *nph4* mutants revealed that the majority of mutations produce stop codons in the Q-rich regions and these severely impair modulation responses governed by *NPH4*. This also suggests that a functional CTD domain is necessary to transduce signals in the *NPH4* auxin transduction cascade.

ETT (*ARF3*), is distinct from other members of the *ARF* family in that it lacks the protein-protein interaction CTD domains III and IV (Sessions et al., 1997). All mutations identified in *ETT* to date affect the DNA binding domain (Sessions et al., 1997). In contrast to *MP*, loss of *ETT* activity alters carpel tissue patterning. *ett* mutants exhibit reduced

apical-basal and also abaxial-adaxial proportions of carpel tissues (Sessions and Zambryski, 1995). A progressive loss of carpel tissue is seen with increasing severity of the *ett* mutant alleles (Sessions et al., 1997). This also tends to reflect an increase in pistil vascular development. Thus *ETT* function in the carpel may protect specific AuxRE sites in gene promoters from the inappropriate activation by other ARFs and prevent formation of proteins responsible for auxin induced development. *ETT* is expressed in abaxial regions of the carpel from stage 5 – 6 flowers and then its expression becomes restricted after stage 9 to the developing vasculature of the carpel (Sessions et al., 1997). *ARF8* also has expression within pistil and silique tissues (Ulmasov et al., 1999b; Vivian-Smith and Koltunow, unpublished data). In chapter 5, *fwf* and *ett*-2 were combined in a double mutant. Both mutations were shown to have independent carpel phenotypes, reflecting that *ETT* and *ARF8* possibly have non-overlapping functions in these tissues and that auxin responses governed by *fwf* do not govern carpel boundary specification in the *ett-2* background.

6.3.2 Transformation of *ARF8* reveals the *fwf* mutation is antimorphic

The mutation identified in the initiation codon of the *ARF8* gene in *fwf* plants and the phenotypes induced when the mutant *ARF8* gene was introduced into both wild type and *fwf* plants is consistent with the hypothesis that a functional but truncated form of the ARF8 protein is translated and that the truncated protein acts in a dominant antimorphic manner to interfere with developmental events. How is the protein acting to induce parthenocarpic silique development? The ORF analysis of the mutant *ARF8* gene predicted a protein product lacking the DBD of ARF8 but containing a portion of the Q-rich region together with the CTD domains III and IV. Absence of the DBD in *fwf* plants means that

the ARF8 protein can not bind to the promoters of auxin responsive genes to repress their transcription, as would possibly occur normally during fertilization.

The hypothetical truncated protein in *fwf* may instead allow activation of auxin responses through the dimerization of the ARF8 CTD with other members of the ARF or Aux / IAA family that are normally involved in post-fertilization-induced fruit development, thus enabling parthenocarpic silique formation. Addition of the truncated protein into wild type plants may interfere with suppressive activities of the endogenous protein, while the introduction of the truncated protein into mutant *fwf* plants might result in other abnormalities associated with competitive binding of the truncated ARF8 CTD with other regulatory proteins. The 5' upstream region of the *ARF8* gene has an AuxRE in its promoter and therefore the activity of the truncated protein would be subjected to self-regulation over the course of auxin mediated responses. These hypotheses can be directly tested by the introduction of truncated versions of the *ARF8* gene and by the transformation of truncated versions of other Q-rich *ARF*s into wild type plants to assess which regions are required for the activation of parthenocarpy.

Further dependencies of silique and ovule development on *FWF* and subsequent auxin signal transduction could also be tested. Studies of *fwf* / *ARF8* expression through *in situ* techniques could reveal whether *FWF* / *ARF8* is expressed in domains similar to *MP* in the carpel. Double mutants with auxin mutants in *ARF* and *Aux* / *IAA* families may reveal further information on how *fwf* regulates parthenocarpic silique development.

6.3.3 Is the *FWF* gene transcriptionally regulated through CArG and homeodomain protein binding motifs?

As suggested earlier, the proximity of the CArG-box and *Athb1* binding motifs indicate that these motifs could be important in the control *FWF* expression. How would

the CArG-box and homeodomain DNA binding motifs regulate *FWF*? In yeast the homeodomain protein MATα2 can effectively homodimerize and bind to sequences containing a homeodomain-binding site (Gehring et al., 1994). The DNA binding affinity of MATα2 increases 50-100 fold when MATα2 forms a complex with the MCM1 MADS-box protein that can cooperatively bind to a 31 bp α2-specific operator DNA containing the homeodomain-binding sequences plus a flanking CArG-box motif for the MCM1 protein (Tan and Richmond, 1998). Repression is only mediated through the α2-specific operator DNA when Ssn6 (a tetratricopeptide repeat protein) and Tup1 (a beta-transducin repeat protein) proteins are brought to the α2-MCM1 complex (Keleher et al., 1992; Smith and Johnson, 2000a; Smith and Johnson, 2000b).

In *Arabidopsis* it is possible that proteins like AG and BEL could regulate *ARF8* transcription through the CArG-box and homeodomain motifs in a similar manner to that observed in yeast. Either the AG or BEL proteins could bind individually, or together, to the CArG-box and homeodomain motifs and thereby regulate the level of *FWF* expression. It is also possible that AG and other homeodomain proteins might competitively bind these motifs by an exclusion process. This model is not purely speculative because mutations in *LEUNIG* (*LUG*), a gene with similarity to Tup1 from yeast, also cause homeotic transformation of sepals to carpels with ectopic ovule primordia, and petals into stamens (Conner and Liu, 2000). Consistent with this hypothesis *LUG* has an expression domain similar to *AG* (Conner and Liu, 2000) suggesting that LUG might act as a transcriptional corepressor of AG function like yeast.

AG and *BEL* expression domains are congruent with models described in chapter 3.4.1 and 4.4.3 whereby *FWF* has a central role in controlling fertilization-dependent silique elongation by regulating auxin signal transduction and canalization collectively from the inner integument, endothelium and female gametophyte. Expression domains of

AG occur early in ovule primordia and then later in the endothelium (Reiser et al., 1995). The expression of *BEL* overlaps to some degree with *AG*, but is mainly expressed in the integument primordia and chalazal region (Reiser et al., 1995). These expression patterns would ensure the correct temporal expression of *FWF* during ovule development and then at anthesis prior to fertilization. Other genes that hetero- or homo-dimerize with *FWF* would post-transcriptionally mediate subsequent processes in the auxin signal transduction cascade.

This hypothesis may explain why in chapter 3.3.1 the *fwf* mutation showed altered outer integument morphogenesis in 19% of the *fwf* ovules and in chapter 4.3.2 why the *fwf* mutation enhanced the development of carpelloid structures developing in the *bel1-1* mutant background. In the case of the *bel1-1 fwf* double mutants, *AG* activity together with the truncated *FWF* protein in *bel1-1* ovules and would enhance the growth of the carpelloid structures. Recently Dong et al., (2000) also showed that constitutive expression of a *BEL*-like gene *MDH1* in *Arabidopsis*, that was previously found to be differentially expressed during apple fruit development, reduced silique growth. The constitutive over-expression of *MDH1* could thus block normal *AG* or *BEL* activity, accounting for the reduced silique development following pollination. Thus it is therefore possible that the ovule identity functions seen when *AG* is over-expressed (Mizukami and Ma, 1992; Ray et al., 1994) and the reduction in silique growth via the over-expression of the *BEL*-like gene (Dong et al., 2000), represent threshold effects acting through the 5' CArG-box and homeodomain binding motifs of *FWF*.

In chapter 5 it was shown that stamen identity, normally controlled by *AGAMOUS*, was carpelloid in the presence of both the *fwf* and *spy-4* mutations. Again *AG* activity together with the *fwf* protein could convert stamenoid identity to carpelloid identity, because the partial loss in the multifunctional role played by *FWF* would promote cellular

differentiation. Likewise the epistasis of the *ful-7* mutation to the *fwf* mutation (chapter 3) could indicate that the *FUL* MADS-box protein might be essential for the activation of *FWF* specifically in the carpel valve through the CArG-box motif. Experiments where *FUL*, *AG* and *BEL* expression is altered, may reveal the role these DNA binding motifs play in silique and ovule development.

Chapter 7: General discussion

7.1 Conclusion and future directions

This thesis describes how I have used *Arabidopsis* as a model system to study the initiation of fruit development. The central question of this thesis was to understand how fruit initiate and form parthenocarpic fruit in the absence of fertilization and seed initiation. Morphological events of fruit (silique) development in *Arabidopsis* were studied and experiments were carried out to examine how exogenous phytohormones induce fruit development and affect cell division and expansion processes in wild type and mutant backgrounds (chapter 2 and 3). A variety of phytohormones were shown to induced fruit development independent of fertilization and application of GA proved the most efficient. Genetic analysis of silique development following phytohormone application to gibberellin perception and biosynthesis mutants provided evidence that gibberellins control anticlinal mesocarp cell division in ancillary manner to a primary auxin-like response during the initiation of parthenocarpic and seeded fruit (chapter 2). The molecular characterization of a parthenocarpic mutant, *fruit without fertilization* (chapter 3 and 6), led to the cloning of a gene regulating the initiation of fruit development and aspects of silique morphogenesis.

The *FWF* gene was shown to encode the auxin response factor gene, *ARF8*, demonstrating that auxin responses play a fundamental role early in the initiation of silique development and silique morphogenesis. Genetic analysis showed that auxin responses in *fwf* are initiated either separately or collectively from within the inner integument, endothelium and female gametophyte of the ovule, and are then transmitted to the carpel margin. The exact mechanism of signal transmission remains unknown, but a model incorporating the role of polar auxin transport was presented. The ovule plays a critical role in the transmission of signals regulating fruit set.

Genetic analysis of parthenocarpic fruit development also uncovered several other genetic pathways that cooperate together with the primary auxin signal. One pathway

important in the control of parthenocarpic fruit initiation includes ethylene perception (chapter 4). It was shown that integumentary cell layers together with ethylene responses modulate silique development (chapter 4) and I suggested that ethylene perception may have a role controlling polar and lateral movement of auxin in these tissues.

An interaction was shown to occur between *FWF*, *ATS* and *GAI* that affected anticlinal mesocarp cell division and consequently silique elongation. *GAI* is a member of the *SCR*-like gene family and fine-mapping *ATS* and characterization of the *ats* lesion indicated it could be another member of the family, but the gene needs to be cloned and the *ats* lesion complemented to verify this. Surrounding floral whorls also inhibit silique development in the *fwf* background, but this inhibition is not seen in the *ats* background. Cloning *ATS* will also enable the investigation of this phenomenon.

The analysis of the fruit initiation in this thesis suggests that the signal transduction process leading to fruit development occurs in a linear manner affected by two or more feedback loops. In the first, auxin has a primary role affecting secondary morphogenic signals (gibberellins) that provide ancillary roles controlling asymmetric cell division. This feedback loop comprises the late steps in gibberellin biosynthesis (*GA4* and *GA5*) and gibberellin perception partly mediated by the *GRAS* member *GAI*. In the second auxin responses could determine aspects of vascular differentiation and therefore might act as a gatekeeper to influence nutrient mobilization and the primary steps in gibberellin biosynthesis (*GA1*). Fertilization dependent events regulate the auxin response, but it is necessary to determine whether fertilization immediately initiates an auxin biosynthesis burst or whether auxin responses are directly instigated by the activity of the *FWF* gene.

Genetic analysis in chapter 4 and 5 also suggested that ARF8 activity might be dependent on AG activity, a transcription factor important for conferring stamen, carpel and ovule identity (Bowman et al., 1999). Tissue proliferation was altered in all of these

organs in *spy-4 fwf* and in ovules from *bel1-1 fwf* mutants, suggesting that *ARF8* may provide the means by which *AG*, a gene with orthologues in all angiosperms controls cellular proliferation in C-class organs after organ specification. Therefore I propose that common fruit developmental unit exists and that auxin forms an integral part of this unit and acts to control both organ initiation and then cellular proliferation. Considering that this developmental unit is of interest to us, one might begin to understand how this ancestral regulatory unit might have evolved to control fruit morphogenesis.

7.2 Evolutionary origins of fruits and developmental modularity

Plants first developed naked seeds some 350 million years ago and then later developed carpels and flowers as a way to protect developing seeds, and also attract pollinators (Theissen et al., 2000). Unlike some Cycad members which possess megasporophylls having naked seeds borne on what resemble modified leaf margins (Hill, 1994), all angiosperms characteristically bear seeds enclosed within carpelloid structures. The earliest fossil evidence of a closed angiosperm carpel is of *Archaefructus* from rockbeds near Beijing, China and dates to 142 million years ago (Sun et al., 1998). Fossil flowers show conduplicate carpels initiated from the axils of an inflorescence and pea pod-shaped fruits bearing two to four developing seed, showing that the fruit modestly expanded to accommodate developing seeds. The highest living concentration of primitive flowering plant families occurs in the rainforests of northeast Queensland (Mummery and Hardy, 1995). Many basal angiosperms from this region have fleshy multi-carpel fruits, pointing towards a Gondwanan origin for angiosperm diversity (Mummery and Hardy, 1995). The closed angiosperm carpel may have arisen to first, to protect seeds, but subsequently evolved additional capabilities to disseminate seed effectively by herbivorous megafauna. Innovations such as the modification of leaf-like organs, reproductive branches

and dormant seeds in early angiosperms provide evidence of considerable hormonal control and phenotypic adaptability.

The MADS box gene *AGAMOUS* was present in both the most ancestral forms of angiosperms and gymnosperms but is absent from ferns (Theissen et al., 2000). In *Arabidopsis AG* provides both C-class carpel identity and D-class ovule organ identity (Theissen et al., 2000). Conifer homologues of *Arabidopsis AG* also have conserved gene function (Tandre et al., 1995; Tandre et al., 1998) indicating that the ancestral function was probably to specify primary identity of sporophyllous organs (Theissen et al., 2000). By contrast the *FRUITFULL* MADS-box gene is closely related to the *AP1* or *SQUAMOSA* clade of MADS-box genes that control A-class sepal and perianth identity (Theissen et al., 2000). In *Arabidopsis FUL* controls carpels identity and vascular tissue development (Gu et al., 1998). During evolution of early angiosperm fruit form and composition, key carpel development genes such as *AG* and *FUL* may have been coopted into new functions initially regulating carpel structure, and then in turn controlling downstream events in fruit development.

In *Arabidopsis thaliana*, auxin response factors such as *ETT* and *FWF*, in conjunction with *SPY*, appear to play an important role after carpel organ identity is established to control carpel morphogenesis. The *spy-4 fwf* double mutant phenotype resembles more primitive flower forms that have perianth-like stamens and unfused carpels, indicating that the *spy-4* and *fwf* mutations interrupt several C-class morphogenesis and tissue proliferation steps. The exact role for *SPY* in flower development and morphogenesis is difficult to discern since it appears to integrate a variety of signals at different developmental steps (Blázquez and Weigel, 2000; chapter 5).

Vascular differentiation may have been associated with megasporophyll evolution so as to supply nutrients to developing seed. *In situ* data for *MP* (Hardtke and Berleth,

1998) also suggests a role for this Q-rich *ARF* gene in provascular tissues because *MP* may play a role activating auxin signaling between the ovule and carpel. In this thesis auxin responses have also been shown to act later, in fruit initiation, having a dual role in cell expansion and vascular differentiation.

7.3 Recruitment of networks and canalization of auxin responses

The recruitment and cooption of homeotic genes was probably an essential component in the evolution and modification of leaves into carpel-like structures seen today (Alvarez and Smyth, 1999; Bowman et al., 1999; Gillaspy et al., 1993). Fruit are also thought to have recruited regulatory networks from leaves and then developed their own physiological properties. In chapter 3 and 4 I describe a model based partly upon the leaf canalization model described by (Mattsson et al., 1999; Sieburth, 1999) in which auxin flows from the ovule to control the growth and vascular differentiation of the mature carpel during the transition to silique development. In this model ovule and integument integrity are essential for the movement of morphogens directing silique initiation. The *FWF* gene might be involved in a positive feedback process integral to the canalization process since the *FWF* promoter region contains an ER7-like auxin response element (chapter 6). Alternatively ER7-like element could be involved in buffering an auxin response threshold level, amplifying an auxin response, or sustaining a particular auxin response within the ovule or carpel following fertilization. The proliferation of carpel-like structures in *bel1-1 fwf* mutants suggests that the element in the *FWF* promoter might be involved in directing tissue proliferation intrinsically by a positive feedback mechanism. Shuffling and mutation within promoter elements appear to be important factors influencing the evolution of gene expression in growth hormone biosynthesis genes in vertebrate species (Chuzhanova et al., 2000). Similarly the shuffling of promoter elements in the *knotted1* gene from plants

causes drastic alteration in plant morphogenesis (Chen et al., 1997). Future attention should be given to an examination of the elements in the *ARF8* promoter, as the canalization process may have been important factor for adapting the growth and determination of the megasporophyll organs.

7.4 Cell division and expansion

Factors controlling fruit growth in other species have been attributed to the cell number within the carpel at anthesis, or the amount of cell division during the early stages of fruit development because these appear to be associated with variation in final fruit size (Coombe, 1975). In *Arabidopsis* cell expansion induced by auxin responses was the most important factor in initiating silique growth, but mesocarp division that occurred normal to the plane of elongation subsequently influenced the final length attained by the *Arabidopsis* silique (chapter 2 and 3). *ATS* and *GAI* were identified as significant factors controlling mesocarp cell division in *Arabidopsis* siliques. In other fruit species flesh components have their own distinctive timing and direction of division and it remains to be determined how *ATS* and *SCR*-like members control overall fruit growth. It remains possible that *SCR*-like genes play a dual role, not only specifying asymmetric cell division processes but selecting whether cell files are responsive to one endogenous stimulus or another.

Additional factors that affect cell division in *Arabidopsis* carpels and siliques have also been identified. These include the *CLAVATA1*, *CLAVATA3* and *WUSCHEL* genes (Schoof et al., 2000) and the *CYP78A9* gene (Ito and Meyerowitz, 2000). Molecular genetics in *Arabidopsis* could be used to identify genes regulating the different types and planes of cell division important for generating cells with different fates and essentially fruit form.

One simplistic model pertaining to the common fruit ancestral developmental unit could be that *AG* initially specifies organ identity. Subsequent steps in morphogenesis would be dependent on cellular expansion initiated by auxin, followed by cell division processes involved in organogenesis. The initiation of lateral root primordia (Malamy and Benfey, 1997) and floral organ initiation in shoot apical meristems (Reinhardt et al., 2000) have similar initial steps in organogenesis. These steps could be envisaged to happen during carpel and ovule morphogenesis and also during fruit development, except in the later, fruit organ morphogenesis is controlled via long-range communication and ancillary morphogenic molecules.

7.5 Modularity in organ development: Integument and ovule

Double mutant studies between *fwf*, and *bel1-1* or *spy-4* support that *ARF8* has a developmental role in determining ovule morphogenesis and that the development of the outer integument may be dependent on auxin as a morphogen. Both *AG* and *BEL* have been shown to play a complementary role in ovule primordia initiation and morphogenesis (Western and Haughn, 1999). The outer integument is thought to be derived from a modified stipule (Gasser et al., 1998). In chapter 6 *FWF* was shown to encode *ARF8* and putative CArG-box and homeodomain binding sites were found in the *ARF8* promoter region. The developmental significance of the putative motifs await further experimentation but their identification supports the hypothesis that *ARF8* transcription may be developmentally controlled by transcriptional factors such as the MADS-box *AG* and the homeodomain *BELL*. Expression of *AG* within the inner integument is also consistent with the developmental genetic data that suggests the inner integument, endothelium and gametophyte are essential domains for *ARF8* expression in order for parthenocarpic silique development to occur in the *fwf* mutant background (chapter 4).

During the course of this research the *INNER NO OUTER* gene, a member of the *YABBY* gene family, was cloned and found to regulate the early steps in the abaxial growth of the outer integument (Villanueva et al., 1999). In wild type ovules *INO* expression is confined abaxial regions of ovule primordia at stage II, to regulate outer integument primordia initiation (Villanueva et al., 1999). In mutant *bel1-1* plants *INO* expression extends into a ring that surrounds the ovule primordia and extends into the funiculus region (Villanueva et al., 1999). The phenotype of the *bel1-1 fwf* double mutant includes an aberrant long funiculus and the radial growth of carpel-like organs (chapter 4).

Considering that exogenous auxin can induce organ development (Reinhardt et al., 2000) and that *INO* is expressed in the incipient outer integument primordia, it was considered plausible that the *INO* promoter might contain elements that determined the initiation and the growth of the outer integument. The *INO* promoter was inspected and it was uncovered that the upstream region contains an AuxRE similar to the ER9 element (Guilfoyle et al., 1998a; Figure 7.1). This might suggest that *INO* is an auxin regulated gene. Inspection of all other promoter regions of *YABBY* members (Siegfried et al., 1999) for the presence of AuxREs using the computer programs described in chapter 6, failed to find any AuxRE elements (Figure 7.1).

As *ARF8* contains potential CArG-box and homeodomain (*Athb1*) binding motifs, a model for the regulation of *INO* and outer integument growth is presented in Figure 7.1. *AG* and or *BELL* could bind to the *ARF8* promoter (Figure 7.1A) and activate the transcription of *ARF8* (Figure 7.1B). Depending on other factors, the ARF8 protein (Figure 7.1C) would bind to an ARF already occupying the AuxRE site in the *INO* promoter region (Figure 7.1D) and activate the transcription and translation of *INO* (Figure 7.1E).

In the *fwf* mutant, the truncated *ARF8* molecule would allow activation of *ARF* members occupying AuxRE sites within the *INO* promoter (Figure 7.1D) and permit the

aberrant transcription of *INO* (Figure 7.1E). In *fwf* mutants this may account for the reinforced growth of the outer integument and aberrant funiculus development observed in the *bel1-1* mutant (chapter 4) and the longer outer integuments observed in *fwf* (chapter 3). Future work could focus on testing whether this sequence of events determines the growth and development of the outer integument. Further work is also needed to determine whether *ARF8* and *AG* expression domains overlap in the endothelium to understand *FWF*'s multifunctional role in morphogenesis.

7.6 Other determinants of fruit growth and downstream targets

During the course of this research other factors influencing parthenocarpy were identified. These included ovule receptivity, the ecotype in which the parthenocarpic response was induced and the requirement for emasculation of the surrounding floral whorls. The latter was ameliorated by the presence of the *ats* mutation. Ovule receptivity might be an important factor in parthenocarpic varieties if the ovule is the primary source of auxin for sustained fruit development. This explanation may also explain why the number of fertilized ovules is important in determining fruit size in horticultural species.

Ecotype backgrounds also affect the phenotype of *mea* (*fis1*), *fis* (*fis2*) and *fie* (*fis3*) mutants (Chaudhury et al., 1997). It is unknown whether these specific differences seen in Col-1 and L.*er* ecotypes are related factors affecting the silique and seed initiation response. Future studies could also focus on identifying these factors.

Transgenic plants that contain the *DefH-IAA* construct which confers localized auxin synthesis in ovules have seedless parthenocarpic fruit of comparable size to seeded fruit (Ficcadenti et al., 1999; Rotino et al., 1997), it follows that sink strength could be determined by auxin or the creation of vascular networks facilitating the mobilization of carbohydrates. Genes encoding sucrose synthase isoforms have been isolated from

Figure 7.1 Model for the regulation of the *INNER NO OUTER* (*INO*) gene by *ARF8* during outer integument growth. (A) AGAMOUS and BELL may bind CArG-box and homeodomain binding motifs (HD-motif) in the *ARF8* promoter respectively. (B) These facilitate the transcription of the *ARF8* gene. (C) The translated ARF8 protein may bind an ARF occupying the AuxRE site located at 855 bp upstream of the ATG translation initiation start site in the *INO* promoter (D). (E) Activation of transcription and translation of *INO* would subsequently occur and initiate outer integument morphogenesis.

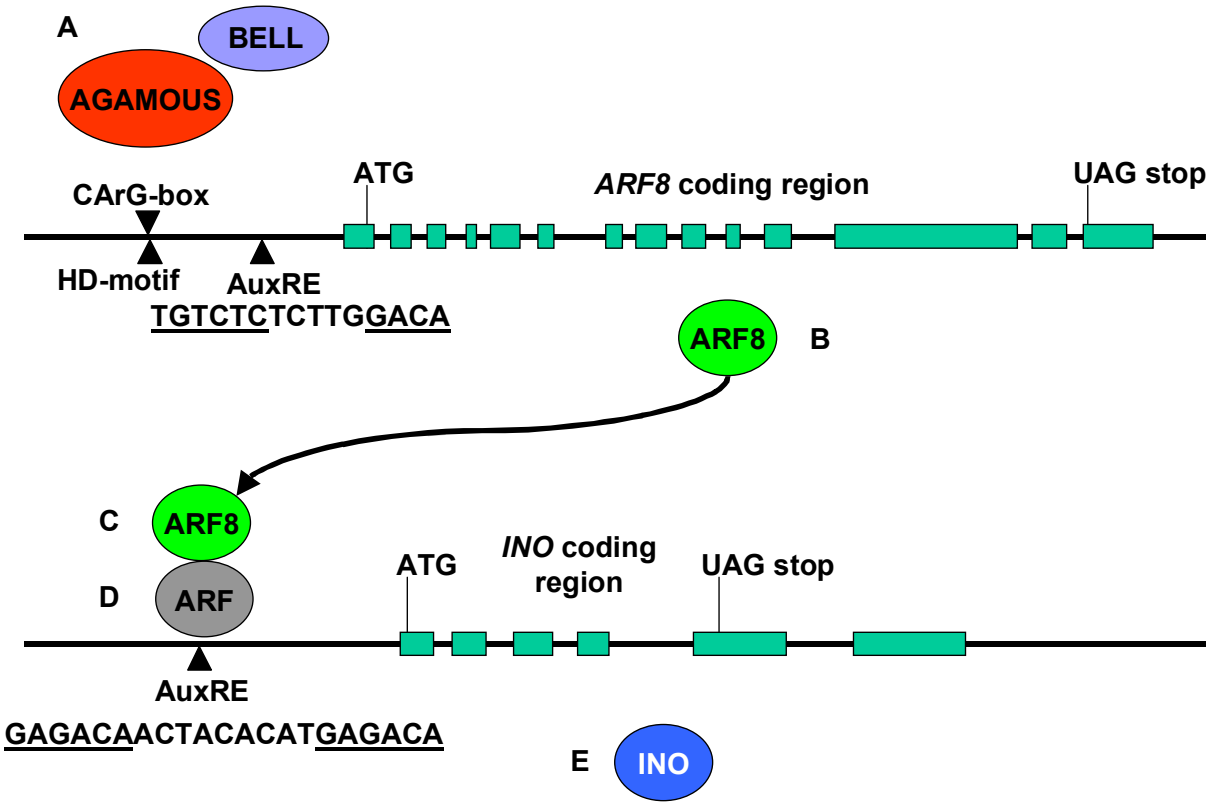
A
BELL
AGAMOUS
ATG
ARF8 coding region
UAG stop
CArG-box
HD-motif
AuxRE
TGTCTCTCTTGGACA
ARF8
B
C
ARF8
D
ARF
ATG
INO coding region
UAG stop
AuxRE
GAGACAACTACACATGAGACA
E
INO

Arabidopsis (Chopra et al., 1992). Plasma membrane sucrose proton symport carriers in *Arabidopsis* have also been identified and characterized and these have been shown to be expressed in the ovule and funiculus during silique development (Stadler et al., 1999). Studies could determine the relationship between auxin responses and vascular development and sucrose transport during fertilization-dependent events to establish their order. Additional studies could focus on how cell wall modification enzymes are activated during the growth and expansion of the fruit.

7.7 Questions and future work concerning *FWF*

Determination of the spatial and temporal expression of *FWF* via *in situ* analysis, and resolving how the *fwf* mutant produces and expresses the putative truncated *ARF8* protein predicted from DNA sequence, are essential experiments to understand how the fruit developmental program is initiated in *Arabidopsis*. *In situ* analysis of *FWF* expression should enable correlative resolution of the early and late function of *FWF* in controlling carpel morphogenesis and may also indicate if *FWF* participates in ovule morphogenesis. Immuno-localization, however, will be necessary to understand the action of the truncated ARF8 protein produced in the *fwf* mutant. Immuno-localization of FWF during fertilization-dependent fruit development will help towards our understanding of the repressive role FWF plays in the inner integument, endothelium and female gametophyte. Ovule mutants such as *nozzle* (Balasubramanian and Schneitz, 2000) and female gametophyte defective mutants detailed in (Christensen et al., 1998) could be utilized for *in situ* and immuno-localization experiments to define whether *FWF* is gametophytically expressed.

Experiments where the expression of *FWF* is examined in mutants where *AG* expression is altered could be used diagnostically to test whether *FWF* is regulated by *AG*

activity. The polycomb mutation *curly leaf-2* (*clf*), that expresses *AG* constitutively (Goodrich et al., 1997) could be used for this objective. It is interesting to note that in *clf* mutants the leaves remain small, reduced in structure and never expand (Goodrich et al., 1997). One hypothesis for this phenotype might be that ectopic *AG* activity regulates *ARF8* transcription, which in turn has a negative effect on leaf expansion because of reduced auxin responses. To test whether functional *ARF8* activity forms the basis for the reduced leaf expansion phenotype, one could simply cross the *fwf* and *clf-2* mutants together and examine the resultant leaf structure in the double mutant. Theoretically, the *fwf* mutation should restore leaf expansion in *clf* because auxin responses would be activated rather than repressed. Alternatively to reveal whether *AG* controls *FWF* transcription, one might analyze the function of the CArG box and homeodomain motifs found in the *ARF8* promoter region (chapter 6) and determine if the AG and BEL proteins bind to these motifs.

The ability to substitute gene functions in other species by heterologous transgene expression is a stringent test for gene function. Truncated forms of the *FWF* gene could be expressed in other species to test conservation of function and also assess whether the Q-rich and C-terminal portion of the ARF are able to induce fruit development independent of fertilization in a variety of different species.

Other questions remain about auxin signal transduction. *MP* is expressed in the ovule, funiculus and lateral vascular bundle of the carpel (Hardtke and Berleth, 1998). Do other Q-rich related members of the *ARF* family like *MP*, *NPH4* and *ARF6* participate in the control fruit development? How does the DNA binding domain activate or protect AuxREs during fertilization-dependent silique development? The Aux / IAA family of proteins have been shown to interact with ARF8 in a yeast two hybrid system (Tatematsu et al., 2000). How do the Aux / IAA family of proteins interact with ARF8 C-terminal

domain in the ovule? Physical interaction has also been shown between the *ETT* and *FIL* proteins (Watanabe et al., 1999). This suggests that there might other physical partners to ARF proteins other than just the Aux / IAA family. What are these? Ubiquitination and proteolysis has been shown to an important component of auxin signal transduction (Gray et al., 1999). How does proteolysis activity affect the action of ARF and Aux / IAA members?

Does auxin or an *ARF* initiate the parthenocarpic response? Or does the fruit development program just require *ARF8* activity to mediate the auxin signal transduction and canalization process? Considering that *NPH4* is involved in phototropic responses (Stowe-Evans et al. 1998; Harper et al. 2000), and that the *fis-2* penetrance is altered under different light environments (chapter 4), does *ARF* and homeodomain activity relating to phototropic responses (Morelli and Ruberti, 2000) affect silique and seed initiation? What are the upstream elements of *ARF8*? Do they include the repressive complex formed by MEA, FIS and FIE?

7.8 Horticultural implications

A primary role for auxin in fruit development in other species is supported by the work of (Ficcadenti et al., 1999; Rotino et al., 1997) in which parthenocarpic fruit set was induced transgenically by targeting the expression of auxin biosynthetic gene to ovule tissues. In this thesis a mutated form of *ARF8* was shown to induce fruit development in *Arabidopsis thaliana* (chapter 6). It follows then that truncated forms of Q-rich ARFs might be used to induce parthenocarpy in a variety of horticultural species.

Natural parthenocarpy in tomato is controlled by several different loci (chapter 1). As one locus controlling the molecular basis for parthenocarpy in *Arabidopsis* has now been identified, the molecular basis for natural parthenocarpy in other species where the

genetic system has been defined, can now be investigated. For instance segregating parthenocarpic tomato populations for *pat* and *pat-2* loci could be tested for allelic cosegregation of auxin response genes or *ARF8* homologues to parthenocarpic plants. An experimental approach such as this may constitute a starting point to identifying the molecular basis for natural parthenocarpy in other species. Discovering the molecular basis for parthenocarpy in other horticultural species would expedite breeding seedless fruit crops.

The diversity and structure of fruit shape and size presents a new problem for horticulture and may require an understanding of the interactions occurring between the ovule and the carpel. As *Arabidopsis* is a relatively simple fruit and other horticulturally important fruit appear far more complex in structure, other genetic systems like tomato might have to be utilized to identify or uncover molecular aspects regarding metabolic processes or physiological conditions following fruit set. However, as discussed earlier the diversity and complexity of fruit structure may be due in part to common developmental units controlled by MADS-box genes such as *AG*, auxin response factors and *GRAS* genes which might direct whether one particular tissue type is responsive to a particular endogenous morphogen. *GRAS* genes are conserved throughout higher plants (chapter 4) and their role in fruit morphogenesis could be studied in other fruit crops as a means to manipulate cell division process and possibly fruit structure, size and quality.

Appendices

1.1 Development of new SSLPs and CAPS markers

Fine mapping of *ats* and *fwf* required the development of new CAPS and SSLP markers because of the limited markers were available in the AthPhyC to DFR region. New CAPS and SSLP markers were designed to sequence specific sites in the *Arabidopsis* genome spanning this region. Oligonucleotide primers were designed using the *Primer 3* program (Rozen and Skaletsky, 1997) by choosing a sequenced region from physically placed BACs, P1, TACs or YAC end sequences (KAOS database). Sequences for PCR amplification were typically selected between 0.8 to 1.5 kb in length.

Table 8.1 shows the primer pairs that were tested for new polymorphisms in addition to previously identified SSLP and CAPS markers (TAIR database) that were used in this study to locate the *fwf* and *ats* mutations. To test new primer pairs for polymorphisms, PCRs were carried out as described by Glazebrook et al., (1998) on genomic DNA isolated as described by Edwards et al., (1991). Conditions for PCR were optimized so that a single PCR product was observed on a 1% agarose gel. Occasionally, PCRs could not be optimized and multiple products were observed. Reactions yielding additional products were examined for the presence of the expected PCR product, and if it was present, digestions were performed bearing in mind the additional PCR products.

PCR reactions were performed on genomic DNA prepared from L.*er*, Col-4, and a F_1 heterozygous plant and examined for SSLPs on 1% and 4% agarose gels. Those primers yielding SSLPs (Figure 8.1A) and were used in linkage analysis.

To assess for CAPS polymorphisms, amplified PCR products were diluted and digested to completion with restricted endonucleases. PCR products were digested with a battery of different enzymes. Each digest was performed in a single 20 µl reaction according to the manufacturers specifications. Digested PCR products for L.*er*, Col-4 and heterozygous individuals for each different enzyme were compared on 4% agarose gels to

Figure 8.1 Developing new CAPS and SSLP polymorphisms. New primer pairs were initially tested for SSLP polymorphisms. (A) An example of the MNJ8a SSLP. PCR products not yielding SSLPs were digested with a battery of different restriction endonucleases to screen amplified DNA for CAPS polymorphisms (B). B, shows the MJG14 #2 CAPS marker and C, shows the ARF8a CAPS polymorphism. L, L.*er* DNA; H, heterozygote L.*er* / Col-4 DNA; C, Col-4 DNA.

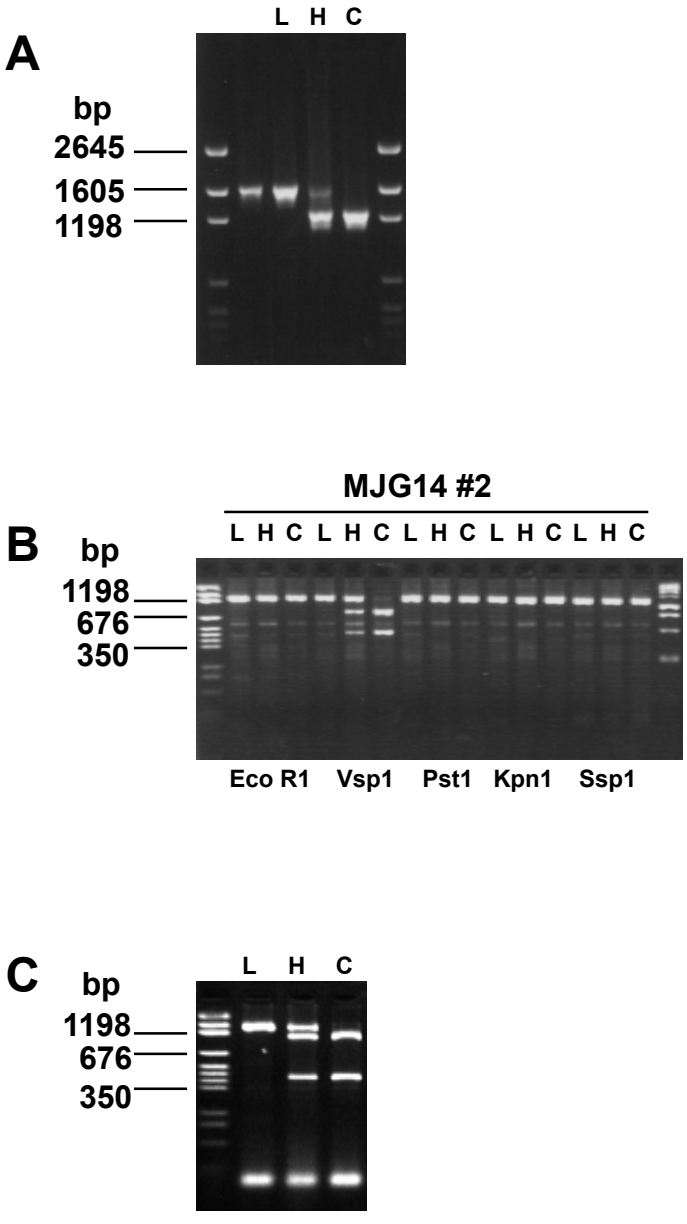
A
L H C
bp
2645
1605
1198
B
MJG14 #2
L H C L H C L H C L H C L H C
bp
1198
676
350
Eco R1
Vsp1
Pst1
Kpn1
Ssp1
C
L H C
bp
1198
676
350

reveal CAPS polymorphisms (Table 8.1, Figure 8.1B and 8.1C). The length of PCR products from each digestion was checked with the expected digestion patterns and sequence data. New CAPS and SSLP markers were then tested against recombinant populations for correct segregation ratios and linkage.

Table 8.1: Oligonucleotides primers used in mapping and cloning *fwf* and *ats*

Marker/source	Sequence (5'-3')	Polymorphism
[a]nga249	TACCGTCAATTTCATCGCC GGATCCCTAACTGTAAAATCCC	SSLP
[a]nga151	GTTTTGGGAAGTTTTGCTGG CAGTCTAAAAGCGAGAGTATGATG	SSLP
[a]nga106	GTTATGGAGTTTCTAGGGCACGF TGCCCCATTTTGTTCTTCTC	SSLP
[a]nga139	AGAGCTACCAGATCCGATGG GGTTTCGTTTCACTATCCAGG	SSLP
[a]AthS0262	TTGCTTTTTGGTTATATTCGGA ATCATCTGCCCATGGTTTTT	SSLP (repeat)
[a]nga76	GGAGAAAATGTCACTCTCCACC AGGCATGGGAGACATTTACG	SSLP*
[b]GA3	CCCTGCAGGAAGTGAGGT ACATCAAGATTTTGAAACTAG	SSLP (indel)
[a]AthPhyC	CTCAGAGAATTCCCAGAAAAATCT AAACTCGAGAGTTTTGTCTAGATC	SSLP (repreat)
[c]T30G6 #1	GCATCGATCTCTGTTTGGGA AAATGCTGGTCATTCGGTTG	N.D.
[c]F5H8 #1	CTCTGGGCTGAGTGTCAAGC AGCACCCTCTGCCCAATAGT	N.D.
[d]MDK17 #1	TTTTGATATTGCTTTTCTCCATGA GATTTTAACCCGCGATACACC	CAPS (*Acs* I)
[c]MLF18 #1	CGACATAAGTATGGAGTTGCCA TTAATGAGATCGTGTGGGTGAG	CAPS (*Acc* I/*Pst* I)*
[c]MLF18 #2	TTTGTCAATGTTGGGTTCCG GGGAGACGGGTGAGACAAAT	Col-4 dominant
[c]MLF18 #3	GGATTTTTCGCGGTTATGGT GGGAGACGGGTGAGACAAAT	Col-4 dominant
[d]K15O15 12819F 13190R	CAGATGAATGATCCGTTGAGC GATTCGATGGGGCATGACTA	CAPS (*Pst* I)

[c]ARF8 –1830F	CTCGAGTGAGAAGTCTATGATG	cloning primer
[c]ARF8 –80R	CTGCAGTAGCTATAACTCTTTAGC	cloning primer
[c]ARF8 –44F	CCTAGGGTTTTCAAAGTTTGGTT	cloning primer
[c]ARF8 –1R	CTCGAGTTCAACTTCAAGAA	cloning primer
[c]K15O15 15394R	GGGTATGTGACCATCAACTTCC	ATA / ATG polymorphism (*Hsp92 II*)
[c]K15O15 16183R	ACAGAGCCTCCGTGGTTTCT	cloning primer
[c]ARF8a (+1478F) (+2817R)	GAGCTCCTTTAAGACAGCAGTTTGT CCTAGGAAAGTTTAGTTACCCTGAGAC	CAPS (*Acc* I)
[c]ARF8 +2481F	GGTACCAGAAGATGTGCATCAAATGGG	cloning primer
[c]MJG14 #2	GGATCGTTAGGCAATGGGAT TGGATACGATGGGGACAAAA	CAPS (*Vsp* I)
[c]MNJ8a	ATAGCCAGGGCCAAATATGC TGGAGAATCTGGGAGCATTG	SSLP (large indel)
[c]MPA22 #1	TCCGTAAACCATGTTCGTTCA GTAACGTCCTTCCAAACCCG	CAPS (*Taq I*)
[a]AthS0191	TGATGTTGATGGAGATGGTCA CTCCACCAATCATGCAAATG	SSLP (repeat)
[a]RBCS-Ba	TATCGACAATTTATTGTGG TGAATGGAGCGACCATGGTGGCCTGAGCCGG	CAPS (*Ssp* I)
[e]EMB506	AGTGATTGGGAAGATGACTC TCTGCAAGGCTCCAACTTGAAC	CAPS (*Bcl I*)
[f]MEE6 #2	TTGAGCTACTATGGATAGTCTAG GTTGGTTCAATCGAATCGCC	SSLP (large indel)
[f]1MYC6	CTTGCTCATAGAGACTCGC GCACGTGGCGTATACTG	CAPS (*Hind III*)
[f]MBK23B	GATGGAGCCAAGAGACAATC TCATTGTCATCTTCTGGTGC	CAPS (*Acc I* and *Msp I*)
[c]MJC20 #2	CCTCACCAATGAGCCTTTCA CGCAGATCGGATTCGAGTAA	CAPS (*Vsp I*)
[c]MDH9 #1	TTCGGTTTGGATGATGTTGG CCCCTGCAACCATAAGAACA	Col-4 dominant
[a]DFR	AGATCCTGAGGTGAGTTTTTC TGTTACATGGCTTCATACCA	CAPS (*Taq* I)
NPTII	GCCAAGCTCTTCAGCAATA GGCACAACAGACAATCGG	transformant checking (628 bp product)

[a] from TAIR at http://www.arabidopsis.org/maps/CAPS_Chr5.html

[b] donated by Dr Chris Helliwell
[c] Developed this study
[d] Developed this study in conjunction with the L.*er* sequence database at The Institute for Genomic Research (TIGR, http://www.tigr.org/tdb/at/atgenome/Ler.html)
[e] (Albert et al., 1999)
[f] donated by Jason Walker and Prof John Larkins
* Unreliable polymorphisms

All PCR amplifications for CAPS and SSLPs were performed according to Konieczny and Ausubel, (1993) or Bell and Ecker, (1994) respectively. PCR reactions were performed on a Hybaid (Hybaid Ltd., Middlesex, UK). Annealing temperatures were 55°C except for the following primer pairs. Primers with 53°C anneal were MLF18 #1 and #2, ARF8a, MJG14 #2, MNJ8a, 1MYC6, MDH9 #1. The MEE6 #2 marker used an annealing temperature of 58°C with 5 mM $MgCl_2$. Dominant PCR markers are polymorphisms in which the PCR product is either absent or present in one parental background.

Appendix 1.2

Sequencing reactions

Sequencing reactions were preformed using BigDye™ Terminators (Perkin Elmer, Foster City, CA). In a 200 μl PCR tube, 8 μl terminator mix was combined with 200 – 500 *n*g of template DNA and 3.2 *p*mol of primer. The volume was diluted to 20 μl with deionized water. Cycle sequencing was performed in a PCR cycler (Hybaid Ltd., Middlesex, UK) using rapid thermal ramping. A cycle of 96°C for 10 sec, 50°C for 5 sec, 60°C for 4 min was repeated 25 times and then held at 4°C indefinitely.

Purification of extension products was achieved through the following steps. 2 μl of 3 M sodium acetate pH 5.2 and 50 μl of 95% ethanol was added to the sequencing reaction. The tube was vortexed and left at room temperature for 15 min. Tubes were then spun at 14 000 rpm for 30 min and then the supernatant was discarded. The pellet was rinsed with 250 μl of 70% ethanol and spun for 5 min. The supernatant was discarded and pellet dried in a heating block at 90°C for 1 min.

Publications

During the course of this research chapter 2 was published as a paper in Plant Physiology. Chapters 3 and 4 are presently being submitted as two papers to Development and chapter 6 is currently being examined for a patent. † Designates that this poster received a poster prize.

Papers

Vivian-Smith, A. and Koltunow, A. (1999). Genetic analysis of growth-regulator-induced parthenocarpy in *Arabidopsis*. Plant Physiology 121: 437-451

Published proceedings

Koltunow, A.M., Vivian-Smith, A., and Sykes, S.R. (2000). Molecular and conventional breeding strategies for seedless *Citrus*. In R. Goven, and E.E, Golschmidt (eds) 1st International *Citrus* Biotechnology Symposium. Acta Horticulturae 535: 169-174

Koltunow, A.M., Brennan, P., Protopsaltis, P., and Vivian-Smith, A. (1998). Seedless Citrus using molecular strategies. In M. Omura, T. Hayashi, and N.S. Scott, (eds) *Breeding and Biotechnology for fruit trees*: Proceedings of the 2nd Japan-Australia International Workshop, pp 98-104.

Abstracts and papers presented

Vivian-Smith A., Chaudhury, A.M., and Koltunow A.M. (2000). Surrounding floral organs and ovule structure influence parthenocarpic silique development in the

Arabidopsis fwf mutant. 11th International conference on Arabidopsis Research, 24th – 28th June, University of Wisconsin, Madison.

Vivian-Smith A., Chaudhury, A.M., and Koltunow A.M. (1999). Analysis of fertilization independent fruit development in *Arabidopsis fwf1* mutant. 10th International meeting on Arabidopsis Research, 4th – 8th July, Melbourne, Australia

Vivian-Smith A., and Koltunow, A.M. (1999). Plant growth regulator induced fruit development in *Arabidopsis*. 10th International meeting on Arabidopsis Research, 4th – 8th July, Melbourne, Australia.

Koltunow, A.M., Vivian-Smith, A., and Sykes, S. (1998). Molecular strategies for seedless citrus. 1st International Citrus Biotechnology Symposium, 29th November – 3rd December, Eilat, Israel.

†**Vivian-Smith A. Chaudhury, A.M. and Koltunow A.M.K.** (1998). Genetic and hormonal control of fertilization independent fruit set. 38th Annual Australian Society of Plant Physiology, 28th September – 1st October, Adelaide, Australia.

Vivian-Smith A. (1998). Fruit development and parthenocarpy - sex, lies and hormones. 6th Floral Retreat Warrawong Sanctuary, Adelaide Oct 1st to 3rd 1998.

Vivian-Smith, A., and Koltunow, A.M. (1998). Genetic and hormonal control of fertilization independent fruit set in *Arabidopsis*. 15th International Congress of Sexual Plant Reproduction, 16th – 21st August, Wageningen, The Netherlands.

Vivian-Smith A. Chaudhury, A.M. and Koltunow A.M.K. (1997). Hormonal and genetic control of parthenocarpy in *Arabidopsis*. 37th Annual Australian Society of Plant Physiology, 29th September – 2st October, Melbourne, Australia.

Vivian-Smith A. and Koltunow A.M. (1997). Hormonal and genetic control of parthenocarpy in *Arabidopsis*. 5th International Congress of Plant Molecular Biology, 21-27th September, Singapore.

Vivian-Smith, A., Luo. M., Barker, S.J., Chaudhury, A., and Koltunow, A.M. (1997). Hormonal and genetic control of parthenocarpy in *Arabidopsis*. 2nd Plant Hormone Meeting, 11th-13th April, Mt. Macedon, Victoria, Australia.

References

Abel, S., Oeller, P. W. and Theologis, A. (1994). Early auxin-induced genes encode short-lived nuclear proteins. *Proc. Natl. Acad. Sci.* **91**, 326-330.

Acton, T. B., Mead, J., Steiner, A. M. and Vershon, A. K. (2000). Scanning mutagenesis of *MCM1*: residues required for DNA binding, DNA bending, and transcriptional activation by a MADS-box protein. *Mol. Cell. Biol.* **20**, 1-11.

Albert, S., Despres, B., Guilleminot, J., Bechtold, N., Pelletier, G., Delseny, M. and Devic, M. (1999). The *EMB506* gene encodes a novel ankyrin repeat containing protein that is essential for the normal development of *Arabidopsis* embryos. *Plant J.* **17**, 169-179.

Alonso, J. M., Hirayama, T., Roman, G., Nourizadeh, S. and Ecker, J. R. (1999). *EIN2*, a bifunctional transducer of ethylene and stress responses in *Arabidopsis*. *Science* **284**, 2148-2152.

Alvarez, J. and Smyth, D. R. (1999). *CRABS CLAW* and *SPATULA*, two *Arabidopsis* genes that control carpel development in parallel with *AGAMOUS*. *Development* **126**, 2377-2386.

Archbold, D. D. and Dennis, F. G. (1985). Strawberry receptacle growth and endogenous IAA content as affected by growth regulator application and achene removal. *J. Am. Soc. Hort. Sci.* **110**, 816-820.

Aubert, D., Chevillard, M., Dorne, A. M., Arlaud, G. and Herzog, M. (1998). Expression patterns of *GASA* genes in *Arabidopsis thaliana*: The *GASA4* gene is up-regulated by gibberellins in meristematic regions. *Plant Mol. Biol.* **36**, 871-883.

Baker, S. C., Robinson-Beers, K., Villanueva, J. M., Gaiser, J. C. and Gasser, C. S. (1997). Interactions among genes regulating ovule development in *Arabidopsis thaliana*. *Genetics* **145**, 1109-1124.

Balasubramanian, S. and Schneitz, K. (2000). *NOZZLE* regulates proximal-distal pattern formation, cell proliferation and early sporogenesis during ovule development in *Arabidopsis thaliana*. *Development* **127**, 4227-4238.

Ballas, N., Wong, L. M., Ke, M. and Theologis, A. (1995). Two auxin-responsive domains interact positively to induce expression of the early indoleacetic acid-inducible gene PS-IAA4/5. *Proc. Natl. Acad. Sci.* **92**, 3483-3487.

Barendse, G. W. M., Kepczynski, J., Karssen, C. M. and Koornneef, M. (1986). The role of endogenous gibberellins during fruit and seed development: Studies on gibberellin-deficient genotypes of *Arabidopsis thaliana*. *Physiol. Plantarum* **67**, 315-319.

Bell, C. J. and Ecker, J. R. (1994). Assignment of 30 microsatellite loci to the linkage map of *Arabidopsis*. *Genomics* **19**, 137-144.

Ben-Cheikh, W., Perez-Botella, J., Tadeo, F. R., Talon, M. and Primo-Millo, E. (1997). Pollination increases gibberellin levels in developing ovaries of seeded varieties of citrus. *Plant Physiol.* **114**, 557-564.

Berleth, T. and Mattsson, J. (2000). Vascular development: Tracing signals along veins. *Curr. Opin. Plant Biol.* **3**, 406-411.

Bevan, M. (1984). Binary *Agrobacterium* vectors for plant transformation. *Nucleic Acids Res.* **12**, 8711-8721.

Bharathan, G., Janssen, B. J., Kellogg, E. A. and Sinha, N. (1999). Phylogenetic relationships and evolution of the KNOTTED class of plant homeodomain proteins. *Mol. Biol. Evol.* **16**, 553-563.

Blázquez, M. A., Green, R., Nilsson, O., Sussman, M. R. and Weigel, D. (1998). Gibberellins promote flowering of *Arabidopsis* by activating the *LEAFY* promoter. *Plant Cell* **10**, 791-800.

Blázquez, M. A. and Weigel, D. (2000). Integration of floral inductive signals in *Arabidopsis*. *Nature* **404**, 889-892.

Bowman, J. (1993). *Arabidopsis*: An atlas of morphology and development. New York: Springer-Verlag.

Bowman, J. L., Baum, S. F., Eshed, Y., Putterill, J. and Alvarez, J. (1999). Molecular genetics of gynoecium development in *Arabidopsis*. *Curr. Top. Dev. Biol.* **45**, 155-205.

Bowman, J. L., Drews, G. N. and Meyerowitz, E. M. (1991). Expression of the *Arabidopsis* floral homeotic gene *AGAMOUS* is restricted to specific cell types late in flower development. *Plant Cell* **3**, 749-758.

Bowman, J. L. and Eshed, I. (2000). Formation and maintenance of the shoot apical meristem. *Trends Plant Sci.* **5**, 110-115.

Bowman, J. L. and Smyth, D. R. (1999). *CRABS CLAW*, a gene that regulates carpel and nectary development in *Arabidopsis*, encodes a novel protein with zinc finger and helix-loop- helix domains. *Development* **126**, 2387-96.

Bünger-Kibler, S. and Bangerth, F. (1982). Relationship between cell number, cell size and fruit size of seeded fruits of tomato (*Lycopersicon esculentum* Mill.), and those induced parthenocarpically by the application of plant growth regulators. *Plant Growth Regul.* **1**, 143-154.

Busch, M. A., Bomblies, K. and Weigel, D. (1999). Activation of a floral homeotic gene in *Arabidopsis*. *Science* **285**, 585-587.

Cano-Medrano, R. and Darnell, R. L. (1997). Cell number and cell size in parthenocarpic vs. pollinated blueberry (*Vaccinium ashei*) fruits. *Ann. Bot.* **80**, 419-425.

Cary, A. J., Liu, W. and Howell, S. H. (1995). Cytokinin action is coupled to ethylene in its effects on the inhibition of root and hypocotyl elongation in *Arabidopsis thaliana* seedlings. *Plant Physiol.* **107**, 1075-1082.

Chaudhury, A. and Peacock, W. J. (1994). Isolating apomictic mutants in *Arabidopsis thaliana* - prospects and progress. In *Apomixis: exploiting hybrid vigour in rice*, (G. S. Khush, eds), pp. 67-71, International Rice Research Institute, Manila, Philippines.

Chaudhury, A. M., Lavithis, M., Taylor, P. E., Craig, S., Singh, M. B., Singer, E. R., Knox, R. B. and Dennis, E. S. (1994). Genetic control of male fertility in *Arabidopsis thaliana*: Structural analysis of premeiotic developmental mutants. *Sex. Plant Reprod.* **7**, 17-28.

Chaudhury, A. M., Letham, S., Craig, S. and Dennis, E. S. (1993). *amp*1 - a mutant with high cytokinin levels and altered embryonic pattern, faster vegetative growth, constitutive photomorphogenesis and precocious flowering. *Plant J.* **4**, 907-916.

Chaudhury, A. M., Ming, L., Miller, C., Craig, S., Dennis, E. S. and Peacock, W. J. (1997). Fertilization-independent seed development in *Arabidopsis thaliana*. *Proc. Natl. Acad. Sci.* **94**, 4223-4228.

Chen, J. J., Janssen, B. J., Williams, A. and Sinha, N. (1997). A gene fusion at a homeobox locus: Alterations in leaf shape and implications for morphological evolution. *Plant Cell* **9**, 1289-1304.

Chen, R., Hilson, P., Sedbrook, J., Rosen, E., Caspar, T. and Masson, P. H. (1998). The *Arabidopsis thaliana AGRAVITROPIC 1* gene encodes a component of the polar-auxin-transport efflux carrier. *Proc. Natl. Acad. Sci.* **95**, 15112-15117.

Chiang, H.-H., Hwang, I. and Goodman, H. M. (1995). Isolation of the Arabidopsis *GA4* locus. *Plant Cell* **7**, 195-201.

Cho, H. T. and Kende, H. (1997). Expression of expansin genes is correlated with growth in deepwater rice. *Plant Cell* **9**, 1661-1671.

Chopra, S., Del-favero, J., Dolferus, R. and Jacobs, M. (1992). Sucrose synthase of Arabidopsis: Genomic cloning and sequence characterization. *Plant. Mol. Biol.* **18**, 131-134.

Christensen, C. A., Subramanian, S. and Drews, G. N. (1998). Identification of gametophytic mutations affecting female gametophyte development in *Arabidopsis*. *Dev. Biol.* **202**, 136-151.

Christensen, S. K., Dagenais, N., Chory, J. and Weigel, D. (2000). Regulation of auxin response by the protein kinase *PINOID*. *Cell* **100**, 469-478.

Chuang, C. F. and Meyerowitz, E. M. (2000). Specific and heritable genetic interference by double-stranded RNA in *Arabidopsis thaliana*. *Proc. Natl. Acad. Sci.* **97**, 4985-4990.

Chuzhanova, N. A., Krawczak, M., Nemytikova, L. A., Gusev, V. D. and Cooper, D. N. (2000). Promoter shuffling has occurred during the evolution of the vertebrate growth hormone gene. *Gene* **254**, 9-18.

Clark, S. E., Jacobsen, S. E., Levin, J. Z. and Meyerowitz, E. M. (1996). The *CLAVATA* and *SHOOT MERISTEMLESS* loci competitively regulate meristem activity in *Arabidopsis*. *Development* **122**, 1567-1575.

Clough, S. J. and Bent, A. F. (1998). Floral dip: A simplified method for *Agrobacterium*-mediated transformation of *Arabidopsis thaliana*. *Plant J.* **16**, 735-743.

Conner, J., and Liu, Z. (2000). *LEUNIG*, a putative transcriptional corepressor that regulates *AGAMOUS* expression during flower development. *Proc. Natl. Acad. Sci.* **97**, 12902-12907

Conway, L. J. and Poethig, R. S. (1997). Mutations of *Arabidopsis thaliana* that transform leaves into cotyledons. *Proc. Natl. Acad. Sci.* **94**, 10209-10214.

Coombe, B. G. (1975). The development of fleshy fruits. *Ann. Rev. Plant Physiol.* **27**, 507-528.

Cowling, R. J., Kamiya, Y., Seto, H. and Harberd, N. P. (1998). Gibberellin dose-response regulation of *GA4* gene transcript levels in *Arabidopsis*. *Plant Physiol.* **117**, 1195-1203.

D'Aoust, M. A., Yelle, S. and Nguyen-Quoc, B. (1999). Antisense inhibition of tomato fruit sucrose synthase decreases fruit setting and the sucrose unloading capacity of young fruit. *Plant Cell* **11**, 2407-2418.

de Bouille, P., Sotta, B., Miginiac, E. and Merrien, A. (1989). Hormones and pod development in oilseed rape (*Brassica napus*). *Plant Physiol.* **90**, 876-880.

De Martinis, D. and Mariani, C. (1999). Silencing gene expression of the ethylene-forming enzyme results in a reversible inhibition of ovule development in transgenic tobacco plants. *Plant Cell* **11**, 1061-1072.

Denny, O. J. (1992). Xenia includes metaxenia. *HortScience* **27**, 722-728.

Di Laurenzio, L., Wysocka-Diller, J., Malamy, J. E., Pysh, L., Helariutta, Y., Freshour, G., Hahn, M. G., Feldmann, K. A. and Benfey, P. N. (1996). The *SCARECROW* gene regulates an asymmetric cell division that is essential for generating the radial organization of the *Arabidopsis* root. *Cell* **86**, 423-433.

Dolan, L. and Okada, K. (1999). Signalling in cell type specification. *Semin. Cell Dev. Biol.* **10**, 149-156.

Dong, Y. H., Yao, J. L., Atkinson, R. G., Putterill, J. J., Morris, B. A. and Gardner, R. C. (2000). *MDH1*: an apple homeobox gene belonging to the *BEL1* family. *Plant Mol. Biol.* **42**, 623-633.

Dornelas, M. C., Van Lammeren, A. A. and Kreis, M. (2000). *Arabidopsis thaliana* SHAGGY-related protein kinases (AtSK11 and 12) function in perianth and gynoecium development. *Plant J.* **21**, 419-429.

Drews, G. N., Bowman, J. L. and Meyerowitz, E. M. (1991). Negative regulation of the *Arabidopsis* homeotic gene *AGAMOUS* by the *APETALA2* product. *Cell* **65**, 991-1002.

Drews, G. N., Lee, D. and Christensen, C. A. (1998). Genetic analysis of female gametophyte development and function. *Plant Cell* **10**, 5-17.

Edwards, K., Johnstone, C. and Thompson, C. (1991). A simple and rapid method for the preparation of plant genomic DNA for PCR analysis. *Nucleic Acids Res.* **19**, 1349.

Eeuwens, C. J. and Schwabe, W. W. (1975). Seed and pod wall developments in *Pisum sativum* L. in relation to extracted and applied hormones. *J. Exp. Bot.* **26**, 1-14.

Elliott, R. C., Betzner, A. S., Huttner, E., Oakes, M. P., Tucker, W. Q., Gerentes, D., Perez, P. and Smyth, D. R. (1996). *AINTEGUMENTA*, an *APETALA2*-like gene of *Arabidopsis* with pleiotropic roles in ovule development and floral organ growth. *Plant Cell* **8**, 155-168.

El-Otmani, M., Lovatt, C. J., Coggins, C. W. and Agusti, M. (1995). Plant growth regulators in Citriculture: Factors regulating endogenous levels in citrus tissues. *Crit. Rev. Plant Sci.* **14**, 367-412.

Eshed, Y., Baum, S. F. and Bowman, J. L. (1999). Distinct mechanisms promote polarity establishment in carpels of *Arabidopsis*. *Cell* **99**, 199-209.

Fei, H. and Sawhney, V. K. (1999). Role of plant growth substances in *MS33*-controlled stamen filament growth in *Arabidopsis*. *Physiol. Plantarum* **105**, 165-170.

Fernandez, D. E., Heck, G. R., Perry, S. E., Patterson, S. E., Bleecker, A. B. and Fang, S. C. (2000). The embryo MADS domain factor *AGL15* acts postembryonically. Inhibition of perianth senescence and abscission via constitutive expression. *Plant Cell* **12**, 183-98.

Ferrándiz, C., Pelaz, S. and Yanofsky, M. F. (1999). Control of carpel and fruit development in *Arabidopsis*. *Annu. Rev. Biochem.* **68**, 321-354.

Ficcadenti, N., Sestili, S., Pandolfini, T., Cirillo, C., Rotino, G. L. and Spena, A. (1999). Genetic engineering of parthenocarpic fruit development in tomato. *Molecular Breeding* **5**, 463- 470.

Fos, M., Nuez, F. and García-Martínez, J. L. (2000). The gene *pat-2*, which induces natural parthenocarpy, alters the gibberellin content in unpollinated tomato ovaries. *Plant Physiol.* **122**, 471-479.

Fukaki, H., Wysocka-Diller, J., Kato, T., Fujisawa, H., Benfey, P. N. and Tasaka, M. (1998). Genetic evidence that the endodermis is essential for shoot gravitropism in *Arabidopsis thaliana*. *Plant J.* **14**, 425-30.

Gälweiler, L., Guan, C., A, M. l., Wisman, E., Mendgen, K., Yephremov, A. and Palme, K. (1998). Regulation of polar auxin transport by *AtPIN1* in *Arabidopsis* vascular tissue. *Science* **282**, 2226-22230.

García-Martínez, J. L., López-Diaz, I., Sánchez-Beltrán, M. J., Philllips, A. L., Ward, D. A., Gaskin, P. and Hedden, P. (1997). Isolation and transcript analysis of

gibberellin 20-oxidase genes in pea and bean in relation to fruit development. *Plant Mol. Biol.* **33**, 1073-1084.

García-Martínez, J. L., Martí, M., Sabater, T., Maldonado, A. and Vercher, Y. (1991a). Development of fertilized ovules and their role in the growth of the pea pod. *Physiol. Plantarum* **83**, 411-416.

García-Martínez, J. L., Santes, C., Croker, S. J. and Hedden, P. (1991b). Identification, quantification and distribution of gibberellins in fruits of *Pisum sativum* L. cv. Alaska during pod development. *Planta* **184**, 53-60.

García-Martínez, J. L., Sponsel, V. M. and Gaskin, P. (1987). Gibberellins in developing fruits of *Pisum sativum* cv. Alaska: studies on their role in pod growth and seed development. *Planta* **170**, 130-137.

Gasser, C. S., Broadhvest, J. and Hauser, B. A. (1998). Genetic analysis of ovule development. *Ann. Rev. Plant Physiol. Plant Mol. Biol.* **49**, 1-24.

Gasser, C. S. and Robinson-Beers, K. (1993). Pistil development. *Plant Cell* **5**, 1231-1239.

Gehring, W. J., Qian, Y. Q., Billeter, M., Furukubo-Tokunaga, K., Schier, A. F., Resendez-Perez, D., Affolter, M., Otting, G. and Wuthrich, K. (1994). Homeodomain-DNA recognition. *Cell* **78**, 211-223.

George, W. L., Scott, J. W. and Splittstoesser, W. E. (1984). Parthenocarpy in tomato. *Hortic. Rev.* **6**, 65-84.

Gil, P. and Green, P. J. (1996). Multiple regions of the *Arabidopsis SAUR-AC1* gene control transcript abundance: The 3' untranslated region functions as an mRNA instability determinant. *EMBO J.* **15**, 1678-1686.

Gillaspy, G., Ben-David, H. and Gruissem, W. (1993). Fruits: A developmental perspective. *Plant Cell* **5**, 1439-1451.

Glazebrook, J., Drenkard, E., Preuss, D. and Ausubel, F. M. (1998). Use of cleaved amplified polymorphic sequences (CAPS) as genetic markers in *Arabidopsis thaliana*. In *Methods in molecular biology*, (J. M. Martínez-Zapater and J. Salinas, eds), pp. 173-182, Humana Press, Totowa, N.J.

Gonzalez, M. V., Coque, M. and Herrero, M. (1998). Influence of pollination systems on fruit set and fruit quality in Kiwifruit (*Actinidia deliciosa*). *Ann. Appl. Biol.* **132**, 349-355.

Goodrich, J., Puangsomlee, P., Martin, M., Long, D., Meyerowitz, E. M. and Coupland, G. (1997). A Polycomb-group gene regulates homeotic gene expression in *Arabidopsis*. *Nature* **386**, 44-51.

Granell, A., Harris, N., Pisabarro, A. G. and Carbonell, J. (1992). Temporal and spatial expression of a thiolprotease gene during pea ovary senescence, and its regulation by gibberellin. *Plant J.* **2**, 907-915.

Gray, W. M., del Pozo, J. C., Walker, L., Hobbie, L., Risseeuw, E., Banks, T., Crosby, W. L., Yang, M., Ma, H. and Estelle, M. (1999). Identification of an SCF ubiquitin-ligase complex required for auxin response in *Arabidopsis thaliana*. *Genes Dev.* **13**, 1678-1691.

Grossniklaus, U., Vielle-Calzada, J. P., Hoeppner, M. A. and Gagliano, W. B. (1998). Maternal control of embryogenesis by *MEDEA*, a polycomb group gene in *Arabidopsis*. *Science* **280**, 446-450.

Gu, Q., Ferrándiz, C., Yanofsky, M. and Martienssen, R. (1998). The *FRUITFULL* MADS-box gene mediates cell differentiation during *Arabidopsis* fruit development. *Development* **125**, 1509-1517.

Guardiola, J. L., Barrés, M. T., Albert, C. and García-Luis, A. (1993). Effects of exogenous growth regulators on fruit development in Citrus unshiu. *Ann. Bot.* **71**, 169-176.

Guilfoyle, T., Hagen, G., Ulmasov, T. and Murfett, J. (1998a). How does auxin turn on genes? *Plant Physiol.* **118**, 341-347.

Guilfoyle, T. J., Ulmasov, T. and Hagen, G. (1998b). The ARF family of transcription factors and their role in plant hormone- responsive transcription. *Cell. Mol. Life. Sci.* **54**, 619-627.

Gustafson, F. G. (1936). Inducement of fruit development by growth promoting chemicals. *Proc. Natl. Acad. Sci.* **22**, 629-636.

Gustafson, F. G. (1939). The natural cause of parthenocarpy. *Am. J. Bot.* **26**, 135-138.

Gustafson, F. G. (1942). Parthenocarpy: Artificial and natural. *Botanical Review* **8**, 599-654.

Hardtke, C. S. and Berleth, T. (1998). The *Arabidopsis* gene *MONOPTEROS* encodes a transcription factor mediating embryo axis formation and vascular development. *EMBO J.* **17**, 1405-1411.

Harper, R. M., Stowe-Evans, E. L., Luesse, D. R., Muto, H., Tatematsu, K., Watahiki, M. K., Yamamoto, K. and Liscum, E. (2000). The *NPH4* locus encodes the auxin response factor *ARF7*, a conditional regulator of differential growth in aerial *Arabidopsis* tissue. *Plant Cell* **12**, 757-770.

Hedden, P. and Kamiya, Y. (1997). Gibberellin biosynthesis: Enzymes, genes and their regulation. *Ann. Rev. Plant Physiol. Plant Mol. Biol.* **48**, 431-460.

Heinemeyer, T., Wingender, E., Reuter, I., Hermjakob, H., Kel, A. E., Kel, O. V., Ignatieva, E. V., Ananko, E. A., Podkolodnaya, O. A., Kolpakov, F. A. (1998).

Databases on Transcriptional Regulation: TRANSFAC, TRRD, and COMPEL. *Nucleic Acids Res.* **26**, 364-370.

Heisler, M. G. B., Bylstra, Y. M. and Smyth, D. R. (1999). Patterns of expression of the carpel development gene *SPATULA*. *10th International Conference on Arabidopsis Research*. 4th-8th July, Melbourne, Australia.

Helariutta, Y., Fukaki, H., Wysocka-Diller, J., Nakajima, K., Jung, J., Sena, G., Hauser, M. T. and Benfey, P. N. (2000). The *SHORT-ROOT* gene controls radial patterning of the *Arabidopsis* root through radial signaling. *Cell* **101**, 555-567.

Hertzberg, M. and Olsson, O. (1998). Molecular characterisation of a novel plant homeobox gene expressed in the maturing xylem zone of *Populus tremula* x *tremuloides*. *Plant J.* **16**, 285-295.

Herzog, M., Dorne, A. M. and Grellet, F. (1995). *GASA*, a gibberellin-regulated gene family from *Arabidopsis thaliana* related to the tomato *GAST1* gene. *Plant Mol. Biol.* **27**, 743-752.

Higo, K., Ugawa, Y., Iwamoto, M. and Korenaga, T. (1999). Plant cis-acting regulatory DNA elements (PLACE) database: 1999. *Nucleic Acids Res.* **27**, 297-300.

Hill, K. D. (1994). Three new species of *Cycas* from the Northern Territory of Australia. *Telopea* **5**, 693-701.

Hobbie, L. (1998). Auxin: Molecular genetic approaches in *Arabidopsis*. *Plant Physiol. Biochem.* **36**, 91-102.

Hobbie, L., Timpte, C. and Estelle, M. (1994). Molecular genetics of auxin and cytokinin. *Plant Mol. Biol.* **26**, 1499-1519.

Hua, J. and Meyerowitz, E. M. (1998). Ethylene responses are negatively regulated by a receptor gene family in *Arabidopsis thaliana*. *Cell* **94**, 261-271.

Hua, J., Sakai, H., Nourizadeh, S., Chen, Q. G., Bleecker, A. B., Ecker, J. R. and Meyerowitz, E. M. (1998). *EIN4* and *ERS2* are members of the putative ethylene receptor gene family in *Arabidopsis*. *Plant Cell* **10**, 1321-1332.

Huang, H., Mizukami, Y., Hu, Y. and Ma, H. (1993). Isolation and characterization of the binding sequences for the product of the *Arabidopsis* floral homeotic gene *AGAMOUS*. *Nucleic Acids Res.* **21**, 4769-4776.

Hulme, A. C. (1970). The biochemistry of fruits and their products. Academic Press, London.

Hülskamp, M., Kopczak, S. D., Horejsi, T. F., Kihl, B. K. and Pruitt, R. E. (1995). Identification of genes required for pollen-stigma recognition in *Arabidopsis thaliana*. *Plant J.* **8**, 703-714.

Ito, T. and Meyerowitz, E. M. (2000). Overexpression of a gene encoding a cytochrome P450, *CYP78A9*, induces large and seedless fruit in *Arabidopsis*. *Plant Cell* **12**, 1541-1550.

Jacobs, W. P. (1952). The role of auxin in differentiation of xylem around a wound. *Am. J. Bot.* **39**, 301-309.

Jacobsen, S. E., Binkowski, K. A. and Olszewski, N. E. (1996). *SPINDLY*, a tetratricopeptide repeat protein involved in gibberellin signal transduction in *Arabidopsis*. *Proc. Natl. Acad. Sci.* **93**, 9292-9296.

Jacobsen, S. E. and Oleszewski, N. E. (1993). Mutations at the *SPINDLY* locus of *Arabidopsis* alter signal transduction. *Plant Cell* **5**, 887-896.

Jensen, P. J. and Bandurski, R. S. (1994). Metabolism and synthesis of indole-3-acetic acid (IAA) in *Zea mays*. Levels of IAA during kernel development and the use of *in vitro* endosperm systems for studying IAA biosynthesis. *Plant Physiol.* **106**, 343-351.

Johnson, P. R. and Ecker, J. R. (1998). The ethylene gas signal transduction pathway: A molecular perspective. *Annu. Rev. Genet.* **32**, 227-54.

Kang, H. G., Jun, S. H., Kim, J., Kawaide, H., Kamiya, Y. and An, C. (1999). Cloning and molecular analyses of a gibberellin 20-oxidase gene expressed specifically in developing seeds of watermelon. *Plant Physiol.* **121**, 373- 382.

Keleher, C. A., Redd, M. J., Schultz, J., Carlson, M., and Johnson, A. D. (1992). Ssn6-Tup1 is a general repressor of transcription in yeast. *Cell* **68**, 709-719.

Khan, S. (1994). Ethylene and other signals involved in the pollination-induced senescence of climacteric flowers. Honors Thesis, Department of Botany, University of Queensland, Brisbane.

Khripach, V. A., Zhabinskii, V. N. and de Groot, A. E. (1999). Brassinosteroids: A new class of plant hormones. Academic Press, San Diego.

Kieber, J. J., Rothenberg, M., Roman, G., Feldmann, K. A. and Ecker, J. R. (1993). *CTR1*, a negative regulator of the ethylene response pathway in *Arabidopsis*, encodes a member of the *raf* family of protein kinases. *Cell* **72**, 427-441.

Kim, I. S., Okubo, H. and Fujieda, K. (1992). Endogenous levels of IAA in relation to parthenocarpy in cucumber (*Cucumis sativus* L.). *Scientia-Horticulturae* **52**, 1-8.

Kim, I. S., Yeoung, Y. R. and Yoo, K. C. (1995). Comparison of endogenous hormone in the sarcocarp and placental tissue of parthenocarpic and seeded cucumber fruits. *J. Kor. Soc. Hortic. Sci.* **36**, 601-607.

Kim, J., Harter, K. and Theologis, A. (1997). Protein-protein interactions among the Aux/IAA proteins. *Proc. Natl. Acad. Sci. U S A* **94**, 11786-91.

Kojima, K., Shiozaki, K., Koshita, Y. and Ishida, M. (1999). Changes of endogenous levels of ABA, IAA and GA-like substances in fruitlets of parthenocarpic persimmon. *J. Jpn. Soc. Hortic. Sci.* **68**, 242- 247.

Koltunow, A. M. (1993). Apomixis: Embryo sacs and embryos formed without meiosis or fertilization in ovules. *Plant Cell* **5**, 1425-1437.

Komori, S., Soejima, J., Tsuchiya, S., Masuda, T., Bessho, H. and Ito, Y. (1997). Two types of unfruitfulness found in artificial pollination experiments of apple. *J. Jpn. Soc. Hortic. Sci.* **66**, 289-295.

Koncz, C., Chua, N.-H. and Schell, J. (1992). Methods in *Arabidopsis* research. World Scientific Publishing Co. Pte. Ltd., Singapore.

Konieczny, A. and Ausubel, F. M. (1993). A procedure for mapping *Arabidopsis* mutations using co-dominant ecotype- specific PCR-based markers. *Plant J.* **4**, 403-410.

Koornneef, M., Elgersma, A., Hanhart, C. J., van Loenen-Martinet, E. P., van Rijn, L. and Zeevart, J. A. D. (1985). A gibberellin insensitive mutant of *Arabidopsis thaliana*. *Plant Physiol.* **65**, 33-39.

Koornneef, M. and Stam, P. (1992). Genetic analysis. In *Methods in Arabidopsis research*, (C. Koncz, N.-H. Chua and J. Schell, eds), pp. 83-99, World Scientific Publishing Co. Pte. Ltd., Singapore.

Koshioka, M., Nishijima, T., Yamazaki, H., Liu, Y., Nonaka, M. and Mander, L. N. (1994). Analysis of gibberellins in growing fruits of *Lycopersicon esculentum* after pollination or treatment with 4-chlorophenoxyacetic acid. *J. Hortic. Sci.* **69**, 171-179.

Kumcha, U. (1999). The effects of cultural practices and environmental factors on fruit development in lychee (*Litchi chinesis* Sonn.). Ph.D. Thesis, Department of Agriculture, University of Queensland, Brisbane.

Langridge, U., Schwall, M. and Langridge, P. (1991). Squashes of plant tissue as substrate for PCR. *Nucleic Acids Res.* **19**, 6954.

Larsen, P. B., Woltering, E. J. and Woodson, W. R. (1993). Ethylene and interorgan signaling in flowers following pollination. In *Plants signals in interactions with other organisms*, (I. Raskin and J. Schultz, eds), pp. 112-122, American Society of Plant Physiologists, Rockville, MD.

Léon-Kloosterziel, K. M., Keijzer, C. J. and Koornneef, M. (1994). A seed shape mutant of *Arabidopsis* that is affected in integument development. *Plant Cell* **6**, 385-392.

Lester, D. R., Ross, J. J., Davies, P. J. and Reid, J. B. (1997). Mendel's stem length gene (*Le*) encodes a gibberellin 3 beta-hydroxylase. *Plant Cell* **9**, 1435-1443.

Leyser, O. and Berleth, T. (1999). A molecular basis for auxin action. *Semin. Cell Dev. Biol.* **10**, 131-137.

Liljegren, S. J., Ferrándiz, C., Alavarez-Buylla, E. R., Pelaz, S. and Yanofsky, M. F. (1998). *Arabidopsis* MADS-box genes invovled in fruit dehiscence. *Flowering News Letter* **25**, 9-19.

Lin, S., George, W. L. and Splittstoesser, W. E. (1984). Expression and inheritance of parthenocarpy in 'Severianin' tomato. *J. Hered.* **75**, 62-66.

Luo, M., Bilodeau, P., Dennis, E. S., Peacock, W. J. and Chaudhury, A. (2000). Expression and parent-of-origin effects for *FIS2*, *MEA*, and *FIE* in the endosperm and embryo of developing *Arabidopsis* seeds. *Proc. Natl. Acad. Sci.* **97**, 10637-10642.

Luo, M., Bilodeau, P., Koltunow, A., Dennis, E. S., Peacock, W. J. and Chaudhury, A. M. (1999). Genes controlling fertilization-independent seed development in *Arabidopsis thaliana*. *Proc. Natl. Acad. Sci.* **96**, 296-301.

Lyndon, R. F. (1990). Plant Development. Unwin Hyman Ltd., London.

Malamy, J. E. and Benfey, P. N. (1997). Organization and cell differentiation in lateral roots of *Arabidopsis thaliana*. *Development* **124**, 33-44.

Mapelli, S., Cantoni, M., Bricchi, D., Soressi, G. P. and Stamova, L. (1993). Influence of *pat2* gene on phytohormones, fruit set and fruit yield in Mediterranean mild climate. *Proceedings of the XIIth Eucarpia meeting on tomato genetics and breeding.* pp 95-100, 27th-31st July, MARITSA Vegetable Crops Research Institute, Plovdiv, Bulgaria.

Mapelli, S., Frova, C., Torti, G. and Soressi, G. P. (1978). Relationship between set, development and activities of growth regulators in tomato fruits. *Plant Cell Physiol.* **19**, 1281-1288.

Mattsson, J., Sung, Z. R. and Berleth, T. (1999). Responses of plant vascular systems to auxin transport inhibition. *Development* **126**, 2979-2991.

Mazzucato, A., Taddei, A. R. and Soressi, G. P. (1998). The parthenocarpic fruit (*pat*) mutant of tomato (*Lycopersicon esculentum* Mill.) sets seedless fruits and has aberrant anther and ovule development. *Development* **125**, 107-114.

Mazzucato, A., Testa, G., Biancari, T. and Soressi, G. P. (1999). Effect of gibberellic acid treatments, environmental conditions, and genetic background on the expression of the parthenocarpic fruit mutation in tomato. *Protoplasma* **208**, 18- 25.

Mehouachi, J., Iglesias, D. J., Tadeo, F. R., Agusti, M., Primo-millo, E. and Talon, M. (2000). The role of leaves in citrus fruitlet abscission: Effects on endogenous gibberellin levels and carbohydrate content. *J. Hortic. Sci. Biotech.* **75**, 79-85.

Meinke, D. W. and Sussex, I. M. (1979). Embryo lethal mutants of *Arabidopsis thaliana*. A model system for genetic analysis of plant embryo development. *Dev. Biol.* **12**, 50-61.

Meyerowitz, E. M. (1997). Genetic control of cell division patterns in developing plants. *Cell* **88**, 299-308.

Meyerowitz, E. M., Bowman, J. L., Brockman, L. L., Drews, G. N., Jack, T., Sieburth, L. E. and Weigel, D. (1991). A genetic and molecular model for flower development in *Arabidopsis thaliana*. *Dev. Suppl.* **1**, 157-167.

Meyerowitz, E. M., Running, M. P., Sakai, H. and Williams, R. W. (1998). Multiple modes of cell division control in *Arabidopsis* flower development. *Symp. Soc. Exp. Biol.* **51**, 19-26.

Mizukami, Y. and Ma, H. (1992). Ectopic expression of the floral homeotic gene *AGAMOUS* in transgenic *Arabidopsis* plants alters floral organ identity. *Cell* **71**, 119-131.

Modrusan, Z., Reiser, L., Feldmann, K. A., Fischer, R. L. and Haughn, G. W. (1994). Homeotic transformation of ovules into carpel-like structures in *Arabidopsis*. *Plant Cell* **6**, 333-349.

Mordhorst, A. P., Voerman, K. J., Hartog, M. V., Meijer, E. A., van Went, J., Koornneef, M. and de Vries, S. C. (1998). Somatic embryogenesis in *Arabidopsis thaliana* is facilitated by mutations in genes repressing meristematic cell divisions. *Genetics* **149**, 549-563.

Morelli, G. and Ruberti, I. (2000). Shade avoidance responses. Driving auxin along lateral routes. *Plant Physiol.* **122**, 621-626.

Muller, A., Guan, C., Galweiler, L., Tanzler, P., Huijser, P., Marchant, A., Parry, G., Bennett, M., Wisman, E. and Palme, K. (1998). *AtPIN2* defines a locus of *Arabidopsis* for root gravitropism control. *EMBO J.* **17**, 6903-6911.

Mummery, J. and Hardy, N. (1995). Australia's Biodiversity - An overview of selected significant components. Biodiversity Series, Paper No. 2. Biodiversity Unit Report, Department of Environment, Sport and Territories, Canberra.

Murashige, T. and Skoog, F. (1962). Medium for growth and bioassays with tobacco tissue cultures. *Plant Physiol.* **15**, 473-497.

Nagpal, P., Walker, L. M., Young, J. C., Sonawala, A., Timpte, C., Estelle, M. and Reed, J. W. (2000). *AXR2* encodes a member of the Aux/IAA protein family. *Plant Physiol.* **123**, 563-574.

Nemhauser, J. L., Feldman, L. J. and Zambryski, P. C. (2000). Auxin and *ETTIN* in *Arabidopsis* gynoecium morphogenesis. *Development* **127**, 3877-3888.

Nemhauser, J. L., Zambryski, P. C. and Roe, J. L. (1998). Auxin signaling in *Arabidopsis* flower development? *Curr. Opin. Plant. Biol.* **1**, 531-535.

Nitsch, J. P. (1950). Growth and morphogenesis of the strawberry as related to auxin. *Am. J. Bot.* **37**, 211-215.

Nitsch, J. P. (1970). Hormonal factors in growth and development. In *The biochemistry of fruits and their products*, vol. 1 (A. C. Hulme, eds), pp. 427-472, Academic Press, London.

Nuez, F., Costa, J. and Cuartero, J. (1986). Genetics of the parthenocarpy for tomato varieties 'Sub-Arctic Plenty', '75/59' and 'Severianin'. *Z. Pflanzenzuecht* **96**, 200-206.

Oeller, P. W., Keller, J. A., Parks, J. E., Silbert, J. E. and Theologis, A. (1993). Structural characterization of the early indoleacetic acid-inducible genes, PS-IAA4/5 and PS-IAA6, of pea (*Pisum sativum* L.). *J. Mol. Biol.* **233**, 789-798.

Oeller, P. W. and Theologis, A. (1995). Induction kinetics of the nuclear proteins encoded by the early indoleacetic acid-inducible genes, PS-IAA4/5 and PS-IAA6, in pea (*Pisum sativum* L.). *Plant J.* **7**, 37-48.

Ohad, N., Margossian, L., Hsu, Y.-C., Williams, C., Repetti, P. and Fischer, R. L. (1996). A mutation that allows endosperm development without fertilization. *Proc. Natl. Acad. Sci.* **93**, 5319-5324.

Ohad, N., Yadegari, R., Margossian, L., Hannon, M., Michaeli, D., Harada, J. J., Goldberg, R. B. and Fischer, R. L. (1999). Mutations in *FIE*, a WD polycomb group gene, allow endosperm development without fertilization. *Plant Cell* **11**, 407-416.

Okada, K., Ueda, J., Komaki, M. K., Bell, C. J. and Shimura, Y. (1991). Requirement of the auxin polar transport system in early stages of *Arabidopsis* floral bud formation. *Plant Cell* **3**, 677-684.

Okamuro, J. K., Caster, B., Villarroel, R., Van Montagu, M. and Jofuku, K. D. (1997). The AP2 domain of *APETALA2* defines a large new family of DNA binding proteins in *Arabidopsis*. *Proc. Natl. Acad. Sci.* **94**, 7076-7081.

Okamuro, J. K., den Boer, B. G., Lotys-Prass, C., Szeto, W. and Jofuku, K. D. (1996). Flowers into shoots: Photo and hormonal control of a meristem identity switch in *Arabidopsis*. *Proc. Natl. Acad. Sci.* **93**, 13831-13836.

O'Neill, S. D. (1997). Pollination regulation of flower development. *Annu. Rev. Plant Physiol. Plant Mol. Biol.* **48**, 547–574.

O'Neill, S. D. and Nadeau, J. A. (1997). Post-pollination flower development. *Hortic. Rev.* **19**, 1-58.

O'Neill, S. J., Nadeau, J. A., Zhang, X. S., Bui, A. Q. and Halevy, A. H. (1993). Interorgan regulation of ethylene biosynthetic genes by pollination. *Plant Cell* **5**, 419-432.

Ortiz, R. and Vuylsteke, D. (1995). Effect of the parthenocarpy gene P-1 and ploidy on fruit and bunch traits of plantain banana hybrids. *Heredity* **75**, 460-465.

Orzáez, D., Blay, R. and Granell, A. (1999). Programs of senescence in petals and carpels of *Pisum sativum* L. flowers and its control by ethylene. *Planta* **208**, 220-226.

Ozga, J. A., Brenner, M. L. and Reinecke, D. M. (1992). Seed effects on gibberellin metabolism in pea pericarp. *Plant Physiol.* **100**, 88-94.

Page, R. D. M. (1996). TreeView: An application to display phylogenetic trees on personal computers. *Computer application in the Biosciences* **12**, 357-358.

Parinov, S., Sevugan, M., De, Y., Yang, W. C., Kumaran, M. and Sundaresan, V. (1999). Analysis of flanking sequences from dissociation insertion lines. A database for reverse genetics in *Arabidopsis*. *Plant Cell* **11**, 2263-2270

Pecaut, P. and Philouze, J. (1978). A *sha pat* line obtained by natural mutation. *Rep. Tom. Genet. Coop.* **28**, 12.

Peng, J., Carol, P., Richards, D. E., King, K. E., Cowling, R. J., Murphy, G. P. and Harberd, N. P. (1997). The *Arabidopsis GAI* gene defines a signaling pathway that negatively regulates gibberellin responses. *Genes Dev.* 23, 3194-3205.

Peretó, J. G., Beltrain, J. P. and García-Martínez, J. L. (1988). The source of gibberellins in the parthenocarpic development of ovaries in topped plants. *Planta* **175**, 493-499.

Pharis, R. P. and King, R. (1985). Gibberellins and reproductive development in seed plants. *Ann. Rev. Plant Physiol.* **36**, 517-568.

Phillips, A. L. (1998). Gibberellins in *Arabidopsis*. *Plant Physiol. Bioch.* **36**, 115-124.

Phillips, A. L., Ward, D. A., Uknes, S., Appleford, N. E., Lange, T., Huttly, A. K., Gaskin, P., Graebe, J. E. and Hedden, P. (1995). Isolation and expression of three gibberellin 20-oxidase cDNA clones from *Arabidopsis*. *Plant Physiol.* **108**, 1049-1057.

Philouze, J. (1983a). Attempts to map *pat-2*. *Tomato. Genet. Coop. Rep.* **33**, 9.

Philouze, J. (1983b). Epistatic relations between *ls* and *pat-2*. *Tomato Genet. Coop. Rep.* **33**, 9-12.

Pike, L. M. and Peterson, C. R. (1969). Inheritance of parthenocarpy in the cucumber (*Cucumis sativus* L.). *Euphytica* **18**, 101-105.

Pommer, C. V., Pires, E. J. P., Terra, M. M. and Passos, I. R. S. (1996). Streptomycin-induced seedlessness in the grape cultivar Rubi (Italia Red). *American Journal of Enology and Viticulture* **47**, 340-342.

Prohens, J., Ruiz, J. J. and Nuez, F. (1998). The inheritance of parthenocarpy and associated traits in pepino. *J. Am. Soc. Hortic. Sci.* **123**, 376- 380.

Przemeck, G. K., Mattsson, J., Hardtke, C. S., Sung, Z. R. and Berleth, T. (1996). Studies on the role of the *Arabidopsis* gene *MONOPTEROS* in vascular development and plant cell axialization. *Planta* **200**, 229-237.

Pysh, L. D., Wysocka-Diller, J. W., Camilleri, C., Bouchez, D. and Benfey, P. N. (1999). The *GRAS* gene family in *Arabidopsis*: Sequence characterization and basic expression analysis of the *SCARECROW-LIKE* genes. *Plant J.* **18**, 111-119.

Quandt, K., Frech, K., Karas, H., Wingender, E. and Werner, T. (1995). MatInd and MatInspector - New fast and versatile tools for detection of consensus matches in nucleotide sequence data. *Nucleic Acids Res.* **23**, 4878-4884.

Rao, G. U., Jain, A. and Shivanna, K. R. (1992). Effects of high temperature stress on *Brassica* pollen: Viability, germination and ability to set fruits and seeds. *Ann. Bot.* **69**, 193-198.

Rappaport, L. (1979). Applications of gibberellins in agriculture. In *Plant growth substances*, (F. Skoog, eds), pp. 377-391, Springer-Verlag, New York.

Raventos, D., Meier, C., Mattsson, O., Jensen, A. B. and Mundy, J. (2000). Fusion genetic analysis of gibberellin signaling mutants. *Plant J.* **22**, 427-438.

Ray, A., Robinson-Beers, K., Ray, S., Baker, S. C., Lang, J. D., Preuss, D., Milligan, S. B. and Gasser, C. S. (1994). *Arabidopsis* floral homeotic gene *BELL* (*BEL1*) controls ovule development through negative regulation of *AGAMOUS* gene (*AG*). *Proc. Natl. Acad. Sci.* **91**, 5761-5765.

Rebers, M., Kaneta, T., Kawaide, H., Yamaguchi, S., Yang, Y. Y., Imai, R., Sekimoto, H. and Kamiya, Y. (1999). Regulation of gibberellin biosynthesis genes during flower and early fruit development of tomato. *Plant J.* **17**, 241-250.

Reinhardt, D., Mandel, T. and Kuhlemeier, C. (2000). Auxin regulates the initiation and radial position of plant lateral organs. *Plant Cell* **12**, 507-518.

Reiser, L. and Fischer, R. L. (1993). The ovule and the embryo sac. *Plant Cell* **5**, 1291-1301.

Reiser, L., Modrusan, Z., Margossian, L., Samach, A., Ohad, N., Haughn, G. W. and Fischer, R. L. (1995). The *BELL1* gene encodes a homeodomain protein involved in pattern formation in the *Arabidopsis* ovule primordium. *Cell* **83**, 735-742.

Rhee, S. Y., Weng, S., Flanders, D., Cherry, J. M., Dean, C., Lister, C., Anderson, M., Koornneef, M., Meinke, D. W., Nickle, T. (1998). Genome maps 9. *Arabidopsis thaliana*. Wall chart. *Science* **282**, 663-667.

Rice, P. (1994). Genetics Computer Group EGCG Program manual. The Sanger Centre, Cambridge.

Robertson, M., Swain, S. M., Chandler, P. M. and Olszewski, N. E. (1998). Identification of a negative regulator of gibberellin action, *HvSPY*, in barley. *Plant Cell* **10**, 995-1007.

Rodrigo, M. J., García-Martínez, J. L., Santes, C., Gaskin, P. and Hedden, P. (1997). The role of gibberellins A_1 and A_3 in fruit growth of *Pisum sativum* L. and the identification of gibberellins A_4 and A_7 in young seeds. *Planta* **201**, 446-455.

Roe, J. L., Nemhauser, J. L. and Zambryski, P. C. (1997). *TOUSLED* participates in apical tissue formation during gynoecium development in *Arabidopsis*. *Plant Cell* **9**, 335-353.

Roman, G., Lubarsky, B., Kieber, J. J., Rothenberg, M. and Ecker, J. R. (1995). Genetic analysis of ethylene signal transduction in *Arabidopsis thaliana*: Five novel mutant loci integrated into a stress response pathway. *Genetics* **139**, 1393-1409.

Rotino, G. L., Perri, E., Zottini, M., Sommer, H. and Spena, A. (1997). Genetic engineering of parthenocarpic plants. *Nat. Biotechnol.* **15**, 1398-1401.

Rozen, S. and Skaletsky, H. J. (1997). Primer3. Whitehead Institute/MIT Center for Genome Research. http://www-genome.wi.mit.edu/genome_software/other/primer3.html.

Rudich, J., Baker, L. R. and Sell, H. M. (1977). Parthenocarpy in *Cucumis sativus* L. as affected by genetic parthencarpy, thermo-photoperiod and femaleness. *J. Am. Soc. Hort. Sci.* **102**, 225-228.

Russell, S. (1993). The egg cell: Development and role in fertilization and early embryogenesis. *Plant Cell* **5**, 1349-1359.

Sabatini, S., Beis, D., Wolkenfelt, H., Murfett, J., Guilfoyle, T., Malamy, J., Benfey, P., Leyser, O., Bechtold, N., Weisbeek, P. et al. (1999). An auxin-dependent distal organizer of pattern and polarity in the *Arabidopsis* root. *Cell* **99**, 463-472.

Sachs, T. (1991). Pattern formation in plant tissues: Developmental and cell biology. *Development Supplement* **1**, 833-893.

Sakai, H., Hua, J., Chen, Q. G., Chang, C., Medrano, L. J., Bleecker, A. B. and Meyerowitz, E. M. (1998). *ETR2* is an *ETR1*-like gene involved in ethylene signaling in *Arabidopsis*. *Proc. Natl. Acad. Sci.* **95**, 5812-5817.

Santes, C. M., Hedden, P., Sponsel, V. M., Reid, J. B. and García-Martínez, J. L. (1993). Expression of the *le* mutation in young ovaries of *Pisum sativum* and its effects on fruit development. *Plant Physiol.* **101**, 759-764.

Sato-Nara, K., Yuhashi, K. I., Higashi, K., Hosoya, K., Kubota, M. and Ezura, H. (1999). Stage- and tissue-specific expression of ethylene receptor homolog genes during fruit development in muskmelon. *Plant Physiol.* **120**, 321-330.

Sauter, M., Mekhedov, S. L. and Kende, H. (1995). Gibberellin promotes histone H1 kinase activity and the expression of cdc2 and cyclin genes during the induction of rapid growth in deepwater rice internodes. *Plant J.* **7**, 623-632.

Sawa, S., Ito, T., Shimura, Y. and Okada, K. (1999a). *FILAMENTOUS FLOWER* controls the formation and development of *Arabidopsis* inflorescences and floral meristems. *Plant Cell* **11**, 69-86.

Sawa, S., Watanabe, K., Goto, K., Liu, Y.-G., Shibata, D., Kanaya, E., Morita, E. H. and Okada, K. (1999b). *FILAMENTOUS FLOWER*, a meristem and organ identity gene of Arabidopsis, encodes a protein with a zinc finger and HMG-related domains. *Genes Dev.* **13**, 1079-1088.

Sawhney, V. K. and Greyson, R. I. (1973). Morphogenesis of the *stamenless-2* mutant in tomato. I. Comparative description of the flowers and ontogeny of stamens in the normal and mutant plants. *Am. J. Bot.* **60**, 514-523.

Scheres, B. (2000). Non-linear signaling for pattern formation? *Curr. Opin. Plant Biol.* **3**, 412-417.

Scheres, B. and Benfy, P. N. (1999). Asymmetric cell division in plants. *Ann. Rev. Plant Physiol. Plant. Mol. Biol.* **50**, 505-537.

Schneitz, K., Hülskamp, M., Kopczak, S. D. and Pruitt, R. E. (1997). Dissection of sexual organ ontogenesis: A genetic analysis of ovule development in *Arabidopsis thaliana*. *Development* **124**, 1367-1376.

Schneitz, K., Hülskamp, M. and Pruitt, R. E. (1995). Wild-type ovule development in *Arabidopsis thaliana*: A light microscope study of cleared whole-mount tissue. *Plant J.* **7**, 731-749.

Schoof, H., Lenhard, M., Haecker, A., Mayer, K. F., Jurgens, G. and Laux, T. (2000). The stem cell population of *Arabidopsis* shoot meristems in maintained by a regulatory loop between the *CLAVATA* and *WUSCHEL* genes. *Cell* **100**, 635-644.

Schumacher, K., Schmitt, T., Rossberg, M., Schmitz, G. and Theres, K. (1999). The *LATERAL SUPPRESSOR* (*LS*) gene of tomato encodes a new member of the VHIID protein family. *Proc. Natl. Acad. Sci.* **96**, 290-295.

Schwabe, W. W. (1971). Chemical modification of phyllotaxis and its implications. *Sym. Soc. Exp. Biol.* **25**, 301-322.

Schwabe, W. W. and Mills, J. J. (1981). Hormones and parthenocarpic fruit set: A literature survey. *Hortic. Abstr.* **51**, 661-699.

Sedgley, M., Newbury, H. J. and Possingham, J. V. (1977). Early fruit development in the watermelon: Anatomical comparison of pollinated, auxin-induced parthenocarpic and unpollinated fruits. *Ann. Bot.* **41**, 1345-1355.

Seki, M., Ito, T., Shibata, D. and Shinozaki, K. (1999). Regional insertional mutagenesis of specific genes on the CIC5F11/CIC2B9 locus of *Arabidopsis thaliana* chromosome 5 using the *Ac*/*Ds* transposon in combination with the cDNA scanning method. *Plant Cell Physiol.* **40**, 624-639.

Sessa, G., Morelli, G. and Ruberti, I. (1993). The *Athb-1* and *-2* HD-Zip domains homodimerize forming complexes of different DNA binding specificities. *EMBO J.* **12**, 3507-3517.

Sessa, G., Morelli, G. and Ruberti, I. (1997). DNA-binding specificity of the homeodomain-leucine zipper domain. *J. Mol. Biol.* **274**, 303-309.

Sessions, A., Nemhauser, J. L., McColl, A., Roe, J. L., Feldmann, K. A. and Zambryski, P. C. (1997). *ETTIN* patterns the *Arabidopsis* floral meristem and reproductive organs. *Development* **124**, 4481-4491.

Sessions, R. A. and Zambryski, P. C. (1995). *Arabidopsis* gynoecium structure in the wild type and in *ettin* mutants. *Development* **121**, 1519-1532.

Sieburth, L. E. (1999). Auxin is required for leaf vein pattern in *Arabidopsis*. *Plant. Physiol.* **121**, 1179-1190.

Siegfried, K. R., Eshed, Y., Baum, S. F., Otsuga, D., Drews, G. N. and Bowman, J. L. (1999). Members of the *YABBY* gene family specify abaxial cell fate in *Arabidopsis*. *Development* **126**, 4117-4128.

Silverstone, A. L., Chang, C.-W., Krol, E. and Sun, T-P. (1997a). Developmental regulation if the gibberellin biosynthetic gene GA_1 in *Arabidopsis thaliana*. *Plant J.* **12**, 9-19.

Silverstone, A. L., Ciampaglio, C. N. and Sun, T-P. (1998). The *Arabidopsis RGA* gene encodes a transcriptional regulator repressing the gibberellin signal transduction pathway. *Plant Cell* **10**, 155-169.

Silverstone, A. L., Mak, P. Y. A., Martínez, E. C. and Sun, T.-P. (1997b). The new *RGA* locus encodes a negative regulator of gibberellin response in *Arabidopsis thaliana*. *Genetics* **146**, 1087-1099.

Smith, R. L., and Johnson, A. D. (2000a). Turning genes off by Ssn6-Tup1: A conserved system of transcriptional repression in eukaryotes. *Trends Biochem Sci.* **25**, 325-330

Smith, R. L., and Johnson, A. D. (2000b). A sequence resembling a peroxisomal targeting sequence directs the interaction between the tetratricopeptide repreats of Ssn6 and the homeodomain of α2. *Proc. Natl. Acad. Sci.* **97**, 3901-3906

Smith, R. F., Wiese, B. A., Wojzynski, M. K., Davison, D. B. and Worley, K. C. (1996). BCM search launcher - An integrated interface to molecular biology data base search and analysis services available on the world wide web. *Genome Res.* **6**, 454-462.

Spence, J., Vercher, Y., Gates, P. and Harris, N. (1996). 'Pod shatter' in *Arabidopsis thaliana*, *Brassica napus* and *Brassica juncea*. *J. Microscopy* **181**, 195-203.

Sponsel, V. M. (1983). The localization, metabolism and biological activity of gibberellins in maturing and germinating seeds of *Pisum sativum* cv. Progess No. 9. *Planta* **159**, 454-468.

Sponsel, V. M., Schmidt, F. W., Porter, S. G., Nakayama, M., Kohlstruk, S. and Estelle, M. (1997). Characterization of new gibberellin-responsive semidwarf mutants of *Arabidopsis*. *Plant Physiol.* **115**, 1009-1020.

Spurr, A. R. (1969). A low viscosity epoxy resin embedding medium for electron microscopy. *J. Ultrastruct. Res.* **26**, 31-43.

Srinivasan, A. and Morgan, D. G. (1996). Growth and development of the pod wall in spring rape (*Brassica napus*) as related to the presence of seeds and exogenous phytohormones. *J. Agr. Sci.* **127**, 487-500.

Stadler, R., Truernit, E., Gahrtz, M. and Sauer, N. (1999). The AtSUC1 sucrose carrier may represent the osmotic driving force for anther dehiscence and pollen tube growth in *Arabidopsis*. *Plant J.* **19**, 269-278.

Steindler, C., Carabelli, M., Borello, U., Morelli, G. and Ruberti, I. (1997). Phytochrome A, phytochrome B and other phytochromes(s) regulate *ATHB-2* gene expression in etiolated and green *Arabidopsis* plants. *Plant Cell Environ.* **20**, 759-763.

Steindler, C., Matteucci, A., Sessa, G., Weimar, T., Ohgishi, M., Aoyama, T., Morelli, G. and Ruberti, I. (1999). Shade avoidance responses are mediated by the *ATHB-2* HD-zip protein, a negative regulator of gene expression. *Development* **126**, 4235-4245.

Stevens, W. L. (1939). Tables of the recombination fraction estimated from the product ratio. *J. Genet.* **39**, 171-180.

Stowe-Evans, E. L., Harper, R. M., Motchoulski, A. V. and Liscum, E. (1998). *NPH4*, a conditional modulator of auxin-dependent differential growth responses in *Arabidopsis*. *Plant Physiol.* **118**, 1265-1275.

Strobeck, M. W., Knudsen, K. E., Fribourg, A. F., DeCristofaro, M. F., Weissman, B. E., Imbalzano, A. N. and Knudsen, E. S. (2000). *BRG-1* is required for RB-mediated cell cycle arrest. *Proc. Natl. Acad. Sci.* **97**, 7748-7753.

Sun, G., Dilcher, D. L., Zheng, S. and Zhou, Z. (1998). In search of the first flower: A jurassic angiosperm, *Archaefructus*, from northeast china. *Science* **282**, 1692-1695.

Sun, T.-P. and Kamiya, Y. (1994). The *Arabidopsis GA1* locus encodes the cyclase ent-kaurene synthetase A of gibberellin biosynthesis. *Plant Cell* **6**, 1509-1518.

Sun, T.-P. and Kamiya, Y. (1997). Regulation and cellular location of *ent*-kaurene synthesis. *Physiol. Plantarum* **101**, 701-708.

Swain, S. M., Ross, J. J., Reid, J. B. and Kamiya, Y. (1995a). Gibberellin and pea seed development: Expression of the *lhi*, *ls* and, *le5839* mutations. *Planta* **195**, 426-433.

Swain, S. M., Ross, J. R. and Kamiya, Y. (1995b). Gibberellins and pea seed development. *Planta* **195**, 426-433.

Sykes, S. R. and Lewis, S. (1996). Comparing Imperial mandarin and Silverhill satsuma mandarin as seed parents in a breeding program aimed at developing new seedless citrus cultivars for Australia. *Aust. J. Exp. Agric.* **36**, 731-738.

Szymkowiak, E. J. and Sussex, I. M. (1993). Effect of *lateral suppressor* on petal initiation in tomato. *Plant J.* **4**, 1-7.

Takeno, K. and Ise, H. (1992). Parthenocarpic fruit set and endogenous indole-3-acetic acid content in ovary of *Cucumis sativus* L. *J. Jpn. Soc. Hortic. Sci.* **60**, 941-946.

Talon, M., Hedden, P. and Primo Millo, E. (1990a). Gibberellins in *Citrus sinensis*: A comparison between seeded and seedless varieties. *J. Plant Growth Regul.* **9**, 201-206.

Talon, M., Koornneef, M. and Zeevaart, J. A. D. (1990b). Endogenous gibberellins in *Arabidopsis thaliana* and possible steps blocked in the biosynthetic pathways of the semi-dwarf *ga4* and *ga5* mutants. *Proc. Natl. Acad. Sci.* **87**, 7983-7987.

Talon, M., Koornneef, M. and Zeevart, J. A. D. (1990c). Accumulation of C19-gibberellins in the gibberellin-insensitive dwarf mutant *gai* of *Arabidopsis thaliana*. *Planta* **182**, 501-505.

Talon, M., Zacarias, L. and Primo-Millo, E. (1990d). Hormonal changes associated with fruit set and development in mandarins differing in their parthenocarpic ability. *Physiol. Plantarum* **79**, 400-406.

Talon, M., Zacarias, L. and Primo-Millo, E. (1992). Gibberellins and parthenocarpic ability in developing ovaries of seedless mandarins. *Plant Physiol.* **99**, 1575-1581.

Tan, S. and Richmond, T. J. (1998). Crystal structure of the yeast MATalpha2/MCM1/DNA ternary complex. *Nature* **391**, 660-666.

Tandre, K., Albert, V. A., Sundas, A. and Engstrom, P. (1995). Conifer homologues to genes that control floral development in angiosperms. *Plant Mol. Biol.* **27**, 69-78.

Tandre, K., Svenson, M., Svensson, M. E. and Engstrom, P. (1998). Conservation of gene structure and activity in the regulation of reproductive organ development of conifers and angiosperms. *Plant J.* **15**, 615-623.

Tatematsu, K., Liscum, E. and Yamamoto, K. T. (2000). The molecular interaction between NPH4 / ARF7 and MSG2 / IAA19 in the yeast two-hybrid system. *11th International Conference on Arabidopsis Research*, 24th-28th June, University of Wisconsin, Madison.

Theissen, G., Becker, A., Di Rosa, A., Kanno, A., Kim, J. T., Münster, T., Winter, K. U. and Saedler, H. (2000). A short history of MADS-box genes in plants. *Plant Mol. Biol.* **42**, 115-149.

Thornton, T. M., Swain, S. M. and Olszewski, N. E. (1999). Gibberellin signal transduction presents the *SPY* who O-GlcNAc'd me. *Trends Plant Sci.* **4**, 424-428.

Tissier, A. F., Marillonnet, S., Klimyuk, V., Patel, K., Torres, M. A., Murphy, G. and Jones, J. D. (1999). Multiple independent defective suppressor-mutator transposon insertions in *Arabidopsis*: A tool for functional genomics. *Plant Cell* **11**, 1841-1852.

Torii, K. U., Mitsukawa, N., Oosumi, T., Matsuura, Y., Yokoyama, R., Whittier, R. F. and Komeda, Y. (1996). The *Arabidopsis ERECTA* gene encodes a putative receptor protein kinase with extracellular leucine-rich repeats. *Plant Cell* **8**, 735-746.

Ulmasov, T., Hagen, G. and Guilfoyle, T. J. (1997a). ARF1, a transcription factor that binds to auxin response elements. *Science* **276**, 1865-1868.

Ulmasov, T., Hagen, G. and Guilfoyle, T. J. (1999a). Activation and repression of transcription by auxin-response factors. *Proc. Natl. Acad. Sci.* **96**, 5844-5849.

Ulmasov, T., Hagen, G. and Guilfoyle, T. J. (1999b). Dimerization and DNA binding of auxin response factors. *Plant J.* **19**, 309-319.

Ulmasov, T., Murfett, J., Hagen, G. and Guilfoyle, T. J. (1997b). Aux / IAA proteins repress expression of reporter genes containing natural and highly active synthetic auxin response elements. *Plant Cell* **9**, 1963-1971.

Urao, I., Yamaguchi-Shinozaki, I. and Shinozaki, I. (2000). Two-component systems in plant signal transduction. *Trends Plant Sci.* **5**, 67-74.

van der Knaap, E., Jagoueix, S. and Kende, H. (1997). Expression of an ortholog of replication protein A1 (RPA1) is induced by gibberellin in deepwater rice. *Proc. Natl. Acad. Sci.* **94**, 9979-9983.

van der Knaap, E., Kim, J. H. and Kende, H. (2000). A novel gibberellin-induced gene from rice and its potential regulatory role in stem growth. *Plant Physiol.* **122**, 695-704.

van der Knaap, E. K. M. (1998). Identification of gibberellin-induced genes in deepwater rice and the role of these genes in plant growth. Ph.D. Thesis, Michigan State University, Michigan.

van Huizen, R., Ozga, J. A. and Reinecke, D. M. (1997). Seed and hormonal regulation of gibberellin 20-oxdiase expression in pea pericarp. *Plant Physiol.* **115**.

van Huizen, R., Ozga, J. A., Reinecke, D. M., Twitchin, B. and Mander, L. N. (1995). Seed and 4-chloroindole-3-acetic acid regulation of gibberellin metabolism in pea pericarp. *Plant Physiol.* **109**, 1213-1217.

Van Overbeek, J., Conklin, M. E. and Blakeslee, A. F. (1941). Factors in coconut milk are essential for growth and development of very young *Datura* embryos. *Science* **94**, 350-351.

Vardy, E., Lapushner, D., Genizi, A. and Hewitt, J. (1989a). Genetics of parthenocarpy in tomato under a low temperature regime: I. Line RP75/79. *Euphytica* **41**, 1-8.

Vardy, E., Lapushner, D., Genizi, A. and Hewitt, J. (1989b). Genetics of parthenocarpy in tomato under a low temperature regime: II. cultivar 'Severianin". *Euphytica* **41**, 9-15.

Varge, A. and Bruinsma, J. (1976). Roles of seeds and auxins in tomato fruit growth. *Z. Pflanzenphysiol.* **80**, 95-104.

Vercher, Y. and Carbonell, J. (1991). Changes in the structure of ovary tissues and in the ultrastructure of mesocarp cells during ovary senescence or fruit development induced by plant growth substances in *Pisum sativum*. *Physiol. Plantarum* **81**, 518-526.

Vercher, Y., Carrasco, P. and Carbonell, J. (1989). Biochemical and histochemical detection of endoproteolytic activities involved in ovary senescence or fruit development in *Pisum sativum*. *Physiol. Plantarum* **76**, 405-411.

Vercher, Y., Molowny, A. and Carbonell, J. (1987). Gibberellic acid effects on the ultrastructure of the endocarp cells of unpollinated ovaries of *Pisum sativum*. *Physiol. Plantarum* **71**, 302-308.

Vercher, Y., Molowny, A., Lopez, C., García-Martínez, J. L. and Carbonell, J. (1984). Structural changes in the ovary of *Pisum sativum* L. induced by pollination and gibberellic acid. *Plant Sci. Lett.* **36**, 87-91.

Vielle-Calzada, J. P., Thomas, J., Spillane, C., Coluccio, A., Hoeppner, M. A. and Grossniklaus, U. (1999). Maintenance of genomic imprinting at the *Arabidopsis medea* locus requires zygotic DDM1 activity. *Genes Dev.* **13**, 2971-2982.

Villanueva, J. M., Broadhvest, J., Hauser, B. A., Meister, R. J., Schneitz, K. and Gasser, C. S. (1999). *INNER NO OUTER* regulates abaxial-adaxial patterning in *Arabidopsis* ovules. *Genes Dev.* **13**, 3160-3169.

Wardlaw, I. F. (1990). The control of carbon partitioning in plants. *The New Phytologist* **116**, 341-381.

Watanabe, K., Sawa, S. and Okada, K. (1999). FIL protein interacts with ETTIN protein in yeast two-hybrid system. *10th International Conference on Arabidopsis Research*, 4th-8th July, Melbourne, Australia.

Western, T. L. and Haughn, G. W. (1999). *BELL1* and *AGAMOUS* genes promote ovule identity in *Arabidopsis thaliana*. *Plant J.* **18**, 329-336.

Wisman, E., Cardon, G. H., Fransz, P. and Saedler, H. (1998). The behavior of the autonomous maize transposable element *En*/*Spm* in *Arabidopsis thaliana* allows efficient mutagenesis. *Plant Mol. Biol.* **37**, 989-999.

Wittich, P. E. (1998). Seed development and carbohyrates. Ph.D. Thesis, *Laboratorium Plantencytologie en -morfologie*, van de Landbouwuniversiteit, Wageningen.

Worley, C. K., Zenser, N., Ramos, J., Rouse, D., Leyser, O., Theologis, A. and Callis, J. (2000). Degradation of Aux / IAA proteins is essential for normal auxin signaling. *Plant J.* **21**, 553-562.

Wysocka-Diller, J. W., Helariutta, Y., Fukaki, H., Malamy, J. E. and Benfey, P. N. (2000). Molecular analysis of *SCARECROW* function reveals a radial patterning mechanism common to root and shoot. *Development* **127**, 595-603.

Xu, Y. L., Li, L., Wu, K. Q., Peeters, A. J. M., Gage, D. A. and Zeevaart, J. A. D. (1995). The *GA5* locus of *Arabidopsis thaliana* encodes a multifunctional gibberellin 20-oxidase: Molecular cloning and functional expression. *Proc. Natl. Acad. Sci.* **92**, 6640-6644.

Yamaguchi, S., Smith, M., Brown, R. G. S., Kamiya, Y. and Sun, T. P. (1998). Phytochrome regulation and differential expression of gibberellin 3ß-hydroxylase genes in germinating *Arabidopsis* seeds. *Plant Cell* **10**, 2115-2126.

Yanofsky, M. F., Ma, H., Bowman, J. L., Drews, G. N., Feldmann, K. A. and Meyerowitz, E. M. (1990). The protein encoded by the *Arabidopsis* homeotic gene *AGAMOUS* resembles transcription factors. *Nature* **346**, 35-39.

Yasuda, S. (1930). Parthenocarpy induced by the stimulus of pollination in some plants of the *Solanaceae*. *Agriculture and Horticulture* **5**, 287-294.

Yasuda, S. (1935). Parthenocarpy caused by the stimulation of pollination in some plants of the *Cucurbitaceae*. *Agriculture and Horticulture* **10**, 1385-1390.

Yephremov, A. and Saedler, H. (2000). Technical advance: Display and isolation of transposon-flanking sequences starting from genomic DNA or RNA. *Plant J.* **21**, 495-505.

Zhang, J. Z. and Somerville, C. R. (1997). Suspensor-derived polyembryony caused by altered expression of valyl-tRNA synthetase in the *twn2* mutant of *Arabidopsis*. *Proc. Natl. Acad. Sci.* **94**, 7349-7355.

Zrenner, R., Salanoubat, M. and Willmitzer, L. (1995). Evidence of the crucial role of sucrose synthase for sink strength using transgenic potato plants (*Solanum tuberosm* L.). *Plant J.* **7**, 97-107.